Université de Lille

PhD Thesis

presented with a view to obtaining the degree of

Doctor of Science

from the University of Lille

École doctorale Biologie Santé

2021/2022

Laure Deramoudt

Presented and defended on 26th September 2022

« B cells and humoral immunity in demyelinating diseases of the central nervous system »

Jury members:

President:

Monsieur le Professeur Patrick Vermersch
MD, PhD, PU-PH – Neurologist – Lille University

Reviewers:

Monsieur le Professeur Alexander Flügel
Professor and director of the Institute for Neuroimmunology and Multiple Sclerosis Research, University of Göttingen

Monsieur le Docteur Guillaume Dorothée
Research Director – inserm UMR-S 938 – Team leader « *Système Immunitaire et Neuroinflammation* » – Saint Antoine research centre, Paris

Examinateur:

Madame le Docteur Anneli Peters
Research Group Leader – *T:B cell interactions* – institute of Clinical – Neuroimmunology, Munich

Thesis Director :

Monsieur le Docteur Lennart MARS
Researcher – inserm UMR-S 1172 – Team leader NEMESIS « *Neuroinfammation & Multiple Sclerosis* » – Lille University

ACKNOWLEDGEMENTS

To my thesis director, Dr. Lennart Mars

Thank you for your trust, your availability and for the transmission of your knowledge.
I am honored to have been able to contribute to the various innovative projects of your laboratory at the interface between fundamental and clinical neuroimmunology.

To the members of this jury

Thank you for having accepted to reside in my thesis jury and for your time in the reading of this manuscript. Looking forward to your comments and suggestions.
Dear Pr. Patrick Vermersch, I would like to thank you, who have honored me with the privilege of presiding over this thesis defense
Dear Pr. Alexander Flügel, I would like to thank you sincerely for your consideration of this work. It is a great privilege to have you on this jury.
Dear Dr Guillaume Dorothée, I would like to thank you for having accepted to be the rapporteur of this work and thank you very much for your advises during the monitoring PhD committee.
Dear Dr Anneli Peters, I would like to warmly thank you for agreeing to be a member of my thesis jury.

I would also like to warmly thank all the people with who I have enjoyed working, who have helped, supervised, advised and comforted me and from whom I have learned so much:

- Warmly thanks to Dr. Nathalie Journiac, in particular for her expertise, support and advice. Thank you for training me so well with experimental neuroimmunology.
- Thanks to my colleagues from the NEMESIS (Neuro-inflammation and Multiple Sclerosis) team and more broadly the LilNCog (Lille Neuroscience and Cognition) with a special thanks for the supportive administrative team, Céline, Nathalie, Sophie and Marion and also to Pierre Semaille for his help with genotyping.
- I would like to thank in particular Dr. Shin-Yi Yu for her expertise in glycosylation ; Dr. Edmone Dewaeles for helping me so well during my last year of thesis and a special thanks to Dr. Florent Salvador, thank you for working together and for your cheerfulness. I would also like to thank Marie Delbeke for her help and Carine Hauspie for her expertise in the development of ELISA. Many thanks to the students who participated in this research project, in particular Claire, Nachiati, Aude and Carole.
- Thanks very much to Pr. Hélène Zephir, it was rewarding to collaborate on the great B cell repertoire.

- Thanks to the cytometry and cell sorting platform of the Bio Imaging Center of the University of Lille, especially Nathalie Jouy and Emilie Floquet for your precious help on the platform and for the discovery of the SP6800.
- I would like to thank the EOPS 1 teams and more specifically Mélanie.
- Thanks to the LFB Biotechnology and specially to Céline Monnet and Mathilde Bas, their expertise in Fc- engineering and glyco-engineering formed the basis of this wonderful project.
- Thanks to to Pr. Hélène Zephir (Lille) and Romain Marignier (Lyon) for the serum and CSF samples from the biobank of the NOMADMUS and OFSEP protocols.
- Thanks to Pr. Yann Guerardel and UGSF team (Unité de Glycobiologie Structural et Fonctionelle) for expertise on the glycans analysis.
- Thanks to Raphaëlle Romieu-Mourez for INFINITy U1291 for the reading of ELISPOT plates.
- Thanks to the Pr. Dr. Jan Bauer from Vienna Brain institute for the histochemistry and immunohistochemistry and the valuable zoom exchanges.
- I thank the ANR and ARSEP for funding this research project.
- Thank you to the whole CERIM team for their support in the writing of this thesis and especially to Anaïs and Laurine for their unfailing support.

Personal acknowledgements

To my family, I would like to express my deepest thanks to my parents for their unfailing support and encouragement throughout my studies. Thanks to my brothers Charles and Thibaut with whom I shared my studies at the Faculty of Pharmacy.

To Norbert, thank you for being there for me and for taking such good care of me.

My thanks also go to my friends, always at my side even when the kilometers separate us:

- To all my friends at the Faculty of Pharmacy of Montpellier :

and especially to Marine, Loriane, Sophie, Laura, Sarah, Lauren Blandine and Camille. I keep in mind all these moments of joy that punctuated our lives as Montpellier students, hoping that there will be many more in our lives as pharmacists. I would also like to thank Florine, Marie, Laura, Jérémie, Nolwenn, Marion, Laurence, Roxane and the other members of the group: may our meetings together remain a tradition.

- Thank you to the F... you know the following, Anaïs, Amayelle, Anne-Sophie, Claire and Laureen, you have made the North so welcoming. I thank you for your support and especially for having filled these 5 years of internship/thesis with laughter and memorable weekends, I hope to spend many more in your company. Special warmly thanks to Anaïs for your understanding and your support. I also would like to thank very much Laurine for your presence and your good mood. And long live the board games.
- Thanks to Mathilde and Florent for their help in this thesis.

- Thanks to FWA crossfit and all the team for their welcome.
- Thanks to PhD DC for the support I found there and the great people I have met.

PREFACE

After completing my pharmacy studies at the University of Montpellier, motivated by innovation, I pursued a career at the interface of scientific innovation and biotechnology aimed to human benefit.

With a particular interest in immune-mediated inflammatory diseases, I joined the Lille University Hospital to train in translational research. I enrolled in a double internship in pharmacy / PhD to study the pathophysiology of autoimmune demyelinating diseases. I was able to do my PhD in the fundamental research laboratory of Dr Lennart MARS, enriched by the proximity of the multiple sclerosis clinic directed by Pr Patrick Vermersch and Pr Hélène Zephir.

This manuscript reflects my four years of thesis work, which allowed me to acquire the technical and scientific background in order to better understand autoimmune diseases of the central nervous system. My work is dedicated to the role of B cells in the physiopathology of demyelinating diseases in particular in Multiple Sclerosis (MS) and a novel demyelinating disease driven by a focal antibody response against Myelin Oligodendrocyte Glycoprotein (MOG) called MOG-antibody associated disease (MOGAD). This work was possible with the help of translational research approaches and with the use of selected animal models.

Initially I studied the involvement of a subpopulation of proinflammatory B cells characterized by the expression of the transient activation marker 4-1BBL in the pathophysiology of MS using an EAE MOG model induced in 4-1BBL KO mice. This work allowed me to defend my pharmacy thesis in 2020 and is therefore not detailed in this document. My PhD thesis is dedicated to two studies. I had the opportunity to study the repertoire of MOG specific B cells in a spontaneous model of experimental auto-immune encephalomyelitis which allowed a co-first author publication together with Florent Salvador. My primary study focused on Fc-glycosylation and its ability to dictate the pathogenicity of MOG specific antibodies in the context of MOGAD. This project is nearing completion and a manuscript will be submitted for publication in the coming months.

ABSTRACT IN ENGLISH

Demyelination, inflammation and neurodegeneration are the hallmarks of two paradigmatic diseases of the central nervous system (CNS): multiple sclerosis (MS) and myelin oligodendrocyte glycoprotein-associated diseases (MOGAD). MS is a chronic disease that mobilises the immune response in recurrent waves before evolving into a progressive disease. In contrast, MOGAD is an inflammatory disease with a focal antibody (Ab) response. In these distinct demyelinating diseases, the B cell response remains a relevant but unresolved mediator of inflammation.

In this thesis we investigate two aspects of the B cell response. First, we study the clonality of MOG-specific B cell response in a spontaneous model of experimental autoimmune encephalomyelitis (EAE). In a second approach we address the Fc-glycosylation profile of disease-related antibodies in MOGAD and MS and study their pathogenic traits experimental models.

To investigate the clonal expansion of auto reactive B cells in autoimmune demyelinating disease, a spontaneous EAE model was used. These mice express a transgenic TCR (TCR^{1640}) specific for I-As:MOG_{92-106}. In our animal facility, 94% of TCR^{1640} spontaneously developed a chronic paralytic EAE between 60 and 500 days of age. It is known that this auto reactive immune response is triggered by the microbiota in the gut-associated lymphoid tissue. Our study indicates that the MOG-specific B cells ($MOGtet^{+}$ B cells) cumulate in the brain-draining cervical lymph nodes and among the brain immune infiltrate of diseased mice. Repertoire analysis provided evidence of clonal B cells expansion. This study implicates clonal expansion and CNS infiltration of B cells iin the development of spontaneous autoimmune demyelinating EAE.

Abs exert their function through binding to Fc receptors and complement. For IgG, this tightly regulated process relies on the structural heterogeneity of the IgG-Fc domain resulting from differences between the four subclasses (IgG1, IgG2, IgG3 and IgG4). This position is changing. N-glycosylation associated with the asparagine 297 (N297) influences binding to both classical Fc-gamma receptors (FcRs) and non-classical type II receptors.

Deep analysis of the salient glycan features on disease-related Abs from MS and MOGAD revealed a clear dichotomy. The glycosylation profile of MOG-specific Abs in MOGAD revealed a striking enrichment in Fc-domains with an inflammatory signature, which was absent in both healthy individuals and MS patients. Furthermore, Fc-glycovariants of a monoclonal MOG-

specific Ab were compared in vivo demonstrating that the MOGAD-related Fc-glycosylation profile dictated the pathogenicity of autoantibodies.

My thesis deepens the understanding of the MOG-specific B cell response in autoimmune demyelinating disease of the CNS. Notably I demonstrate a salient Fc-glycosylation feature associated with the MOG-specific IgG1 response driving MOGAD. In experimental models, this salient trait strongly augmented Ab pathogenicity. This translational approach demonstrates the major role of N-glycosylation and in particular hypofucosylation in the emerging demyelinating inflammatory disorders associated with MOG.

Key words: neuro immunology, autoantibodies, Fc-glycosylation, Multiple sclerosis, Neuromyelitis optica, autoimmune experimental encephalomyelitis

ABSTRACT IN FRENCH

La démyélinisation, l'inflammation et la neurodégénérescence sont des caractéristiques de deux maladies paradigmatiques du système nerveux central (SNC) : la sclérose en plaques (SEP) et les maladies associées à la glycoprotéine de l'oligodendrocyte de la myéline (MOGAD). La SEP est une maladie chronique qui mobilise la réponse immunitaire par vagues récurrentes avant d'évoluer vers une maladie progressive. En revanche, les MOGAD sont des maladies inflammatoires avec une réponse focale des anticorps (Ac). Dans ces maladies démyélinisantes distinctes, la réponse des lymphocytes B (LB) reste un médiateur de l'inflammation pertinent mais non résolu.

Dans cette thèse, nous étudions deux aspects de la réponse des lymphocytes B. Premièrement, nous étudions la clonalité de la réponse des LB spécifiques de MOG dans un modèle spontané d'encéphalomyélite auto-immune expérimentale (EAE). Dans une deuxième approche, nous nous penchons sur le profil de glycosylation du fragment cristallisable (Fc) des anticorps liés aux MOGAD et à la SEP et nous étudions leurs traits pathogéniques dans des modèles expérimentaux.

Pour étudier l'expansion clonale des LB auto-réactifs dans les maladies démyélinisantes auto-immunes, un modèle spontané d'EAE a été utilisé. Ces souris expriment un TCR transgénique (TCR^{1640}) spécifique de I-As:MOG_{92-106}. Dans notre animalerie, 94% des TCR^{1640} ont développé spontanément une EAE chronique paralytique entre 60 et 500 jours d'âge. Il est connu que cette réponse immunitaire auto-réactive est déclenchée par le microbiote dans le tissu lymphoïde associé à l'intestin. Notre étude indique que les LB spécifiques de MOG (LB MOGtet^{+}) s'accumulent dans les ganglions cervicaux drainant le cerveau et parmi l'infiltrat immunitaire cérébral des souris malades. L'analyse du répertoire a fourni des preuves de l'expansion clonale des LB. Cette étude implique l'expansion clonale et l'infiltration des LB dans le SNC dans le développement de l'EAE démyélinisant auto-immun spontané.

Les Acs exercent leur fonction en se liant aux récepteurs Fc et au complément. Pour les IgG, ce processus étroitement régulé repose sur l'hétérogénéité structurelle du domaine IgG-Fc résultant des différences entre les quatre sous-classes (IgG1, IgG2, IgG3 et IgG4). Ce positionnement est en train de changer. La N-glycosylation associée à l'asparagine 297 (N297) influence la liaison aux récepteurs Fc-gamma classiques (FcRs) et aux récepteurs non classiques de type II.

Une analyse approfondie des caractéristiques marquantes des glycanes sur les Acs liés à la maladie de la SEP et dans les MOGAD a révélé une nette divergence. Le profil de N-glycosylation des Acs spécifiques de MOG dans les MOGAD a révélé une signature inflammatoire marquante,, qui était absente chez les individus sains et les patients atteints de SEP. En outre, les Fc-glycovariants d'un Ac monoclonal spécifique de MOG ont été comparés *in vivo*, démontrant que le profil de Fc- glycosylation Fc lié aux MOGAD dictait la pathogénicité des auto-anticorps.

Ma thèse approfondit la compréhension de la réponse des LB spécifiques de MOG dans les maladies démyélinisantes auto-immunes du SNC. Je démontre notamment une caractéristique majeure de la Fc-glycosylation associée à la réponse IgG1 spécifique de MOG qui conduit aux MOGAD. Dans des modèles expérimentaux, ce trait marquant a fortement augmenté la pathogénicité de l'Ac. Cette approche translationnelle démontre le rôle majeur de la N-glycosylation et en particulier de l'hypofucosylation dans les troubles inflammatoires démyélinisants émergents associés à MOG.

Mots clés : neuro-immunologie, autoanticorps, Fc-glycosylation, Sclérose en plaques, Neuromyélite optique, Encéphalomyélite expérimentale auto-immune.

INDEX

LIST OF ABBREVIATIONS

Ab	Antibody
ADCC	Antibody-dependent cellular cytotoxicity
ADEM	Acute disseminated encephalomyelitis
Ag	Antigen
AID	Auto-immune disease
AID	Activation-induced cytidine deaminase
AIRE	Auto-immune regulatory element
ANO2	anoctamine 2
APC	Antigen presenting cells
AQP4	Aquaporine 4
BBB	Blood-Brain Barrier
BCR	B cell receptor
BCS	Body condition score
BCSFB	Blood-CSF barrier
BLI	Biolayer interferometry
BM	Bone marrow
CBA	Cell-based Assay
CDC	Complement-dependent cytotoxicity
CHO	Chinese hamster ovary
CIS	Clinically isolated syndrome
CLR(s)	c-type lectin receptors
CNS	Central nervous system
CSF	Cerebrospinal fluid
CSR	Class-switch recombination
DC	Dendritic Cell
DC-SIGN	Dendritic cell-specific intercellular adesion molecule-3-grabbing nonintegrin
EAE	Experimental autoimmune encephalopathy
EBNA-1	EBV nuclear antigen 1
EBV	Epstein-Barr virus
ELF	Ectopic lymphoid follicle
Fab	Fragment antigen-binding
FBS	Fetal Bovine Serum
Fc	Crystallizable fragment

FcR(s)	Receptors for Fc fragments of IgG
FDC	Follicular dendritic cells
Foxp3	Forkhead Box P3
FUT8	Fucosyltransferase 8
GC	Germinal center
GWAS	Genome-wide association studies
HC	Heavy chain
LC	Light chain
HEK	Human Embryonic Kidney
I.V	Intravenously
IC	Immune complex
IDO	indolamine 2,3 dioxygénase
IFN	Interferon
Ig	Immunoglobulin
iGB	Induced germinal center B cells
IL	Interleukin
IS	Immune System
ITAM	Immunoreceptor Tyrosine Activating Motif
JKT	Jurkat
KO	Knock Out
MALDI	Matrix assisted laser desorption ionisation
MBP	Myelin Basic Protein
MHC	Major histocompatibility complex
MOG	Myelin oligodendrocyte glycoprotein
MOGAD	MOG antibody associated disease
MS	Multiple sclerosis
MS-PP	Multiple Sclerosis Primary Progressive
MS-PS	Multiple Sclerosis Secondary Progressive
MS-RR	Multiple Sclerosis Recurrent-Remittent
mTEC	Medullary thymic epithelial cells
NGA	Next Generation Antibodies
NK	Natural killer
NMO	Neuromyelits optica
NMOSD	Neuroromyelitis Optica Spectrum disoders
NS	Not significant
ON	Optic neuritis
OR	Odds ratio

PLP	ProteoLipid Protein
PMA	phorbol myristate acetate
pMHC	peptide-MHC
PRR	Pattern recognition receptors
RAG	Recombination activating Gene
rhMOG	Recombinant Human MOG
RR	Recurrent-Remittent
RSS	Recombination signal sequence
SC	Spinal Cord
SEM	Standard error of the mean
SH	Somatic hypermutations
SLE	Systemic Lupus Erythematosus
TCR	T cell receptor
Tfh	Follicular helper T cell
Tg	Transgenic
TM	Transverse myelitis
TREC	T-cell Receptor Excision Circle
Treg	Regulatory T cells
WT	Wild type

APPENDICES

LIST OF FIGURES

I. Definition and interaction between the immune and the central nervous system

A. The central nervous system

The central nervous system (CNS) consists of the brain and spinal cord and also optic nerve and retina. It organizes, controls and regulates essential body functions such as motor skills, perception, intellectual functions, emotions, behavior and organ function. Sensory and effector information is carried to and from the CNS by the nerves that make up the peripheral nervous system. The CNS is surrounded by the meninges, fibrous membranes with a protective function. In the parenchyma of the brain and spinal cord, a distinction is made between white matter and grey matter: while the white matter consists mainly of neuronal extensions and glial cells, the grey matter contains the cell bodies of neurons. The brain and spinal cord (SC) is immersed in cerebrospinal fluid (CSF), which acts as a buffer for the CNS by providing mechanical protection, chemical stability and waste removal. CSF is produced continuously by plasma filtration through the ependymal cells of the choroid plexuses, interfaces between the blood and the CNS found in the ventricles.

The cellular components of the CNS consist of neurons and glial cells (**Figure 1**). Neurons are the main cognitive actors in the CNS, transmitting information in the brain and in the periphery using electrical impulses or chemical signals. The nerve impulse travels along the axon. Neuron have almost no capacity for self-renewal, a feature shared only few other structures. For their functioning, neurons interact with supporting cells: glial cells. Glial cells include: astrocytes, oligodendrocyte and microglia. Astrocytes are star-shaped cells that provide nutrients and regulate the chemical environment of neurons. They also help to reinforce the synapses. Oligodendrocytes in the CNS and Schwann cells in the peripheral nervous system produce a lipid membrane that surrounds axons called myelin. This protective sheath protects the axons and speeds up the nerve impulse by clustering the ion channels, which improves the speed of conduction. Demyelination, due to the damage of oligodendrocytes and myelin sheath, can lead to neurological manifestations associated with demyelinating diseases of the CNS [1,2].

Finally, microglia are a distinct population in the CNS, they do not originate from the same embryonic stage of development as other glial cells. They are the main innate immune cells of the CNS and they contribute to the maintenance of the environment with a unique homeostatic molecular signature. These tissue resident macrophages are essential immune sentinel, as they are critical innate immune sensors, they maintain homeostasis by the phagocytose of apoptotic neurons. [3,4]. Single cell analyses by *Mrdjen et al. (2018)* have recently revealed the presence of non-parenchymal immune cells at CNS-associated interfaces, which include border-associated macrophages (BAMs), dendritic cells (DCs), innate lymphoid cells and T-cells [5,6].

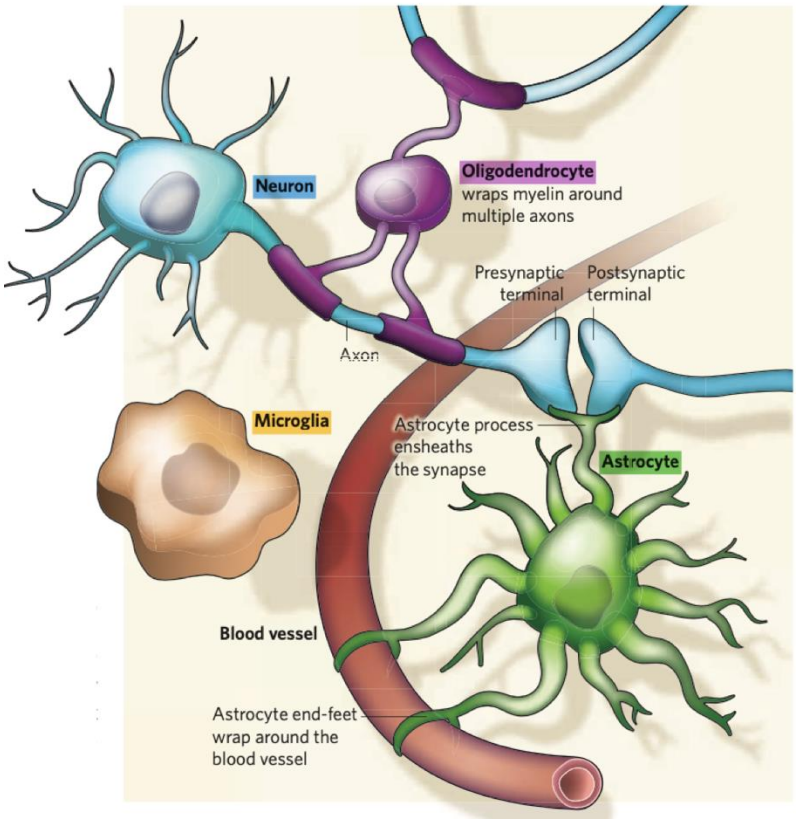

Figure 1: The cellular components of CNS parenchyma

(From Allen and Barres, 2009)

Illustration of neurons and glials cells that constitute the SNC and there interactions.

The CNS has different protective mechanisms that explain its highly controlled interaction with the immune system. It has long been recognised as a site of "immuno-privilege", a notion introduced by Medawar in 1948 [7]. This status dictated that immunogenic agents can persist in the CNS parenchyma without inducing an adaptive immune response [8]. The passive concept of the CNS parenchyma being sealed from the immune system has long evolved. But an active system that tightly regulates when and how immune intervention may be tolerated is in place. To explain CNS immune surveillance, it is important to start with the anatomical features and in particular the barrier or interface systems that integrate the CNS (**Figure 2**):

- ***The blood-CSF barrier (BSCFB), "the educational barrier":*** This barrier surrounds the choroid plexus, a structure that is responsible for the production of CSF found in the ventricles. The stroma of the choroid plexus contains vessels that do not have the same structure as those of the cerebral capillaries, and thus allow cells or molecules to pass through more or less freely, thus maintaining homoeostasis and the protein and cell composition of the CSF [9]. This barrier can be overcome by activated effector cells at the steady state and this allow CSF immune surveillance.
- ***The blood-brain barrier (BBB), "the true barrier":*** This barrier surrounds the microvessels located in the parenchyma. It is an endothelial barrier formed by a monolayer of endothelial cells with tight junctions resting on a continuous basement membrane that splits in places to accommodate pericytes (smooth muscle cells that ensure the contractility of the microvessels). This membrane is composed of an astroglial endfeet structure, the *glial limitans*. The perivascular space is filled with CSF. This space opens to the subarachnoid lepto-meninges on the surface of the brain. This barrier prevents the invasion of leukocytes mediated by fetaures which ensures the maintenance of its sealing. This barrier requires an "opening" for the infiltration of immune cells and this is possible in pathological pro-inflammatory conditions where perivascular cuffs can develop. These structures are composed of immune cells and this is what leads to parenchymal immune cells infiltrate [10].
- ***The meninges*** cover the surface of the CNS and connect the BBB and the Blood-CSF barrier. There are composed of three membranes that protect the brain and SC. This three layered membrane consist of the dura mater, arachnoid mater, and the pia mater [11]. The dura mater is the outermost layer. It is a thick, leather-like membrane with fenestrated blood vessels without tight junctions. The arachnoid and the pia mater together constitute the leptomeninges, also called subdural meninges. It is important to note the presence of meningeal lymphatic vessels. Around these vessels we find an endothelial monolayer with serrated junctions but without the astroglial endfeet structure. This meningeal vessels allow the drainage of macromolecules and immune cells. Various immune cells populate the meninges, like macrophages, in the steady state, which can changes during aging and neurodegenerative disorders [12].

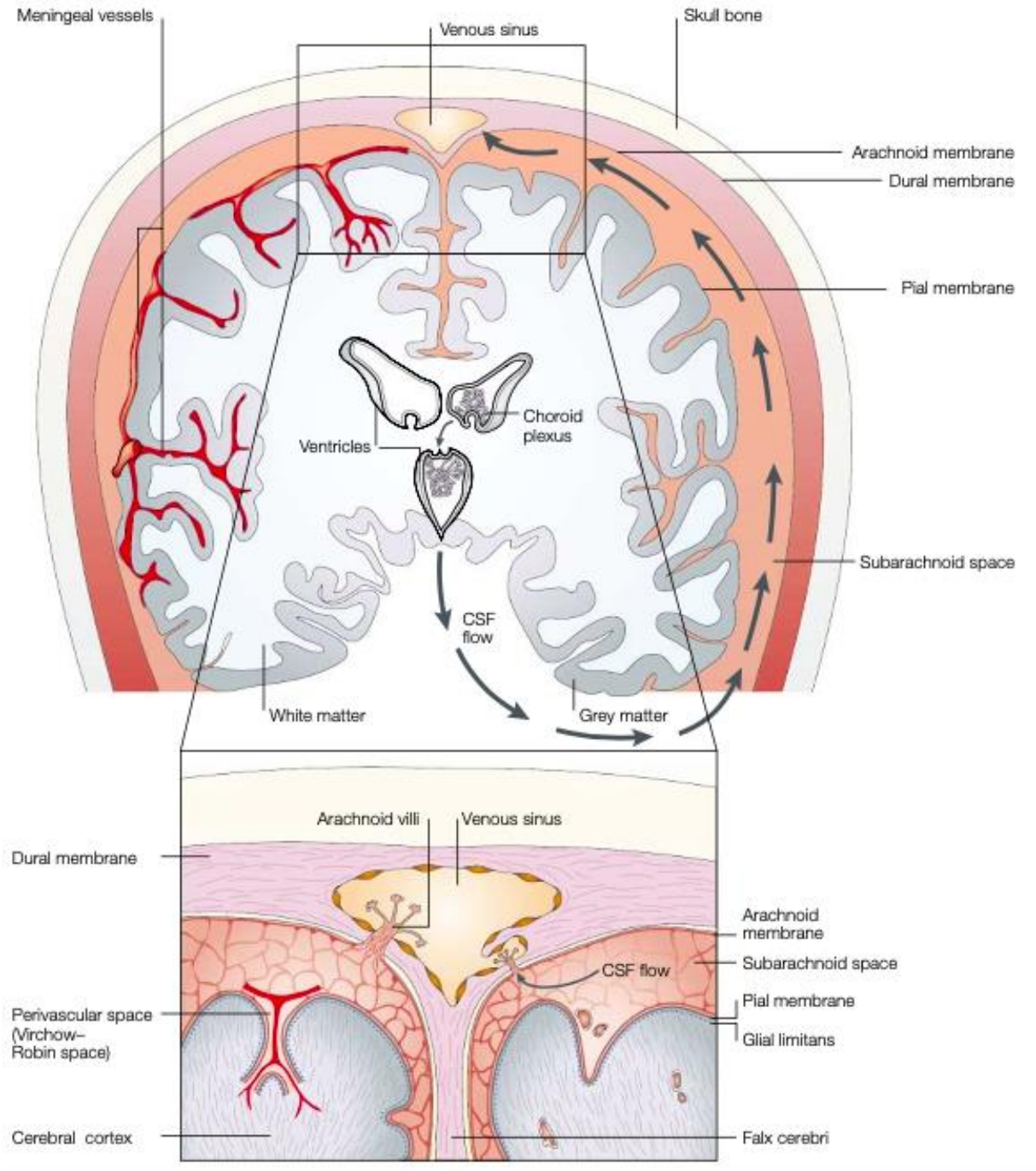

Figure 2: Anatomical structures of the brain

(From Ransohoff and al. 2003)

The terminal branches of the internal carotid arteries supply the paranchyma. These follow the surface of the brain to the subarachnoid space.
At the location where vessles enter the parenchyma, they are first surrounded by the perivascular space which is connected to the subarachnoid space.
Ventricles secrete CSF.

The lack of MHC molecule expression by CNS parenchymal cells, and the anti-inflammatory nature of the CNS tissue environment - help to explain the specialized and largely attenuated nature of CNS inflammatory responses, which is extremely important for the preservation of the delicate, non-regenerative tissue elements of the CNS. However, immune surveillance is present in the central nervous system and takes place in the meningeal compartment through functional lymphatic vessels that are connected to the deep cervical lymph nodes [13–15].
However, failure to control immune responses in the CNS can result in chronic immuno-pathological disorders, such as multiple sclerosis and neuromyelitis optica [14]. The infectious agent may also escape immune clearance and establish persistence or latency in the parenchyma [16].

B. The immune system

The network of cells, tissues and molecules that provide protects organism from disease is called the immune system (IS). The IS protects the body against infectious diseases and cancers by recognising and neutralising microbial pathogens and tumour cells. Lymphoid organs and tissues are strategically positioned over the body, and immune cells circulate in and between these organs via blood or lymphatics. This vital system is divided into two functional components: innate immunity and adaptive immunity; which cooperate to exert immune function[17]. Innate immunity also known as natural immunity or non-specific immunity, was the first to be established during evolution. It is based on defence mechanisms that are present from birth (innate) and therefore do not require learning (acquired). These innate mechanisms are rapidly mobilised by reactions to conserved signals derived from infection, malignancy or tissue damage. Adaptive immunity is found in all jawed vertebrates. This branch is an adjusts to the specific pathogen that is being encountered. Such acquired immunity is specific to a single protein fragment called an antigen (Ag). Antigen specificity affords the adaptive immune response with a decisive advantage because during a second encounter with the same pathogen, the response induced is faster and more effective. This immunological memory is highlighted in vaccination strategies. Effective immunity regulates both the innate and adaptive immunity response which are complementary and not mutullaly exclusive.

1. Lymphoid organs

The IS is composed of primary and secondary lymphoid organs.
The primary lymphoid organs are responsible for the production of all the cell lineages of the IS that derive from communes hematopoietic stem cells. **Thymus** and **bone marrow** (BM) are the two primary lymphoid organs found in humans. The innate immune response originates from the bone marrow where hematopoietic stem cells differentiate into myeloid progenitors which are the progenitors of granulocytes (eosinophils, basophils, neutrophils) monocytes

(precursor of dendritic cells (**DC**) and macrophages) as well as erythrocytes and platelets. The acquired immune response matures in either the thymus or bone marrow. The B cell lineage matures in the BM while CD4 and CD8 T cell mature in the thymus. Secondary lymphoid organs are the spleen, lymph nodes and lymphoid tissues associated with the mucosa: MALT (Mucose associated lymphoid tissue). The secondary lymphoid organs provide the architecture to control the cellular cooperation required for the activation of the adaptive immune response. Mature lymphocytes circulate between lymphoid organs searching for their cognate antigen. The T cells reside in the paracortex where DCs charged with antigen from drained tissue circulate. T cell priming will allow some T cells penetrate to adjacent B cell follicles where in conjunction with follicular DC expressing native antigen. Germinal centers may be induced to initiate the humoral response.

The spleen is the most voluminous secondary lymphoid organ. The structure of the spleen is such that it is divided into two compartments: the red pulp, which represents 99% of its volume, is rich in macrophages and serves mainly for the degradation of red blood cells; the white pulp, located around the arterioles, is full of lymphoid cells. It is in the white pulp that the adaptive immune response can be initiated. It is composed of distinct zones for B cells and T cells, which are surrounded by the marginal zone - a region that contains subsets of macrophages and B cells. While blood flows freely through the marginal zone, the white pulp is excluded from the bloodstream, and specific signals are required to enter it. This allows the spleen to mount the adaptive immune response and effectively remove pathogens from the blood [18].
Lymph nodes are formed by chains of lymph nodes connected to lymphatic vessels. They are at the crossroads of the haemolymphatic circulation. Lymphoid follicles, rich in B cells, are present in the cortical zone and the paracortical zone contains mainly T cells. Of particular interest are the deep cervical lymph nodes which interact with meningeal lymphatic vessels as mentioned above.

2. Leukocytes and myeloids cells

Leukocytes are divided into two major lineages: lymphoid and myeloid.
The lymphoid lineage is composed of:

- $CD4^+$ helper T cells essential for the coordination of the humoral and cellular response and the maintenance of immune tolerance.
- cytotoxic $CD8^+$ T cells essential for lysis of infected cells and immunity to cancer.
- B lymphocytes which produce antibodies responsible for humoral immunity.

The lymphoid compartment is also composed of innate cells, indeed, Natural killer cells (NK cells) and γδ T cells are cytotoxic lymphocytes that stand at the interface of innate and adaptive immunity. They constitute a first line of defense against infection and malignant tumors. The myeloid lineage is composed of innate cells capable of phagocyting and presenting antigen:

monocytes, macrophages and dendritic cells. Dendritic cells are essential in the initiation of the adaptive response due to their role as antigen presenting cells (APCs). The myeloid compartment is also composed of cells capable of phagocyting and secreting their granules: granulocytes (neutrophils, basophils, eosinophils) and mast cells (**Figure 3**).

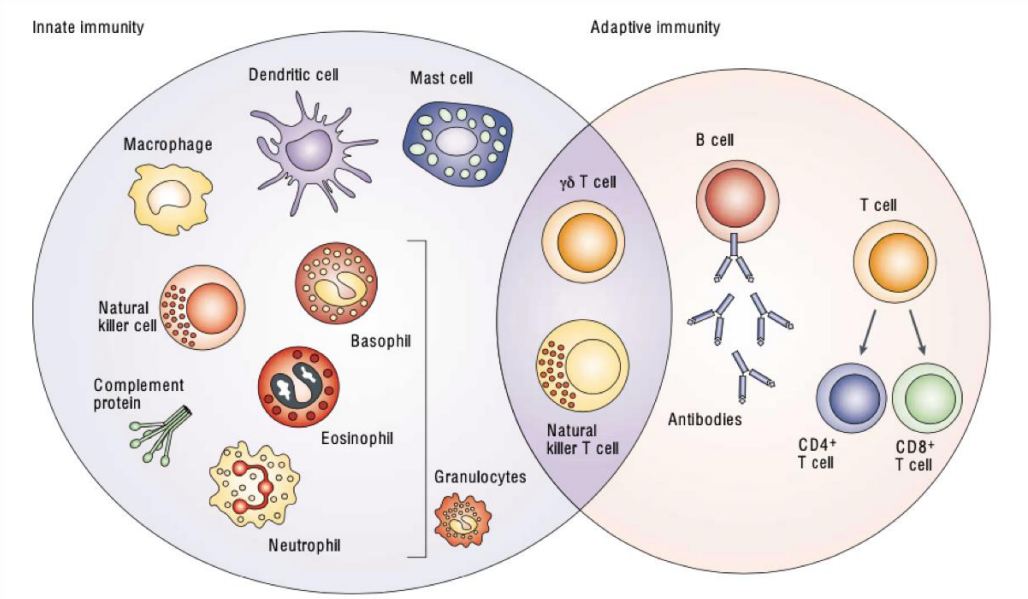

Figure 3: Cells and soluble factors involved in the innate and adaptive immune responses

(From Dranoff and al. 2004)

3. Recognition of micro-organisms

The innate immune response needs to be activated to perform its function. This is done via a number of cell and intracellular surface receptors that recognize molecular sequences. Pathogens are thus recognized via conserved receptors: PRRs (pattern recognition receptors). They recognize particular patterns present only in micro-organisms: PAMPs (pathogen-associated molecular pattern). PRRs are also able to recognize signals of cellular damage: DAMPs (damage-associated molecular pattern) which induce an immune response in case of sterile lesions. There are different types of PRRs localized between the membrane, the cytosol and the endosome to best detect pathogens. These PRRs include TLR (Toll like receptor) membrane receptors, cytosolic NLR (Nod like receptor) receptors and c-type lectin receptors (CLRs). Signaling through the PRRs activates the NLRP3 inflammasome, a multimolecular complex that promotes the maturation of the inflammatory cytokines interleukin-1β and interleukin-18, by cleaving them via activation of its caspase 1 [19]. This early activation allows granulocytes, mast cells, monocytes and dendritic cells to mount short lived effectors that constrain infection by phagocytosis, cytosolic release and secretion of toxic mediators including reactive oxygen species.

The innate immune response engages the activation of the acquired T cell response. T cell activation requires the T cell receptor (**TCR**) to recognize small antigenic peptides in the context of the major histocompatibility complex (**MHC**). This capacity to present antigen to T cells is restricted to a subset of immune cells. These antigen-presenting cell (APC) function include macrophages, mast cells, dendritic cells and B cells, but only dendritic cells can effectively prime naive T cells according to their capacity to migrate to the T cells zone and express costimulatory molecules for the activation of naïve T cells. Antigen presentation elicits a clonal T cell response that is selected from a diverse repertoires of TCRs. Peptide-MHC (**pMHC**) Recognition is mediated by determinant and complementary regions of the TCR for which the required diversity is achieved by somatic recombination of variable (v), joining (j) and diversity (d) genes, complemented by joining mechanisms [20]. TCRs are very sensitive and are thus able to discriminate pMHC complexes that differ by a single amino acid. Such structural antigenic variations alter the half-life of the TCR's association with the MHC-peptide complex within the immunological synapse, giving the TCR the ability to translate antigenic strength into a proportional activation of downstream signaling cascades. [21,22]. Contrary to the initial belief that each TCR had a unique antigenic target, it is now commonly accepted that TCRs are poly-specific [23]. This feature is essential to ensure the required diversity in the face of the almost unlimited variation of microbe-derived antigens. The disadvantage is that polyspecificity leads to an intrinsic presence of benign autoreactivity in the peripheral T cell repertoire.

In contrast to T cells, B cells recognize Ag in its native form through the BCR (*B cell receptor*). As with the TCR, diversity in the LB repertoire is ensured by recombination of the variable (v), junctional (j) and diversity (d) genes of the heavy and light chain variable domains. B cells will leave the bone marrow and enter dedicated areas in the secondary lymphoid organs. The antigen-activated B cells will differentiate into antibody-producing plasma cells. This process is controlled and conditioned by the presence of activated $CD4^+$ helper T cells. These follicular helper T cells will engage the B cells in the germinal centers.

There is a constant probability that the immune system will recognize self antigens. this is largely due to the fact that the process of TCR generation is anticipated rather than instructed. The resulting autoreactive lymphocytes might, under appropriate conditions, be able to mount an immune response against the body's structures, with potentially severe damage to self-tissues, a phenomenon known as autoimmunity. Nevertheless, the low prevalence of autoimmune diseases in the general population (3-8%) is explained by the existence of multiple active and passive mechanisms that prevent autoreactive lymphocytes from being able to initiate such a response, establishing a state of immunological tolerance towards the self.

II. Ontogeny of B cells

This thesis focuses on the role of autoreactive B cells in the pathophysiology of CNS inflammatory demyelinating diseases.

A. B lymphoiesis and B repertoire

The human B cell repertoire is 10^9 to 10^{12} different B cells that are distinguished by their BCR. However, there are 30,000 human genes and more than 10^9 different immunoglobulins (Ig) that define the B cell repertoire. This diversity is largely generated by random rearrangement of a set of gene segments that encode for regions of variability, junctions and constancy. Recombination of the gene segments is ensured by the Recombination activating Gene (**RAG**).

Lymphopoiesis takes place in the bone marrow in the periphery of the bone in endosteal niches. It begins with the common lymphoid progenitor (CLP) expressing CD34 receptor and proceeds to differentiation through the **pre-pro B stage** expressing CD79 (Ig-α/Ig-β) intra-cytoplasmic. IL-7 receptor is expressed on its surface and allows further progression to the **pro-B stage**. At this stage the cell expresses CD79 and the Stem Cell Factor (SCF) receptor produced by marrow stromal cells on its surface. This SCF stimulates further differentiation, enabling intense proliferation of the cells, which then differentiate into the **late pro-B stage**. The cells in this stage have the particularity of expressing the first specific marker of the B lineage: CD19 as well as MHC-II. So far the cell has initiated recombination of gene segments by associating a diversity gene and a junction gene during the pre-pro B stage and continues between the Pro B stage and the broad pre B stage the association between V_H and DJ_H segments. This enables cells of **large pre-B stage** to express an immunoglobulin heavy chain associated with the surrogate light chain (SLC) at their membrane. Then cells will undergo a phase of intense proliferation and move into the **small pre-B stage** and it is at this stage that the cell will begin to rearrange its light chains and will exit the bone marrow and give rise to the **naïve mature B stage**. In the naive mature B stage the cell co-expresses mature IgM with IgD associated with the co-stimulatory molecules CD79a CD79b [24] (**Figure 4**).

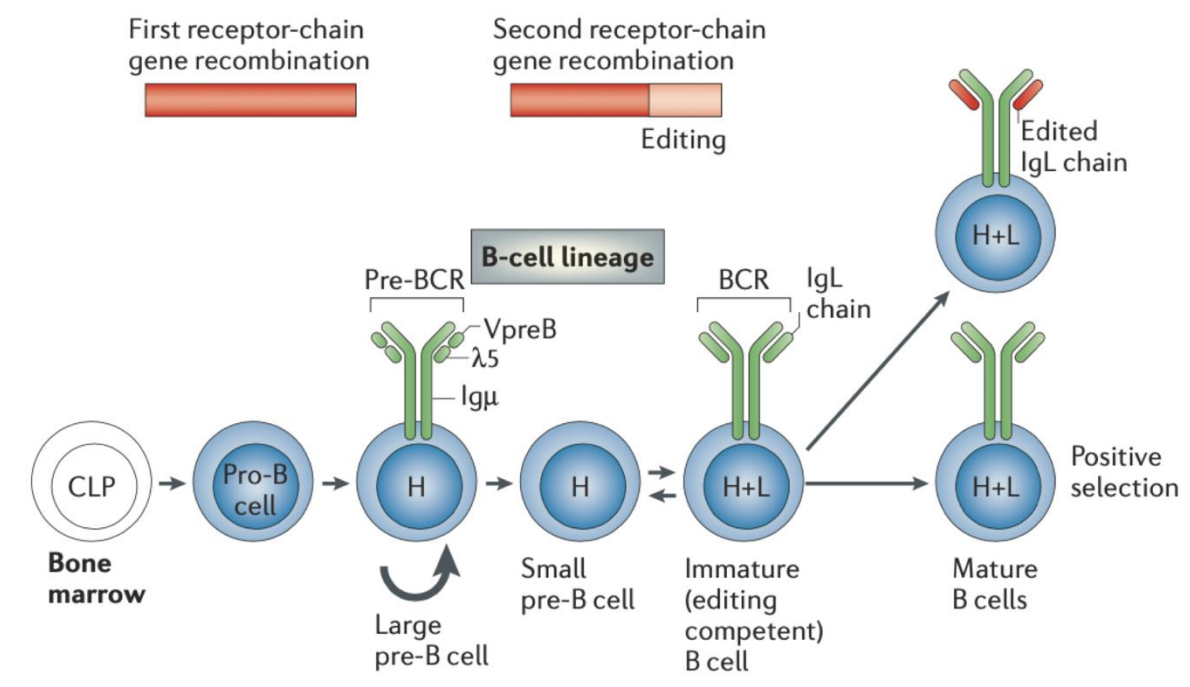

Figure 4: Schematic representation of the steps in BCR synthesis during B lymphopoiesis

(From Nimazee and al., 2006)

The loci that code for the heavy chain are located on chromosome 14 (14q32). They are organised with gene segments of variability (V), diversity (D), joining (J) and those coding for the constant part (C). The loci encoding the lambda and kappa light chains are respectively on chromosome 22 (22q11) and chromosome 2 (2p12). These chains have only diversity genes and junction genes. The process of VDJ recombination therefore takes place during lymphopoiesis and begins with the association of a diversity gene with a junction gene in a random pattern. It continues with the association of a variability segment with DJ segment and this will form the variable part of the immunoglobulin. From these two somatic recombination mechanisms, a pre-messenger RNA will be transcribed which will carry the VDJ segment joined to the constant parts thanks to alternative splicing. Such recombinations are based on a set of structures and in particular the **RSS** for recombination signal sequences which are present only at the loci coding for the heavy and light chains and the TCR genes. They are composed of one heptamer with one nonamer separated by 12 or 23 nucleotides. The RSS sequences are complementary to each other, so the combination of two RSSs results in a particular structure which is the origin of the combination of a variability gene and a joining gene. During deletion recombination, the two RSSs face each other forming a loop. Pairing of the RSS is mediated by the RAG-1/RAG-2 recombinase complex and allows the intergenic part (the loop) between the two genes undergoing recombination to be cut, and repair is achieved by the ubiquitous DNA repair complex NHEJ. If the RSS are reversed, the excision loop is retained. The VDJ rearrangement allows the creation of unique sequences that will

code for immunoglobulins but this is not sufficient to explain the variability of the repertoire. So to increase this diversity of the repertoire there are different mechanisms that come into play, what. They will intervene in particular at the time of the cuts by the RAG-1/RAG-2 complex where nucleotide deletions will be made upstream of the variability genes, downstream of the junction genes and on either side of the diversity genes. In addition, TdT (terminal deoxytransferase) will be able to insert additional nucleotides. These mechanisms are at the origin of the CDR3 hypervariable regions which constitute in part the paratope of immunoglobulin.

In summary, the diversity of the repertoire is ensured by the random combination of VDJ genes, their junctions with nucleotide breaks and additions, and the association between a heavy chain and a light chain. [25,26] (**Figure 5**).

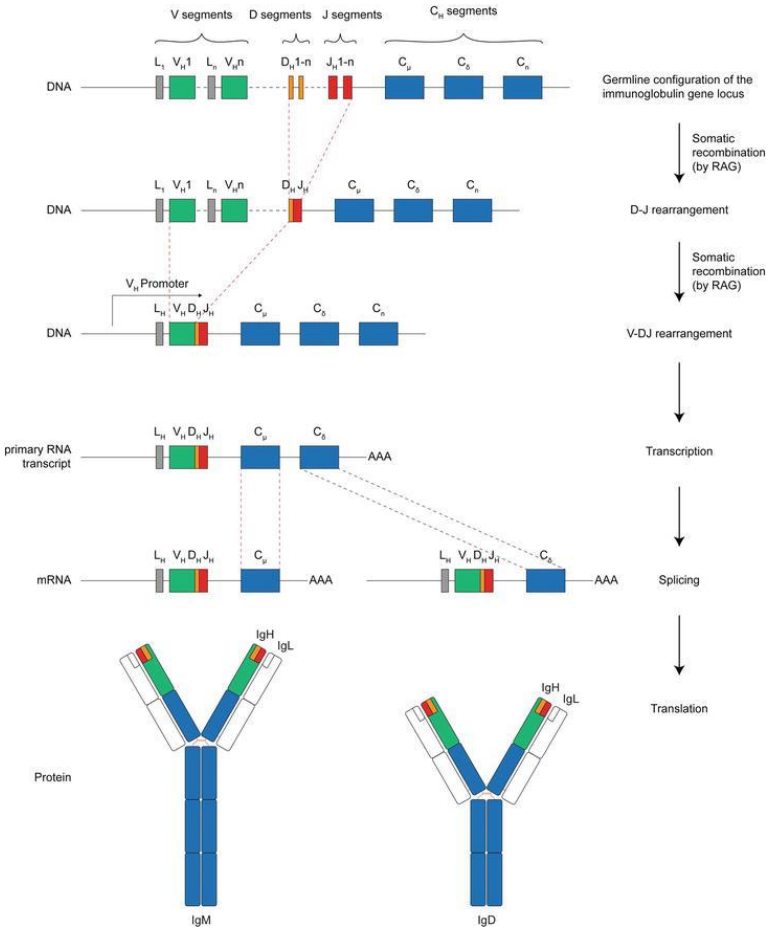

Figure 5: schematic representation of VDJ recombination

(From Backhaus and al., 2018)

B. Humoral adaptive response process

1. Initiation of the germinal center reaction

Naive mature B cells circulate in the blood stream with each clone expresses a unique BCR. The BCR is pentameric, composed of two identical heavy chains with the variable region consisting of the VDJ recombination and the constant region. Associated with two light chains consisting of a variable and a constant domain. The paratope is the antigen recognition site consisting of the variable region of the heavy and light chains. The BCR alone is not able to transduce a signal. For this, the presence of co-stimulatory molecules is essential, these are the CD79a (Ig-α) CD79b (Ig-β).

Cognate stimulation of the BCR can be provided by a conformational antigens, a linear antigen or a neoantigen created by proteolysis. The recognition of the antigen enables B cell activation, wich induces the expression of proteins that promote the survival and proliferation of the activated B cell. In addition, internalization of the BCR-antigen complex promotes the antigen-presentation capacity through MHC-II soliciting cognate interactions with $CD4^+$ helper T cells of similar specificity.

Within the secondary lymphoid organs (spleen or lymph node), T cells are located in the paracortex and B cells form discrete follicles in the cortex. These follicles form crownd follicular dendritic cells (FDCs) that *via* the production of CXCL13 chemoattract CXCR5 expressing naïve B cells. Upon antigen engagement by the BCR, the costimulatory molecules CD79a and CD79b induce a signalling cascade involving the BTK signaling protein for Brutone Tyrosine Kinase, which results in the activation of the B cell. B cell migration to the T-B follicle border driven by CCR7, CCL19 and CCL21 produced by high endothelial venules of the paracortex. Activated B cells expressing peptide-MHC (pMHC) complexes of internalized antigen screen the primed T cell response for cognate supports. Soliciting effective B-T cooperation notably through the engagement of CD40 – CD40L, ICOS-ICOSL and the absence of FAS-Ligand, will result the rapid and extensive proliferation of the stimulated B cells. This response initiates the germinal center reaction. It is at the junction between the T-zone and the B-zone that **B-T cooperation** takes place, notably through the engagement of CD40-CD40L, the expression of ICOS-ICOSL [27] (**Figure 6**).

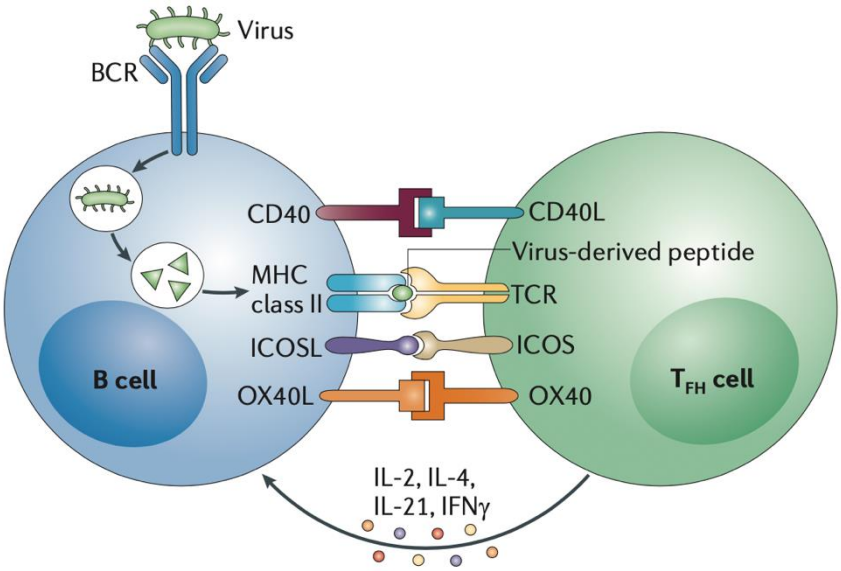

Figure 6: B-T cooperation

(Adapted from *Swain, 2012*)

Cooparation between Tfh and b cells occurs in germinal center in the junction zone between zone T and zone B

2. Germinal center reaction

Seeding of the early activated B cells in the B cells follicles form nascent Germinal center (GC). These structure can be spatially devided into **dark and light zones**. The dark zones are cellulary dense with proliferating B cells that undergo **somatic hypermutations** (SH), a process that introduces mutatiosn in the Ig CDRs with the objective of creating BCRs of higher affinity.

During the intense multiplication of lymphocytes in the dark zone, there is a multiplication of the genetic heritage of each of the cells and at the level of the genes which code the variable part of the Ig, an enzyme: **AID,** for activation-induced cytidine deaminase, will intervene and create deaminations of the cytosines which will entail their replacement by uracils. The subsequent repair randomly replaces these uracils with any other nucleotide, thus creating point mutations. Selection of affinity maturation among the somatic hypermutations B cells requires the implication of follicular dendritic cells and a dedicated T cell subset, coined follicular helper T cells (Tfh), that differentiate from the primed T cell response and migrate to the B cell follicles owing to the expression of CXCR5 [28]. SH B cells are prone to die, but increased BCR affinity results in increased pMHC epitope density augmenting competitive access to Tfh mediated survival signals. The remaining cells can be recycled to follow a new phase of proliferation and hypermutation or leave the follicle as memory B cell or plasmocyte. [29].

In parallel, isotype switching occurs, which changes the nature of the heavy chain. At the end of these steps in the clear zone, two types of cells are obtained: plasma cells that secrete antibodies and memory B cells [30,31] (**Figure 7)**.

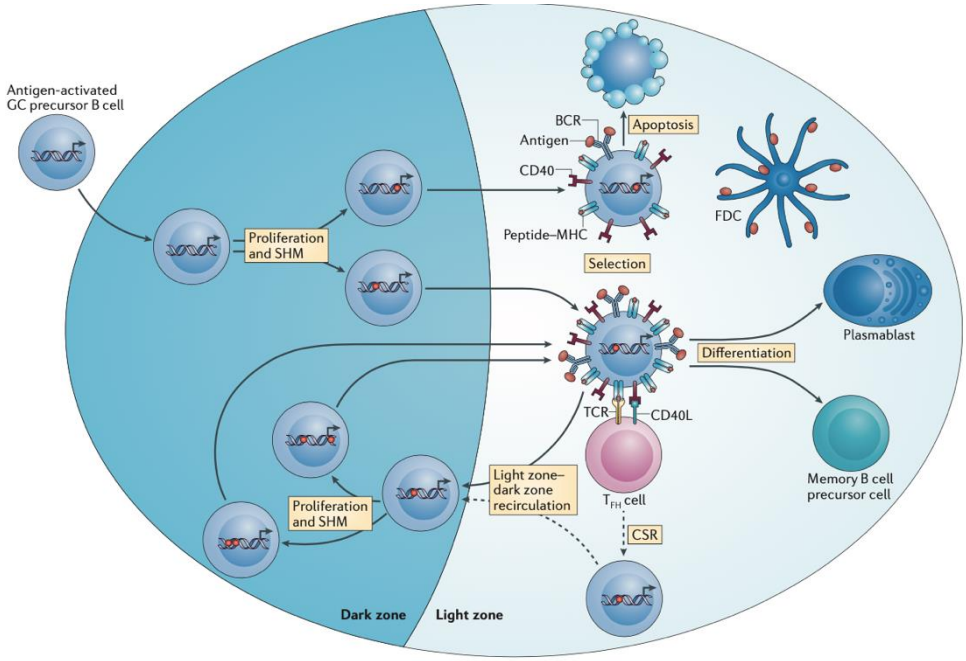

Figure 7: Dynamic of B cell in germinal centre

(From Nilushi S. De Silva and Ulf Klein, 2015)

With SHM for immunoglobulin somatic hypermutation and CSR for Class-switch recombination

3. Class-switch recombination

Class-switch recombination (CSR) changes the nature of the heavy chain associated with the variable region which is conserved. The enzyme AID is involved in this process. Cytokines produced by the T follicular helper lymphocyte (Tfh) guide the choice of the new heavy chain. The expression of ICOS on the surface of Tfh and the production of IL-21 are important for the entry of the B cell into isotypic switching. B cell will stop expressing its Ig and will enter a phase of rearrangement of the constant parts.It is the type of cytokines produced by Tfh that guide the switch: for example the production of IL-4 allows switching to IgE or Ig4 ; la production de TGFβ production lead to the switching to IgA [32].

CSR is essential for an optimal immune response by allowing the synthesis by B cells of the Ig whose isotype is most adapted to the antigen encountered. Indeed, antibodies (Abs) exert their function by binding their crystallizable fragment (Fc) to distinct Fc receptors and to complement. For IgG, this tightly regulated process relies on the structural heterogeneity of the Ig-Fc domain that results from differences in affinity between the four subclasses (IgG1, IgG2, IgG3 and IgG4).

4. Extra follicular activation and follicular kinetics

A response can be made in the absence of persistent B-T cooperation. This is the extra follicular response. The differentiation of these B cells takes place outside the GC in the T-zone. This leads to the differentiation of these cells into short-lived plasma cells. These plasma cells are generated more rapidly than those leaving the GC, but provide a critical first birth of antibodies to neutralize the encountered infection. These plasma cells did not undergo somatic hypermutation or class switch recombination, thereby products low affinity IgM antibodies.

III. Tolerance and autoimmune diseases

A. Structure and function of the T cell receptor

Antigen-presentation and clonal selection are central to efficient immunity. These processes require MHC-restriction, and a clonal TCR repertoire adapted to different lineages/subsets.

1. Structure of the T cell receptor

The T cell receptor is a disulfide-linked heterodimer of two distinct TCR chains. The large majority of conventional lymphocytes T express an α chain paired with a β chain (95%), the remaining minority a γ and δ chain. $\alpha\beta$ T cells express a highly diverse TCR repertoire that is restricted to either conventional or non-conventional MHC molecules. The diversity of the $\gamma\delta$ TCRs is more restrained, can be engaged by antigens independently of MHC-restriction, and are suggested to react to stress-induced antigen-modifications. Each chain of the TCR has a distal variable domain and a proximal constant domain which prolongs to a transmembrane portion followed by an intracytoplasmic domain. In order to translate TCR engagement into T cell activation the TCR is associated with the signal transduction module; the CD3 complex. This complex is composed of four molecules of the immunoglobulin superfamily forming an extracellular domain on either side of the TCR and divided into two heterodimers γ/ε and δ/ε. It is also composed of a dimer ζ/ζ or ζ/η which is situated between the two TCR chains and a long intracellular domain containing 6 activation motifs ITAM (Immunoreceptor Tyrosine Activating Motif). The other CD3 chains provide an additional 4 ITAM motifs [33,34].

Similar to the BCR, the diversity of the TCR repertoire results from three main mechanisms: combinatorial diversity, junctional diversity and pairing diversity of the two chains forming the TCR. The TCR gene segments are located in man on chromosome 14 for the α and δ chains and on chromosome 7 for the β and γ chains. The β and δ chains comprise variability (V), diversity (D), and joining (J) segments while the α and γ chains comprise only V and J segments. On either side of these segments are the **RSS** for recombination signal sequence which are recognized by the V(D)J recombinase, and enzymatic complex containing **RAG** (Recombination Activating Gene) 1 and 2 enzymes in combination with double strand DNA repair proteins. The ensuing combinatorial diversity is explained by the number of possible combinations during the assembly of VDJ segments. The junctional diversity is responsible for most of the diversity of the TCR repertoire, with the intervention of the Artemis protein, which is capable of making sharp or offset cuts. This random process is estimated to generate a theoretical 10^{15} distinct TCRs [35,36]. The number of T cells in the human body is however limited to 10^{12} comprising roughly 10^{8} distinct TCR clonotypes. If TCRs were to be mono-specific this diversity is largely insufficient to provide effective coverage to the estimated

$1.6*10^{16}$ theroretical 14-mer peptides able to bind the host MHC (estimated at 1%). This reiterates the importance of **TCR polyspecificity** stipulating that each TCR may recognize a broad arrays of epitopes, yet this remains specific as TCR will recognize only a minute fraction of the presentable epitopes estimated at 1 in 10^{10}. The polyspecificity is explained by multiple different mechanisms, including conservation of TCR contact residues, molecular mimicry, conservation of the antigenic landscape of pMHC molecules. This increases the breath of an individual's T cell repertoire at the cost of increasing TCR autoreactivity.

2. Structure of the MHC molecules

Located on chromosome 6 in man and 17 in mice, the locus encoding the major histocompatibility complex is polygenic and highly polymorphic. Class I MHC molecules comprise a single alpha chain of three domains which is stabilised with a 12 KDa light chain subunit, β2-microglubulin. Class II MHC molecules are heterodimers of an α and β chain each containing 2 alpha domains. In man class I locus encodes HLA-A, HLA-B, HLA-C and the non-classical HLA-E and HLA-G, the class II locus encodes HLA-DQ, HLA-DR, HLA-DP. The murine locus for class I encodes H-2L, H2-D, and H-2K, the class II locus comprises H2-IE and H2-IA.

The source of peptides that are presented on MHC molecules differs. MHC-II molecules are only present on antigen-presenting cells which specialise in phagocytosing extracellular proteins to be endocytosed, digested in lysosomes, before pMHC-II antigen-loading. The co-receptor CD4 binds MHC-II to stabilise TCR-MHC interactions and initiate CD3 signalling by juxtaposting the LCK kinase bound to its intracellular domain. T cells expressing CD4 are coined “helper” T cells as they owing to their role in activating MHC-II myeloid cells or B cells conditional to the presentation of cognate antigen. MHC-I is expressed on all nucleated cells and presents antigen derived from endogenous cytosolic proteins. In case of infection pMHC-I expressing cells solicit elimination by cytotoxic T lymphocytes. This is associated with the expression of the CD8 co-receptor that similar to its CD4 counterpart juxtaposes the LCK kinase proximate to the CD3 ITAMs.

MHC haplotypes are among the strongest genetic factors determining immune efficacy in health and disease. The reason is that the MHC binding grooves are polymorphic and impact on the epitope repertoire available for antigen-presentation. The peptide binding grooves in both the class I and II complexes is structured with two elongated α-helices that astride a floor formed by a seven-stranded β -sheet. Within this structure binding-pockets favour interaction with defined amino-acid side-chains present in the epitope backbone. The biochemical nature of these pockets therefore defines the binding-motif required for epitopes to stably integrate the MHC binding groove. Of note is that the class-I binding groove maintains a closed formation

limiting presentation of 8 to 10-mer epitopes. The MHC-II binding groove, that arises from the α and β strains remains open allowing binding of epitopes that vary in length.
Additional non-conventional MHC molecules exist including CD1d, able to present glycolipids to invariants NKT cells or the non-polymorphic MHC MR1 able to bind microbial vitamin B metabolites to mucosal associated invariant T cells (MAIT).

B. T cell ontogeny

T cells develop in the thymus where signaling events triggered by the T cell receptor control TCR selection, MHC-restriction, and T cell lineage commitment.

1. Stages of thymic T cell maturation

As illustrated in Figure 8, lymphoid progenitors enter the thymus from the blood stream via the cortical-medullary junctions owing to the expression of the homing receptor CCR9. Cytokine release by epithelial cells in the cortex, including SCF, IL-7 and Notch-1 ligands ensure the survival and early differentiation of the progenitors. Expression of the stem cell growth factor receptor (CD117) indicates their differentiation into early thymic progenitors (ETP). These first stage precursors (CD44+CD25-) are negative for both co-receptors ($CD4^-CD8^-$) and remain pluripotent able to differentiate into DCs, NK cells and macrophages in addition to T cells. Subsequent maturation stages of the DN stage can be divided four subpopulations based on expression of CD44 and CD25: CD44+CD25- (DN1), CD44+CD25+ (DN2), CD44-CD25+ (DN3) and CD44-CD25-(DN4) (**Figure 8)**. Notch1 receptor signaling transitions DN1 ETP precursors into DN2a during which the precursor cells lose their pluripotency in favor of T cell engagement. Progression towards the DN2b stage coincides with the induction of RAG1 expression and gradually increasing levels of the pre-TCRα. At this stage the γδ and β loci will compete for functional rearrangement, the success of which will govern αβ or γδ commitment. The very large majority of DN2a thymocytes will commit to the αβ lineage. TCR signalling induced by a successfully rearranged TCRβ chain complexed with the pre-TCRα indicates the end of the DN3a stage in addition to 2 important outcomes. β-selection will signal the rearrangement of the α chain locus causing the irreversible excision of the δ locus from the genome, which can be detected as T-cell Receptor Excision Circles (TREC) in the cytoplasm. Second, the rearrangement and expression of the alternative β chain allele is halted, a process known as allelic exclusion. This process critically abolishes the possibility of expressing two distinct β chains within the same T cell. TCR α chains are not subjected to a similar mechanism permitting a minority of peripheral T cells to express a dual TCR, both comprising the same β chain but each associated with a distinct, successfully rearranged α chain.

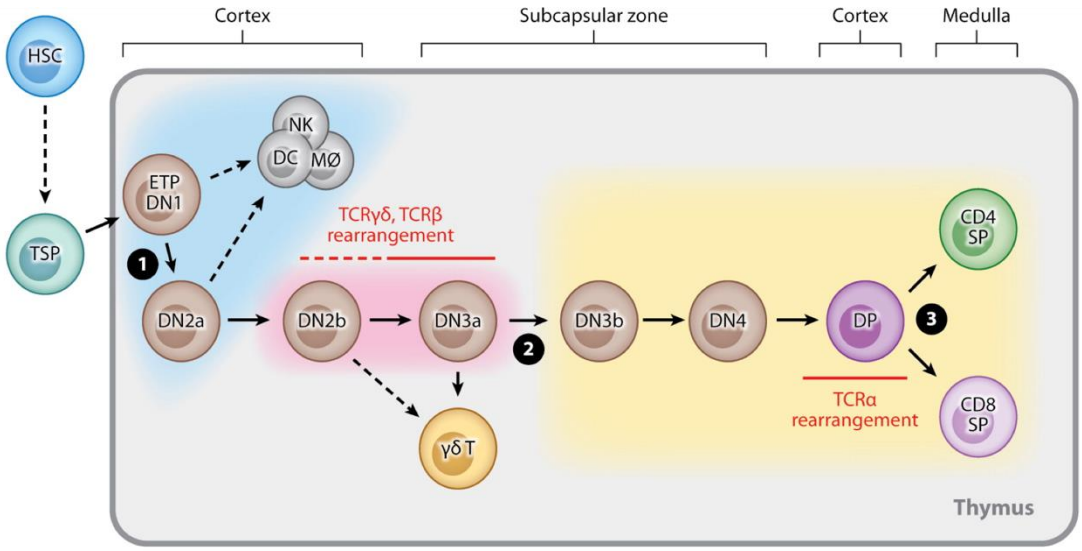

Figure 8: Overview of thymocytes development

(From Koch and Radtke, 2011)

This diagram describes the main stages of T cell maturation in the thymus. T cell progenitors derived from hematopoietic stem cells migrate from the bone marrow to enter the thymus in the cortical zone and migrate towards the medullary zone where the central clonal selection steps take place. Distinct thymocyte stages are defined: CD4-CD8- double negative (DN), CD4+CD8+ double positive (DP) and CD4+CD8- or CD4-CD8+ single-positive (SP). CD44 and CD25 denote four major subpopulations of DN cells: $CD44^{+}CD25^{-}$ (DN1), $CD44^{+}CD25^{+}$ (DN2), $CD44^{-}CD25^{+}$ (DN3) and $CD44^{-}CD25^{-}$(DN4).
Critical checkpoints during early thymocyte development are indicated by the circled numbers. Their key steps are framed by different colours: 1 - the DN1 checkpoint (blue shading), 2 - the β selection checkpoint (pink shading), 3 - the positive and negative selection checkpoint (yellow shading).

2. Positive selection

Triggering of the pre-TCR complex signals survival and expansion of the DN3b thymocytes and their Notch1 dependent maturation to the DN4 stage. Migration from the subcapsular zone to the cortex, the anatomical site that will instruct the selection of thymocytes expressing a functional αβ TCR. Positive selection ensures restriction to the MHC of the host, a feature that is crucial to limit TCR activation solely by antigens presented in the context of MHC. In the periphery self-antigen pMHC complexes maintain T cell homeostasis by providing basal TCR tickling. Second, positive selection will also affirm compatibility between MHC restriction and co-receptor compatibility. This is why positive selection impacts on double-positive (DP) thymocytes that arise from DN4 thymocytes by upregulating the CD4 and CD8 co-receptors. The DP thymocytes strongly express RAG1 and RAG2 nucleases required for the rearrangement of the Vα and Jα segments in order to generate a functional TCRα chain able to combine with the selected TCR β chain. DP thymocytes are prone to die due to their downmodulation of the IL-7 receptor and low-expression of the Bcl-2 survival factor. In the absence of selection the DP thymocytes will die of neglect. In order to survive, DP thymocytes

inspect pMHC complexes expressed on cortical thymic epithelial cells (cTECs) which express high levels of MHC I and MHC II molecules complexed with endogenous self-peptides. Cognate TCR recognition of sufficient strength rescues the DP thymocyte and induces the CCR7 chemokine receptor allowing the migration to the thymic medulla.

3. CD4 versus CD8 lineage commitment

At the end of positive selection the high expression of the TCR $\alpha\beta$ enables DP thymocytes to commit to the CD4 and CD8 single-positive (SP) lineages. Lineage commitment is instructed. A default reduction of CD8 expression creates $CD4^{hi}CD8^{lo}$ thymocytes that are interrogated at this stage. In the case of productive MHC II interaction the stabilization and signal transduction afforded by the CD4 co-receptor permits sustained TCR signalling driving GATA-3 and Th-POK transcription. The transcription factor Th-POK is sufficient to engage CD4 lineage commitment. CD8 lineage commitment has similarities to a default pathway. In the case of MHC I binding the reduced CD8 co-receptor expression fails to stabilise or potentiate the interaction. But TCR engaged combined with IL-7R signalling driven by stromal cell secreted Il-7 favor survival and drive the transcription factor Runx3 which antagonizes Th-POK. CD8 lineage commitment ensues [37,38].

4. Negative selection and central tolerance

The importance of negative selection, which purges thymocytes with high affinity for self pMHC complexes, is intuitive given that tolerance to self is vital. The rigours of negative selection are encountered upon migration of the positively selected thymocytes to the thymic medulla. At the cortico-medullary junction the large majority of thymocytes will be purged. This process is driven by the promiscuous expression of tissue specific self-antigens by medullary thymic epithelial cells (mTEC). Transfer of antigen from mTECs to adjacent DCs provides the myeloid cells with the scaffold to interrogate thymocytes for TCRs specific for ubiquitous and tissue-specific self-antigens expressed by the organism. It is through this mechanism that negative selection takes place: thymocytes that recognize MHC-peptide complexes of self with high avidity are eliminated from the repertoire [39].

This central elimination of self-reactive thymocytes is a major step in the selection of a peripheral T repertoire with controlled self-reactivity. The expression of two transcription factors in mTECs are critical for this process: **AIRE** (autoimmune regulatory element) and the FEZF-2 (Family Zinc finger - 2). The absence of either results in APACED (autoimmune polyendocrinopathy candidiasis ectodermal dystrophy) or severe autoimmunity, respectively. The AIRE transcription factor allows mTECs to mirror the proteome of self-antigens present

within the organism. AIRE functions by loosening epigenetic regulation by targeting regions of inactive chromatin leading to low-level expression of hundreds of genes in a terminally differentiated cell type devoid of the transcription factors and chromatin configurations that regulate transcription of the respective genes in tissue cells [40,41].

5. FoxP3 regulatory T cells

Central tolerance is not only achieved through recessive mechanisms. Dominant mechanisms relying on the induction of T cells able to restrain immune responses in order to prevent immune pathology and autoimmunity also find their ontogeny in the thymus. Natural regulatory T cells (nTregs), as opposed to induced Tregs (iTregs), originate from the thymus where they differentiate at the HSA^+CD4^+ SP stage from thymocytes expressing a TCR with high avidity for self-pMHC complexes. The transcriptional program determining the differentiation of Tregs is controlled by the nuclear factor Foxp3. Genetic perturbation of the gene encoding Foxp3 causes the IPEX syndrome in humans (X-linked immunoregulation, polyendocrinopathy and enteropathy syndrome) a rare multiorgan autoimmune disease [40]. Immune tolerance is therefore achieved by eliminating self-reactive T cells and inducing $FoxP3^+$ Treg. The relative contribution of these two mechanisms depends on the expression profile of the self-antigen. Indeed, ubiquitous proteins will impose a dominant negative selection due to their high expression in thymus. In contrast, AIRE driven expression of tissue-specific antigens, will drive elimination of the highest-avidity thymocytes, but moderate avidity result in an equilibrated output of FoxP3 Tregs and conventional T cells (Tconv) [42].

Within the secondary lymphoid organs Treg cumulate in the lymph nodes that drain their cognate self-antigen. Comparison of the repertoires of Tregs and conventional $TCD4^+$ cells shows that there is little overlap between the two repertoires and that Tregs have a high percentage of TCRs recognizing self-antigens, while conventional T cells have almost none [43]. Functionally, Tregs exert their guardian role via multiple mechanisms. Tregs can interfere with inflammation via the production of immunosuppressive cytokines such as IL-10, TGFβ and IL-35. Tregs can starve effector T cells from their growth factor Il-2 owing to their constitutive expression of the high-affinity IL-2 receptor (CD25). Treg control dendritic cell activation. The expression of CTLA-4, a ligand for CD80 and CD86 with higher affinity as CD28, allows Tregs to interfere with the co-stimulatory pathway of APCs. Stimulation of CD80/CD86 by CTLA-4 drives the expression of IDO (indolamine 2,3 dioxygénase) by DCs. This enzyme catabolizes tryptophan into kynurenine, this deprives T cells from this essential amino acid while kynurenine refrains T cells proliferation and promotes cell apoptosis. Some Tregs have been ascribed as cytotoxic to effector T cells and activated APCs owing to their release of granzymes and perforin. Strikingly, Tregs optimize their intervention by co-expressing transcription factors involved in effector T cell polarization (T-bet, RORγt, Gata3)

leading to co-migration and co-localisation of effector T cells and Tregs at the site of inflammation [44,45].

6. Activation and Lineage of T cell subpopulations

a) T cell activation

After thymic egress mature naïve T cells patrol through the secondary lymphoid organs [46]. Within the T cell zones these resting T cells screen dendritic cells for the presentation of cognate antigens. The activation of naïve T cells requires three complementary signals. TCR triggering via pMHC complexes, co-stimulation via co-receptors and their ligands and the presence of cytokines for effector orientation.

The primary signal for T cell activation is mediated by the TCR upon cognate engagement of the pMHC complex. In order to stabilise this interaction between T cells and APCs the binding of mutual adhesion molecules allows the formation of the immunological synapse. The supra molecular activation cluster (SMAC) creates a specialized contact area between the membranes of the T cell and APC. Within this area three functionally distinct segments can be identified. The central SMAC (cSMAC) concentrates the TCR, the CD4/CD8 co-receptors and the co-stimulatory molecules. The peripheral SMAC (pSMAC) encircles the cSMAC and contains larger adhesion molecules LFA-1 the ligand of ICAM-1 stabilises the cSMAC. Beyond the pSMAC lies the distal SMAC (dSMAC) which contains large molecules able to inactivate the TCR signaling complex, such as the CD45 phosphatase. This structurally controlled interaction is essential as it clusters the TCR signaling machinery. Moreover, it guards the sensitivity of the TCR allowing quantitative differences in TCR signaling strength to reflect epitope variations of as little as one amino acid. In conjunction with co-stimulation afforded by co-stimulatory molecules induced on activated APCs a number of signaling cascades is induced proportional to TCR signaling strength. Phosphorylation of the CD3 ITAMs is initiated by the Src kinase Lck bound to the intracellular domain of the CD4 and CD8 co-receptors. ZAP-70 docks to the phosphorylated ITAMS via its SH2 domains and is itself phosphorylated by Lck. Phosphorylated ZAP-70 phosphorylates the adapter proteins LAT and SLP76. This scaffold allows for the recruitment of a variety of other signaling molecules including Phospholipase C gamma 1 (PLCγ1), growth factor receptor-bound protein 2 (Grb-2) and its related adapter proteins (GAD). PLCγ1 is critical for the induction of the calcium flux that is initiated by the hydrolysis of phophatidylinocytol (4,5)-biphosphate to inositol 1,4,5-triphosphate (IP3) and diacylglycerol (DAG). Binding of IP3 to its endoplasmic reticulum membrane receptor mobilises the calcium flux. Other distal signalling pathways include the mitogen-activated protein kinases (MAPK). Driven by the kinase ERK (extracellular signal-regulated protein kinase) this pathway is associated with cytokine release, cell proliferation by activating the transcription factors AP1, which complexed with NFAT regulates cytokines

including IL-2, IL-4 and IFNγ. The PKC/NFκB pathway is critical for cytokine expression by genes harbouring the NFκB DNA-binding sites, of which TNFα is a critical example. Lastly, the PI3K/AKT/mTOR pathway regulates cellular processes including metabolism, and cell survival via, for instance, the induction of FOXO1.

Activation of T cells modifies the expression of molecules at it's cell surface. The receptors retaining T cells in the secondary lymphoid organs like CD62L and CCR7 are downmodulated. Temporal retention in the T cell zones is maintained by the transient expression of CD69. Activated T cells induce expression of the high affinity IL2-receptor (CD25) to drive T cell proliferation by autocrine IL-2 production. CD44 is expressed to serve as a retention receptor at sites of inflammation and their migration is towards inflammatory sites requires LFA-1 and VLA-4.

b) Effector $CD4^+$ T cell subpopulations

The $CD4^+$ T cell response has evolved different effector arms required for the efficient neutralization of different pathogens. TCR signal strength and the cytokine milieu provided by TLR stimulated APCs dictate the differentiation of the distinct T cell subsets which is established by the action of dedicated transcription factors. Reciprocal regulation affirms T cell differentiation in that the expression of subset specific factors antagonizes the differentiation into alternative subsets. The three main effector subpopulations are Th1, Th2 and Th17 characterised by specific cytokine profiles (**Figure 9**).

(1) Th1 differentiation and characteristics:

Th1 is involved in the eradication of intracellular pathogens such as viruses or bacteria. These pathogens drive the release of IL-12 by DCs which triggers STAT-4 expression in T cells upon engagement of the IL-12 receptor. STAT-4 drives the expression of the hallmark effector cytokine IFN-γ [47]. The master regulator of the Th1 phenotype, T-bet, is induced by autocrine IFN-γ activity promoting STAT-1 phosphorylation. IFN-γ is a critical effector cytokine that in conjunction with CD40L instructs macrophages to kill engulfed pathogens. It instructs isotype switching of the humoral response, as has been discussed in "**Ontogeny of B cells**". Critically for immunity for viral infections, IFN-γ stimulates host cells to increase pMHC I expression eliciting the protective function of the cytotoxic CD8 T cell response.

(2) Th2 differentiation and characteristics

-4 is produced by basophils and has as such been indicated to serve as primary source for the differentiation of Th2 cells. This CD4 T cells subset is mobilized to eliminate extracellular pathogens such as intestinal parasites or toxoplasma. IL-4 receptor signaling activates STAT-6 which amplifies IL-4 synthesis and induces the expression of the master regulator GATA-3. GATA-3 programs Th2 cells to produce secrete IL-5 and IL-13, in addition to IL-4. IL-5 enables differentiation, activation and recruitment of eosinophils. IL-13 and IL-4 promote differentiation of B cells into IgE-producing plasma cells. IgE has a prominent role in mast cell degranulation [48].

(3) Th17 differentiation and characteristics

Th17 cells were discovered in experimental autoimmune encephalomyelitis (EAE) owing to the discrepancy that mice deficient in the IL-12 subunit p40 were resistant to EAE whereas mice deficient in P35 were not. This was due to the effect of the IL-23 cytokine that shares the p40 subunit with IL-12. This cytokine pairs p40 with p19, which when genetically inactivated also conferred resistance to EAE. Stimulating effector memory T cells with IL-23 identified IL-17A, IL-17F and IL-21 as their hallmark cytokine. These Th17 cells have since been demonstrated as essential in the defense against bacteria and fungi, as they locate at mucosal surfaces. Th17 differentiation is initiated by the cytokines IL-6 and TGF-β, boosted by IL-1β. This induces IL-21 that drives STAT-3 activation which in turn drives expression of the master regulator RORγt as well as the expression of the IL-23 receptor. IL-23 stimulation permits terminal differentiation of the Th17 subset [49]. The effector cytokine IL-17 allows the efficient recruitment of neutrophilic granulocytes to sites of infection.

Other subsets include Th9 cells which are related to Th2 cells in that they require the GATA-3 master regulator. They are differentiated by IL-4 and TGF-β and are implicated in immunity against helminth infections and tumors. Th22 cells are related to Th17 cells in that they are mobilized during mucosal immunity. IL-22 requires the aryl hydrocarbon receptor (AhR) and STAT-3. Their differentiation requires IL-6, IL-23, IL-1β, FICZ, a TGFβ receptor inhibitor and absence of IFNγ and IL-17.

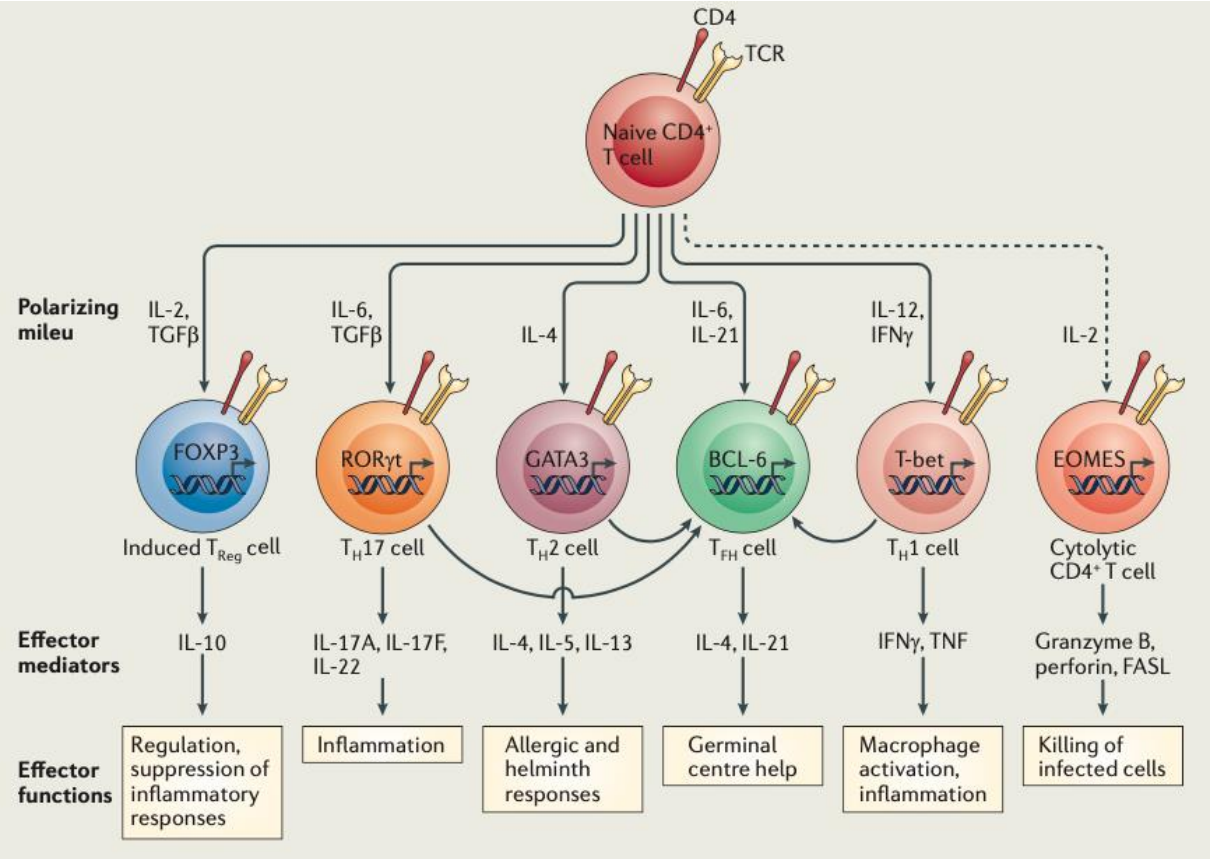

Figure 9: Different subpopulations of CD4⁺ T cell

(From *Swain, 2012*)

c) Cytotoxic CD8 T cells

The cytotoxic adaptive response mainly involves CD8 T cells but other lymphocyte populations are also involved such as Tγδ and more rarely Th1. CD8 T cell activation requires pMHC-I activation in conjunction with co-stimulation. Their survival and function can be modulated by Il-7, IL-15 and IL-18. CD8 T cell priming requires the licensing of DCs by effector CD4+ T cells of similar specificity. Antigen-presentation by licensed DCs, concomitant with IL-2, IL-12 and IL-21 optimize the priming of cytotoxic CD8 T cells. Cytotoxic CD8 T cells require T-bet for the type 1 phenotype and Eomes for their cytotoxic activity.

Mature cytotoxic CD8 T cells are critical effectors to control viral infection and tumor elimination. These CTLs lyse target cells in an antigen-driven manner using three possible pathways: the secretion of cytokines with anti-microbial activity that include IFNγ and TNFα, the exocytosis of lytic granules oriented by the immune synapse: perforin and granzymes; the Fas death receptor pathway which sees pMHC-I stimulation induced Fas-L on effector CD8 T cells which in turn engages Fas on the infected target cell affording direct apoptosis.

.

C. Autoimmunity and autoimmune diseases

More than 80 autoimmune diseases (AID) have now been described. They can be systemic, such as systemic lupus erythematosus, which can affect several organs like the skin, joints, kidneys or CNS. IADs can also be organ-specific, as in type 1 diabetes affecting the pancreas. In these diseases, loss of tolerance of B or T cells is frequently implicated. Indeed the HLA locus is commonly associated with an increased risk of susceptibility to autoimmune diseases [50].

Combination of several factors (genetic, environmental or immunological) can lead to a disruption of tolerance and result in an immune response directed against the self that may result in the development of an AID. Indeed, genetic polymorphisms that influence immune checkpoints can favour the emergence of autoimmunity. Tissue damage caused by local infections has an intrinsic risk of triggering organ-specific autoimmunity once the initial infection is under control. It's the principle of **epitope spreading.** This is the case with the example of TMEV (Theiler's murine encephalomyelitis virus) infection in SJL/J mice which induces prolonged CNS demyelination. This demyelination is explained by the activation of an autoreactive T response against myelin sheath proteins.

This autoreactive response is due to the dissemination of epitopes as a result of tissue damage induced by the viral infection. APCs are indeed capable of presenting self-antigens derived from cell debris or from phagocytosis of apoptotic cells. This is not a cross-reaction between TMEV and myelin-derived antigens. CNS APCs therefore present myelin antigens 40 days after viral infection. TCD4 first targets the myelin peptide $PLP_{139-151}$ of the proteolipid protein (PLP). Later on, TCD4s specific for $PLP_{178-191}$ and PLP_{56-70} are found. Even later TCD4 specific to MOG_{92-106} another myelin component protein MOG myelin oligodencrocyte glycoprotein is found [51–53].

In addition, microorganisms frequently contain antigens that share common motifs with tissue antigens, a process known as **molecular mimicry**.

This mimicry can present a risk of autoimmunity, particularly for tissue self-antigens that have had partial negative selection. Therefore, in genetically predisposed individuals, this type of mechanism could lead to an autoimmune response. A striking example is narcolepsy induced after an infection or vaccination against H1N1. [13,14].

Another example related to the context of this thesis work is Epstein-Barr virus (EBV) infection and Multiple Sclerosis (MS). Several studies have identified EBV-infected B cells in the brains of MS patients [56,57], but the link between EBV infection and multiple sclerosis is still an unresolved issue. One of the mechanisms put forward is molecular mimicry, whereby EBV viral protein sequences mimic human myelin proteins. Indeed, isolated t cells show a cross-reaction

between MBP and EBV antigen, in particular EBV nuclear antigen 1 (EBNA-1). It has been shown that there are (**Figure 10**) :

- Serum antibodies from MS patients cross-reacting between the EBNA-$1_{411-440}$ epitope and the human chloride channel protein, anoctamine 2 (ANO2), which is associated with nerve impulses in axons [58].
- MS serum antibodies targeting EBNA-$1_{411-426}$ and self-reactive T cells cross-reacting with myelin basic protein (MBP) [59,60].
- Antibodies in the CSF of MS patients, targeting EBNA-$1_{386-405}$ residues and reacting with a cell adhesion molecule, glialCAM [61].

These studies highlight different amino acid related regions of EBNA-1 which may result in epitope spreading [62].

It should be noted that molecular mimicry is not the only suspected mechanism in the link between EBV infection and MS development. There is also transformation of B cells with latent membrane proteins: LMP2A and LMP1 which respectively mimic CD40 receptor signalling giving rise to pathogenic plasmablasts [63].

This example of EBV and MS is evidence of the complexity of autoimmune disease induction and that it is indeed multifactorial.

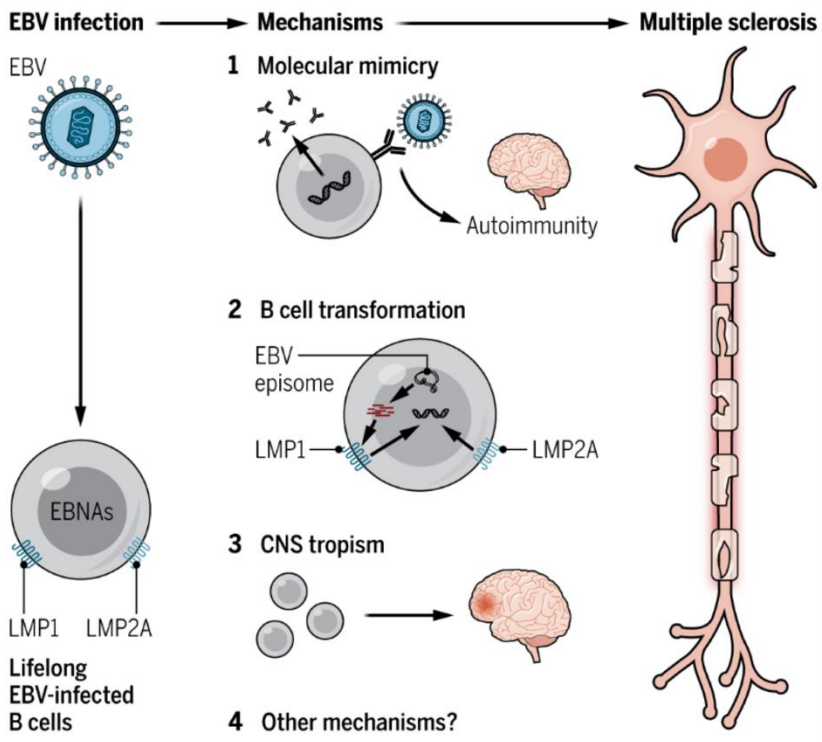

Figure 10: Epstein-Barr virus infection and Multiple Sclerosis initiation

(William H. Robinson and Lawrence Steinman, Science 2022)

IV. Demyelinating diseases of the central nervous system

This project is situated in the context of demyelinating diseases of the central nervous system which are inflammatory autoimmune diseases that affect the myelin sheath. These diseases are caused by a variety of factors: genetic, due to primary inflammatory processes such as infection or dut to autoimmune processes. However these diseases share a **causal immune response** with a true pathogen-specific targeting.

These diseases include those with an **acute course** where the immune response is interventional such as neuromyelitis optica (NMO) or acute disseminated encephalomyelitis (ADEM) ; and the one with a **chronic course** where the immune response is compartmentalised such as multiple sclerosis (MS).

The project emphasis is on MS and a subgroup of diseases derived from NMO: MOGAD for myelin oligodencrocyte associated disease.

A. Multiple sclerosis

Multiple sclerosis is a chronic inflammatory disease that affects the CNS. It is characterized by the presence of multifocal lesions of demyelination in the parenchyma.

MS has been extensively studied. Robert Carswell and Jean Cruveilhier first described in 1838 the disease by documenting their independent observation of unusual lesions of the spinal cord. It was in 1849 that Friedrich Von Frerichs described the disease's clinical symptoms: involuntary movement, ocular damage and damage to cognitive functions. And finally, it is thanks to the work of Jean Martin Charcot in 1868 that MS was considered a disease in its entirety.

1. Diagnosis of the disease

The diagnosis of MS is based on several criteria, called "McDonald's criteria" [64]. They are based on a cerebral MRI evaluation with the following criteria [65,66] (**Figure 11**):

- **Spatial dissemination criteria**: multiplicity of lesions and their location.
- **Temporal dissemination criteria**: appearance of new lesions and evolution of pre-existing lesions over time
- Presence of oligoclonal bands in the cerebrospinal fluid suggestive of the presence of intrathecal immunoglobulin G (IgG).
- On the differential diagnosis (HIV, Lyme disease, syphilis)

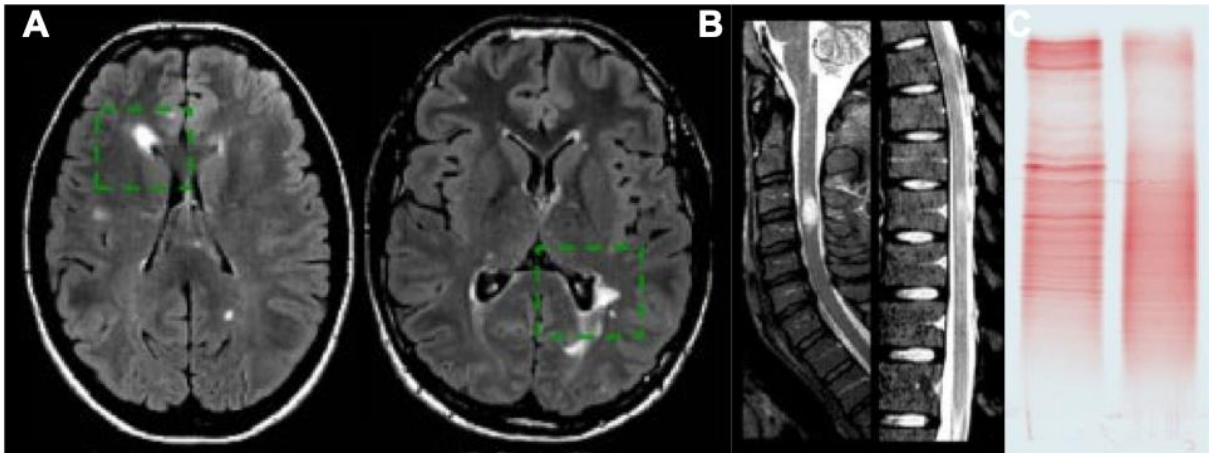

Figure 11: Illustration of the diagnostic criteria for MS

(From Filippi and al. 2019 and Compston and Coles, 2008)

Example of typical juxtacortical lesions in MS (**A**) Example of spinal cord injuries in the cervical and thoracic spine (**B**) Positive oligoclonal bands after protein electrophoresis of cerebrospinalfluid of MS patient (**C**).

The clinic of MS varies from patient to patient. There are different forms of MS. The most common form is the relapsing-remitting (**MS-RR**) form, which is found in 85% of patients. It is characterized by alternating phases of exacerbation (or relapses) and phases of remission during which there is a partial or total recovery of symptoms. In the course of time, the disease mostly develops into a secondary progressive form (**MS-SP**) characterised by significant neuronal deterioration, neurodegeneration. In 10 to 15% of patients, the disease evolves progressively from the beginning of the disease, in which case we speak of primary progressive forms (**MS-PP**). [66,67].

The specificity of the adaptive immune response in MS remains an active area of investigation. The prevailing view is that multiple antigens can be the target of the immune response in a given patient and that this profile fluctuates over time [68].

2. Pathophysiology and clinical signs

MS is characterised by more or less extensive areas of demyelination, called plaques, located in the white matter and also in the grey matter of the brain and spinal cord. The symptomatology is directly related to the topography of the lesions, and reflects their spatial and temporal dissemination. This is why the disease manifests itself differently from one person to another. The symptoms are varied and may correspond to [69] :

- **Sensory disorders**: these may be manifested by paresthesia (tingling, pins and needling), dysesthesias or by Lhermitte's sign (sensation of electric discharge in the spine when the neck is flexed).
- **Motor disorders**: these can be expressed by paralysis or muscle weakness. The patient feels a heaviness, a drop in muscle tone that can lead to difficulties in walking or balance problems.
- Physical **exhaustion**.
- Visual impairment: this is reflected in a decrease in visual acuity, which may be accompanied by orbital pain.
- **Cognitive disorders**: depression, dementia, etc.
- **Bladder and bowel disorders**

These clinical signs are often grouped under the term " relapse ".

3. Epidemiology

Multiple sclerosis is the leading cause of non-traumatic disability in young adults. The average age of onset is 30 years, although there are also pediatric forms and forms that begin after the year 50. The estimated number of people affected by MS is 2.5 million worldwide, including 1 million in Europe [70].

It is found in all regions of the world but its prevalence varies according to latitude. Indeed, several studies show that the prevalence is higher in North America and Europe, while it is lower in sub-Saharan Africa and East Asia, or higher in industrialised countries [71]. The incidence of the disease is higher in women, resulting in a higher male to female ratio [72].

4. Genetic and environmental risk factors

The MS's etiology remains unknown to this day, but a number of genetic and environmental factors are considered to be risk factors for the disease. The family prevalence of MS is 13% and the risk of recurrence within a family increases according to genetic sharing. Thus the risk in monozygotic twins is 35%, 6% in dizygotic twins and 3% in siblings [65].

Genome-wide association studies (GWAS) have identified over 200 genetic variants that predispose to MS [73]. Most of these variants code for molecules involved in the immune system. This is the case for the HLA-DRB1*1501 alleles and its associated haplotypes such as HLA-DR2 [74]. There are also genes coding for the α chains of interleukin 7 (IL-7) receptors,

for example. The risk of developing MS associated with these risk genes, especially the HLA genes, may be strongly influenced by other environmental factors such as smoking or infections [75]. Indeed, smokers with the HLA-DRB1*1501 allele have a higher risk of developing the disease (Odds Ratio 13,5 [8,1-22,6]) [76].

The natural interaction of micro-organisms with the commensal gut flora shapes the composition and differentiation of the adaptive immune response [77]. However, microbial infections have an inherent risk of inducing autoimmune inflammation. This is the case for example with: *Yersinia enterocolitica* and Basedow disease [78]. As discussed in the chapters on autoimmune diseases (III.C), infection with EBV is closely linked to MS. In their latest publication, Bjornevik et al in 2022 [56] analyzed the presence of anti-EBV antibodies in the serum of 801 MS patients from a cohort of more than 10 million people in the US military over a 20-year period. Of the 801 MS cases, 35 were initially EBV-negative, and of these 35 patients, 34 were infected with EBV before the onset of MS. EBV seropositive was therefore almost ubiquitous at MS initiation. Other studies highlight the link between EBV and MS and show that EBV infection has a higher risk of developing the disease (OR 16,03 [9,42-27,3]) [79,80]. Smoking is also an identified risk factor [81]. On the other hand, there are beneficial environmental factors such as the protective effect of vitamin D induced by sunlight [82,83].

5. Treatment and management of MS

Currently, there is no cure for MS. The disease's treatment is multidisciplinary and includes the treatment of moderate to intense attacks, long-term treatments and care of symptoms [84].

a) Treatment of MS relapses

The aim is to reduce the patient's pain during the onset of relapses. These include intravenous glucocorticoids: **Methylprednisolone**.

b) Long-term treatment

With the long term treatments, the aim is to reduce the progression of the disease. The most effective treatments for delaying the disease progression are based on two modes of action:

- Reduction of pro-inflammatory cells: we find here molecules like: **ocrelizumab** (humanized anti-CD20 monoclonal antibody inducing depletion of B cells expressing this surface antigen). The recombinant **IFN-β** (recombinant which modulates the inflammatory response). **Glatiramer acetate** (a peptide analogue of the myelin basic protein that prevents antigen presentation by APCs). The **mitoxantrone** (DNA intercalant which has an immunosuppressive effect.

- ❖ Inhibition of cell migration to the CNS: **Natalizumab** (monoclonal antibody that binds to alpha4ß1 integrin and thus block the interaction between this integrin and the molecule VCAM-1 (*Vascular Cell Adhesion Molecule*-1) which prevents diapedesis of lymphocytes across the BBB). **Fingolimod** (selective immunosuppressant that modulates sphingosine-1-phosphate receptors).

The problem with long-therm treatments is the occurrence of serious side effects such as infections due to the immunosuppressive effect of these drugs. The future objective is to develop more specific therapies to reduce adverse effects. Other therapeutic areas are also being developed, such as new therapies based on nerve fibre protection and remyelination, with the example of anti-LINGO-1 [65,85].

c) Associated treatments

The associated treatments are the symptomatic treatments due to the disease or to the undesirable effects of the basic treatments. They may or may not be medicinal and include, among other things, psychological support for the patient, functional re-education with the physiotherapist and also hygienic and dietary advice to limit as far as possible the factors that trigger relapses.

6. Fundamental Immunopathology of MS

a) Immuno-pathological mechanisms involved

The CNS infiltrate of the immune response is common to all forms of MS. The lesions found in MS are characterized by the presence of activated microglia and activated infiltrating myeloid cells in the periphery [86]. The inflammatory response is determined by the adaptive immune response including T cells [87]: Th1 $CD4^+$ T cells producing INF-γ and Th17 $CD4^+$ T cells producing IL-17 [86] and $CD8^+$ T cells [88,89]. B cells are also part of the CNS infiltrating cells [90].

In MS Recurrent-Remittent focal lesions are found. These lesions are characterized by deep astrocytic scarring, axonal loss and remyelination of various extents. In RRMS it's a dynamic. Different waves of immune cell infiltrates lead to plaque formation [66,86]. Consistent with the location of the lesions, in RRMS the immune response is prone to target neuronal antigens, including components of myelin. Autoreactivity directed against myelin contributes to the loss of oligodendrocytes and subsequent demyelination of axons. Axon damage is mediated by mitochondrial damage induced by oxidative stress generated by activated microglia leading to their hypoxia [91].

The microglia's contribution is variable. Microglia can either contribute to inflammation or promote repair by removing neuronal debris and supporting remyelination.

The disease is progressive over time and in the majority of cases, patients eventually develop a secondary progressive form (SP-MS).

Inflammation is found in both RR-MS and SP-MS. However, there are significant differences in the organisation of the immune response *in situ.*

RR-MS is a dynamic disease in which distinct waves of infiltrating immune cells cause clinical relapses of the disease. The lesions found in the white matter are active. This is associated with a degradation of the blood-brain barrier allowing macrophages and $CD8^+$ T cells to infiltrate the CNS parenchyma. In the progressive phase, the BBB remains intact and the inflammatory response is compartmentalized. The anatomy of the demyelinating lesions evolves with the development of lesions in the cortex. Lesional demyelination occurs by expansion of existing lesions, with few *de novo* lesions occurring in the white matter. Chronic neuronal damage or neurodegeneration is significant. Les lésions sont à expansion lente dans la SEP progressive. Lesions are slowly expanding in progressive MS. Active tissue damage is mainly associated with activation of pro-inflammatory microglia, recruitment of macrophages as in the dynamic RR [92,93]. Adjacent to the cortical demyelinating lesions are ectopic lymphoid follicles (ELFs) in the meninges near the brain surface [70]. These structures resemble germinal centers that promote B cells and are suspected of maintaining helper T cells and Th17 T cells (**Figure 12**). These tertiary lymphoid structures characterise the chronic and diffuse inflammatory response and are seen in progressive forms of MS [94,95]. Indeed, at this stage of the disease the inflammatory reaction is compartmentalized and functions independently of the peripheral influx of immune cells.

These pathological processes are accentuated with ageing patients [96]. Indeed, comorbidities increase with time and the mechanisms of remission diminish [97]. Persistent diffuse inflammation leads to progressive senescence of the immune system [98].

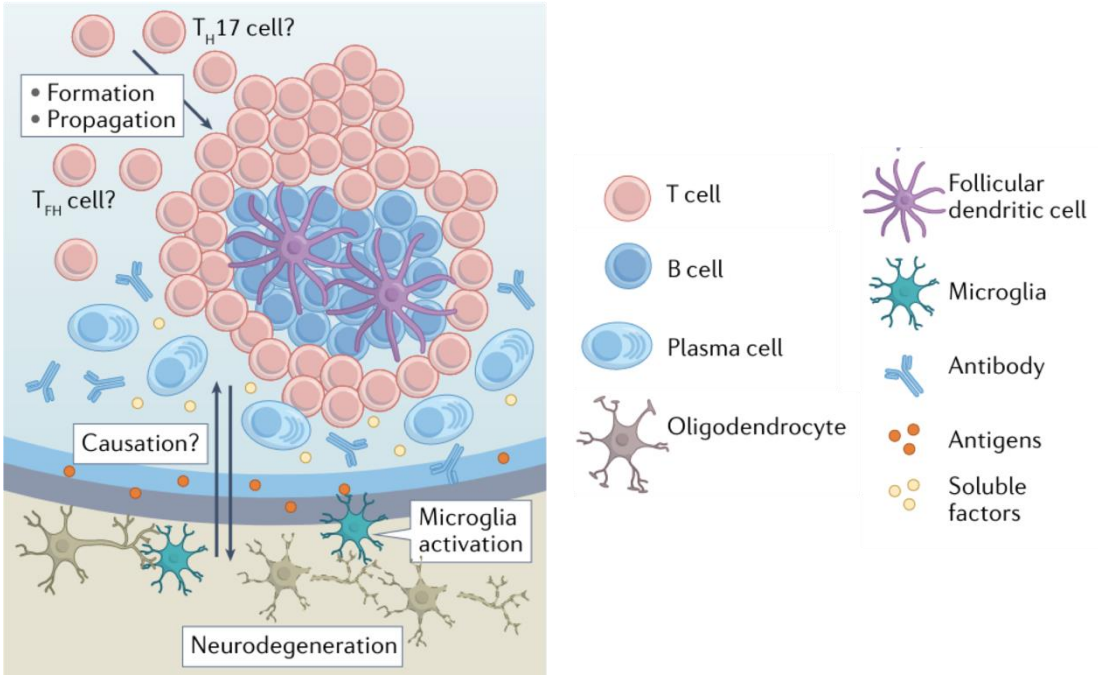

Figure 12: Representation of ectopic lymphoid follicles in the meninges

(Adapted from Attfield and al., 2022)

b) Antibody and B lymphocytes in MS pathophysiology

In the case of multiple sclerosis (MS), several lines of evidence implicate antibodies [99]. Antibody and complement deposits are frequently detected in active demyelinating lesions [87,100,101]. The presence of antibodies in cerebrospinal fluid (CSF) coincides with infiltration of plasma cells, suggesting in situ production of antibodies. This process is likely to be antigen driven since the CSF IgG proteome and CSF B cell transcriptome show shared clonotypes [102,103]. Antibody detection in CSF is pathologically relevant because patients negative for oligoclonal bands develop milder disease [104]. In addition, plasma exchange therapy, which removes soluble factors from the bloodstream, improves MS in a subset of patients [105,106]. In MS, antibody specificity is still largely debated, but the prevailing idea is that in a given patient, multiple autoantigens can be targeted by the immune response and that this profile fluctuates with disease progression. disease [68].

This cellular function of B cells has been studied using experimental models of MS with experimental autoimmune encephalopathy (EAE). Immunisation with recombinant human MOG protein (rhMOG) induces an MS-like disease in mice with a myelin-specific T and B cell response. In this model the pathogenicity of B cells is due to humoral and cellular mechanisms. Indeed, plasma cells secrete pathogenic antibodies that cause complement-dependent demyelination. In addition, they have an essential role as antigen presenting cells. This role has been demonstrated in the B cells MHC-II deficient mouse model which has been shown

to be resistant to EAE [107]. This is an unexpected result because MHC-II deficiency selectively targets the humoral response. The cellular immune response mediated by $CD4^+$ T cells and macrophages is in principle sufficient to induce a disease [108]. It turns out here that it had not been established, suggesting an indispensable role for B cells in the establishment of a cellular response through antigen presentation. Another experiment also demonstrated this cellular role independent of antibody production with mice expressing a MOG BCR specific (IgHMOG). These mice were compared with a new IgHMOG variant in which the secretion of transgenic antibodies to MOG was disabled. Both genotypes remained fully susceptible to rhMOG-induced EAE, providing strong evidence that invalidation of antibody secretion did not alter the pathogenicity of B cells in rhMOG EAE.[107].
This fundamental demonstration and the clinical efficacy of Ocrelizumab highlight B cells as mediators of inflammation. The cellular role of B cells is not yet well defined. Memory B cells may present myelin-derived peptides to T cells, resulting in pathogenic activation of T cells [109]. The worsening of MS was associated with the presence of LBs in the meninges at the level of ELFs, co-located with T cells. [94].

Other central nervous system demyelinating diseases have demonstrated a more targeted autoantibody response. Neuromyelitis Optica Spectrum Disorders (NMOSD) emerged as antibody-mediated demyelinating diseases. Patients produce antibodies against aquaporin 4 (AQP-4) or against the MOG protein. Neutralization of this humoral response by B cell depletion, complement inhibition, or blockade of IL-6 binding to its receptor has recently been shown to provide clear clinical benefit. [110,111].

B. Neuromyelitis optica and its subgroup of diseases.

Neuromyelitis Otica (NMO) is a rare disease, characterized by myelitis and optic neuritis. The history of neuromyelitis optica is related to multiple sclerosis but is less well known. Eugène Devic and Fernand Gault first described this syndrome at « Congrès français de médecine » in 1894. By grouping similar cases, they proposed to consider NMO as a disease in its own right « Ces seize cas de myélite aiguë accompagnés de névrite optique sont suffisants pour légitimer la création d'un type clinique, ou plutôt d'un syndrome auquel on pourrait donner le nom de neuro-myélite optique" [112]. However, NMO or Devic's syndrome was long considered a variant of MS. It was only in 2004 that V. Lennon and B. Weinshenker identified autoantibodies targeting aquaporin4 (**AQP4**) in a cohort of NMO patients but not in MS patients [113,114]. Aquaporin 4 is the most. numerous water channel protein of the CNS mainly expressed by astrocytes. Patients with NMO, AQP4-IgG presented other clinical signs than optic nerve or spinal cord involvement. Cerebral involvement was indeed observed with area postrema syndrome (nausea vomiting and hiccups) as an example of clinical manifestations. In addition, partial involvement of isolated myelitis or optic neuritis was demonstrated and it

was through the addition of these observations that the term NMO spectrum disorder (NMOSD) was created and in 2015 the diagnostic criteria were published : international Panel for NMO diagnosis (IPND) [115]. Thus, the concept of AQP4-negative NMOSD came to light, raising the possibility that other autoantibodies could explain similar syndromes.
Subsequent studies using cell-based assays (CBA) with a conformational **MOG** protein have resulted in the detection of anti-MOG antibodies confirming the detection of MOG-IgG in 30-70% of patients with seronegative NMOSD [116,117]. NMOSDs positive for anti-MOG antibodies are therefore referred to **MOGAD** for myelin oligodendrocyte associated diseases [118,119]. A nomenclature based on the specificity of autoantibodies has been established and a distinction is made between NMO-AQP4 and MOGAD [117].

In NMO around 80% of cases are caused by AQP4-IgG. Around the NMO-AQP4 negative there is around 10-40% of cases caused by MOG-IgG [120].

1. Epidemiology

NMO is found in all the country and all the ethnicities [121] (**Figure 13**). Several studies of the prevalence and incidence had been done but differences have emerged certainly because the disease newly described and the diagnostic criteria or more simply the test for anti-MOG or anti-AQP4 autoantibodies may differ from one study to another.

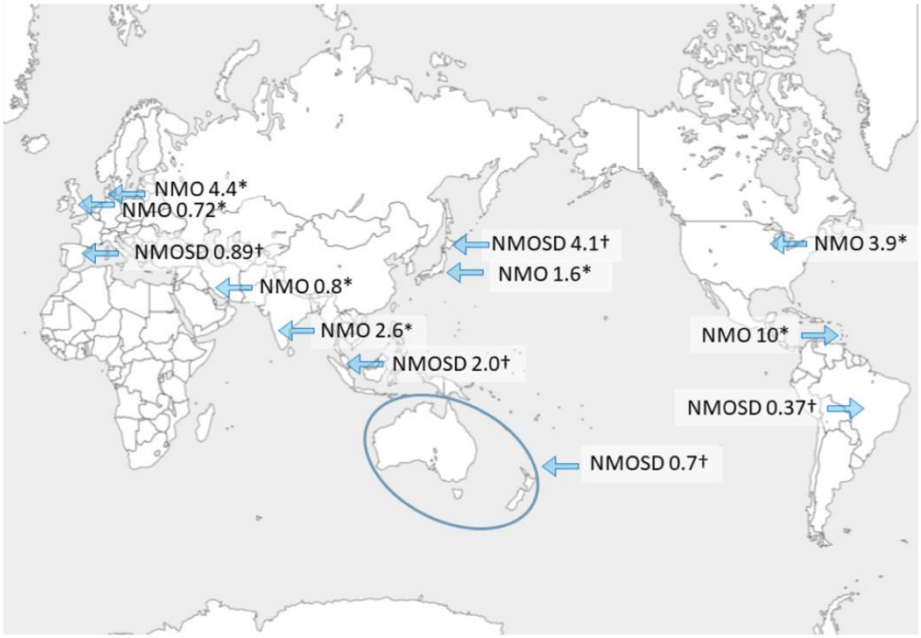

Figure 13: Prevalence of NMO worldwide with two difference diagnostic criteria

(From Masahiro Mori and al., 2018)

Prevalence with 2006 Wingerchuk diagnostic criteria for NMOSD of 2006***** or with the International consensus diagnostic criteria of 2015 **†**.

NMO can occur at any age. In NMO-AQP4 patients the median age of disease onset is 40 years. For MOGAD patients, the median age of onset is 31 years. NMO-AQP4 is more common in women than in men (female to male 8.1:1; P<0.001) [122]. The female preponderance is much less pronounced in patients with seronegative NMO and in those with MOGAD [123–125].

2. Genetic and environmental risk factors

Recent studies have been carried out on the impact of genetic and environmental factors as an example here is two studies one on the genetic impact and the other on the environmental risks:

- A study in the Dutch population investigate the link between HLA and NMO-AQP4 or MOGAD disease. They concluded that there was a difference. Indeed, they showed a strong association with HLA-A*01, -B*08, and -DRB1*03 and NMO-AQP4 patients, suggesting a role for this haplotype in the etiology of this disease. In contrast, in MOGAD, no evidence of HLA association in these disorders was found [126].
- Regarding environmental risks, a study was carried out in children. They found that exposure to other young children may be an early protective factor against the development of NMO, as has already been reported for MS. This is consistent with the hypothesis that infections contribute to changes in disease risk [127].

3. Diagnosis and clinical presentations and diagnosis

The predominant clinical signs of NMO are optic nerve damage and transverse myelitis. However, cerebral and brainstem lesions may occur in some patients. Due to the location of the lesions, the associated clinic may vary :

a) Optic Neuritis

Optic neuritis (**ON**) was present at disease onset in 74% of MOGAD patients and in 50% of NMO-AQP4 patients. ON is an inflammation of the optic nerve revealed by a decrease in visual acuity or an alteration of the visual field of rapid installation over 24-72 hours. Visual discomfort is usually associated with and/or preceded by periorbital pain increased by eyeball movements. NO can also lead to a decrease in contrast sensitivity, a dyschromatopsia (red/green axis). NMO frequently results in scotomas (an area of the visual field with decreased visual acuity) in both MOGAD and NMO-AQP4 patients. In the acute stage, the fundus examination is most often normal, the inflammation of the optic nerve being preferentially located in the posterior part of the optic nerve or in the optic chiasm. The ON relapse of NMO is clinically distinguished from other causes by its severity: the decrease in visual acuity is profound, the visual sequelae frequent and the relapses numerous [128].

b) Transverse myelitis

Transverse myelitis (**TM**) was presented by 34% of MOGAD patients and 52% of NMO-AQP4 patients at disease onset. This spinal cord injury results in acute onset spinal cord symptoms with a maximum of symptoms between 4 hours and 3 weeks, and is responsible for motor, sensory and vesico-sphincter impairment, often severe. The motor impairment concerns the lower limbs or all four limbs, and may lead to tetraplegia. It may be associated with painful muscle spasms significantly more frequently than in other causes of spinal cord injury. Neuro-perineal damage can be responsible for acute urinary retention, transit arrest and sexual dysfunction. Vesico-sphincter sequelae are frequent, often poorly investigated, with a major impact on quality of life [129].

c) Other clinical signs

As mentioned previously, a post-traumatic syndrome may also be associated especially with NMO-AQP4, just as diencephalon involvement (especially thalamus and hypothalamus) is exceptional but suggestive. Clinical presentations include in particular: sleep disorders (narcolepsy or hypersomnia), eating disorders (hyperphagia) or thermoregulation disorders. In MOGAD patient and not NMO-AQP4, we find children affected with the clinical presentation of ADEM (acute disseminated encephalomyelitis) [119,125,130,131].

NMO most often manifests itself in iterative relapses that can be spaced from a few weeks to several decades apart. The relapse corresponds to neurological symptoms that set in rapidly, in a few hours to a few days, with a maximum of symptoms that are often very severe, sometimes even life-threatening, and with an often poor recovery without treatment. The potential for residual disability is major from the first attack. This severity underlines the crucial importance of early diagnosis. The course of this type of disease is usually relapsing, with children being more prone to monophasic expression of the disease [132,133].

d) Diagnosis

Diagnosis of the disease is based initially with serology and the detection of anti-AQP4 and anti-MOG autoantibodies. For this purpose, CBAs are performed and the general consensus among experts is that human full-length protein should be used as the antigenic substrate.
Imaging examinations by MRI allow the exploration of a neurological episode (relapse) of NMO. They identify inflammatory involvement confirming the relapse suspected on the basis of clinical data and they provide qualitative elements allowing the etiological diagnosis to be oriented towards an NMO rather than towards another inflammatory disease of the central nervous system (**Figure 14**). CSF examination is not essential but can be part of the initial evaluation, it allows to confirm the inflammation. Indeed, cellularity is increased in 14 to 79% of cases and may be well above 50/mm3. It is often made up of lymphocytes and monocytes,

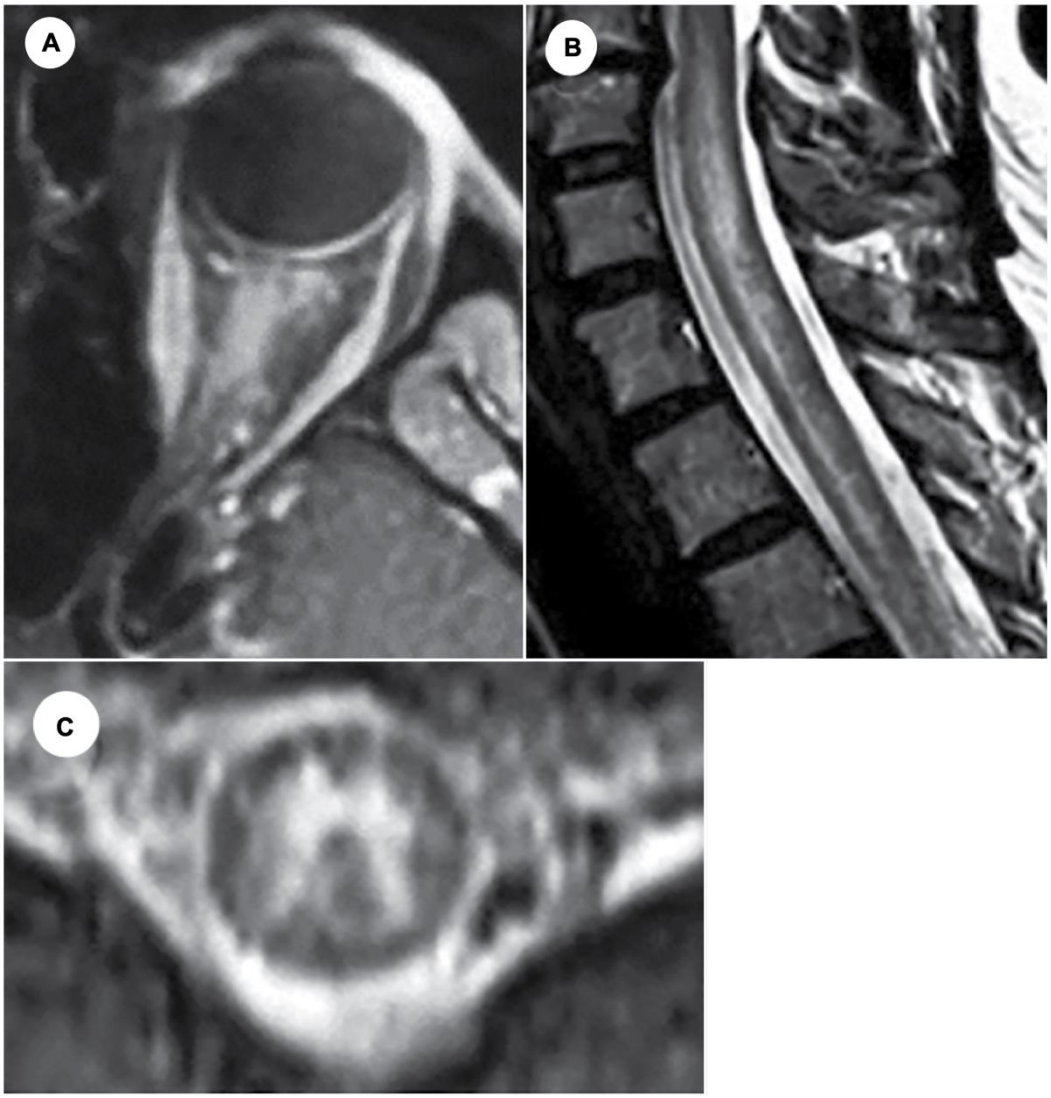

Figure 14: MRI from MOGAD patient

(Adapted from Sven Jarius and al. , 2020 and Jarius and al., 2016)

(**A**) Lesion of the optic neuritis in the anterior parts. (**B**) Longitudinal and extensive lesion in spinal cord (**C**) Lesion in the central portion of the spinal cord with a typical H-shaped lesion found in MOGAD patients.

4. Physiopathology

In NMO, the lesions contain antibody and complement deposits.

The pathophysiology involved in MOGAD differs from that involved in NMO-AQP4.

The disappearance of AQP-4-expressing astrocytes characterizes NMO-AQP4, whereas in MOGAD, antibodies (IgG1 isotype) target mature oligodendrocytes expressing MOG protein [134]. Complement, antibodies, and infiltrating immune cells are found at the lesions. IgG and complement deposits are less pronounced and less frequent in patients with MOG-IgG than in those with NMO-AQP4. Macrophages and TCD4$^+$ T cells dominate the infiltrate compared to TCD8$^+$ and B cells are present but in smaller numbers [135]. Tissue damage is characterized by demyelination, oligodendrocyte loss and axonal scarring. In contrast to NMO-AQP4, astrocytes are spared: there is no dystrophy and aquaporin-4 expression persists. Compared to MS, the immune response in MOGAD seems to differ in the absence of oligoclonal bands and the accumulation of inflammatory cells in the CSF. In addition, CD8$^+$ T cells are less dominant in the lesions unlike in multiple sclerosis (**Figure 15**).

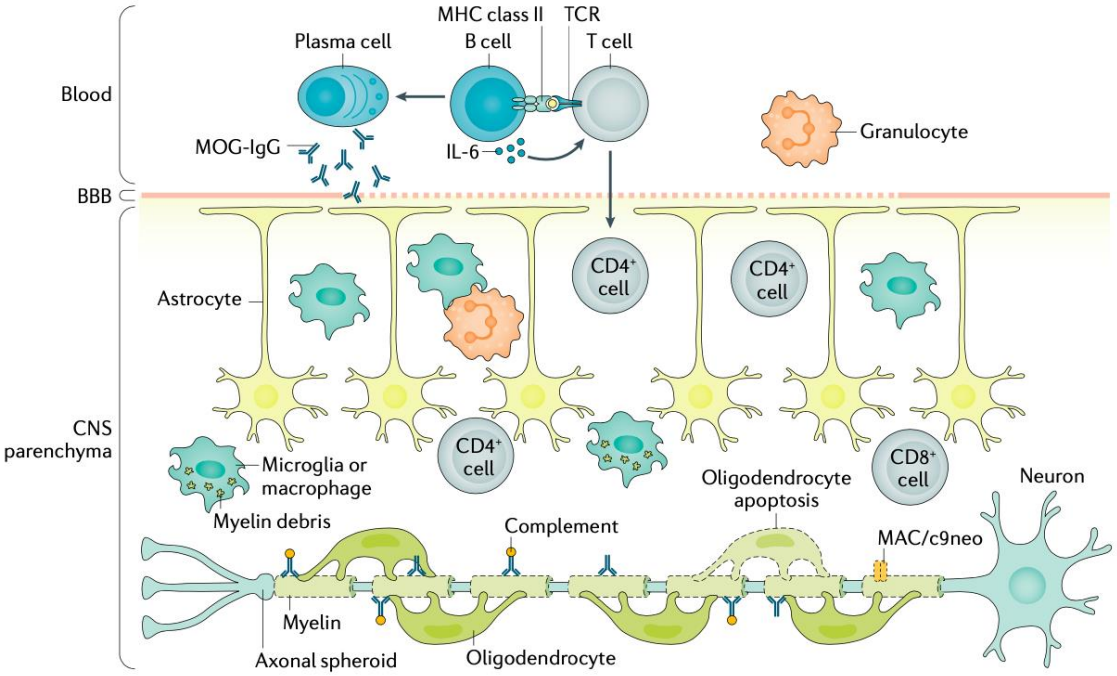

Figure 15: Supposed pathophysiology of MOGAD

(From Sven Jarius and al. , 2020)

In MOGAD, the cellular infiltrate found is composed of microglia, macrophages, T cells (mainly CD4+ rather than CD8+) and granulocytes (neutrophils and possibly eosinophils). Immunoglobulin deposits are typically IgG (not usually IgM), and complement (C9neo included) can be detected in macrophages and along myelin sheaths in areas of active demyelination

5. Management of the disease

The management of a neuromyelitis optica relapse represents a therapeutic emergency due to the risk of disabling sequelae and, in addition to the functional prognosis, the possible threat to life. At the same time, long-term treatment is essential in order to reduce the risk of relapses, the repetition of which can lead to serious functional sequelae.

a) Treatment of the relapse

The onset of a relapse requires emergency hospital care to start corticosteroid therapy as soon as possible, which may be combined with plasma exchange. High-dose corticosteroid therapy (methylprednisolone) (1 g/d) is given by intravenous bolus. If necessary, the association with plasma exchange is initiated as soon as possible. In any case, confirmation of autoantibody positivity is necessary to initiate treatment. Indeed, recent data strongly suggest that prompt initiation of plasma exchange improves the functional prognosis of the relapse compared with the administration of corticosteroids alone [136,137]

b) Long-term treatment

The aggressive nature of the disease and its functional consequences, directly related to the inflammatory relapse, make it necessary to seek the advice of an expert center to discuss the implementation of basic immunosuppressive treatment as soon as the disease is diagnosed.
The treatment decision is made in consultation with the reference center. The initiation of treatment must be in order to control the risk of a new attack of the disease as quickly as possible. The treatment of NMOSD is mostly done outside of the MA. Recently published phase III trials (testing eculizumab, satralizumab, rituximab and inebilizumab) will help redefine treatment strategies. The duration of the background treatment is unknown at this time:

(1) Rituximab

Rituximab (anti-CD20), which has been authorized and validated in hematological and rheumatic diseases, has been used in open-label situations of NMOSD refractory to more traditional immunosuppressive drugs (azathioprine, mycophenolate mofetil, cyclophosphamide, mitoxantrone). According to the NOMADMUS database, in France, 45% of patients with NMO-AQP4 are treated with rituximab. This number rises to 80% when analyzed over the last 2 years. This use of rituximab or its biosimilars remains off-label, but is currently a first-line option. Treatment is administered IV every 6 months [138].

(2) anti-IL-6 therapy

IL6 is an important cytokine in plasma cell survival. High levels of IL6 are observed in the serum and plasma of NMOSD patients. Case series have observed that tocilizumab (anti-RIL6) controls the frequency of relapses in patients with NMOSD refractory to either conventional immunosuppressive therapy or rituximab. Thus, tocilizumab is currently used off-label for refractory MODS. Two phase III trials published in 2019 affirm the value of satralizumab (anti-

RIL6 administered subcutaneously every 2 and then 4 weeks) in the control of NMO in adult or pediatric patients, alone or in combination with oral immunosuppressive therapy [139,140].

(3) Other treatments

These three treatments : Azathioprine Mycophenolate mofetil Mitoxantrone have proven their effectiveness in reducing NMO relapses.

Improving the quality of life of patients also involves therapeutic patient education, enabling them to better understand their disease and its implications. This therapeutic patient education can take several forms. It generally consists of group or individual workshops aimed at acquiring self-care and psycho-social skills. It can also involve cooperation with patient associations.

C. Transgenic mouse models of demyelinating disease of the central nervous system

The animal model used to study CNS autoimmunity is the **experimental autoimmune encephalomyelitis** (EAE) which can immitted demyelination, cell and tissue damage like oligodendrocyte loss, axon damage that are encountered in patients with demyelinating CNS inflammatory disease. The first model of EAE was obtained in monkeys in 1933 by Thomas Rivers following repeated vaccination of brain material inducing demyelinating lesions similar to those seen in MS patients [141]. EAE was then induced in different mammalian species and in particular in rodents (rats, mice) allowing the modelling of different forms of MS: acute monophasic, recurrent remittent or chronic progressive. EAE is widely used to model the main features of multiple sclerosis, with several key clinical and pathophysiological differences between human CNS autoimmunity and EAE. Nevertheless, many EAE models have been developed to study one or several aspects of this demyelinating disease and are therefore essential for a better understanding of inflammatory demyelinating diseases of the CNS.

EAE consists of inducing CNS inflammation by immunizing with myelin autoantigens such as myelin oligodendrocyte glycoprotein (MOG), proteolipid protein (PLP) or myelin basic protein (MBP) [53].

- **MBP** is a protein necessary for the compaction of myelin. it represents 30% of myelin proteins and unlike the MOG protein, it is found inside the myelin sheath. it thus allows the adhesion of the cytosolic surfaces of the different layers. Several studies have demonstrated a high affinity between the specific T response of the immunodominant peptide MBP_{84-102} in MS. The study of the presentation of this peptide by DR2 showed a high binding affinity of this peptide to the molecules DRB1*0101 DRB1*1501 [142].
- **PLP** is an abundant myelin protein, it makes up 50% of all myelin. It has 4 transmembrane domains that are hydrophilic and conserved between species.
- **MOG** protein was firstly described in 1984 by Christopher Linnington as a target for demyelination by antibodies [143]. It is a protein present on the outer layer of the myelin sheath making it an easily accessible target for antibodies. The T cell response is predominantly directed against the 35-55 and 119-132 regions of MOG found in the extracellular and transmembrane parts of the protein respectively [144] (**Figure 16**). MOG is low in abundance, representing less than 0.1% of myelin proteins. Its expression is restricted to the CNS as it is only produced by oligodendrocytes. MOG is thus a highly immunogenic target [145,146].

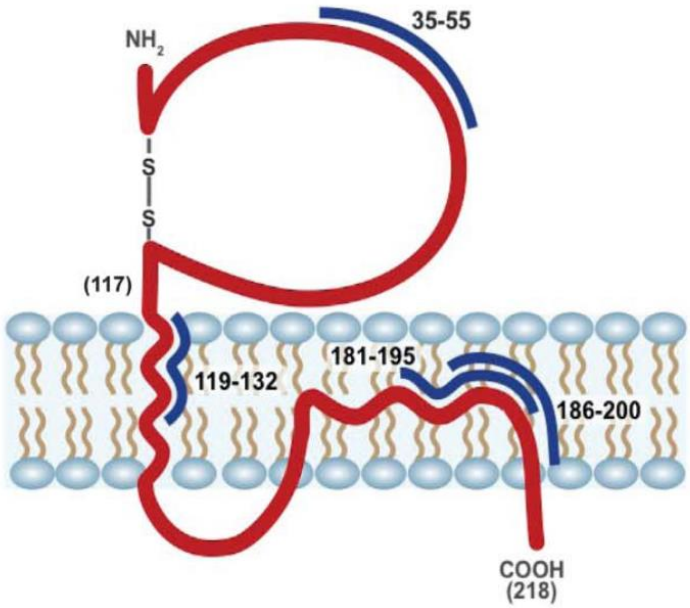

Figure 16: Myelin oligodendrocyte glycoprotein

(from Shetty and al., 2014)

V. Antibodies, structure, functional property and importance of glycosylation of the Fc Fragment

Antibody specificity, isotype, Fc fragment glycosylation and the impact of antibodies in the innate and adaptive immune response are active areas of investigation. The main objective of my thesis project is to evaluate whether the glycosylation of the Fc fragment detected on autoantibodies in anti-MOG antibody-associated demyelinating diseases influences inflammation and disease severity.

A. Antibody structure

Antibodies are the soluble effectors of antigen-specific humoral immunity. They produced by plasma cells. They can be found in serum and other biological fluids.

An antibody has a variable part, capable of recognizing the epitope of an antigen, and an effector part allowing this specific recognition of the antigen to be followed by effects on the immune system.

An antibody is called an immunoglobulin (Ig) because they are found in the α, β and γ globulin protein fractions. In most mammalian species there are five classes of Ig: IgG, IgM, IgA, IgE and IgD. The structure of these five classes is based on a basic structure that is monomeric for IgG, IgE and IgD, dimeric for IgA and pentameric for IgM. The basic structure is Y-shaped and consists of four identical polypeptide chains in pairs (**Figure 17**):

- Two heavy chains (HC) identical to each other and constituted of approximately 450 amino acid (50kDa). There are five types of heavy chains : γ, μ, α, ε et δ also called isotype defines the class of Ig. Some classes are divided into subclasses such as IgG with : IgG1, IgG2, IgG3 et IgG4 corresponding to γ1, γ2, γ3 et γ4 ; or IgA with α1 et α2 for IgGA1 and IgGA2.
- Two light chains (LC) identical to each other and constituted of approximately 220 amino acid (25kDa). There are two types of light chain : κ and λ which can be combined with any HC type. The two LC are identical for one Ig.

HC and LC are composed of domains: two for LC and four for HC held together by disulphide bridges. A domain corresponds to a folding of the polypeptide chain forming a loop of 60 to 70 amino acids held together by an intracatenary bridge and hydrophobic interactions. Each domain is composed of a series of antiparallel pleated β-sheets. One heavy chain is composed of three constants domains CH for constant heavy (CH_1, CH_2 and CH_3) and one variable domain : VH (variable heavy). One light chain is composed of one constant domain : CL (constant light) and one variable domain : VL (variable light). The two association VL-VH form the two variable fragments found at the Ig N-terminus, where antigen binds. This variable fragments show a great diversity of sequences from one Ig to another. Within each variable

domain there are the hypervariable regions, which are three regions of about 10 amino acids with particularly high variability. this high variability is due to the somatic hypermutation mechanism(**c.f II.A**).

The 6 hypervariable regions of an Ig, also known as CDRs for complementary determining region, together with the framework regions form the antigen binding site. Numerous non-covalent bonds (hydrogen, hydrophobic, Van der Waals and electrostatic bonds) are involved in the interaction between the antigen and the amino acids of the binding site. Even though these forces are weak, their large number allows a high binding energy between the epitope and the paratope. The strength of the binding is called affinity. Avidity refers to the strength with which a multivalent antibody binds to a multivalent antigen.

In humans the dominant class of Ig in the blood is IgG. This is the major class in the secondary immune response and constitutes the bulk of plasma gammaglobulin.

The four subclasses of human IgG are named according to their relative serum concentrations: 60% for IgG1, 25% for IgG2 10% for IgG3 and 5% for IgG4. Unlike human IgG, murine IgG is divided into three subclasses (IgG1, IgG2 and IgG3). Murine IgG2 includes the isotypes 2a, 2b and 2c. There are several sequence variants for murine IgG1 and IgG2b [43].

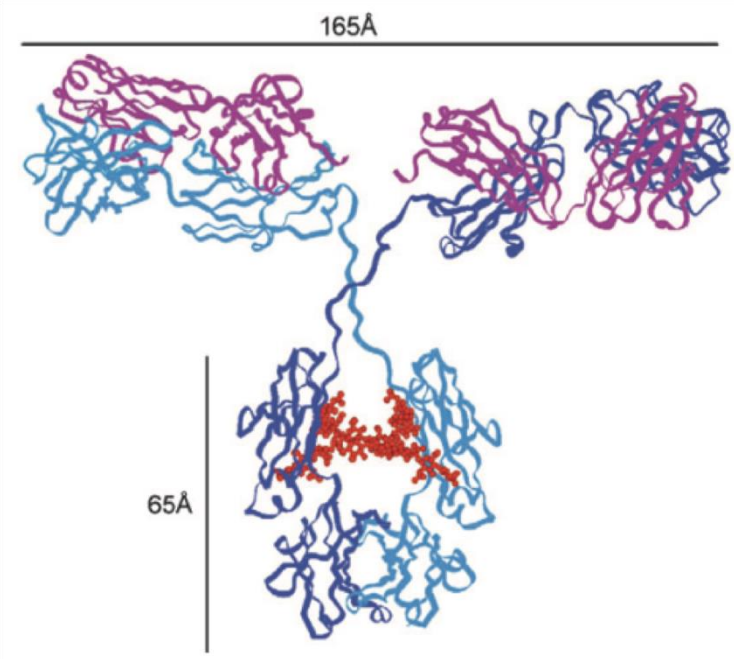

Figure 17: Molecular models of human IgG1 based on the crystal structure

(adapted from : Arnold et al. 2007)

LCs are shown in purple, HCs in blue and interchain sites of N-glycosylation are shown in red

B. Antibody functions

Antibodies have a role in protecting against extracellular pathogens and toxins. They are bi-functional proteins with:

- The Fab fragment for "Fragment antigen-binding": this domain allows binding to the antigen. It is therefore responsible for antigen specificity through hypervariable regions.
- The Fc fragment or crystallizable fragment: made of constant fragments responsible for the effector properties of the Ig with the binding to complement proteins and to Fc-specific receptors: FcRs.

Les actions des anticorps sont donc liés soit à la reconnaissance de l'antigène par la Fab soit à la liaison du Fc au FcRs, on retrouve ainsi

1. Functions related to the Fc fragment:

a) Neutralizing toxins

Many bacteria exert their pathogenicity by secreting toxins. These toxins interact with cell receptors carried by the target cells. Antibodies block the interaction of the toxins with the cell receptors.

b) Preventing infection

Many bacteria have adhesins. Ac can block these adhesion proteins and thus prevent infection.

c) Preventing the spread of infection

Viruses, for example, in order to infect a cell they must bind to a specific membrane receptor. Virus-specific antibodies can block this interaction and thus the spread of the virus by blocking the infection of adjacent cells.

2. Effector functions related to the Fc fragment

An antibody exerts its effector functions through the Fc fragment and its binding to the receptor for that fragment: FcRs or FcRn. Indeed, the immune complex (IC) formed by the recognition of an epitope and the antibody specific to this epitope is recognized *via* its Fc fragment by these receptors.

a) Importance of receptors for Fc fragments of IgG (FcRs)

(1) Opsonisation by antibodies and induction of phagocytosis

Opsonisation is the overlaying of a micro-organism by antibodies to allow phagocytosis. The antibody recognizes the antigen. FcRs on the macrophage recognize the Fc fragment of the antibody bound to the antigen, the immune complex. This recognition activates the phagocyte and triggers phagocytosis of the pathogen.

(2) Induction of NK cytotoxicity: antibody-dependent cellular cytotoxicity (ADCC)

NK cells are considered crucial mediators of ADCC reactions. NK cells solely express the activating FcRs FcγRIII (CD16) and this applies to both humans and mice [147].
This receptor recognizes IgG1 and IgG3 in particular.
Taking the example of viral infections, a cell infected by a virus can express viral proteins on its surface. These viral proteins can be recognized by specific antibodies. Antibodies's Fc fragment can be recognized by the FcγRIII receptor express by NK cells, monocytes or macrophages. Once activated, NK cells are able to lyse the infected cell via the perforin-granzyme system.

(3) Complement-dependent cytotoxicity

Antibodies that bind their antigen can activate the classical complement pathway, C1q binds to the Ig bound to its antigen this activates C1R which cleaves and activates the serine protease C1s. This activation of the classical complement pathway leads to lysis of the cell to which the antibody has attached.

b) The FcRn (receptor for the neonatal Fc fragment) and ½ antibody life

The neonatal IgG Fc receptor (FcRn) is responsible for the transfer of passive humoral immunity from the mother to the newborn in rodents and humans. Maternal IgG can cross the placenta and be released into the fetal bloodstream. At birth, the newborn has a plasma IgG repertoire similar to that of the mother.

In addition throughout life, FcRn contributes to effective humoral immunity by recycling IgG and prolonging its serum ½ life. The ½ life of IgG1, IgG2 and IgG4 is 21 days and only 5 to 7.5 days for IgG3 due to the arginine residue at position 435 replacing histidine in IgG1.

The structure of FcRn is similar between humans, mice and rats. It is in the form of a heterodimer consisting of a soluble light chain β2-microglobulin and a heavy chain in the plasma membrane including a short cytoplasmic part and a transmembrane region with three extracellular domains (α1, α2, α3). It belongs to the MHC class I family of molecules [148].

FcRn is expressed by endothelial cells, epithelial cells, macrophages and monocytes [149]. It binds tightly to the Fc part of IgG at acidic pH (pH 6.0) but not at physiological pH (pH 7.4). It is therefore only after pinocytosis by endothelial cells that Ab can bind to FcRn in endosomes due to the acidic pH 6 of the endosomes. The targeted FcRn-Ab complexes in the endosomes are recycled and the Ab are thus released at the extracellular level thanks to the neutral pH 7.4 [150,151] (**Figure 18**)

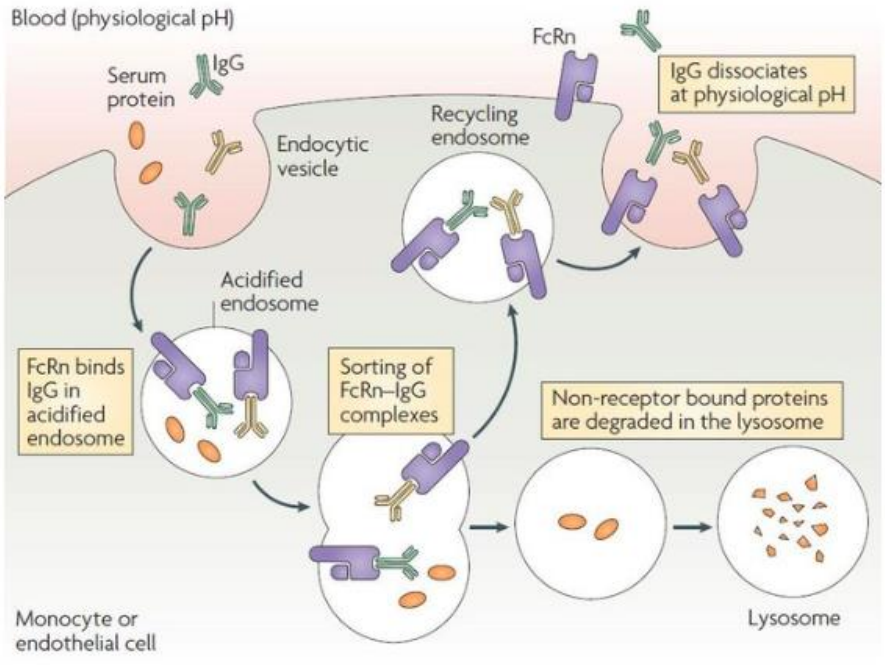

Figure 18: pH-dependent recycling mechanism of IgG following binding to FcRn

(From Roopenian and al. 2007)

C. Focus on Fc receptors for IgG

Immune complexes in addition to their role in antigen removal discussed above; they are also known to have potent immunoregulatory functions, ranging from strong enhancement to complete suppression of antibody responses [152]. These antagonistic activities are explained by the selective engagement of FcγRs and also by the presence of immunoreceptor tyrosine-based activation motif (ITAM) contained in the human FcγRIII and mouse FcγRI or the immunoreceptor tyrosine-based inhibitory motif (ITIM) contained in FcγRIIB human and mouse. These FcγRs belong to the immunoglobulin receptor superfamily.

In mice we found four different classes of Fc receptors have been defined: FcγRI (CD64), FcγRIIB (CD32), FcγRIII (CD16) and FcγRIV (**Figure 19A**). These four different receptors are found in many mammalian species. Genes for these receptors are located on chromosome 1 in humans, chimpanzees and mice, on chromosome 13 in rats. While most species have only one copy of the FcRs genes, duplication and diversification processes have led to the presence of multiple genes in the human genome [147]. This is why we find this orthologues in humans: FcγRIA (CD64), FcγRIIA (CD32a), FcγRIIC, FcγRIIIA (CD16a) and FcγRIIIB and the inhibitory receptor FcγRIIB (CD32b) (**Figure 19**). FcRs are distinguished by their affinity for IgG or by their induced, activating or inhibiting signalling pathway. These receptors are expressed by a wide variety of haematopoietic cells such as: monocytes, macrophages, dendritic cells, basophilic granulocytes and eosinophils.

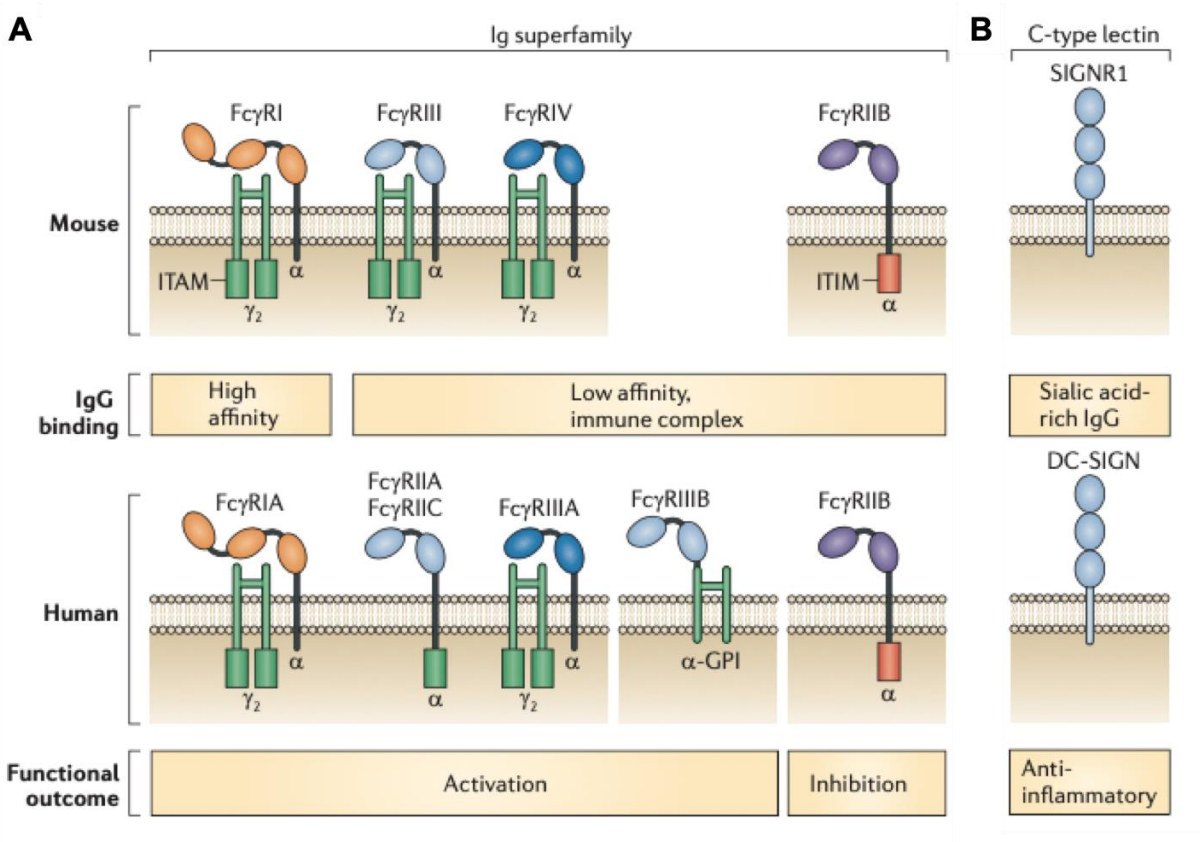

Figure 19: Representations of mouse and human activating and inhibitory FcγRs.

(Adapted From Schwab and Nimmerjahn and al. 2013)

(A) FcγRs of IgG (B) Lectin like receptors

In **Figure 19** from *Schwab and Nimmerjahn and al. Nature 2013* you can see the receptors in humans (bottom) and mice (top). Their immunological role is shown: pro-inflammatory on the left and anti-inflammatory. Are also shown the lectin-like receptors: the mouse protein 1 DC-SIGN (SIGNR1) and its human orthologue DC-specific ICAM3-grabbing non-integrin (DC-SIGN) (**Figure 19B**). It should be noted that, we see that in humans there is a glycosylphosphatidylinositol (GPI)-anchored FcγRIIIB that is exclusively expressed on neutrophils. The level of affinity for IC depends on the IgG isotype. While FcgRI has a high affinity for the constant region of the antibody and a restricted isotype specificity, FcgRII and FcgRIII have a low affinity for the Fc region of IgG but a broader isotype binding pattern [153,154] and FcgRIV is a more recently identified receptor, conserved in all mammalian species with intermediate affinity and restricted subclass specificity [155,156]. It is important to note that murine FcγRIII only binds to IgG1 [157].

In mice, macrophages and monocytes express all activating and inhibitory FcRs. Neutrophils express FcγRIIB, FcγRIII and FcγRIV. Dendritics cells express FcγRI, FcγRIIB and FcγRIII. There is no evidence of FcRs expression by LTs. However, two cell types express only one FcRs [157]:

- B only express the inhibitory FcγRIIB,
- NK cells only express the pro-inflammatory FcγRIII.

NK cells are essential for ADCC, the fact that they express only the FcγRIII receptor underlines the importance of this receptor in the antibody dependent adaptive immune response. Indeed, in mouse models of autoimmune haemolytic anaemia, animal deficient in FcγRIII showed abrogated antibody activity This is also the case in a variety of human autoimmune diseases, such as arthritis and systemic lupus erythematosus (SLE), where aberrant expression or the presence of allelic variants of FcγRs with altered functionality have been observed to contribute to the pathogenesis of these diseases [147,158,159]. The results obtained in mouse models are essential to decipher the role of FcγRs in the activity of different antibody isotypes *in vivo*. Indeed, many of the basic principles and mechanisms underlying these activities have been identified in mice and have been summarised in humans [147].

D. Importance of Fc-glycosylation

It is increasingly proposed that N-glycosylation-binding glycans influence binding to classical Fcγ receptors (FcγRs) and enable binding to non-classical type II receptors [160,161]. This significantly expands the functional potential of the antibody response beyond their isotypes.

Protein N-glycosylation is a highly conserved metabolic process during evolution. It consists of the addition or deletion of different sugars at the glycosylation site depending on the enzymes and substrates present. Human antibodies have an N-glycosylation site on the heavy chain at asparagine 297 (**N297**) of the CH_2 domain on the Fc fragment. Glycosylation represents 2-3% of the mass of 150kDa Ig (**Figure 17**).

In human serum the oligosaccharides present on IgG on Asn297 have a bi-antennate structure. This has an invariable part composed of 7 monosaccharides, 4 N-acetylglucosamine residues (GlcNAc) and 3 mannose residues (Man): $GlcNAc_2Man_3$ (trimannosyl chitobiose). The two mannoses linked in α(1-6) and α(1-3) form the two antennae (**Figure 20**). This "core" can be enriched with different saccharide residues (fucose, galactose, sialic acid, etc.)[109]. This explains the great heterogeneity of IgG glycoforms in serum. The glycosylation profile of IgG varies according to physiological and pathological characteristics [162]. Noteworthy, the mouse equivalent of asparagine is **N174**.

Binding between FcRs and the Fc domain is generally mediated by amino acid interactions [163]. A distinction is made for the FcγRIIIa and FcγRIIIb receptors where carbohydrate interactions between the Fc and FcR allow for high affinity binding [164].

Further extension of the glycan core can occur via the addition of bisecting GlcNAcylation, or the addition of galactose and sialic acid at the terminal level. The addition of terminal sialic acid has a dominant impact on the structure of Fc. Full sialylation of N297 on each of the heavy chains results in a 'closed' Fc domain that attenuates binding to FcRs and complement in favour of binding to type II Fc receptors [161,165].

1. Fc-glycosylation in diseases

In tuberculosis patients, the Fc-glycosylation of patients with latent and active tuberculosis differed [166]. Latency was associated with di-galactosylated N-linked glycans with and without sialylation on IgG Fc that improved bacterial clearance. Conversely, Fc-fucosylation or agalactosylation did not control TB infection. Fucosylation is enriched among dengue virus-reactive but non-neutralising Abs. Afucosylated antibodies provide clearance of dengue, while persistence of dengue in the presence of fucosylated antibodies predisposes to dengue shock syndrome [167]. Antibody-mediated inflammatory diseases show a similar polarisation.

In chronic inflammatory diseases, the Fc-glycome is more diverse. Indeed, changes in IgG Fc-glycosylation are observed in rheumatoid arthritis, lupus, diabetes, Sjögren's disease, inflammatory bowel disease, usually resulting in a significant loss of galactosylation, with

maintenance or increase in fucosylation, even at disease initiation [168,169]. Multiple sclerosis is no exception. Elevated GlcNAc bisecting and reduced Fc-galactosylation were observed in CSF and not in serum of MS patients [170,171]. This Fc-glycosylation profile confers important pro-inflammatory properties by facilitating Fc binding to activating FcγRs [172].

The glycosylation profile of Ab is therefore not invariant and can change according to physiological or pathological conditions. There is accordingly great interest in studying the glycosylation profiles of auto-Ac in MS. They could subsequently be used as biomarkers of this inflammatory disease.

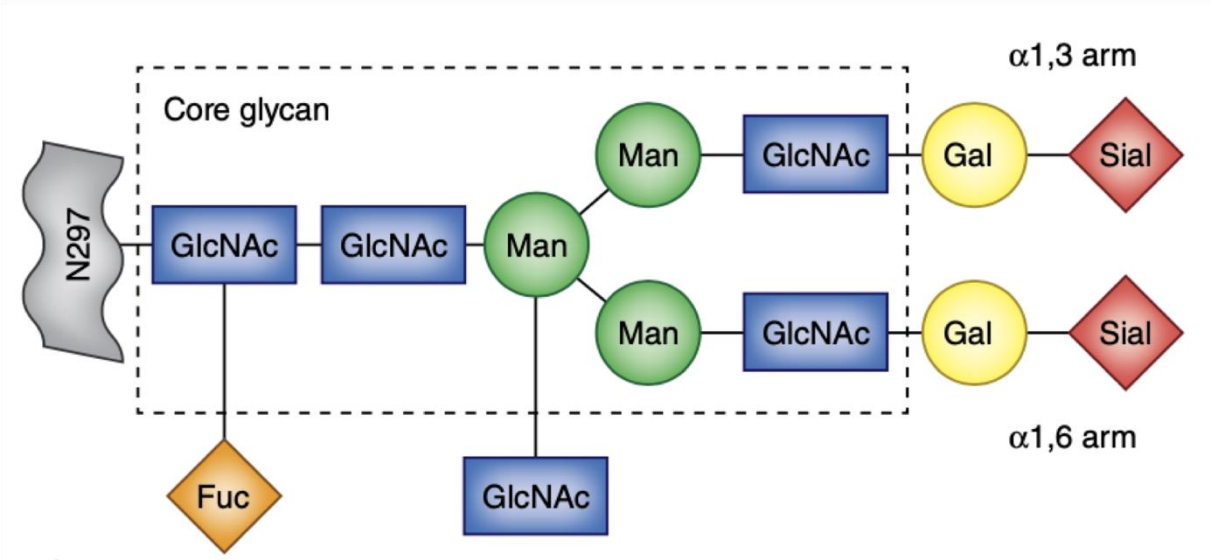

Figure 20: Glycosylation structures attached to Fc Asn297

(Adapted From Pincetic and al, 2014)

The glycan core structure (within the rectangular dotted outline) shows the invariant group of heptasaccharides conjugated to Fc. Sugars beyond the core are attached with varying frequencies. GlcNAc, N-acetylglucosamine; Fuc, fucose; Man, mannose; Gal, galactose; Sial, N-acetylneuraminic acid (sialic acid).

2. Two Fc-glycosylation profiles: fucosylation and sialylation emphasised

Immunologically the impact of fucosylation and sialylation have been studied most extensively. Fucosylation by α-(1,6)-fucosyltransferase 8 (FUT8) is observed on the majority of IgG in healthy individuals [173,174]. This is thought to be a protective trait as Fc domains that lack the branched fucose moiety are known to have an increased affinity for the activating receptor FcγRIIIa (CD16a). This loss of fucose allows for a stabilising interaction between the N-glycan of FcγRIIIa and the afucosylated Fc glycan [164]. This stabilization improves ADCC and monocyte/macrophage activation [175–177].

Sialylation of the Fc-domain has a radically different impact. The addition of terminal sialic acid by β-galactoside α-2,6-sialyltransferase 1 (ST6Gal1) abrogates binding to Type I FcγRs in favour of Type II Fc-receptor binding. Type II family includes the C-type lectin receptor CD209 (DC-SIGN), CD23 (FcεRII), CD22, CLECC4M, CLE4G, and CLEC4A, but this remains a question of controversy [160,163,169,178–180]. Functionally the binding to type II receptors by sialylated antibodies augments activation thresholds for the immune system. This is critical for the affinity maturation of the humoral response. Sialylated Fc upregulate expression of the inhibitory FcγRIIB on germinal center B cells by binding to CD23. Triggering of the FcγRIIB receptor elevates the activation threshold of the B cell receptor (BCR) enforcing the selection of higher affinity B cells to constitute the humoral response [181]. This is essential for vaccine strategies where the induction of sialylated.

VI. Working hypothesis

CNS inflammatory diseases pathophysiology is complex and goes beyond auto-reactivity. Indeed, autoimmunity alone is not sufficient to explain the onset of these diseases. It is associated with immune dysregulation potentially induced by genetic predisposition; with IS immunosenescence (age-related IS dysfunction catalysed by AID) and, at a more advanced stage, with neurodegeneration.

A. Part A : A Evaluation of MOG-specific B cells dynamics at the initiation of spontaneous EAE in secondary lymphoid organs and the brain.

This project resulted in a publication in frontiers in Immunology in 2022 [182]. It investigates the involvement of B cells in the initiation and progression of multiple sclerosis (MS). B cells have a key role in the pathophysiology of multiple sclerosis. This is corroborated by the presence of oligoclonal bands in the cerebrospinal fluid, associated with the presence of ectopic lymphoid follicles, germinal cent like structure found in the meninges.

The objective of this section is to study the clonality of the B cell response targeting MOG. For this purpose, a spontaneous model of experimental autoimmune encephalomyelitis (EAE) was used. The TCR (TCR^{1640}) of these transgenic mice SJL/j strain, is specific for $MOG_{92\text{-}106}$. In our animal facility 94% of the mice expressing TCR^{1640} spontaneously develop chronic paralytic EAE between 60 and 500 days of age.

The immune response is triggered by the microbiota in the gut-associated lymphoid tissue, while there is evidence that maturation of the autoimmune demyelinating response may occur in the cervical lymph nodes due to local brain drainage. Using MOG protein tetramers, specific MOG B cells ($MOGtet^{+}$ B cells) could be traced and located in the cervical lymph nodes and in the brain immune infiltrate of diseased.

With a transgenic mouse model of spontaneous autoimmune encephalomyelitis (EAE) called TCR^{1640}. The TCRs of these transgenic mice, specific for $MOG_{92\text{-}106}$, are thought to recruit MOG-specific B cells from the endogenous repertoire.

B. Part B: Does Fc-glycosylation influence the pathogenicity of antibodies in MOGAD?

In human demyelinating diseases of the central nervous system, the pathogenicity of autoantibodies is a relevant but unresolved issue. Antibody specificity, isotypes, Fc glycosylation and the impact of antibodies in orchestrating the innate and adaptive immune response remain active areas of investigation. The main objective of this research project is to evaluate whether Fc glycosylation detect on autoantibodies in demyelinating diseases influences inflammation and disease severity.

This part of the project investigates via a translational approach the glycosylation of the Fc fragment on the MOG-specific IgG1 response and its potential impact on antibody pathogenicity.

In concomitant research, the glycosylation profile of anti-MOG autoantibodies in MOGAD patients was analyzed with the Dr. Shin Yi Yu glycosylation expertise. In parallel to this study in humans, the impact of Fc glycosylation and more precisely of hypofucosylation highlighted on MOGAD patient was studied through *in vivo* studies in mouse models of Experimental Auto-Immune Encephalomyelitis (EAE) activated by immunization with the MOG_{35-55}.

The antibody chosen was 8-18C5, a murine antibody specific for MOG.

We have designed a study model of the MOGAD starting with a MOG_{35-55} induce EAE supplemented with one 8-18C5 IV injection of 50µg at day 9, just before the onset of disease onset. This model allow to highlight the relevance of Fc-glycosylation on the pathogenicity of antibodies and study the underlying immunopathological factors by investigating the severity of tissue damage and the possible change in the composition and severity of the SI according to the glycosylation profile of the injected antibody. For this purpose, several glycosylation variants of 8-18C5 have been created.

Firstly, to highlight the importance of glycosylation a N-deglycosylated 8-18C5 antibody was created through the treatment with PNGaseF to remove the N-glycosylation.

Secondly to further investigate the impact of the glycosylation patterns as observed in MOGAD patients, several glycovariants of the same 8-18C5 clone were created. For that purpose we have cloned the murin 8-18C5 coding sequence. These recombinants were obtained by transfection using different cell lines:

- **HEK293** (human embryonic kidney cells) producing a fucosylated antibody by transient transfection. The glycoform on N174 is fucosylated so we call the varinats : **G0F**
- **YB2** (rat myeloma derived cells) producing a predominantly hypofucosylated antibody as find in MOGAD patients since YB2 cells are fucosyltransferase (FUT8) Knock-out; by stable transfection. Glycan moiety lacked fucose at 45%. That's why we call this variants **G0.**

- **CHO** (Chinese hamster ovary cells) producing a partially aglycosylated antibody by stable transfection. N174 residues bearing 3 dominant glycoforms: G0F (42%), G1F (21%) and non-glycosylated N174 (27%), a mixed glycosylation profile: **MG**.

PART A :

Evaluation of MOG-specific B cells dynamics at the initiation of spontaneous EAE in secondary lymphoid organs and the brain.

A Spontaneous Model of Experimental Autoimmune Encephalomyelitis Provides Evidence of MOG-Specific B Cell Recruitment and Clonal Expansion

Florent Salvador[1†], Laure Deramoudt[1†], Frédéric Leprêtre[2], Martin Figeac[2], Thomas Guerrier[3], Julie Boucher[1], Mathilde Bas[1], Nathalie Journiac[1], Anneli Peters[4], Lennart T. Mars[1‡] and Hélène Zéphir[1,4,5‡]*

[1] Univ. Lille, Inserm, CHU Lille, Laboratory of Neuroinflammation and Multiple Sclerosis (NEMESIS), UMR-S1172, Lille Neuroscience & Cognition, LICEND, FHU Imminent, Lille, France, [2] UMS2014-US51, Genomics and Structural Platform, Lille University, Lille, France, [3] Univ. Lille, Inserm, CHU Lille, U1286, INFINITE-Institute for Translational Research in Inflammation, Lille, France, [4] Institute of Clinical Neuroimmunology, Hospital and Biomedical Center of the Ludwig-Maximilian University (LMU), Martinsried, Germany, [5] CRC-SEP of Lille, CHU of Lille, Lille, France

The key role of B cells in the pathophysiology of multiple sclerosis (MS) is supported by the presence of oligoclonal bands in the cerebrospinal fluid, by the association of meningeal ectopic B cell follicles with demyelination, axonal loss and reduction of astrocytes, as well as by the high efficacy of B lymphocyte depletion in controlling inflammatory parameters of MS. Here, we use a spontaneous model of experimental autoimmune encephalomyelitis (EAE) to study the clonality of the B cell response targeting myelin oligodendrocyte glycoprotein (MOG). In particular, 94% of SJL/j mice expressing an I-A^{s}: MOG$_{92\text{-}106}$ specific transgenic T cell receptor (TCR^{1640}) spontaneously develop a chronic paralytic EAE between the age of 60-500 days. The immune response is triggered by the microbiota in the gut-associated lymphoid tissue, while there is evidence that the maturation of the autoimmune demyelinating response might occur in the cervical lymph nodes owing to local brain drainage. Using MOG-protein-tetramers we tracked the autoantigen-specific B cells and localized their enrichment to the cervical lymph nodes and among the brain immune infiltrate. MOG-specific IgG1 antibodies were detected in the serum of diseased TCR^{1640} mice and proved pathogenic upon adoptive transfer into disease-prone recipients. The ontogeny of the MOG-specific humoral response preceded disease onset coherent with their contribution to EAE initiation. This humoral response was, however, not sufficient for disease induction as MOG-antibodies could be detected at the age of 69 days in a model with an average age of onset of 197 days. To assess the MOG-specific B cell repertoire we FACS-sorted MOG-tetramer binding cells and clonally expand them *in vitro* to sequence the paratopes of the IgG heavy chain and kappa light chains. Despite the fragility of clonally expanding MOG-tetramer binding effector B cells, our results indicate the selection of a common CDR-3 clonotype among the Igk light

OPEN ACCESS

Edited by:
Abdelhadi Saoudi, INSERM U1043 Centre de Physiopathologie de Toulouse Purpan, France

Reviewed by:
Ché Serguera, Institut National de la Santé et de la Recherche Médicale (INSERM), France
Tommy Regen, Johannes Gutenberg-University Mainz, Germany
Igal Ifergan, University of Cincinnati, United States

***Correspondence:**
Hélène Zéphir
Helene.ZEPHIR@CHRU-LILLE.FR

†These authors have contributed equally to this work

‡These authors share last authorship

Specialty section:
This article was submitted to Multiple Sclerosis and Neuroimmunology, a section of the journal Frontiers in Immunology

Received: *09 August 2021*
Accepted: *11 January 2022*
Published: *03 February 2022*

Citation:
Salvador F, Deramoudt L, Leprêtre F, Figeac M, Guerrier T, Boucher J, Bas M, Journiac N, Peters A, Mars LT and Zéphir H (2022) A Spontaneous Model of Experimental Autoimmune Encephalomyelitis Provides Evidence of MOG-Specific B Cell Recruitment and Clonal Expansion. Front. Immunol. 13:755900. doi: 10.3389/fimmu.2022.755900

chains derived from both disease-free and diseased TCR^{1640} mice. Our study demonstrates the pre-clinical mobilization of the MOG-specific B cell response within the brain-draining cervical lymph nodes, and reiterates that MOG antibodies are a poor biomarker of disease onset and progression.

Keywords: B cell, repertoire, autoimmunity, experimental autoimmune encephalomyelitis (EAE), multiple sclerosis, myelin oligodendrocyte glycoprotein (MOG), TCR^{1640} transgene mouse model, demyelinating antibodies

INTRODUCTION

B cells are essential components of the immune infiltrate that characterizes active demyelinating lesions in multiple sclerosis (MS). The histopathology of patients with relapsing-remitting MS, commonly points to the implication of the humoral response. The localization of plasma blasts and B cells in the perivascular cuffs are associated with the presence of antibodies, activated complement and Fc-receptor expressing myeloid cells indicative of antibody mediated tissue damage (1). The clinical relevance of antibodies is further underlined by the diagnostic value of oligoclonal bands (OCBs) that are present in the cerebrospinal fluid (CSF) of 90% of MS patients. Comparison of transcriptomes of CSF B cells and CSF Ig proteomes revealed that clonally expanded B cells in the CSF produce OCBs (2). Evidence of somatic hypermutation indicates that this is an antigen-driven process (3, 4), which occurs in the brain-draining cervical lymph nodes and possibly in the meningeal ectopic lymphoid structures (5, 6). The specificity of this adaptive immune response is composite and evolves over time (7–9).

Disease progression and worsening are similarly thought to be influenced by the humoral response. The transition to secondary progressive MS (SPMS) is associated with the accumulation of B cells in the leptomeningeal space covering the cortical surface. These ectopic B cell follicles share immunological traits with germinal centers and are thought to contribute to subpial demyelination (10–13). The detrimental nature of the B cell response was formally demonstrated by the therapeutic efficiency of B-cell depletion for both relapsing-remitting (RR) and progressive MS (14–16). This pivotal demonstration is of particular interest as this strategy targets CD20^{+} B cells thus sparing CD20 negative plasmocytes. In MS this results in clinical improvement without reducing IgG titers, nor by impacting plasmocyte frequency implicating a cellular role for B lymphocytes (17).

During the germinal center reaction B cells present antigen to follicular helper T cells in order to control the process of somatic hypermutation (18, 19). Antigen uptake is achieved *via* their B cell receptor (BCR) allowing the internalization, processing and presentation of the captured protein to T cells (20). This route of specific antigen uptake might have larger implications in the context of chronic inflammatory diseases such as MS. Indeed, a selective deficiency of MHC-II in B cells was demonstrated to cause resistance to experimental autoimmune encephalomyelitis (21). Mice expressing the heavy chain of a MOG-specific BCR (IgH^{MOG}) were compared to a novel IgH^{MOG} variant in which the secretion of transgenic MOG-antibodies is invalidated. Both genotypes remained fully susceptible to recombinant human MOG (rhMOG)-induced EAE, formally demonstrating that among transgenic MOG-specific B cells the ability to secrete antibodies did not modify their pathogenicity (21). In MS patients, circulating B cells strongly express MHC II accompanied by the induction of costimulatory molecules (22, 23). These memory B cells can present myelin-derived peptides to T cells, leading to pathogenic T cell activation and CNS homing (24, 25). Their impact on the T cell response is variable. The prominent production of IL-6 by B cells and the reduced magnitude of Th1 and Th17 responses in their absence point to an inflammatory role in MS (21, 26–28). This impact is extended to myeloid cells as the production of GM-CSF by memory B cells favors their differentiation (29). Of similar importance is the discovery that inflammatory B cells are balanced by the induction of regulatory B cells able to reduce the magnitude of inflammation through production of IL-10 and IL-35 (30–32). Plasma cells are similarly endowed with this regulatory capacity (33). Single cell RNA sequencing of CSF B cells in MS revealed clonally related B cells with a pro-inflammatory profile and downregulation of the SMAD/TGF-β1 pathway (34). This B cell cytokine profile might be predictive as in patients with clinically isolated syndrome (CIS) the evolution to MS was associated with a profile favoring IL-6 concomitantly with a loss of IL-10 production (35).

Spontaneous models of EAE provide a complementary paradigm to study myelin-specific B cells over the course of CNS autoimmune disease. Spontaneous EAE develops in the TCR^{1640} transgenic SJL/j mice owing to the expression of an I-A^{s} restricted TCR specific for the MOG peptide 92-106 (MOG$_{92-106}$) on 70% of CD4 T cells (36). Over time, nearly all TCR^{1640} develop inflammatory demyelinating lesions in the brain, optic nerves and spinal cord, reminiscent of the active lesions characteristic of MS. Priming of the adaptive immune response implicates the microbiota given that axenic TCR^{1640} mice refrain from developing clinical or histopathological EAE. In gnotobiotic TCR^{1640} mice, naïve CD4 T cells are likely to be activated within the gut-associated lymphoid tissue (GALT) and re-stimulated within the brain draining cervical lymph nodes by their cognate myelin antigen (37). The microbiota can be instructive to the encephalitogenic immune response as transplanting axenic TCR^{1640} mice with the microbiota of homozygous twins discordant for MS allowed for autoimmune demyelination only in mice receiving the microbiota of the diseased sibling (38).

The TCR^{1640} mice provide an interesting opportunity to study the mobilization of the humoral response. Importantly,

in these mice effector B cells are recruited from a B cell repertoire that is non transgenic and unmanipulated. Germinal centers are detected in the cervical lymph nodes of young RR mice prior to disease onset, implying that TCR^{1640} follicular helper T cells drive the isotype switching and affinity maturation of the MOG-specific B cell response (37). This B cell response is pathogenic as B cell depletion using anti-CD20 monoclonal antibodies prevents the development of spontaneous EAE in the TCR^{1640} mice (36). In this study we used recombinant MOG tetramers to trace the autoantigen-specific B cell response in the TCR^{1640} mice, which developed an acute EAE with late onset in our animal facility. Single B cell expansion provided evidence of a B cell clonotype that emerges over the course of spontaneous autoimmunity in the TCR^{1640} mice.

METHODS

Mice

Heterozygous TCR^{1640} SJL/j (36), homozygous IgH^{MOG} C57BL/6 mice (39), and heterozygous C57BL/6 2D2 mice (40) were housed under specific pathogen-free (SPF) conditions at the animal facility of the University of Lille which is accredited by the French Ministry of Agriculture to perform experiments on live mice in appliance to the French and European regulations on care and protection of the Laboratory Animals (EC Directive 2010/63). Water and food was provided *ad libitum*, hydrogels (Bioservice, Uden, The Netherlands) were added twice weekly. All experimental protocols were approved by the local ethics committee and and the Ministère de l'Enseignement Supérieur de la Recherche et de l'Environnement (5157-2016111011562655) in compliance with European Union guidelines.

EAE Scoring and Induction by Serum Transfer

EAE severity was scored as follows: 0, healthy; 1 for tail atony; 2 for hind limb weakness; 3 for hind limb paralysis; 4 for quadriplegia; 5 for moribund after at least 2 consecutive days of clinical disease. For serum transfer EAE, sera were transferred intravenously, *via* retro-orbital injection in disease-prone 2D2 TCR transgenic recipients. Each recipient received the serum of a single, distinct, donor. On day 0, 2D2 mice received 200 ng of pertussis toxin (List Biological Laboratories, Campbell, CA) intravenously by retro-orbital injection. Two days later a second i.v. injection of pertussis toxin was accompanied by either 50 µL of serum from disease-free TCR1640, diseased TCR1640 or NTL mice or either 50 µL of PBS.

Cell Isolation

Single-cell suspensions were prepared from spleen and cervical lymph nodes by mechanical disruption *via* forcing through 40-µm cell strainers. B-cells were purified using a mouse B-cell isolation kit (EasySTepTM Mouse B cell Isaolation Kit, Stemcell, Köln, Germany). For the isolation of brain infiltrating cells mice were anesthetized with ketamine and transcardially perfused with cold PBS. Brain and spinal cord were collected separately, homogenized and digested with 2 mg/ml collagenase D, 20 µg/ml DNase I, 1 µg/ml TLCK (Roche, Basel, Switzerland) for 30-45 min at 37°C. Adding 60 mM of EDTA stopped the reaction. Cells were then washed, resuspended in 37% of Percoll, layered on 70% Percoll and overlaid with 30% Percoll. After a 20-minute centrifugation at 2000 rpm the mononuclear cells were collected from the interface.

rMOGm Monomer and Tetramer Production

Polyethylenimine linear (PEI, CliniSciences, Nanterres, France) treated HEK cells were transfected with a pTT5 plasmid encoding for a histidine and Avi tagged $MOG_{1\text{-}125}$, according to the protocol described in (41). Transfection efficiency of 21% was determined using a GFP plasmid. After 7 days of culture, supernatants were collected and rhMOG was purified by affinity chromatography using His TrapTM HP columns (Cytivia, Marlborough, MA). rMOG was eluted using an imidazole gradient (Sigma-Aldrich), followed by dialysis against PBS. A single biotin molecule was attached to the AviTag using the biotinylating kit (BirA500 kit, Avidity, Aurora, CO). The single-biotin rMOGm monomer was tetramerized at a ratio of 4mol of biotin rMOGm monomer to 1 mol of FITC or PE-conjugated streptavidin (Biolegend, San Diego, CA). The rMOGm tetramer that we refer to as MOG_{tet} was validated by flow cytometry using splenocytes from IgH^{MOG} mice. Validated MOG_{tet} labelled at least 70% of MOG-specific B cells present among IgH^{MOG} splenocytes.

Flow Cytometry and FACS Sorting

For detection of cell surface markers, cells were stained in FACS buffer (PBS containing 1% BSA and 0.1% NaN_3) with fluorochrome-labelled monoclonal antibodies: APC-Cy7-conjugated anti-CD4 (RM4-5) or BV786-conjugated anti-CD4 (RMA-5], PE-Cy5-conjugated anti-CD19 (6D5) or Pacific-Blue-conjugated anti-CD19 (6D5), Pacific-Blue-conjugated anti-CD38 (6D5), Alexa Fluor 647-conjugated anti-GL-7 (GL7), PE-conjugated anti-CD138 (281-2), FITC-conjugated anti-IgM^b (AF6-78), APC-conjugated anti-CD45.1 (A20), PE-conjugated anti-CD45.2 (104); PerCP-Cy5-conjugated anti-B220 (RA3-6B2), BV-605-conjugated anti-CD19 (1D3), PE-Cy7-conjugated anti-FAS (Jo2), or Pacific-Blue-conjugated anti-CD19 (6D5), FTIC-conjugated anti-IgG1 (A85-1), PE-conjugated anti-IgM (DS-1), PE-conjugated anti-IgM^a (DS-1) (BD Biosciences, San Jose, CA). MOG-specific B cells were detected with single-biotin recombinant mouse MOG_{tet} using streptavidin-FITC or –PE. Viability of cells was evaluated by FACS analysis using 7AAD staining (BioLegend, San Diego, CA). For intracellular staining, cells were fixed and permeabilized in 4% paraformaldehyde/0.1% saponin in HEPES-buffered HBSS and stained intracellularly using the following antibodies: FITC-conjugated anti-IgG1 (185-1), PE-conjugated anti-IgM (DS-1). Samples were acquired using a BD LSRFortessa™ X-20 Cell Analyzer. For the iGB cultures $CD19^+CD20^+CD4^-$ singlets or MOG-tetramer$^+$ $CD19^+CD20^+CD4^-$ singlets were directly sorted into individual wells containing CD40LB feeder cells. Cell-sorting was performed using a FACS Aria III (Becton Dickinson). Analysis was performed using FlowJo (FlowJo, LLC, Ashland, OR) software V10.5.3.

Induced Germinal Center B Cells Single-B-Cell Culture

CD40LB cells are BALB/c 3T3 fibroblasts stably transfected with both CD40L and BAFF that are routinely used to expand purified B cells in a single-cell culture manner (EasySepTM Mouse B cell Isolation Kit, StemCell, Köln, Germany) (42, 43). On day -1, CD40LB feeder cells were seeded into 96-well plates at 600 cells per well in B cell media: RPMI 1640 medium (Gibco™) supplemented with 10% Gibco™ fetal bovine serum, 5.5 X 10^{-5} M 2-ME, 10 mM Gibco™ HEPES, 1 mM sodium pyruvate, 100 U/mL penicillin, 100 µg/mL streptomycin, and 1 X Gibco™ MEME Nonessential Amino Acid (Thermo Fisher Scientific, Waltham, MA). Next day (day 0), recombinant mouse IL-4 (final 2 ng/mL) and IL-21 (final 10 ng//mL) were added to the cultures, and then single B cells were directly sorted into each well using cell sorters (FACS Aria III, Becton Dickinson). On day 2, 50% (volume) of the culture media was removed from cultures and 100% (volume) of fresh BCM was added to the cultures. From day 3 to day 12 maximum, two-thirds of the culture media was replaced with fresh BCM every day. Depending on the cluster's quantity and viability, culture supernatants were harvested between 8 and 12 days for ELISA-analyses, B cell clusters harvested for RNA extraction. To establish cell expansion, we FACS sorted 20 polyclonal or MOGtet+ B cells from each studied organ of each mouse in a dedicated well of a CD40LB containing 96 well plate. Cell expansion was analysed after culture by counting viable cells on a Malassez® with blue trypan dead-cell exclusion. The cell expansion was calculated by dividing the total cell number by the 20 cells originally plated by FACS cell sorting.

Determination of Serum Titers of MOG-Specific Antibodies and of Total IgG1 Antibodies (ELISA)

Serially diluted serum collected from the indicated mice were transferred to 96-well ELISA plates Nunc MaxiSorp™ (Thermo Fisher Scientific, Waltham, MA) precoated with rMOGm or purified anti-IgG1 antibodies. After extensive washing, bound Ig was detected by a sandwich consisting of a biotinylated allotype- and isotype-specific anti-mouse IgG1 labelled with streptavidin-HRP (BD Biosciences, San Jose, CA). A colorimetric reaction was performed with an ATBS (2,2'-Azinobis [3-ethylbenzothiazoline-6-sulfonic acid]-diammonium salt) substrate and absorbance was measured at 405 nm.

RNA Extraction and PCR Analysis for Repertoire Analysis

Total RNA was isolated from B cells clusters after iGB-single culture by TRI Reagent extraction (TRI Reagent® Merck KGaA, Darmstadt, Germany) or the RNAeasy Mini Kit (Qiagen, Courtaboeuf, France), extracted RNA was treated with DNase I (0.1 U/µL, Invitrogen) and cDNA was synthesized using either hexanucleotide or oligo-dT primers and Superscript II Reverse Transcriptase (Invitrogen). We designed and validated primer sets to amplify VDJ gene segments of both the IgG kappa light chain (Igk) and heavy chain (IgHG). To this end, RNA was extracted from iGB cells and reverse-transcribed. Using Igk primer pairs a 500 bp cDNA amplicon was generated encoding the VJ region from either SJL/j or C57Bl/6 mice (**Supplementary Figure S1**). The IgHG primer pair amplified a 400 bp cDNA amplicon from the SJL/j, but not C57Bl6 mice, encoding the IgHG VDJ regions. We next proceeded to determine the BCR rearrangements of the clonal iGB cultures. iGB RNA was extracted from wells with confirmed B cell clusters and reverse-transcribed into cDNA. The variable regions of the IgHG and Igk were amplified by PCR using the above-mentioned primers (**Supplementary Table 1**). PCR products were purified using the QiAquick Gel extraction kit (Qiagen, Courtaboeuf, France) and sequencing confirmed variable parts of murine IgHG and IgHk chains (**Supplementary Figure S1**). PCR conditions used in this study are as follows: IgHG PCR, 94°C for 3 min, followed by 20 cycles of 94°C for 10 s, 67°C for 20 s, 72°C for 20 s, with a progressive determined variation of 0.5°C per cycle;35 cycles of 94°C for 30 s, 57°C for 30 s, 72°C for 1 min; and 72°C for 10 min; and gHk PCR, 94°C for 3 min, followed by 20 cycle of 94°C for 10 s, 68°C for 10 s, 72°C for 20 s with a progressive determined variation of 0.5°C per cycle. VDJ amplimers were gel purified using the QiAquick Gel extraction kit. Sanger sequencing was performed by GENOSCREEN (Lille, France). Sequences obtained for Igk and IgHG chains were submitted to IMGT/V quest and tools (http://www.imgt.org/) to define junction decryptions for each sequences and corresponding amino-acid sequences to determine the different clonotypes.

Statistics

GraphPad PRISM version 9 (San Diego, CA) was used for statistical analyses and graphs. EAE incidence and mortality was analyzed by Kaplan-Meier plots and statistical significance was calculated using the log rank test. Two-way ANOVA was used to compare the clinical evolution of EAE. Linear regression was used to evaluate correlations. A two-tailed unpaired t-test was used for comparing antibody detection, B cell frequencies and the cumulative disease scores. Levels of statistical significance are graded as follows: NS, Not Significant; *$p < 0.05$; **$p < 0.01$; ***$p < 0.001$; ****$p < 0.0001$.

RESULTS

Spontaneous EAE in TCR^{1640} SJL/j Mice

We established the disease incidence and evolution of the TCR^{1640} mice in our local SPF animal facility. Our colony was rederived by *in vitro* fertilization and the first 2 filial generations were analyzed for spontaneous disease evolution. Animals were scored twice weekly for presence or absence of EAE. As demonstrated in **Figure 1A**, over a period of 500 days 94% of mice spontaneously developed EAE, with an increased incidence for female mice. None of the 166 non-transgenic littermates (NTL) developed disease. In the TCR^{1640} mice earliest EAE onset was observed after 57 days with an average onset for the cohort of 197 ± 87 days. Practically, between the age of 60-500 days the

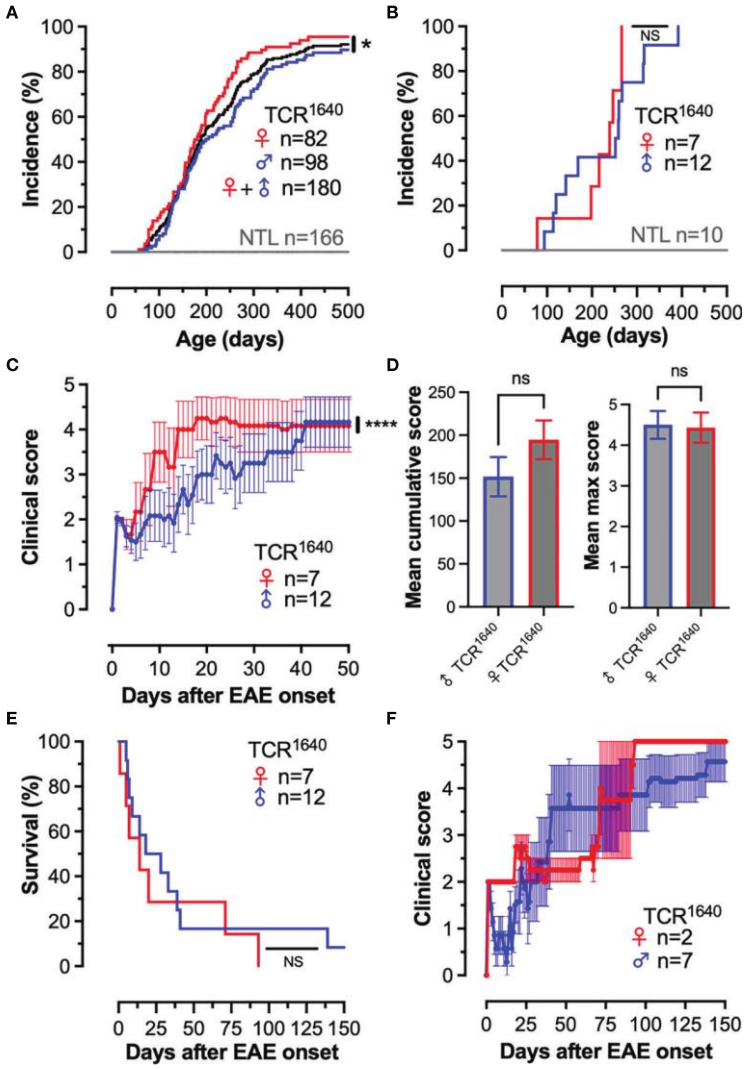

FIGURE 1 | Development of spontaneous progressive EAE in TCR^{1640} mice. **(A)**: Disease incidence over time. EAE onset was monitored twice weekly among male TCR^{1640} (Blue; n = 98) and female TCR^{1640} (Red; n = 82) together with their non-transgenic littermates (Grey; n = 166). Gender independent disease incidence (Black; n = 180). 50% of the TCR^{1640} mice developed EAE after 225 days of age and 80% of mice developed disease after 300 days of age. **(B–F)** Clinical evolution of a dedicated cohort of 19 TCR^{1640} mice and 10 non-transgenic littermates that was monitored daily. **(B)** Disease incidence over time. Male TCR^{1640} (Blue; n = 12) and female TCR^{1640} (Red; n = 7) together with their non-transgenic littermates (Grey; n = 10). **(C)** Clinical disability of female (n = 7) and male (n = 12) TCR^{1640} is presented as the mean EAE score ± SEM for the first 50 days after disease onset. **(D)** Mean cumulative score (left) and mean maximum score (right) for the first 50 days after disease onset. **(E)** Kaplan-Meier curve presenting the probability of survival after disease onset for the male TCR^{1640} (Blue; n = 12) and female TCR^{1640} (Red; n = 7) mice. An acute mortality of 50% is observed for TCR^{1640} mice within 19 days after disease onset. **(F)** The clinical evolution of the remaining 50% of mice surviving beyond 19 days is presented. The mean chronic progressive score +/- SEM is presented for 9 TCR^{1640} mice; male TCR^{1640} (Blue; n = 7) and female TCR^{1640} (Red; n = 2). Log-rank tests were performed for comparisons **(A, B, E)**; 2-way ANOVA **(C)**; Student t-test (**D**, left); Mann Whitney U test (**D**, right). NS, Not Significant; *p < 0.05; ****p < 0.0001.

TCR^{1640} mice developed EAE at an average frequency of 1.5% per week.

A dedicated cohort of 19 TCR^{1640} mice and 10 non-transgenic littermates was monitored daily for a period of 150 days (**Figures 1B–F**). None of the NTL developed EAE, while all of the TCR^{1640} littermates spontaneously developed EAE (**Figure 1B**). Most of the TCR^{1640} mice developed a paralytic disease without relapses, which flared more intensely in female mice (**Figure 1C**). No statistically significant differences were observed for the mean cumulative score and mean maximum score between male and female mice (**Figure 1D**). Mortality exceeded 90% and occurred as early as 6 days after disease onset (**Figure 1E**). In half of the diseased TCR^{1640} mice (46.7%) the clinical evolution was acute causing mortality within 19 days (10.9 days ± 5.7) (**Figure 1E**). The other half that survived beyond 19 days developed a chronic progressive disease (**Figure 1F**).

Our results corroborate the susceptibility of the TCR^{1640} mice to spontaneous autoimmune encephalomyelitis. Contrary to the original description (36), our colony develops an acute or chronic disease as opposed to the relapsing-remitting disease originally reported for the TCR^{1640} mice.

We next assessed if the chronic EAE in TCR^{1640} mice mobilizes the humoral response, as has been reported for the initial RR variant (36). The TCR^{1640} expressed on 70% of CD4 T cells is specific for one $I\text{-}A^{s}$ restricted epitope of myelin oligodendrocyte glycoprotein ($MOG_{92\text{-}106}$) a highly encephalitogenic myelin protein. Pathogenic MOG-antibodies recognize conformational epitopes. To detect their presence in peripheral blood we analyzed their titers by ELISA using recombinant mouse $MOG_{1\text{-}125}$. Serum was collected from diseased TCR^{1640} mice during the first five days after onset together with age- and sex-matched non-transgenic littermates and disease-free TCR^{1640} mice (**Figure 2**). Compared to NTL mice, a significant increase in anti-MOG antibodies was detected in the sera from TCR^{1640} mice, which is coherent with the development of a MOG-specific humoral response in diseased TCR^{1640} mice (**Figure 2B**). Unexpectedly, the disease free TCR^{1640} mice similarly developed a MOG-specific IgG1 response that was significantly increased compared to NTL mice and similar to that detected in diseased TCR^{1640} mice (**Figure 2B**). Total IgG1 titers did not significantly differ between sera from healthy and disease TCR^{1640} mice and NTL mice (**Figure 2A**).

We next correlated the MOG-antibody titers with age and disease severity in order to assess if these factors influence the MOG humoral response. As demonstrated in **Figures 2C, D** neither disease severity in diseased TCR^{1640} mice or age of disease-free and diseased TCR^{1640} mice significantly influenced MOG-antibody titers.

To assess the pathogenicity of the humoral response we transferred individual sera from NTL and TCR^{1640} mice into EAE-prone 2D2 TCR transgenic mice. These mice carry a

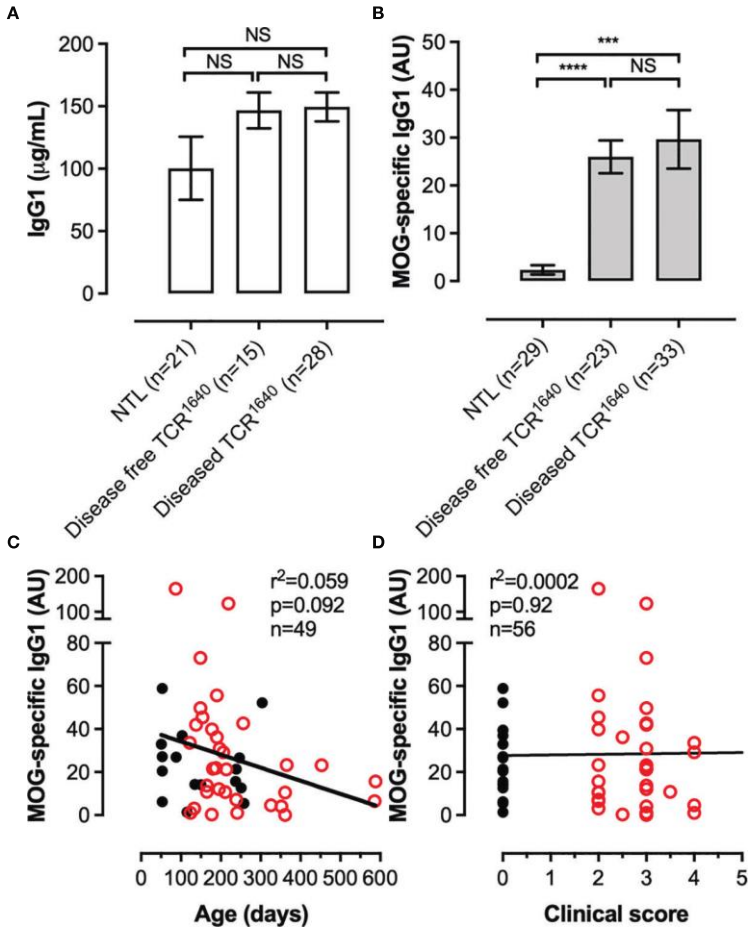

FIGURE 2 | A MOG-specific humoral response develops in TCR1640 mice independent of clinical disease. **(A)** Total IgG1 and **(B)** MOG-specific IgG1 antibodies were detected in the sera of NTL, Disease-free TCR^{1640} and diseased TCR^{1640} mice. Data represents the mean ± SEM of n serum samples. Correlation with **(C)** age or **(D)** clinical intensity of MOG-antibody titres for individual disease-free TCR^{1640} (Black circles, n = 23) and diseased TCR^{1640} mice (Red circles, n = 33). Student t-test **(A, B)**; Fisher exact for linear regressions **(C, D)**. NS, Not Significant; ***$p < 0.001$; ****$p < 0.0001$.

MOG_{35-55} specific transgenic TCR on the C57BL/6 background, but do not develop a MOG-specific B cell response/anti-MOG antibodies (40). Spontaneous EAE development is observed in 1% of our 2D2 colony (data not shown), however, *i.v.* injections of pertussis toxin at a 2-day interval allows for EAE development in 50% of 2D2 mice (**Figure 3A**). When transferring 50 µg of the MOG-specific IgG1 mAb 8-18C5 EAE incidence is raised to 100% causing severe paralytic disease (**Supplementary Figure S2**). The transfer of sera from NTL failed to significantly alter disease incidence and EAE severity compared to PBS controls (**Figures 3A, B**). No difference was observed for the cumulative disease score or the maximum disease score (**Figures 3C, D**). Transfer of sera from disease-free TCR^{1640} mice resulted in disease with reduced severity compared to the PBS controls that reached statistical significance with the 2-way ANOVA (**Figure 3B**). No statistically significant variance was observed for disease incidence, cumulative score, or maximum score between sera from the disease-free TCR^{1640} mice and PBS controls (**Figures 3A, C, D**). By contrast, sera from diseased TCR^{1640} mice induced EAE in 82% 2D2 recipients (**Figure 3A**) and significantly increased the cumulative EAE score relative to the NTL-serum and PBS injected groups (**Figure 3B**). Both the cumulative disease score and maximum disease score increased significantly after transfer of sera from diseased TCR^{1640} mice (**Figures 3C, D**). These findings demonstrate that sera containing MOG-specific antibodies of adult TCR^{1640} mice exacerbate disease in EAE-prone recipients only when derived from diseased TCR^{1640} donor mice.

Tracking MOG-Specific B Cells in the Secondary Lymphoid Organs and Central Nervous System of TCR^{1640} Mice

To identify and track MOG-specific B cells we produced single-biotin avitagged recombinant mouse MOG_{1-125} which was tetramerized using fluorochrome labelled streptavidin (MOGtet). To assess the sensitivity of the MOG_{tet} we serially diluted MOG-specific B cells from $CD45.2^{+/+}$ IgH^{MOG} mice among $CD45.1^{+/+}$ B cells from wild-type C57BL/6 mice (**Figure 4**). The MOG tetramer specifically stained the congenic IgH^{MOG} B cells, with only low frequency labelling

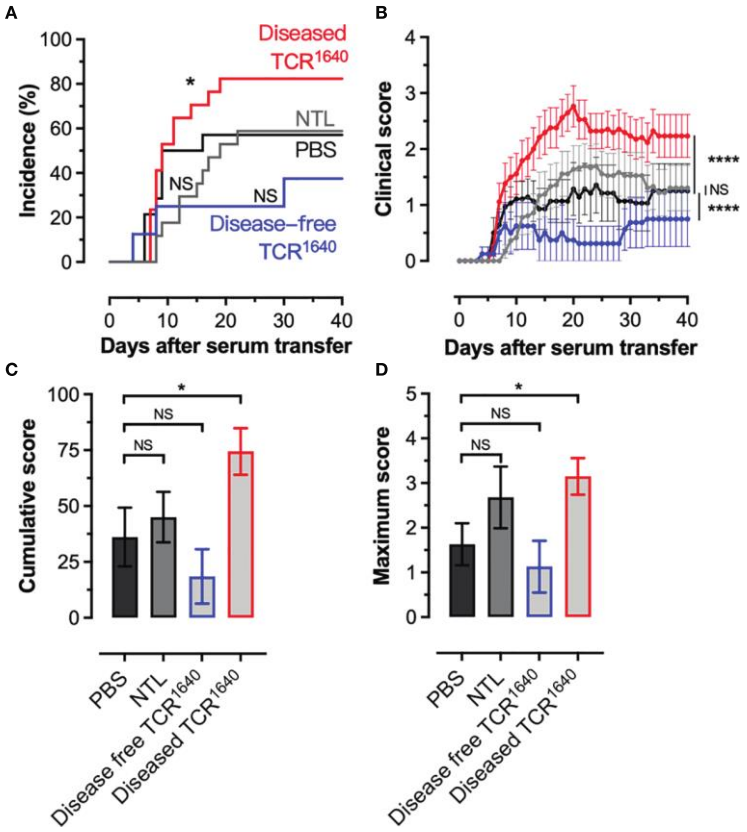

FIGURE 3 | Pathogenicity of MOG-antibodies by serum transfer into EAE prone recipients. **(A, B)** Mild EAE develops in 2D2 MOG-TCR Tg mice after 2 injections (Days 0, 2) of *pertussis* toxin (Incidence 50%). These PT treated 2D2 mice received PBS (n=14) or serum from disease-free TCR^{1640} mice (n = 8), diseased TCR^{1640} mice (n = 17) or NTL mice (n = 18) 2 days after the first PT injection. **(A)** Incidence of EAE over time. **(B)** Mean clinical disability ± SEM presented over time (days after serum transfer). Log-rank test **(A)**, 2-way ANOVA **(B)**, student t-test **(C)**, Mann-Whitney U test **(D)** was used to compare the clinical evolution of EAE. The data was pooled from 4 individual experiments in which sera from single donor mice were transferred into individual 2D2 recipients. NS, Not Significant; *$p < 0.05$; ****$p < 0.0001$.

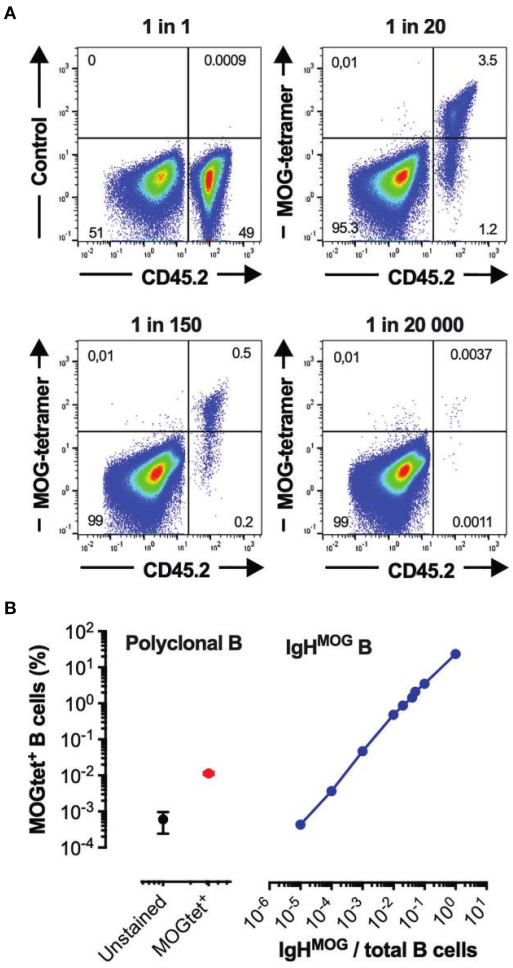

FIGURE 4 | Validation and sensitivity of the recombinant MOG_{1-125}-tetramer. **(A, B)** Purified CD45.2$^{+/+}$ B cells from homozygous C57Bl/6 IgH^{MOG} mice were mixed *in vitro* with purified B cells from congenic CD45.1$^{+/+}$ mice at the indicated ratios. **(A)** A representative flow cytometry profile demonstrating the capacity of Streptavidin-FITC MOG_{1-125}-tetramers to identify IgH^{MOG} B cells among polyclonal CD45.1$^{+/+}$ B cells (Top right, bottom), the Streptavidin-FITC MOG_{1-125}-tetramers were omitted in the control samples (Top left) **(B)** Sensitivity of the Streptavidin-FITC MOG_{1-125}-tetramers in detecting the precursor frequency of the IgH^{MOG} B cells. Left panel, MOG-tet^{+} staining of CD45.1$^{+/+}$ polyclonal B cells (red circle), and the control staining without the MOG_{tet} (black circle). Right panel, MOG-tet^{+} staining off CD45.2$^{+/+}$ IgH^{MOG} B cells serially diluted among CD45.1$^{+/+}$ polyclonal B cells (blue line). The mean +/- SEM is presented from 2 pooled experiments.

among the polyclonal B cells (**Figure 4A**). The IgH^{MOG} MOG-specific B cells could be detected at a minimal frequency of approximately 1 in 10^4 B cells (**Figure 4B**). Next, we performed *ex vivo* analysis of the B cell compartment of NTL and TCR^{1640} mice to enumerate the MOG-specific B cell response. On average 73+/-10% (SEM) of B cells were positive in the MOGtet staining in IgH^{MOG} mice which were included as a positive control (**Figures 5A, B**). By focusing primarily on brain-infiltrating MOG-specific B cells, we chose to preserve all TCR^{1640} mice until the development of clinical EAE. The 2 disease-free mice were excluded from the analysis in **Figures 5B–D** because of the low number of mice for statistics. In adult NTL the frequencies of MOG^{+}_{tet} B cells remained below 0.1% in the spleen and below 0.2% in the brain-draining cervical lymph nodes (cLN) (**Figure 5B**). Upon development of disease the TCR^{1640} mice demonstrated an increase in MOGtet^{+} B cells reaching an average of 1.0+/-0.3% in the cLN (**Figure 5C**). A similar presence of MOG^{+}_{tet} B cells was detected among the mononuclear cells isolated from pooled brains of diseased TCR^{1640} mice, which averaged at 1.0+/-0.2 (**Figure 5D**). These data suggest that in diseased TCR^{1640} mice the MOG-specific B cells reside predominantly in the cLN and brain. We next correlated MOG-specific B cell frequencies with the time after EAE onset to assess any temporality in MOG-specific B cells during EAE progression. In the inflamed brain the proportion of MOG^{+}_{tet} B cells remained relatively stable over time while the precursor frequency of MOG^{+}_{tet} B cells in the cervical lymph nodes was more varied (**Figures 5E, F**). This dataset is coherent with the activation of MOG-specific B cells in the brain-draining cLN prior to infiltration of the inflamed brain.

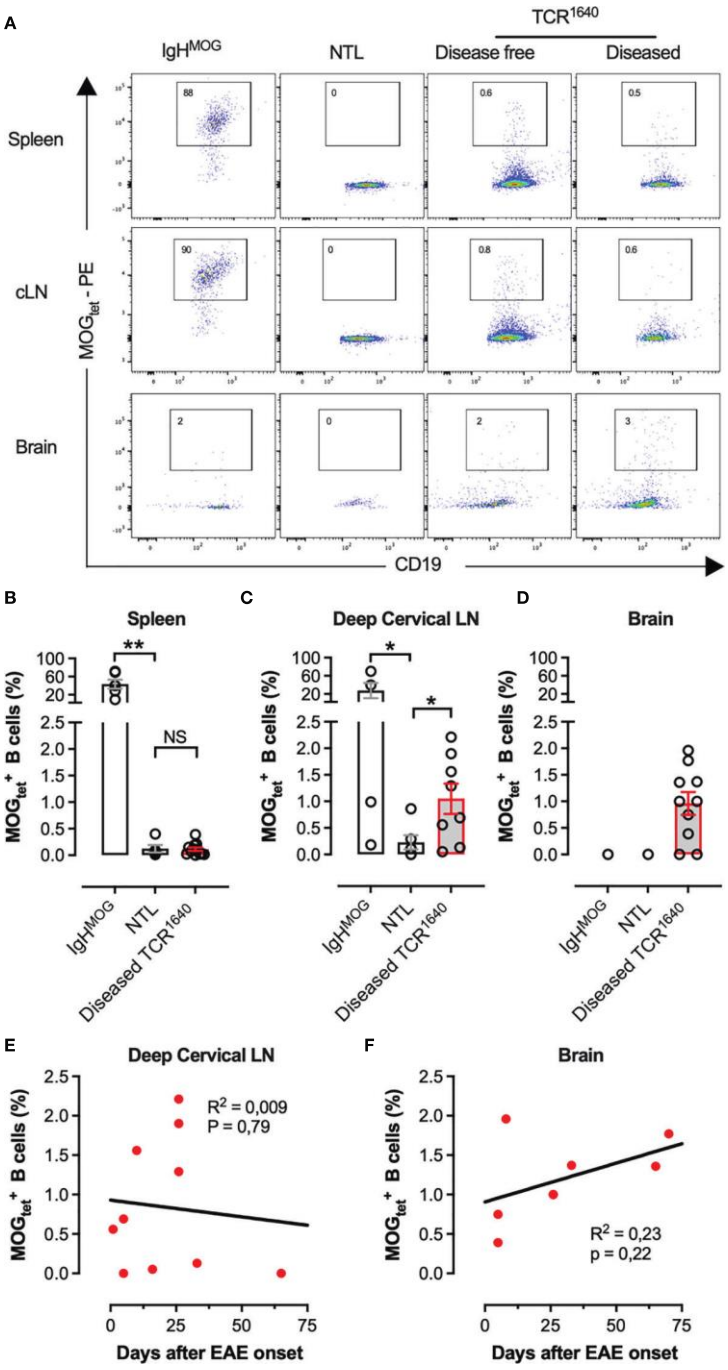

FIGURE 5 | Frequency and localisation of MOG^{+}_{tet} B cells in TCR^{1640} mice; **(A)** A representative flow cytometry profile gated on viable $CD4^{neg}$ $CD20^{+}CD19^{+}$ B cells. MOG_{1-125}-tetramer staining of single cell populations from the spleen (top row), cervical lymph nodes (middle row), and percoll purified mononuclear cells from the brain (Bottom row) are presented from IgH^{MOG} mice (Left column), NTL (center left column), disease-free TCR^{1640} (center right column) and diseased TCR^{1640} mice (right column). Data representative of 3 independent experiments. **(B)** Precursor frequency of MOG^{+}_{test} B cells in the spleen (IgH^{MOG} n = 6; diseased TCR^{1640} n = 12; NTL n = 5), **(C)**, cervical lymph nodes (IgH^{MOG} n = 4; diseased TCR^{1640} n = 8; NTL n = 6), and **(D)** brain (IgHMOG n = 2; diseased TCR^{1640} n = 10; NTL n = 3). The mean frequency of n samples +/- SEM is presented. **(E, F)** Correlation between the frequency of MOG^{+}_{test} B cells and the delay after EAE onset in deep cervical lymph node **(E)** or in brain **(F)** in diseased TCR^{1640} mice. Student t-test **(B, C)**; Fisher exact for linear regressions **(E, F)**. NS, Not Significant; *p < 0.05; **p < 0.01.

Clonality of the MOG-Specific B Cell Response

Adopting a culture system for expansion and differentiation of B cells developed by Kitamura and colleagues, we established a clonal B cell expansion protocol using 3T3 fibroblasts stably transfected with both CD40L and BAFF (CD40LB cells) supplemented with IL-4 and IL-21 (42). This clonal amplification strategy multiplies the genetic material required to sequence the BCR rearrangement of paired heavy and light chains. In parallel, antigen-specificity is determined by ELISA using the supernatants after clonal B cell expansion.

Supplementary Figure S3 and **Figure 6** show the efficacy of expansion of single B cells isolated from BALB/c spleen and from brain infiltrating single B cells of diseased TCR^{1640} mice, respectively, in the induced germinal B cell (iGB) culture. B cell expansion was accompanied by differentiation. *In vitro* flow cytometry analysis of the B cell clusters demonstrated that half of the B cells had differentiated into CD138-positive plasmablasts while the phenotype of the other half showed a germinal center B cell phenotype with limited CD38 expression and strong induction of FAS, GL7 and Peanut agglutinin (**Figure 6A**). In response to the added cytokines IL-4 and IL-21, isotype switching from IgM to IgG1 was observed for 98% of B cells (**Figure 6A**).

The efficacy of expanding single B cells in iGB cultures was similar for B cells isolated from the cLN of disease-free and diseased TCR^{1640} mice. B cell expansion was observed for 46% and 39% of clones with an average fold amplification of 6300 and 4588 for disease-free versus diseased TCR^{1640}, respectively

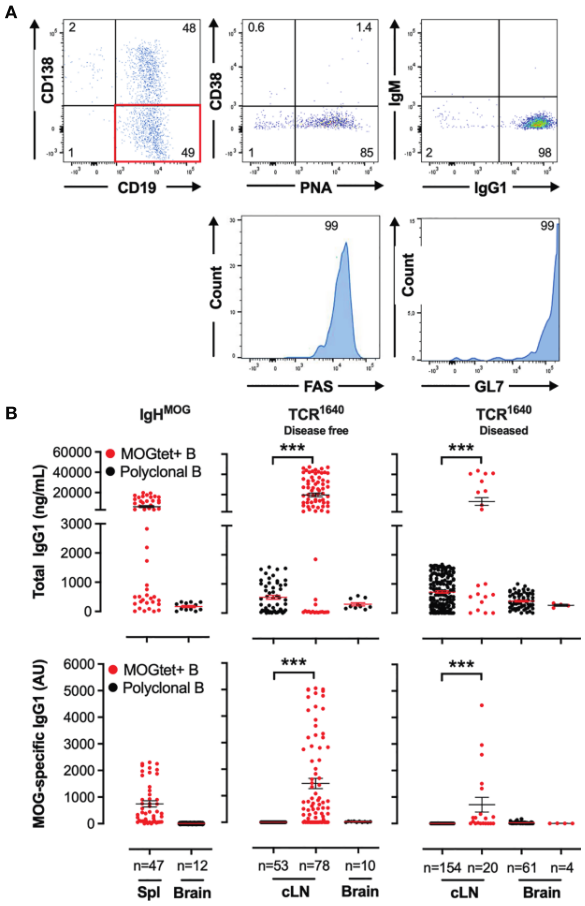

FIGURE 6 | Identification of MOG-specific B cell clones by measuring total IgG1 and MOG-specific IgG1 antibody titres in the supernatants from single-cell iGB cultures. **(A)** Differentiation of clonal B cells into CD138$^+$ plasma cells and CD38$^-$ GL7$^+$FAS$^+$PNA$^+$ germinal centre B cells. iGB cultures of single B cells isolated from the cervical lymph nodes and brain of diseased TCR^{1640} mice were analysed by flow cytometry after 8 days of culture. A representative profile of viable CD19$^+$ B cells demonstrate presence of CD138 plasma cells (Top row, left plot), and gated on CD19$^+$CD138$^-$ B cells (Red quadrant) the expression of CD38 and PNA (top middle, intracellular IgG1 and IgM (top right), and histograms for FAS (bottom left) and GL7 (bottom right). **(B)** Total IgG1 (top row) and anti-MOG IgG1 (bottom row) antibodies were detected in supernatants from spleen, cervical lymph nodes, and brain-derived single B cell iGB cultures from IgH^{MOG} (Left column), disease-free TCR^{1640} (middle column) and diseased TCR^{1640} mice (right column). Clonal B cells were isolated from the polyclonal CD19$^+$ B cell compartment (black circles) or from the CD19$^+$ MOG$^+_{test}$ B cell response (red circles). The individual antibody concentration of n clonal iGB cultures is presented together with the Mean +/- SEM. Data represents the pooled results of 3 independent experiments and was analysed with a t-test. ***$p < 0.001$.

(**Supplementary Figure S4**). Sorting MOG_{tet}-positive B cells from the cLN of disease-free and diseased TCR^{1640} mice permitted the expansion of 40% and 39% of clones with a 5167 and 3233 fold-amplification, respectively (**Supplementary Figure S4**). This demonstrates the efficacy of single-cell iGB cultures derived from the secondary lymphoid organs. The efficacy proved more modest for effector B cells isolated from the brain. Single B cell cultures of B cells from disease-free and diseased TCR^{1640} mice induced expansion in only 3.6% and 13.1% of cultures with a fold-amplification of 1217 and 2686 (**Supplementary Figure S4**). Isolating MOG^{+}_{tet} B cells from the brain of diseased TCR^{1640} mice proved most challenging as only 4% of single-cell cultures showed evidence of abortive proliferation by B cell clusters evolving to rapid cell death (**Supplementary Figure S4**).

To establish specificity of the B cell clones for MOG we collected the culture supernatants of proliferating cultures and determined the concentration of MOG-specific antibodies by ELISA (**Figure 6B**). MOG-specific antibody production could not be detected among the 47 splenic iGB clones derived from NTL mice (data not shown), which is coherent with the low precursor frequency of MOG-specific B cells in the polyclonal repertoire of wild-type mice. For the single cell iGB cultures from the TCR^{1640} mice sorting antigen-specific B cells *via* MOGtet-staining significantly enhanced the efficacy of isolating MOG-specific B cell clones (**Figure 6B**, bottom row). MOG^{+}_{tet} iGB cultures also resulted in higher IgG1 titers compared to the polyclonal iGB cultures. In the MOG^{+}_{tet} iGB cultures from IgH^{MOG} mice all IgG1 antibody producing cultures were MOG-specific (**Figure 6B**). iGB cultures from $MOGtet^{+}$ B cells derived from TCR^{1640} mice induced IgG1 antibody production of which 69% were MOG specific in disease-free mice and 50% were MOG-specific in diseased mice (**Figure 6B**).

The abortive proliferation of brain-derived MOG^{+}_{tet} iGB cultures probably underlies the absence of detectable MOG-specific antibodies in the culture supernatants. Taken together these data demonstrate the efficacy of iGB cultures in expanding polyclonal or tetramer-binding B cells from secondary lymphoïd organs. The iGB cultures proved less efficient in expanding autoantigen-specific B cell clones that were isolated from the inflamed target tissue.

Repertoire Analysis

Few studies have addressed the B cell repertoire in SJL/j mice. Here, a total of 380 iGB cell clusters were analysed. From disease-free TCR^{1640} mice individual polyclonal B cells from the cLN (n=53) and brain (n=10) as well as MOG^{+}_{tet} B cell clones from the cLN (n=78) were sequenced. From diseased TCR^{1640} mice individual polyclonal B cells from the cLN (n=154) and brain (n=61) as well as MOG^{+}_{tet} B cell clones from the cLN (n=20) and brain (n=5) were sequenced. Only 11 IgHG and 21 Igk sequences were obtained (**Tables 1**, **2**) and their VDJ rearrangements were analysed using the IMGT website (http://www.imgt.org). As presented in **Table 1**, 11 unrelated IgHG sequences were obtained providing no evidence of *in vivo* clonal expansion. By contrast, the Igk light chains did provide evidence of selected CDR3 sequences. **Table 2** presents the 21 obtained Igk sequences that were segregated based on MOG specificity. The CDR3 encoding junctional sequences revealed 3 consensus sequences of which 2 are confirmed to be derived from MOG-specific B cell clones. The "CQQXSSYPXTF" sequence was deduced from 13 iGB clones that were derived from diseased (n=11), but also from the cLN of non-diseased (n=2) TCR^{1640} mice. MOG-specificity was confirmed for one clone isolated from brain (n=4) and one clone derived from the cLN (n=7) of diseased TCR^{1640} mice. The majority of iGB clones produced total IgG titers below 1 μg/ml, a concentration insufficient to reliably detect MOG antibodies (ND). A second consensus light chain sequence derived from MOG-specific iGB clones was identified as "CQQHNEXPWTF". This consensus junctional sequence was obtained from clonal B cells isolated from the brain and cLN of diseased TCR^{1640} mice. A third consensual junctional sequence was identified as "CQXGVVTHPX" on kappa light chains derived from the cLN of non-diseased TCR^{1640} mice and was not associated to MOG-reactivity. 2 heavy and light chain pairs were identified. The kappa light-chain V15-103*01-J1*02 with the consensual junctional

TABLE 1 | VDJ rearrangements and junctional sequence of the IgG heavy chain of clonal iGB B cells.

$MOGtet^{+}$	MOGAbs	EAE	Organ	Clonotype	V-geneallele	D-geneallele	J-geneallele	AA junction
-	+	3.5	cLN	6	V1-80*01	D1-1*01	J2*03	CAR RGY XXX SXY XXY X
-	ND	3	cLN	1	V1-18*01 (a)	D2-3*01	J4*01	XQE GXG ISM LWT T
-	ND	3	cLN	3	V5-17*01 (b)	D1-1*01	J3*01	CXX XYX YGS TAW FAX W
-	ND	3	cLN	10	V1-50*01	D1-1*01	J3*01	CAR GGY GSS PAW FAX X
-	ND	3.5	cLN	2	V1-42*01	D3-1*01	J*03	XAR RXR SXW XXX X
-	ND	3	cLN	4	V1-18*01	D2-3*01	J2*03	XAR WGG GFX YX
-	ND	3	cLN	5	V1-69	D1-1*01	J4*01	CAR RGX XSX SXX XXS
-	ND	3	cLN	7	V1-18*01	D2-1*01	J3*01	CAR VNL AWF XYW
-	ND	0	cLN	8	V1-39*01	D4-1*01	J2	CAR RLG REX XXX X
-	ND	3	cLN	9	V1-82*01	–	J2	CAR GXY W
-	ND	3	cLN	11	V1-53*01	D4-1*01	J2	CAR ERX GXX YX
						Consensus sequence		CAR XXX XXX

The first two columns indicate MOG-specificity determined as MOG-tetramer binding during cell-isolation (column 1) or MOG-antibody production determined by ELISA in the iGB culture supernatant (column 2). Columns 3 and 4 refer to the EAE clinical score at the day of sacrifice and the organ from which the B cell clones were isolated. BCR rearrangement is presented as the individual V-D-J gene alleles and the junctional sequence of the hypervariable region. ND (Not detected). (a) and (b) refer to the pair (a) or (b) of IgG heavy and kappa chains from the same iGB culture well (see ***Table 2****).*

*The * refers to the immunoglobulin nomenclature which defines the use of an asterix to refer to different allele polymorphisms.*

+ means positive; - means negative.

TABLE 2 | VJ rearrangements and junctional sequence of the kappa light chain of clonal iGB B cells.

MOGtet+	MOGAbs	EAE	Organ	Clonotype	V-geneallele	D-geneallele	J-geneallele	AA junction
-	+	3	Brain	2	V2-109*01	–	J4*01	CXQ NXE XPW TF
+	+	3	cLN	3	V4-57-1*01	–	J1*01	CQQ HNE XXW TX
-	ND	3	cLN	4	V16-104*01 (a)	–	J1*01	CQQ HNE XXW XX
						Consensus sequence		CQQ HNE XPW TF
-	ND	3	Brain	3	V1-133*01	-	J1*01	CVQ GTH FPX TF
-	ND	3	cLN	6	V4-55*01	-	J2*01	CQQ XSS YPP T
-	-	3	cLN	5	V4-55*01	-	J5*01	CQQ WSS YPL TX
-	ND	3	cLN	13	V4-55*01	-	J5*01	XQQ WDS YPP TF
-	ND	3	cLN	5	V4-57*01	-	J5*01	CQQ RSS YPX TX
-	+	3	Brain	4	V4-61*01	-	J1*01	CQQ YXS YPR TX
-	ND	3	cLN	4	V4-92*01	-	J5*01	CQQ GSS SPL TX
+	+	3	cLN	5	V8-24*01	-	J4*01	CQQ XSG XPX TX
-	ND	0	cLN	1	V8-24*01	-	J2*01	CQQ HYX TPY TX
-	-	0	cLN	3	V8-19*01	-	J5*01	CQN DXS XPX TX
-	ND	3	Brain	2	V8-28*01	-	J4*01	CXQ DHS YPF TX
-	ND	3	Brain	1	V8-30*01	-	J2*01	CQQ YYS YPY TF
-	ND	3	cLN	12	V15-103*01 (b)	-	J1*02	XXQ GXS XXX TX
						Consensus sequence		CQQ XSS YPX TF
-	ND	0	cLN	7	V4-81*01	-	J5*01	XQX GVV THP X
-	ND	0	cLN	8	V6-15*01	-	J1*01	CQX XVV THP X
						Consensus sequence		CQX GVV THP X
-	ND	3	cLN	9	V3-9*01	-	J3*01	XCK VGR FRG RX
-	ND	0	cLN	10	V5-48*01	-	J5*01	CQQ SNX GQP R
-	ND	3	cLN	11	V19-93*01	-	J1*01	CLQ YDN LXT X
						Consensus sequence		CXQ XXX XXX RX

The first two columns indicate presence (+) of MOG-specificity determined as MOG-tetramer binding during cell-isolation or MOG-antibody production in the iGB culture supernatant. Columns 3 and 4 refer to the EAE clinical score at the day of sacrifice and the organ from which the B cell clones were isolated. BCR rearrangement is presented as the individual V-J gene alleles and the junctional sequence of the hypervariable region. The top two consensus sequences (or clonotypes), in white and pink chadings, are associated with MOG-antibody producing and MOGtet+ B cell clones. The third consensus sequence (or clonotype), in orange shading, was identified among cLN B cells of disease free TCR1640 mice. The last group of remaining sequences provided no linear homology (Grey). ND (Not detected). (a) and (b) refer to the pair (a) or (b) of IgG heavy and kappa chains from the same iGB culture well (see ***Table 1****).*

*The * refers to the immunoglobulin nomenclature which defines the use of an asterix to refer to different allele polymorphisms.*

sequence CQQXSSYPXTF was paired with the heavy chain V5-17*01, D1-1*01, J3*01, CXXXYXYGSTAWFAXW. The second BCR comprised a kappa light-chain V16-104*01, J1*01with the consensual junctional sequence CQQ HNE XPW TF was paired with the heavy chain V1-18*01, D2-3*01, J4*01, XQEGXGISM LWTT. The consensual amino-acid sequences of the junctional region were submitted to the protein BLAST tool from NCBI with mus musculus (taxid:10090) as targeted organism (http://blast.ncbi.nlm.gov/Blast.cgi?PAGE=Proteins). This short consensual amino-acid sequence for Igk probed 97 different hits representing for the large majority of other light chain sequences. The distance tree of this analysis (**Supplementary Figure S4**) corroborated the relevance of this consensual amino-acid sequence to rodents and especially mus musculus as part of the Igk region sequences (Fast Minimum Evolution, 0.90 of max sequence difference, distance of Grishin for proteins). These results indicate that despite the limited efficacy shared light chain rearrangements could be identified in the cLN and brain of the TCR^{1640} mice suggestive of clonal expansion.

DISCUSSION

The environment critically influences autoimmune disease (44). Female non-obese diabetic mice spontaneously develop type 1 diabetes in SPF animal facilities while they remain healthy in conventional environments (45). This extends to spontaneous animal models of MS-like disease that have emerged among MOG-specific TCR transgenic mice. On the C57Bl/6 background, the $I\text{-}A^b$: $MOG_{35\text{-}55}$ specific 2D2 TCR transgenic mice were originally ascribed to develop optic neuritis (40), but may develop EAE with an incidence of up to 18% (46, 47), and in our facility the 2D2 colony developed EAE with an incidence of 1% (Data not shown, 2D2 = 199; wild type littermates n=203; monitoring of 250 days). The EAE susceptibility of the TCR^{1640} SJL/j colony housed in our facility was preserved as indicated by the 94% EAE incidence at the age of 500 days. Unlike the originally reported relapsing-remitting disease (36), our TCR^{1640} colony spontaneously developed a chronic progressive EAE that proved moribund for half of the mice within 3 weeks of onset. Clinically, disease was delayed with onset at the age of 225 days for 50% of TCR^{1640} mice, as opposed to an age of 110 days for the original TCR^{1640} colony. A gender difference was observed with disease flaring more quickly in females. Our study thus reiterates the environmental influence of EOPS animal facilities in spontaneous EAE in genetically identical mouse strains.

Within the context of spontaneous EAE, this study assessed the mobilization of MOG-specific B cells from the polyclonal B cell repertoire of TCR^{1640} mice. To this end we produced recombinant MOG tetramers to trace the autoantigen-specific

B cell response in the TCR^{1640} mice. In concordance with previous studies, MOG^{+}_{tet} B cells accumulated in the brain-draining cervical lymph nodes and the brain of TCR^{1640} mice that had spontaneously developed EAE. The specificity of the MOG_{tet} was validated using serially diluted IgH^{MOG} B cells among congenic polyclonal B cells indicating that a clonal frequency of high affinity B cells at 1 in 10^3-10^4, was detectable (**Figure 4**). We confirmed the specificity of the MOG_{tet} for polyclonal B cells using the clonal MOG^{+}_{tet} iGB cultures which demonstrated that all IgG1 antibody producing MOG^{+}_{tet} clones were MOG-specific (**Figures 5**, **6**). The mobilization of the MOG^{+}_{tet} B cell response precedes clinical EAE. In disease-free TCR^{1640} mice MOG-specific B cells could be detected and their iGB cultures demonstrated the production of MOG-specific antibodies by all IgG1 producing clones (**Figures 5**, **6**). This mobilization of the MOG-specific humoral response could be observed as early as 7 weeks by the detection of circulating MOG-specific antibodies in TCR^{1640} sera of disease-free mice (**Figure 2**). The absence of correlation between MOG-antibody titers and spontaneous EAE onset is undoubtedly mediated by the difficulty for antibodies to penetrate the brain parenchyma under physiological conditions. Passive models of MOG-antibody mediated EAE (notably demonstrated with the mouse IgG1 monoclonal antibody 8-18C5) require moderate neuroinflammation and blood-brain-barrier permeability in order to mediate CNS demyelination (48, 49). Our results, using the adoptive serum transfers to EAE-prone 2D2 recipient mice indicate that factors intrinsic to the immune response might influence pathogenicity. Indeed, only the sera from diseased TCR^{1640} mice aggravated EAE relative to the 2D2 recipients receiving PBS. Sera from the disease-free TCR^{1640} mice failed to do so. While other soluble factors such as cytokines or complement may contribute to this difference, antibody intrinsic factors such as isotype, Fc-glycosylation or affinity maturation by clonal selection or somatic hypermutation are likely implicated.

To study the repertoire, we opted for a focused approach combining MOG-tetramers to isolate single B cells and iGB cultures to expand these clones *in vitro*. This approach would have the advantage of identifying the paired heavy and light chains sequences of the MOG-specific B cell responses. The iGB culture of bulk splenic B cells from naive BALB/c or NTL SJL/j mice, and the single cell culture of total/non-antigen-selected) splenic B cells from naive BALB/c or NTL SJL/j mice were highly efficient. Considering single-cell culture of naïve splenic B cells, 70% of BALB/c B cell cultures expanded with a 10^4 fold expansion, corroborating previous reports (42). The efficacy of single-cell iGB cultures is known to be reduced in terms of proportion of clones proliferating as well as their fold expansion, with reductions from 60% for splenic B cells from naïve WT mice to 23% for germinal center B cells from immunized mice (50). For the cervical lymph nodes, we observed an efficacy range between 38-46% for single-cell cultures of polyclonal B cells or MOG^{+}_{tet} B cells from healthy and diseased TCR^{1640} mice. iGB cultures from brain-infiltrating B cells demonstrated low efficacy dropping to only 3.6-13% for polyclonal B cells, and 0-4% for MOG^{+}_{tet} B cells. CNS infiltrating lymphocytes are effector cells prone to undergo activation induced cell death upon *in vitro* reactivation (50). The CD154 expressing, BAFF producing 3T3 fibroblasts were created for the *in vitro* differentiation of mature B cells into germinal center B cells. When applied to tissue infiltrating effector cells their stimulatory capacity might well be in excess.

Despite the constraints in amplifying B cells from the inflamed target tissue we did pursue the sequencing of the expanded iGB clones to identify potential BCR rearrangements associated with MOG-driven disease. Our results revealed shared light chain rearrangements among B cell clones from TCR^{1640} mice suggestive of clonal expansion. Nevertheless, single-cell transcriptomic approaches on non-expanded *ex-vivo* B cells would be required to study the clonality and somatic hypermutations of the antigen-driven B cell response in the TCR^{1640} mice.

CONCLUSION

Our results reiterate that spontaneous EAE in genetically predisposed animals is influenced by the environment under which they are housed. We confirmed that the autoimmune demyelinating humoral response matures in the brain-draining lymph nodes. This process is initiated prior to disease onset, as MOG-antibodies could be detected as early as 7 weeks of age. Sera containing MOG-antibodies proved pathogenic once TCR^{1640} mice had developed disease. The expanded MOG-specific B cell response demonstrated clonal selection as consensus sequences for the junctional region of MOG-reactive kappa light-chains could be identified. Our study indicates that clonal selection and brain infiltration of the MOG-specific humoral response are implicated in a spontaneous model of autoimmune demyelination.

DATA AVAILABILITY STATEMENT

The datasets presented in this study can be found in online repositories. The names of the repository/repositories and accession number(s) can be found in the article/**Supplementary Material**.

ETHICS STATEMENT

All experimental protocols were approved by the local ethics committee and and the Ministère de l'Enseignement Supérieur de la Recherche et de l'Environnement (5157-2016111011562655) in compliance with European Union guidelines.

AUTHOR CONTRIBUTIONS

Conceptualization, AP, LM, HZ. Methodology, MF, NJ, LM, HZ. Investigation, FS, LD, FL, TG, JB, MB, NJ. Data curation, FS, LD, FL, NJ, LM, HZ. Writing, LM, HZ, with input from all authors. Visualization, FS, LD, FL, TG, LM, HZ. Supervision, L.M, HZ. Funding acquisition, AP, LM, HZ. LM and HZ have full access to

all the data in the study and take responsibility for the integrity of the data and the accuracy of the performed analyses.

FUNDING

FS received a scholarship from Institut Roche. The funder was not involved in the study design, collection, analysis, interpretation of data, the writing of this article or the decision to submit it for publication. LD and JB received research scholarship from the Univ of Lille, Departments of Pharmacy or Medicine, respectively. HZ and AP were supported by ARSEP (call for proposal 2014 and 2016). AP was supported by the Emmy Noether Program of the German Research Foundation DFG (PE 2681/1-1). LM is supported by the Institut National de la Santé et de la Recherche médicale (INSERM), the University of Lille, and grants from the Agence Nationale de la Recherche "sugars-in-MS" (ANR-17-CE15-0028), The French MS society (ARSEP, Fondation pour L'aide à la recherche sur la Sclérose en plaques), and the Haut-de-France région.

ACKNOWLEDGMENTS

We thank Dr Dieter Jenne from LMU for sharing the vectors and protocols for recombinant MOG protein production in HEK-Ebna cells. We thank Dr Gurumoorthy Krishnamoorthy and Pr Hartmut Wekerle for scientific advice and the TCR^{1640} and IgH^{MOG} mouse models, Kitamura and colleagues for CD40LB cells. We thank Dr Camille Brochier from Institut Roche for her advice in molecular biology. 40LB cells; Nathalie Jouy Flow cytometry platform, BiCel, Univ Lille; Julien Devassine and Melanie Besegher, Experimental Resources Platform, UMS2014-US41 PLBS. cDNA sequencing.

SUPPLEMENTARY MATERIAL

The Supplementary Material for this article can be found online at: https://www.frontiersin.org/articles/10.3389/fimmu.2022.755900/full#supplementary-material

Supplementary Figure 1 | Amplification of the antibody variable region. Validation of the primer pairs presented in **Table 1**. cDNA was obtained from purified B cells/iGB cells of SJL/J and C57BL/6 mice. Amplified PCR products migrated to expected molecular mass size (close to 500 kDa for IgHG and close to 400 kDa for Igk). Sequencing of the purified amplicon for SJL/J mice confirmed the amplification of the hypervariable regions of murine IgHG and Igk chains (data not shown).

Supplementary Figure 2 | Pathogenicity of monoclonal 8-18C5 IgG1 MOG-specific antibodies by adoptive transfer into EAE-prone recipients. Mild EAE develops in 2D2 MOG-TCR Tg mice after 2 injections (Days 0, 2) of *pertussis* toxin (Incidence 50%). These PT treated 2D2 mice received PBS (n = 4) or 50 µg of 8-18C5 (n = 4), or 50 µl of NTL serum (n=7) 2 days after the first PT injection. Mean clinical disability ± SEM is presented over time (days after serum transfer). 2-way ANOVA.

Supplementary Figure 3 | Differentiation of clonal B cells into $CD138^+$ plasma cells and $CD38^-$ $GL7^+FAS^+PNA^+$ germinal centre B cells. **(A)** iGB cultures of single B cells isolated from BALB/c spleen were analysed by flow cytometry after 8 days of culture. Two representative profiles (left column, middle column) of viable $CD19^+$ B cells stained for CD38, FAS(CD95), GL7, CD138 and intracellular IgG1 and IgM, or with isotype control monoclonal antibody (right column) are presented.

Supplementary Figure 4 | Efficacy of single-cell iGB-culture from FACS-sorted B cells from spleen NTL mice, and from cervical lymph nodes and brain of disease-free- and diseased TCR^{1640} mice. **(A)** Percentage of wells containing iGB clusters and **(B)** mean expansion fold of iGB clusters after 8 to 12 days of single-cell iGB culture.

Supplementary Figure 5 | Distance tree of NCBI protein blasted with mus musculus (taxid:10090) as target organism and the short consensual sequence CQQWSSYPLT as probe (Fast Minim Evolution, 0.90 of max sequence difference, distance of Grishin for proteins).

REFERENCES

1. Lucchinetti C, Brück W, Parisi J, Scheithauer B, Rodriguez M, Lassmann H. Heterogeneity of Multiple Sclerosis Lesions: Implications for the Pathogenesis of Demyelination. *Ann Neurol* (2000) 47(6):707–17. doi: 10.1002/1531-8249(200006)47:6<707::AID-ANA3>3.0.CO;2-Q
2. Obermeier B, Mentele R, Malotka J, Kellermann J, Kümpfel T, Wekerle H, et al. Matching of Oligoclonal Immunoglobulin Transcriptomes and Proteomes of Cerebrospinal Fluid in Multiple Sclerosis. *Nat Med* (2008) 14(6):688–93. doi: 10.1038/nm1714
3. Qin Y, Duquette P, Zhang Y, Talbot P, Poole R, Antel J. Clonal Expansion and Somatic Hypermutation of V(H) Genes of B Cells From Cerebrospinal Fluid in Multiple Sclerosis. *J Clin Invest* (1998) 102(5):1045–50. doi: 10.1172/JCI3568
4. Beltrán E, Obermeier B, Moser M, Coret F, Simó-Castelló M, Boscá I, et al. Intrathecal Somatic Hypermutation of IgM in Multiple Sclerosis and Neuroinflammation. *Brain* (2014) 137(Pt 10):2703–14. doi: 10.1093/brain/awu205
5. Stern JNH, Yaari G, Vander Heiden JA, Church G, Donahue WF, Hintzen RQ, et al. B Cells Populating the Multiple Sclerosis Brain Mature in the Draining Cervical Lymph Nodes. *Sci Transl Med* (2014) 6(248):248ra107. doi: 10.1126/scitranslmed.3008879
6. Lehmann-Horn K, Wang S-Z, Sagan SA, Zamvil SS, von Büdingen H-C. B Cell Repertoire Expansion Occurs in Meningeal Ectopic Lymphoid Tissue. *JCI Insight* (2016) 1(20):e87234. doi: 10.1172/jci.insight.87234
7. Goebels N, Hofstetter H, Schmidt S, Brunner C, Wekerle H, Hohlfeld R. Repertoire Dynamics of Autoreactive T Cells in Multiple Sclerosis Patients and Healthy Subjects: Epitope Spreading Versus Clonal Persistence. *Brain* (2000) 123 Pt 3:508–18. doi: 10.1093/brain/123.3.508
8. Brändle SM, Obermeier B, Senel M, Bruder J, Mentele R, Khademi M, et al. Distinct Oligoclonal Band Antibodies in Multiple Sclerosis Recognize Ubiquitous Self-Proteins. *Proc Natl Acad Sci USA* (2016) 113(28):7864–9. doi: 10.1073/pnas.1522730113
9. Graner M, Pointon T, Manton S, Green M, Dennison K, Davis M, et al. Oligoclonal IgG Antibodies in Multiple Sclerosis Target Patient-Specific Peptides. *PloS One* (2020) 15(2):e0228883. doi: 10.1371/journal.pone.0228883
10. Serafini B, Rosicarelli B, Magliozzi R, Stigliano E, Aloisi F. Detection of Ectopic B-Cell Follicles With Germinal Centers in the Meninges of Patients With Secondary Progressive Multiple Sclerosis. *Brain Pathol* (2004) 14(2):164–74. doi: 10.1111/j.1750-3639.2004.tb00049.x
11. Magliozzi R, Howell O, Vora A, Serafini B, Nicholas R, Puopolo M, et al. Meningeal B-Cell Follicles in Secondary Progressive Multiple Sclerosis Associate With Early Onset of Disease and Severe Cortical Pathology. *Brain* (2007) 130(Pt 4):1089–104. doi: 10.1093/brain/awm038
12. Frischer JM, Bramow S, Dal-Bianco A, Lucchinetti CF, Rauschka H, Schmidbauer M, et al. The Relation Between Inflammation and Neurodegeneration in Multiple Sclerosis Brains. *Brain* (2009) 132(Pt 5):1175–89. doi: 10.1093/brain/awp070
13. Machado-Santos J, Saji E, Tröscher AR, Paunovic M, Liblau R, Gabriely G, et al. The Compartmentalized Inflammatory Response in the Multiple Sclerosis Brain is Composed of Tissue-Resident CD8+ T Lymphocytes and B Cells. *Brain* (2018) 141(7):2066–82. doi: 10.1093/brain/awy151

14. Hauser SL, Waubant E, Arnold DL, Vollmer T, Antel J, Fox RJ, et al. B-Cell Depletion With Rituximab in Relapsing-Remitting Multiple Sclerosis. *N Engl J Med* (2008) 358(7):676–88. doi: 10.1056/NEJMoa0706383
15. Montalban X, Hauser SL, Kappos L, Arnold DL, Bar-Or A, Comi G, et al. Ocrelizumab Versus Placebo in Primary Progressive Multiple Sclerosis. *N Engl J Med* (2017) 376(3):209–20. doi: 10.1056/NEJMoa1606468
16. Hauser SL, Bar-Or A, Comi G, Giovannoni G, Hartung H-P, Hemmer B, et al. Ocrelizumab Versus Interferon Beta-1a in Relapsing Multiple Sclerosis. *N Engl J Med* (2017) 376(3):221–34. doi: 10.1056/NEJMoa1601277
17. Bankoti J, Apeltsin L, Hauser SL, Allen S, Albertolle ME, Witkowska HE, et al. In Multiple Sclerosis, Oligoclonal Bands Connect to Peripheral B-Cell Responses. *Ann Neurol* (2014) 75(2):266–76. doi: 10.1002/ana.24088
18. Chan TD, Wood K, Hermes JR, Butt D, Jolly CJ, Basten A, et al. Elimination of Germinal-Center-Derived Self-Reactive B Cells Is Governed by the Location and Concentration of Self-Antigen. *Immunity* (2012) 37(5):893–904. doi: 10.1016/j.immuni.2012.07.017
19. Tangye SG, Ma CS, Brink R, Deenick EK. The Good, the Bad and the Ugly - TFH Cells in Human Health and Disease. *Nat Rev Immunol* (2013) 13(6):412–26. doi: 10.1038/nri3447
20. Lanzavecchia A. Antigen-Specific Interaction Between T and B Cells. *Nature* (1985) 314(6011):537–9. doi: 10.1038/314537a0
21. Molnarfi N, Schulze-Topphoff U, Weber MS, Patarroyo JC, Prod'homme T, Varrin-Doyer M, et al. MHC Class II-Dependent B Cell APC Function is Required for Induction of CNS Autoimmunity Independent of Myelin-Specific Antibodies. *J Exp Med* (2013) 210(13):2921–37. doi: 10.1084/jem.20130699
22. Genç K, Dona DL, Reder AT. Increased CD80(+) B Cells in Active Multiple Sclerosis and Reversal by Interferon Beta-1b Therapy. *J Clin Invest* (1997) 99 (11):2664–71. doi: 10.1172/JCI119455
23. Aung LL, Balashov KE. Decreased Dicer Expression is Linked to Increased Expression of Co-Stimulatory Molecule CD80 on B Cells in Multiple Sclerosis. *Mult Scler* (2015) 21(9):1131–8. doi: 10.1177/1352458514560923
24. Pierson ER, Stromnes IM, Goverman JM. B Cells Promote Induction of Experimental Autoimmune Encephalomyelitis by Facilitating Reactivation of T Cells in the Central Nervous System. *J Immunol* (2014) 192(3):929–39. doi: 10.4049/jimmunol.1302171
25. Jelcic I, Al Nimer F, Wang J, Lentsch V, Planas R, Jelcic I, et al. Memory B Cells Activate Brain-Homing, Autoreactive CD4+ T Cells in Multiple Sclerosis. *Cell* (2018) 175(1):85–100.e23. doi: 10.1016/j.cell.2018.08.011
26. Bar-Or A, Fawaz L, Fan B, Darlington PJ, Rieger A, Ghorayeb C, et al. Abnormal B-Cell Cytokine Responses a Trigger of T-Cell-Mediated Disease in MS? *Ann Neurol* (2010) 67(4):452–61. doi: 10.1002/ana.21939
27. Barr TA, Shen P, Brown S, Lampropoulou V, Roch T, Lawrie S, et al. B Cell Depletion Therapy Ameliorates Autoimmune Disease Through Ablation of IL-6-Producing B Cells. *J Exp Med* (2012) 209(5):1001–10. doi: 10.1084/jem.20111675
28. Flores-Borja F, Bosma A, Ng D, Reddy V, Ehrenstein MR, Isenberg DA, et al. CD19+CD24hiCD38hi B Cells Maintain Regulatory T Cells While Limiting TH1 and TH17 Differentiation. *Sci Transl Med* (2013) 5(173):173ra23. doi: 10.1126/scitranslmed.3005407
29. Li R, Rezk A, Miyazaki Y, Hilgenberg E, Touil H, Shen P, et al. Proinflammatory GM-CSF-Producing B Cells in Multiple Sclerosis and B Cell Depletion Therapy. *Sci Transl Med* (2015) 7(310):310ra166. doi: 10.1126/scitranslmed.aab4176
30. Fillatreau S, Sweenie CH, McGeachy MJ, Gray D, Anderton SM. B Cells Regulate Autoimmunity by Provision of IL-10. *Nat Immunol* (2002) 3 (10):944–50. doi: 10.1038/ni833
31. Mauri C, Bosma A. Immune Regulatory Function of B Cells. *Annu Rev Immunol* (2012) 30:221–41. doi: 10.1146/annurev-immunol-020711-074934
32. Shen P, Roch T, Lampropoulou V, O'Connor RA, Stervbo U, Hilgenberg E, et al. IL-35-Producing B Cells Are Critical Regulators of Immunity During Autoimmune and Infectious Diseases. *Nature* (2014) 507(7492):366–70. doi: 10.1038/nature12979
33. Matsumoto M, Baba A, Yokota T, Nishikawa H, Ohkawa Y, Kayama H, et al. Interleukin-10-Producing Plasmablasts Exert Regulatory Function in Autoimmune Inflammation. *Immunity* (2014) 41(6):1040–51. doi: 10.1016/j.immuni.2014.10.016
34. Ramesh A, Schubert RD, Greenfield AL, Dandekar R, Loudermilk R, Sabatino JJ, et al. A Pathogenic and Clonally Expanded B Cell Transcriptome in Active Multiple Sclerosis. *Proc Natl Acad Sci USA* (2020) 117(37):22932–43. doi: 10.1073/pnas.2008523117
35. Guerrier T, Labalette M, Launay D, Lee-Chang C, Outteryck O, Lefèvre G, et al. Proinflammatory B-Cell Profile in the Early Phases of MS Predicts an Active Disease. *Neurol Neuroimmunol Neuroinflamm* (2018) 5(2):e431. doi: 10.1212/NXI.0000000000000431
36. Pöllinger B, Krishnamoorthy G, Berer K, Lassmann H, Bösl MR, Dunn R, et al. Spontaneous Relapsing-Remitting EAE in the SJL/J Mouse: MOG-Reactive Transgenic T Cells Recruit Endogenous MOG-Specific B Cells. *J Exp Med* (2009) 206(6):1303–16. doi: 10.1084/jem.20090299
37. Berer K, Mues M, Koutrolos M, Rasbi ZA, Boziki M, Johner C, et al. Commensal Microbiota and Myelin Autoantigen Cooperate to Trigger Autoimmune Demyelination. *Nature* (2011) 479(7374):538–41. doi: 10.1038/nature10554
38. Berer K, Gerdes LA, Cekanaviciute E, Jia X, Xiao L, Xia Z, et al. Gut Microbiota From Multiple Sclerosis Patients Enables Spontaneous Autoimmune Encephalomyelitis in Mice. *Proc Natl Acad Sci USA* (2017) 114(40):10719–24. doi: 10.1073/pnas.1711233114
39. Litzenburger T, Blüthmann H, Morales P, Pham-Dinh D, Dautigny A, Wekerle H, et al. Development of Myelin Oligodendrocyte Glycoprotein Autoreactive Transgenic B Lymphocytes: Receptor Editing *In Vivo* After Encounter of a Self-Antigen Distinct From Myelin Oligodendrocyte Glycoprotein. *J Immunol* (2000) 165(9):5360–6. doi: 10.4049/jimmunol.165.9.5360
40. Bettelli E, Baeten D, Jäger A, Sobel RA, Kuchroo VK. Myelin Oligodendrocyte Glycoprotein-Specific T and B Cells Cooperate to Induce a Devic-Like Disease in Mice. *J Clin Invest* (2006) 116(9):2393–402. doi: 10.1172/JCI28334
41. Perera NC, Wiesmüller K-H, Larsen MT, Schacher B, Eickholz P, Borregaard N, et al. NSP4 Is Stored in Azurophil Granules and Released by Activated Neutrophils as Active Endoprotease With Restricted Specificity. *JI* (2013) 191 (5):2700–7. doi: 10.4049/jimmunol.1301293
42. Nojima T, Haniuda K, Moutai T, Matsudaira M, Mizokawa S, Shiratori I, et al. *In-Vitro* Derived Germinal Centre B Cells Differentially Generate Memory B or Plasma Cells *In Vivo*. *Nat Commun* (2011) 2:465. doi: 10.1038/ncomms1475
43. Haniuda K, Nojima T, Kitamura D. *In Vitro*-Induced Germinal Center B Cell Culture System. *Methods Mol Biol* (2017) 1623:125–33. doi: 10.1007/978-1-4939-7095-7_11
44. Bach J-F. The Effect of Infections on Susceptibility to Autoimmune and Allergic Diseases. *New Engl J Med* (2002) 347(12):911–20. doi: 10.1056/NEJMra020100
45. Mariño E, Richards JL, McLeod KH, Stanley D, Yap YA, Knight J, et al. Gut Microbial Metabolites Limit the Frequency of Autoimmune T Cells and Protect Against Type 1 Diabetes. *Nat Immunol* (2017) 18(5):552–62. doi: 10.1038/ni.3713
46. Bettelli E, Pagany M, Weiner HL, Linington C, Sobel RA, Kuchroo VK. Myelin Oligodendrocyte Glycoprotein-Specific T Cell Receptor Transgenic Mice Develop Spontaneous Autoimmune Optic Neuritis. *J Exp Med* (2003) 197 (9):1073–81. doi: 10.1084/jem.20021603
47. Krishnamoorthy G, Saxena A, Mars LT, Domingues HS, Mentele R, Ben-Nun A, et al. Myelin-Specific T Cells Also Recognize Neuronal Autoantigen in a Transgenic Mouse Model of Multiple Sclerosis. *Nat Med* (2009) 15(6):626–32. doi: 10.1038/nm.1975
48. Reindl M, Linington C, Brehm U, Egg R, Dilitz E, Deisenhammer F, et al. Antibodies Against the Myelin Oligodendrocyte Glycoprotein and the Myelin Basic Protein in Multiple Sclerosis and Other Neurological Diseases: A Comparative Study. *Brain* (1999) 122(Pt 11):2047–56. doi: 10.1093/brain/122.11.2047
49. Flach A-C, Litke T, Strauss J, Haberl M, Gómez CC, Reindl M, et al. Autoantibody-Boosted T-Cell Reactivation in the Target Organ Triggers Manifestation of Autoimmune CNS Disease. *Proc Natl Acad Sci USA* (2016) 113(12):3323–8. doi: 10.1073/pnas.1519608113
50. Kuraoka M, Schmidt AG, Nojima T, Feng F, Watanabe A, Kitamura D, et al. Complex Antigens Drive Permissive Clonal Selection in Germinal

Centers. *Immunity* (2016) 44(3):542–52. doi: 10.1016/j.immuni.2016.02.010

Conflict of Interest: The authors declare that the research was conducted in the absence of any commercial or financial relationships that could be construed as a potential conflict of interest.

Publisher's Note: All claims expressed in this article are solely those of the authors and do not necessarily represent those of their affiliated organizations, or those of the publisher, the editors and the reviewers. Any product that may be evaluated in this article, or claim that may be made by its manufacturer, is not guaranteed or endorsed by the publisher.

PART B

Does Fc-glycosylation influence the pathogenicity of antibodies in MOGAD?

A. Fc glycosylation of disease-related antibodies in inflammatory demyelinating diseases

Antibodies contribute to inflammatory demyelinating diseases. To assess whether Fc-glycosylation impacts the humoral response we analyzed the disease-related IgG response in two paradigmatic demyelinating diseases. MS is a chronic autoimmune disease for which we obtained samples at the earliest stage of disease which is referred to as clinically isolated syndrome (CIS). Serum and cerebrospinal fluid (CSF) as a source of oligoclonal disease-related antibodies was collected. MOGAD is an acute inflammatory demyelinating disease which manifests as clinical attacks mediated by a MOG-specific autoantibody response. Serum was collected at this active stage of disease. The isotype distribution among circulating antibodies in healthy individuals (n=24), patients with MS (n=10) or MOGAD (n=6) revealed minor differences. Indeed relative to the isotypes observed in healthy sera, both MS and MOGAD patients revealed a reduced proportion of IgG3 and IgG4 isotypes. This was concomitant to the MOGAD increase in IgG2. When assessing the Fc-glycome of the IgG1 response the major Fc N297-glycoform identified in the three patient groups was a core glycan structure of seven saccharide units (4 N-acetyl-glucosamine (GlcNAc) and 3 mannose residues, enriched with a single galactose residue (G1). The presence of a branching fucose residue segregated healthy and MS IgG1 from MOGAD. In healthy individuals and MS patients the N-297 glycan moiety of polyclonal serum IgG1 are predominantly (>90%) synthesized with branching fucose residues (Figure 22A; healthy 92.1+/-0.4; MS 91.6+/-0.9) [173,174]. This is distinctly different in MOGAD where branching Fucose residues on serum IgG1 were significantly reduced compared to healthy individuals and MS patients (Figure 22A; 69.2+/-8.4).

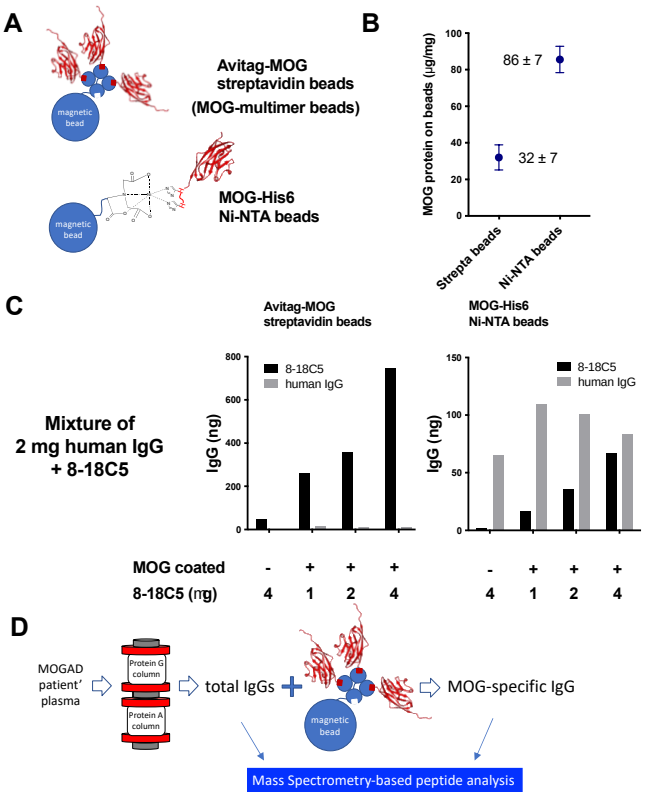

Figure 21: Purification and Fc-glycosylation of MOG-specific antibodies from MOGAD patients.

(**A**) Two magnetic bead formats were compared: Dynabeads™MyOne™ C-1 coated with Streptavidin (MOG-multimer beads) and HisPur™Ni-NTA coated with nickel-charged nitrilotriacetic acid (Ni-NTA). (**B**) The quantity of bait MOG-protein coated on streptavidin and NiNTA beads. (**C**) Purity and efficacy of 8-18-C5 immunoprecipitation when mixed with 2 mg of bulk human IgG using MOG-multimer beads (left column) and MOG-NiNTA beads (right column). (**D**) Current work-flow to purify MOG-specific antibodies from human serum.

Initial Fc-glycosylation is controlled within the germinal centre where antigen-activated T cells direct glycosyltransferase expression by B cells [183]. This motivated us to purify the disease-related MOG-specific antibodies from MOGAD. To this end we created a pTT5 vector encoding the extracellular domain of human MOG_{1-132} with an AviTag-sequence at the N-terminal and a 6-HisTag at the C-terminal. The recombinant was produced by transient transfection in HEK293 cells to allow for human post-translational modifications. We opted for 1 µm magnetic beads to efficiently purify rare auto-antigen specific antibodies (Figure 21A). Nickel-nitrilotriacetic acid (Ni-NTA) coated beads allowed a 2.6-fold higher density of hMOG (86 µg/mg) (Figure 21B). Streptavidin beads provided lower density (32 µg/mg) but allow trimer formation of Avitag biotinylated hMOG. The improved avidity of MOG-multimers considerably ameliorates purification of conformational MOG antibodies [184]. Both MOG-beads were compared for efficacy in purifying MOG-specific mouse IgG1 8-18C5 mAb from a mixture with human serum IgG of healthy individuals [143]. To this end, 1, 2, or 4 µg of 8-18C5 was mixed with 2 mg of human serum IgG isolated from healthy donors by protein A+G chromatography. The MOG coated Ni-NTA beads retained polyclonal human IgG as efficiently as low concentrations of the MOG-specific 8-18C5 (Figure 21C, right). The MOG-multimer beads retained a higher yield of 8-18C5 with higher purity (Figure 21, left) and were selected for the isolation of the MOG-specific antibodies from MOGAD sera.

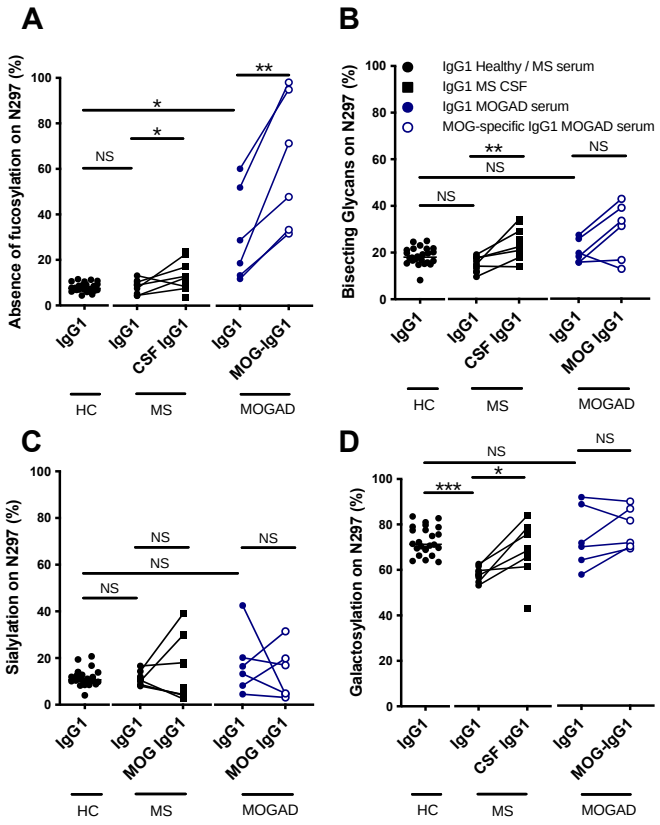

Figure 22: Fc glycosylation of disease-related antibodies in inflammatory demyelinating diseases

(**A-D**) N297 Glycopeptide analysis of 0.5-1 μg MOG-specific IgG1 from sera or 6 MOGAD patients (Blue open circles) or Total IgG1 (Blue close circles), CSF (Black squares) and sera (Black circles) of 10 MS patients, and sera of 24 healthy individuals. Percentage of glycans that are non-fucosylated (**A**), bisecting (**B**), sialylated (**C**) or galactosylated (**D**) on N297 among total

Comparing the Fc-glycosylation profile of disease-related antibodies in MS and MOGAD revealed similar core-glycan structures with both the CSF IgG1 and the MOG-specific IgG1 acquiring a predominantly G1 glycosylation profile of seven saccharide units (4 N-acetyl-glucosamine (GlcNAc) and 3 mannose residues, enriched with a single galactose residue. In contrast, the salient inflammatory traits demonstrated a clear dichotomy. In MS, the N297 glycome of CSF IgG1 demonstrated inflammatory modifications that include the increased prevalence of bisecting GlcNAc and a mild decrease in fucosylation and galactosylation (Figure 22A,B;D). No significant variation in N-sialylation was observed. In MOGAD, the signature observed among total IgG1 was significantly enriched among the disease related MOG-specific Abs (Figure 22A). Their Fc-domains expressed highly inflammatory glycan compositions devoid of branching Fucose residues in 2 patients (hypofucosylation >95%) and averaging at 62,9+/-12,13 (Figure 22A). This demonstrates that the chronic or acute inflammatory processes observed in MS or MOGAD imprint distinct Fc-glycosylation profiles on the disease-related IgG1 response. The highly inflammatory absence of branching fucose residues forms a dominant feature of the MOG-specific IgG1 response in MOGAD.

B. Fc-glycosylation is critical for the effector function of MOG-specific IgG1 antibodies

The distinct Fc-glycosylation profiles observed in two paradigmatic inflammatory demyelinating diseases questions whether the N297 glycan moieties may dictate the pathogenicity of auto-antibodies. To address this in vivo, we established a translational approach using the mouse mAb 8-18C5 that was originally used to identify MOG in 1984 [143]. Importantly, 8-18C5 recognizes a conformational epitope on MOG. It therefore interacts with native MOG in the CNS and not with the MOG-derived peptide 35-55 that is used for disease induction in active EAE [185]. Prior to creating Fc-glycovariants we first assessed whether the glycosylation of the conserved asparagine residue at position 174 is as critical for Fc-effector function as its human homologue N297. To this end we compared the hybridoma derived 8-18C5 with N-glycosidase F treated 8-18C5. As can be observed in Figure 23, the hybridoma derived 8-18C5 contained three major glycovariants. A fucosylated G0F variant with core glycan structure of seven saccharide units (4 N-acetyl-glucosamine (GlcNAc) and 3 mannose residues; a fucosylated G1F variant enriched with a single galactose residue, and a fucosylated G2F variant in which both branches were galactosylated. The N-glycosidase F treated 8-18C5 mAbs expressed a completely deglycosylated N174 (99%).

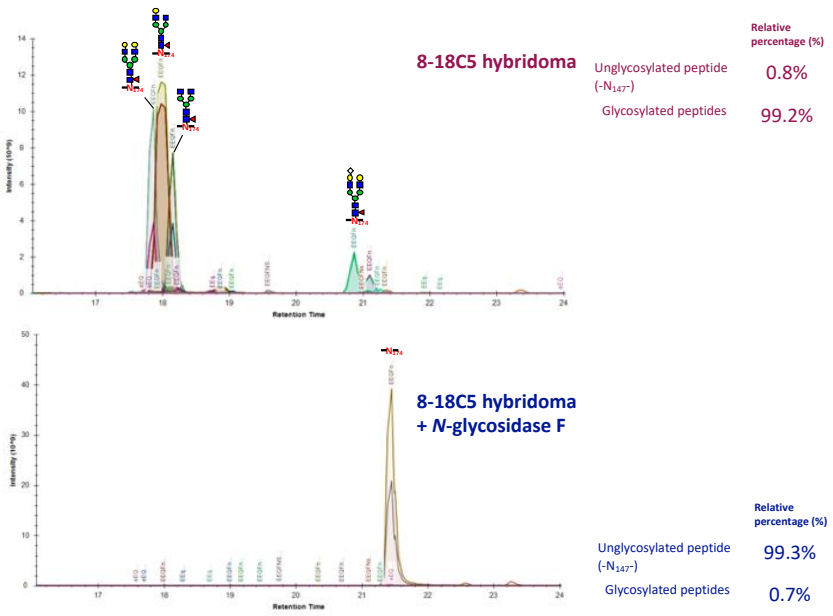

Figure 23: Fc-glycosylation profil of 8-18C5 hybridoma and deglycosylated 8-18C5 mAb

The extracted ion chromatograms of the N174-glycosylated peptide (EEQFN^{174}STFR) of hybridoma derived 8-18-C5 in its native or N-glycosidase treated form.

This deglycosylation resulted in a loss of IgG1 binding to CD16 and CD32a (Figure 24A) and a loss of complement mediated cytotoxicity (Figure 24B) *in vitro*. It should be noted that the antigenic specificity after treatment with PNGAseF remains unchanged (data not shown). The impact of the 8-18C5 glycovariants was assessed in the transcending paralytic disease experimental autoimmune encephalomyelitis (EAE). Active EAE was induced in C57Bl/6 mice by subcutaneous immunization with 100 µg of MOG_{35-55} emulsified in CFA followed by 2

injections of pertussis toxin. On average disease develops 10 days after immunization. One day prior to onset, at day 9, 8-18C5 variants were injected intravenously at a single dose of 50 μg/mouse. The glycosylated 8-18C5 significantly aggravated disease severity compared to the natural disease evolution observed in the PBS injected control group. The 8-18C5 mAbs lacking N-glycosylation had lost their pathogenicity and were unable to modify the natural EAE evolution (Figure 24C). These results demonstrate the cardinal importance of N-glycosylation in mediating the Fc effector function of demyelinating autoantibodies.

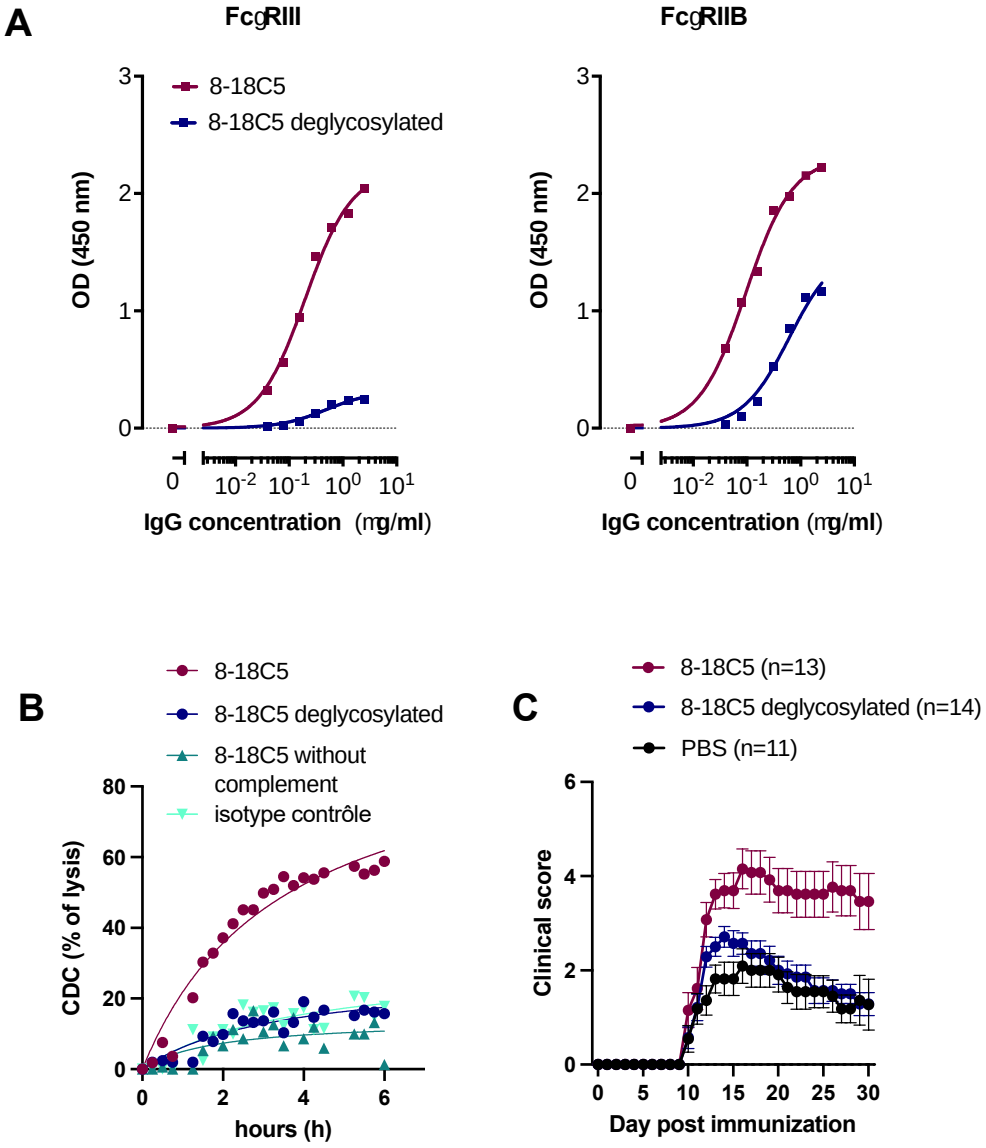

Figure 24: N174-glycosylation is essential for the Fc effector function of mouse IgG1 and the pathogenicity of the MOG-specific 8-18C5 mAb.

(**A**) ELISA serial dilution of native and N-glycosidase treated 8-18C5 on histidine tagged FcγRIII and FcγRIIB coated on NiNTA plates. Representative observation of 4 different experiments (**B**) CDC activity on Jurkat cells expressing MOG. MOG-Jurkat cells were cultured with native 8-18C5, PNGaseF treated 8-18C5, or isotype control IgG1 with fetal calf serum as a source of complement, or heat inactivated FCS. Data are presented as percent lysis over time (hours) analyzed by life imaging with Incucyte (Agilent). (**C**) i.v. injection of 50 μg of 8-18C5 variants 9 days after immunization in active MOG_{35-55} induced EAE. Data is presented as average +/- SEM. Here 3 independent experiments have been grouped.

C. Generating Fc-glycovariants of a clonal MOG-specific IgG1 antibodies

To create Fc-glycovariants the 8-18C5 mAb was cloned *in silico* by combining the Fv domain (VH and VL variable domains) of 8-18C5 with the consensus sequences of the murine IgG1 constant domains. The recombinant 8-18C5 mAbs were produced by transfection of mammalian cell lines imposing different glycosylation profiles. Extracted ion chromatograms of the N174 glycopeptide demonstrated different profiles among the 8-18C5 glycovariants (Figure 25A). The predominant N174 glycoform observed on IgG in healthy mice is G0F [171]. We produced **G0F** and hypofucosylated **G0** variants in HEK and YB2/0 ($FUT8^{-/-}$) cells respectively. The G0F 8-18C5 glycovariant expressed a biantennary glycan moiety on 77% of N174 residues; all G0 moieties integrated a branched fucose (G0F) (Figure 25B). The G0 variant expressed a biantennary glycan moiety on 80% of N174 residues; 45% lacked fucose (G0). CHO cells produced N174 residues bearing 3 dominant glycoforms: G0F (42%), G1F (21%) and non-glycosylated N174 (27%), a mixed glycosylation profile (**MG**). All 8-18C5 glycovariants have been produced using the same expression vector ensuring identical heavy and light chain sequences. As demonstrated in Figure 25C, this ensures identical affinity for their target antigen. ELISA assays using recombinant MOG on NiNTA plates revealed identical dose response curves for the three 8-18C5 glycovariants. In addition, the on-rate constant of the 8-18C5 glycovariants for recombinant MOG_{1-132} was determined by biolayer interferometry (BLI), again confirming identical affinity of the three glycovariants for MOG. The three 8-18C5 glycovariants, are identical in protein sequence, have identical affinity for their target antigen, but carry distinct glycan motifs on the N174.

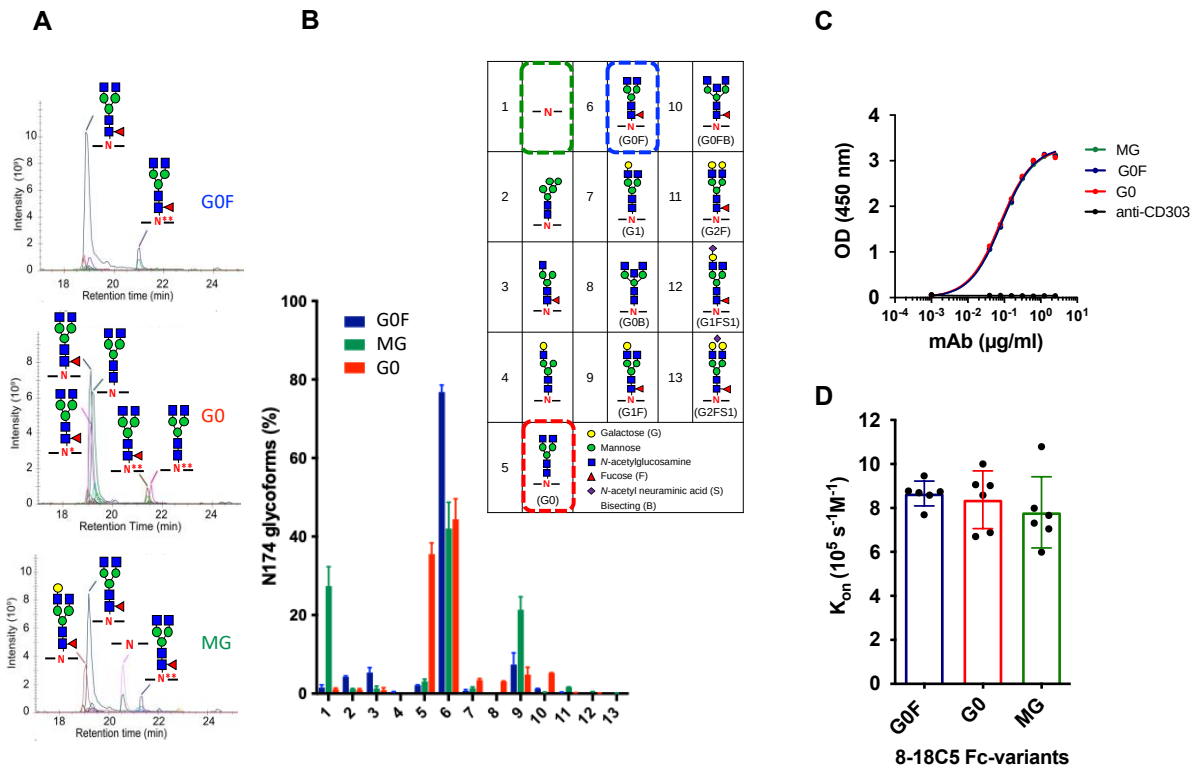

Figure 25: Fc-glycosylation and MOG-affinity of three 8-18C5 glycovariants.

(**A**) The extracted ion chromatograms of the N174-glycosylated peptide (EEQFN^{174}STFR) of recombinant 8-18-C5 produced by HEK (G0F), CHO (MG), and YB2 (G0) cell lines. * and ** indicate natural modifications during the sample preparation. * deamination of Q172; ** methylation of E170. (**B**) Glycopeptide analysis of N174. The histogram shows the proportion of glycoforms described in the table, the most relevant glycoforms are boxed in this table for each glycovariants. (**C**) ELISA serial dilution of 8-18C5 and control (anti-CD303) on MOG_{1-132} coated NiNTA plates. Inset: corresponding EC50 values. (**D**) Biolayer interferometry (BLI) measure of the on-rate constant 8-18C5 glycovariants binding to recombinant MOG_{1-132} using NiNTA
with the biosensors (RED96 OCTET system, Pall ForteBio). Using an unpaired Student's T- test with a 5% risk was used. (p-values < 0.05), no differences were observed between the different glycovariants.

D. Hypofucosylated IgG1 antibodies demonstrate increased affinity to T-haplotype of mouse FcγRIII

As demonstrated in Figure 26 the absence of branching fucose residues on N297 augments the affinity of chimeric IgG1 for CD16. Chimeric antibodies are 60% human. The constant parts of the heavy and light chains (CH and CL) of human an anti-CD20 IgG1 antibodies are grafted onto the respective variable parts (VH and VL) of a murine 8-18C5 antibody.
This difference in affinity is due to carbohydrate interactions between the glycans of Fc-N297 and CD16-N162 that are hindered by a branched fucose residue [186].

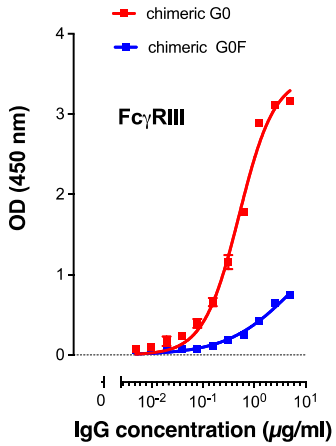

Figure 26: N297 hypofucosylation modify the affinity of chimeric IgG1 for FcgRIII.

ELISA serial dilution of recombinant 8-18C5 chimeric G0 and G0F produced in YB/2 (red), HEK (blue) cells, on histidine tagged human FcgRIII coated.

The impact of N174 hypofucosylation on the affinity of mouse IgG1 for its receptors FcγRIIB and FcγRIII have not been elucidated, not least because the CD16-N162 is not conserved on the mouse FcγRIII [157]. As demonstrated in Figure 27, The G0F and G0 8-18C5 glycovariants demonstrated a similar affinity for the FcγRIIB. The MG 8-18C5 glycovariant demonstrated a lower affinity for FcγRIIB, likely due to the presence of 30% deglycosylated N174 residues.

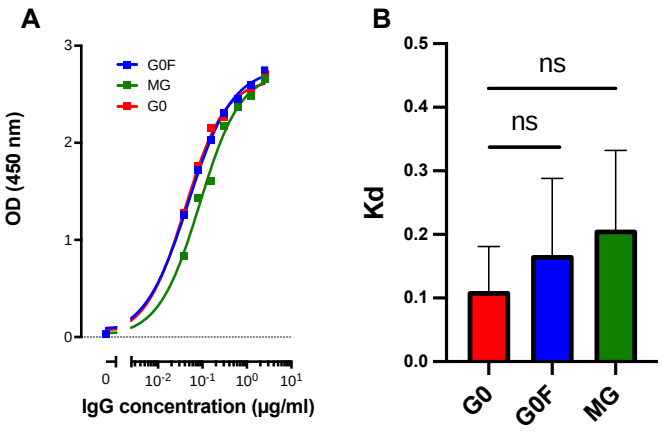

Figure 27: N174 hypofucosylation does not modify the affinity of mouse IgG1 for FcgRIIB.

N174 hypofucosylation does not modify the affinity of mouse IgG1 for FcgRIIB. (**A**) ELISA serial dilution of recombinant 8-18C5 G0, G0F and MG produced in YB/2 (red), HEK (blue) or CHO (green) cells, on histidine tagged murin FcgRIIB coated. (**B**) Kd derived from A from three independent ELISA as presented in A.

The mouse FcγRIII exists in three different haplotypes FcγRIII haplotypes T (C57BL/6 and 10), V (SWR), and H (BALB/c, DBA/1, NZB, NZW, NOD, BXSB, MRL/lpr, CBA), which are depicted in figure 28 H [187]. Both the H and V haplotypes are commercially available. We cloned and produced the T haplotype. The hypoglycosylated MG variant of 8-18C5 revealed a lower affinity compared to the G0F and G0 variants which remained indistinguishable (Fig 28A-B, D-E). This observation was confirmed on Jurkat cells stably co-transfected with both H haplotype FcγRIII and the common gamma chain (Fig 28G). In this assay IgG1 binding to the heterodimeric FcγRIII can be measured by IL-2 release induced by the human Jurkat T cells (Fig 28G). A similar affinity profile was obtained when compared to the recombinant ELISA (Fig 28A), indicating that the co-expression of the common gamma chain did not modify the relative binding of the 8-18C5 glycovariants to the FcγRIII. In contrast, the T haplotype was sensitive to the branching fucose residue on position N147. Figure 5C,F demonstrate the increased affinity of the G0 IgG1 versus the G0F IgG1 that amounts to 1.7 fold, the hypoglycosylated MG variant demonstrated reduced affinity for the FcγRIII T haplotype. This modest augmentation in affinity of the G0 versus G0F variants allowed the validation of C57Bl/6 mice to study the impact of Fc-hypofucosulation on the pathogenicity of demyelinating autoantibodies.

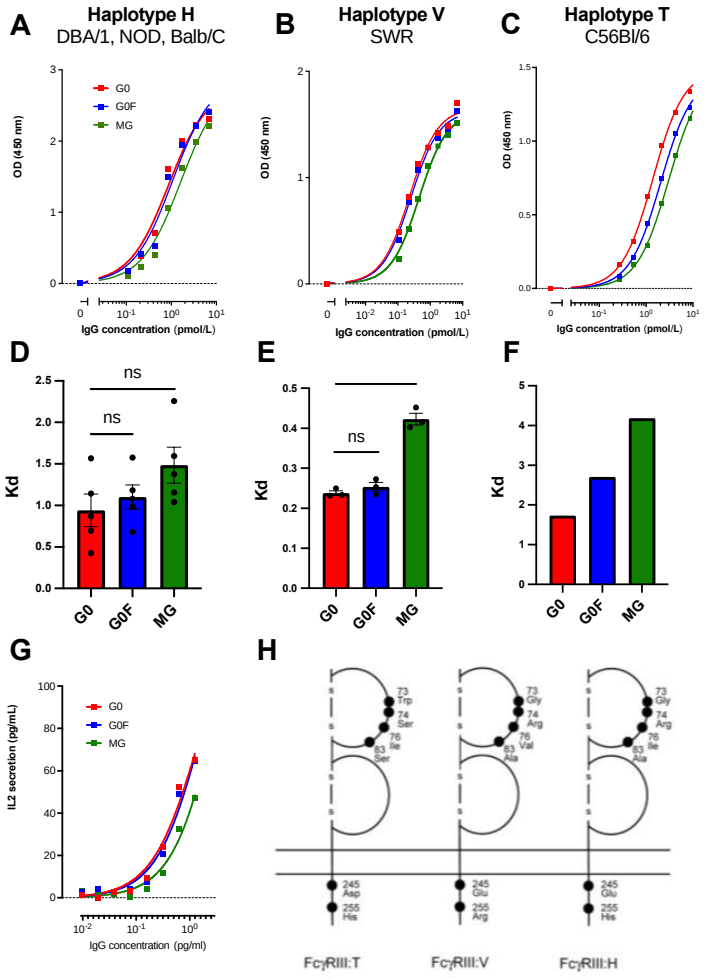

Figure 28: N174 hypofucosylation augments the affinity of mouse IgG1 for FcγRIII of the C57BL/6 haplotype T.

(**A-C**) ELISA serial dilution of recombinant 8-18C5 G0 (red), G0F (blue) or MG (green), on histidine tagged recombinant FcγRIII coated on NiNTA plates. (**A**) ELISA representative of 5 experiments with recombinant FcγRIII haplotype H. (**B**) ELISA representative of 3 experiments FcγRIII haplotype V. (**C**) ELISA FcγRIII haplotype T (**D-F**) Kd (pmol/ml) derived from the results presented in (A-C) calculated with linear regression +/- SEM. (**G**) Serial dilution of recombinant 8-18C5 G0 (red), G0F (blue) or MG (green) cells, in co-culture with Jurkat cells stably transfected with FcγRIII and the common gamma chain. (**E-F**) statistical analyzed performed with unpaired T test. (**H**) Depiction of the T, V, and H haplotypes derived from (Andren et al. 2005).

E. Hypofucosylated 8-18C5 antibodies aggravate autoimmune demyelination in FcγRIII-T mice

To test whether the distinct Fc-glycosylation profiles influence the pathogenicity of demyelinating autoantibodies we made use of the EAE animal model. Mild disease with a maximal score of 2,61+/-0,3 was induced in 94% of mice (PBS group, Figure 29C), half of the mice recovered onwards of day 22 (PBS group, Figure 29C). The 8-18C5 variants were injected intravenously at a single dose of 50 μg/mouse one day prior (day 9) to onset of active EAE (Figure 29A-D). Injection of the 8-18C5 G0F and 8-18C5 G0 significantly aggravated the natural evolution of EAE observed in the PBS group (Figure 29A: 2-way ANOVA PBS vs G0 8-18C5 ****; PBS vs G0F 8-18C5 ****), which was not observed for the hypoglycosylated MG 8-18C5 (PBS vs MG 8-18C5 NS). This hierarchy was also confirmed based on the cumulative disease score which proved most elevated for the G0 8-18C5 injected group (Figure 29D, student t-test). This hypofucosylated G0 variant also significantly reduced the proportion of mice recovering from disease (Figure 29C, PBS vs G0 8-18C5 **). Lastly, during the first week after injection (d10-d18) the 8-18C5 mAbs increased mortality that reached statistical significance only for the G0 8-18C5 mAbs (Figure 29B). Taken together this demonstrates that Fc-glycosylation dictates the pathogenicity of demyelinating IgG1 antibodies. Both the G0F and G0 8-18C5 glycovariants aggravated EAE with the G0 variant causing more severe disease notably in terms of mortality.

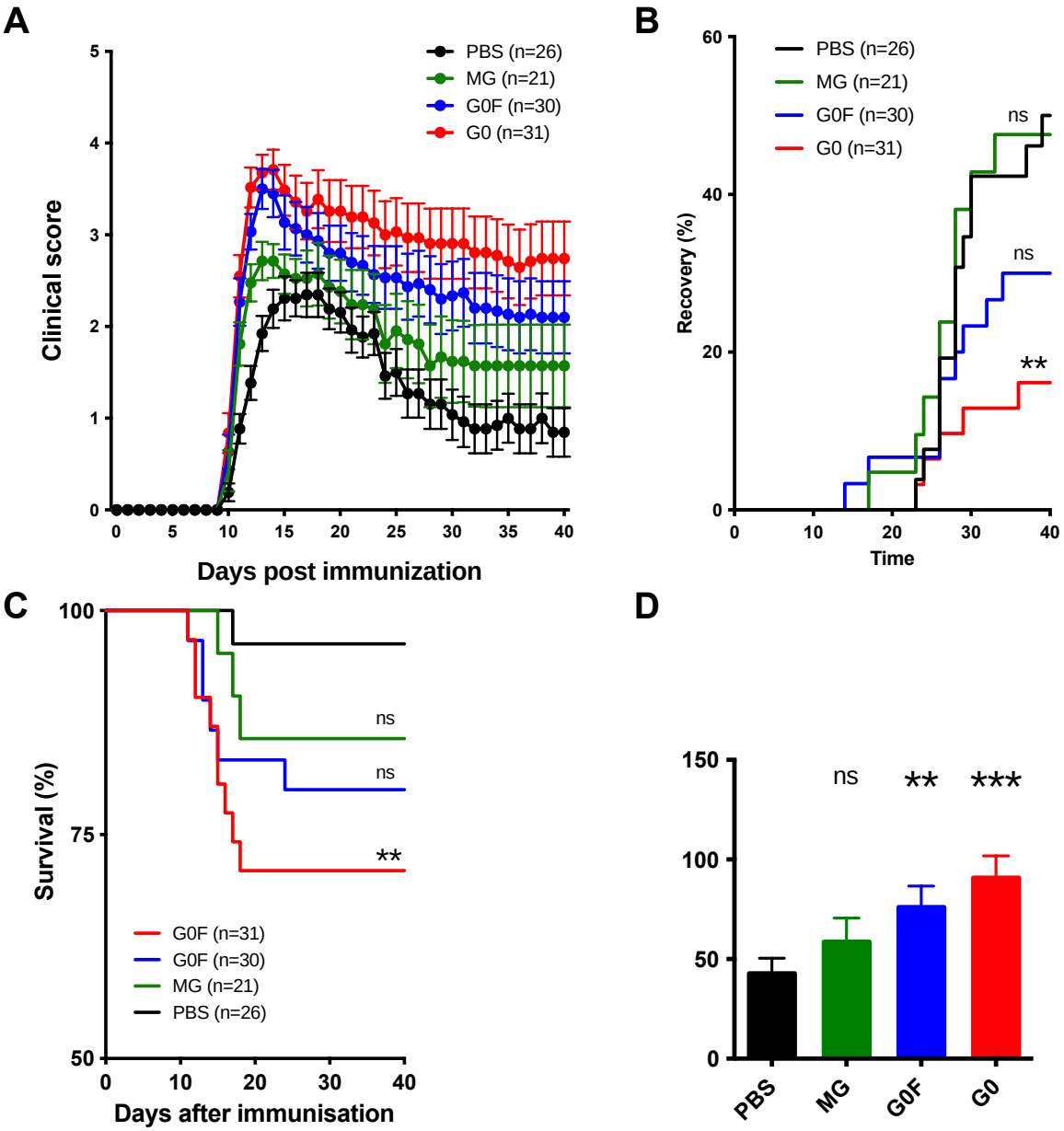

Figure 29: Fc-glycosylation dictates the pathogenicity of 8-18C5 Fc-glycovariants.

For this figure, 6 independent experiments have been grouped. (**A-D**) i.v. injection 9 days after immunization of 50 µg 8-18C5 variants in active MOG_{35-55} induced EAE. PBS (Black), CHO (Green), HEK (Blue), YB2 (Red). (**A**) Clinical evolution. (**B**) Survival. (**C**) Recovery, defined as a persistent absence of neurological symptoms (EAE score 0). (**D**) Cumulative disease score, which represents the sum of all daily disease scores for each mouse. Statistics performed with an unpaired T test (**A,D**) Average +/- SEM. (**B,C**) Performed with a Kaplan-Meier analyze.

F. Hypofucosylated 8-18C5 antibodies potentiate the inflammatory response in the CNS of FcgRIII-T mice

Protocols using persistent high dose injections of 8-18C5 have emphasized the importance of complement mediated demyelination [188]. The punctual injection of 50 μg of 8-18C5 prior to disease onset elicits a broader immune reaction implicating immune-complex phagocytosis by myeloid cells and antigen-presentation to drive the effector T cell response [189]. To assess the cellular mechanisms driving the 8-18C5 induced disease aggravation we focused on CD4 and CD8 T cells, and the recruitment of NK cells (ADCC). Immunohistochemical assessments of the immune composition and correlates of tissue damage were assessed 3 days after 8-18C5 injection (day 12 a.i.). In the spinal cord, the G0 8-18C5 glycovariant significantly increased demyelination as compared to the PBS control group, but also relative to the G0F and MG 8-18C5 treated groups (Figure 30A). The demyelinating lesions were characterized by increased perivascular T cells and NK cell. By contrast, 7 days after 8-18C5 injection the analysis of the mononuclear infiltrate of 4 pooled spinal cords revealed that both the G0F, G0, MG 8-18C5 variants enhanced the accumulation of CD8 T cells (Figure 30). When taking into account the size of the infiltrate the G0F and G0 8-18C5 glycovariants promoted inflammatory infiltration, with the G0 8-18C5 driving the strongest accumulation of CD4 and NK cells (Figure 30C).

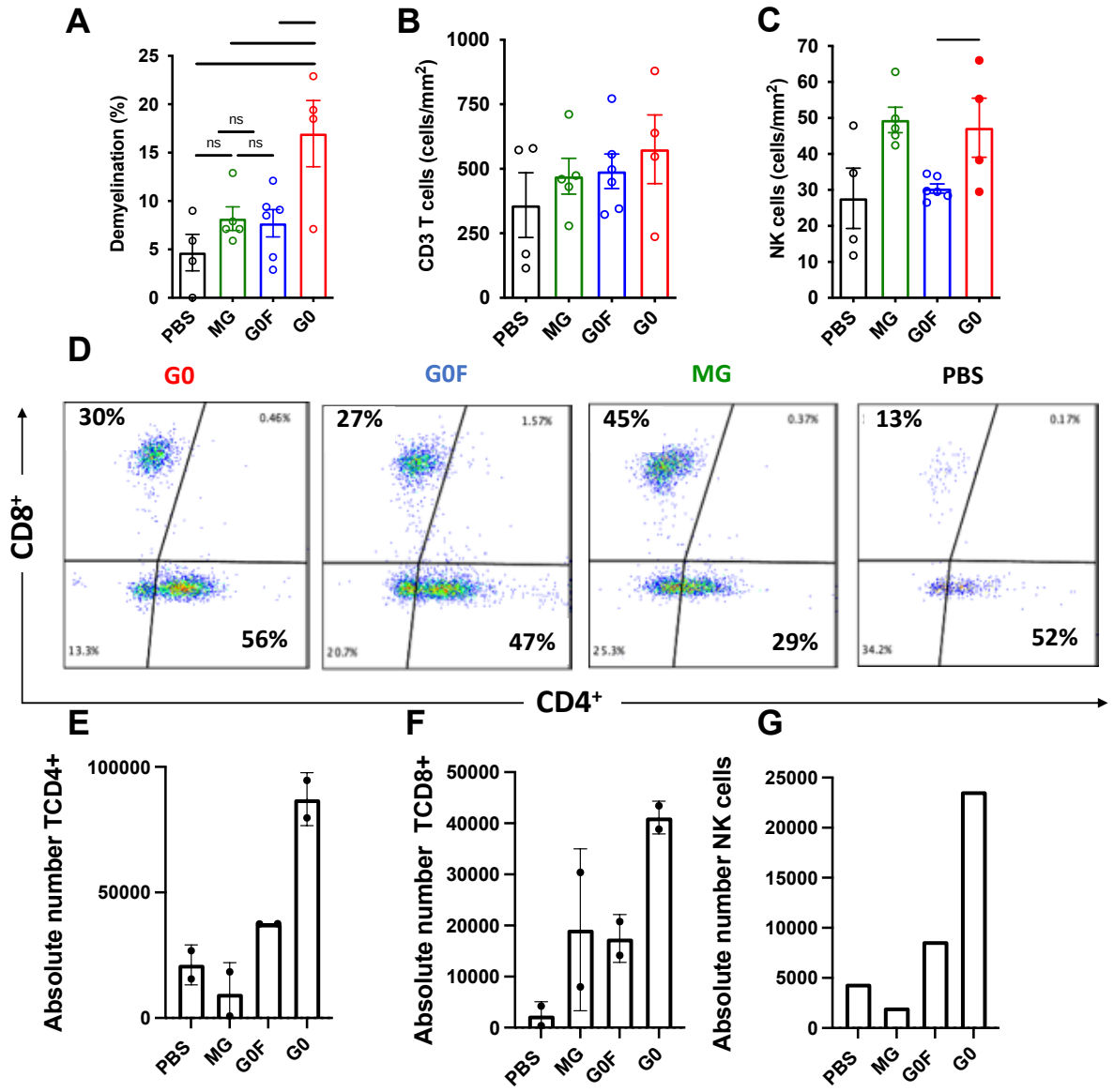

Figure 30: Hypofucosylation potentiates antibody mediated autoimmune demyelination.

(**A-C**) Immunohistochemical analysis of the spinal cord on day 12 after immunisation. 8-18C5 variants (50 μg) were injected i.v. 9 days after immunisation with MOG_{35-55}. PBS (Black), MG (Green), G0F (Blue), G0 (Red). (**A**) Demyelination ; (**B**) CD3 T cells ; (**C**) $CD3^-CD335^+$ NK ; (**B,C**) cells were enumerated from individual spinal cords+/- SEM. Statistical analyze performed with unpaired T test (**D**) Flow cytometry analysis of percoll purified mononuclear cells from the spinal cord on day 16 after immunisation. 8-18C5 variants (50 μg) were injected i.v. 9 days after immunisation with MOG_{35-55}. PBS (Black), MG (Green), G0F (Blue), G0 (Red). CD8β vs CD4 FACS plots of gated viable $CD3^+CD90^+$ T cells. (**E-G**) Absolute numbers of CD4 T cells, CD8β T cells, and $CD3^-CD335^+$ NK cells from pooled spinal cords of 4 mice per group. (**B,C,E,F**) Results from two independent analyzes.

G. 8-18C5 antibodies potentiate the MOG35-55 specific T cell response.

8-18C5 recognizes a conformational epitope on MOG protein and does not interact with the immunodominant MOG_{35-55} -peptide used for EAE induction [185]. MOG is synthesized by oligodendrocytes and not schwann cells, restricting its expression to CNS myelin. Binding of 8-18C5 to CNS myelin causes increased tissue damage that may result in broadened autoantigen-presentation or preferential MOG-specific immunity owing to the phagocytosis of immune complexes by myeloid cells. To address the magnitude of this MOG-specific T cell response we used antigen-recall experiments to enumerate the Th1 (Figure 31A,B,C) and Th17 (Figure 31D,E,F) response by Elispot. Among brain mononuclear cells, we observed an expansion of the MOG_{35-55}-specific IFNγ producing T cells (Figure 31C). The Th17 response was triggered by MOG_{35-55} antigen recall in PBS, MG 8-18C5 and notably the G0 8-18C5 treated mice, but not in the 8-18C5 HEK treated mice (Figure 31F). This dichotomy of 8-18C5 G0F and G0 in driving the Th1 versus Th17 response was also observed in the secondary lymphoid organs. In the spleen, we analyzed the antigen-recall response of purified CD4 T cells and revealed that both the G0F and G0 8-18C5 variants significantly increased the MOG_{35-55} induced Th1 response as detected by IFNγ Elispot (Figure 31B). By contrast the Th17 antigen-recall response was only potentiated by the G0 8-18C5 glycovariant (Figure 31E).

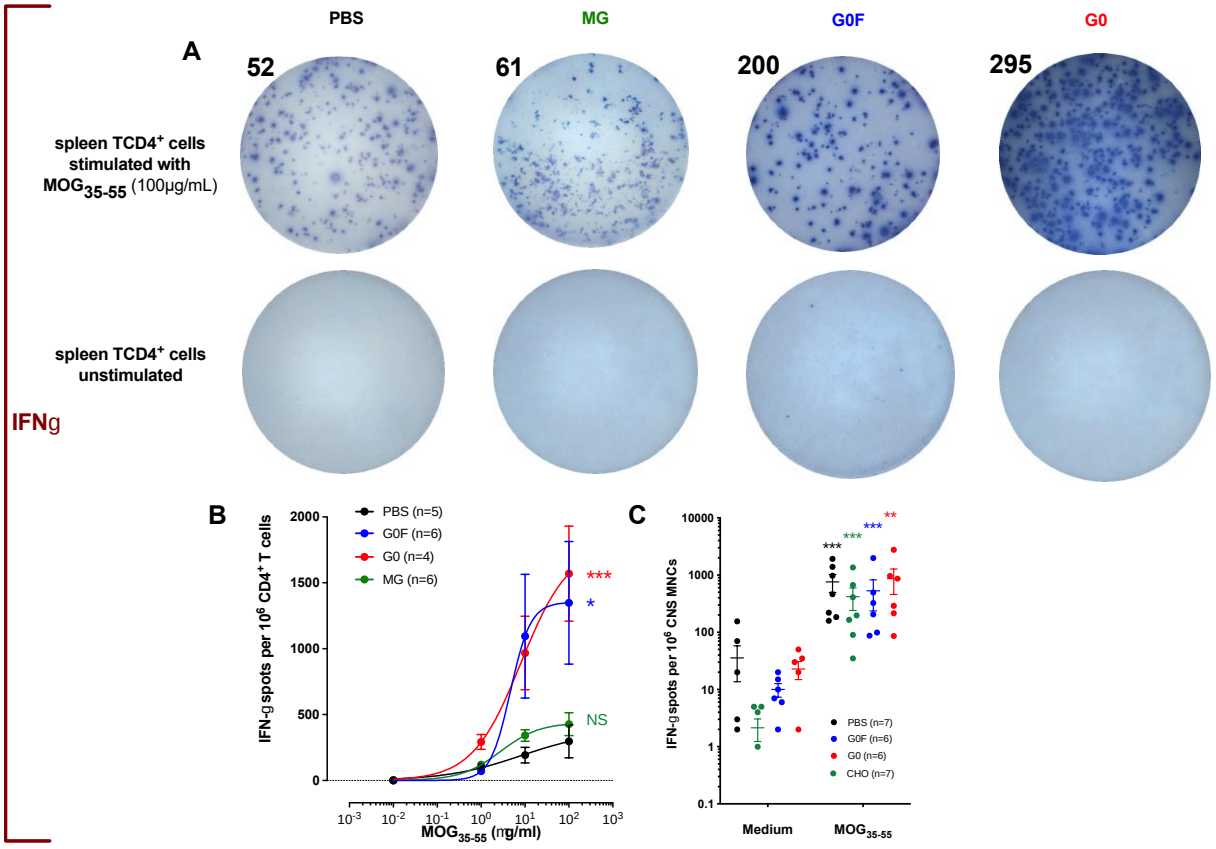

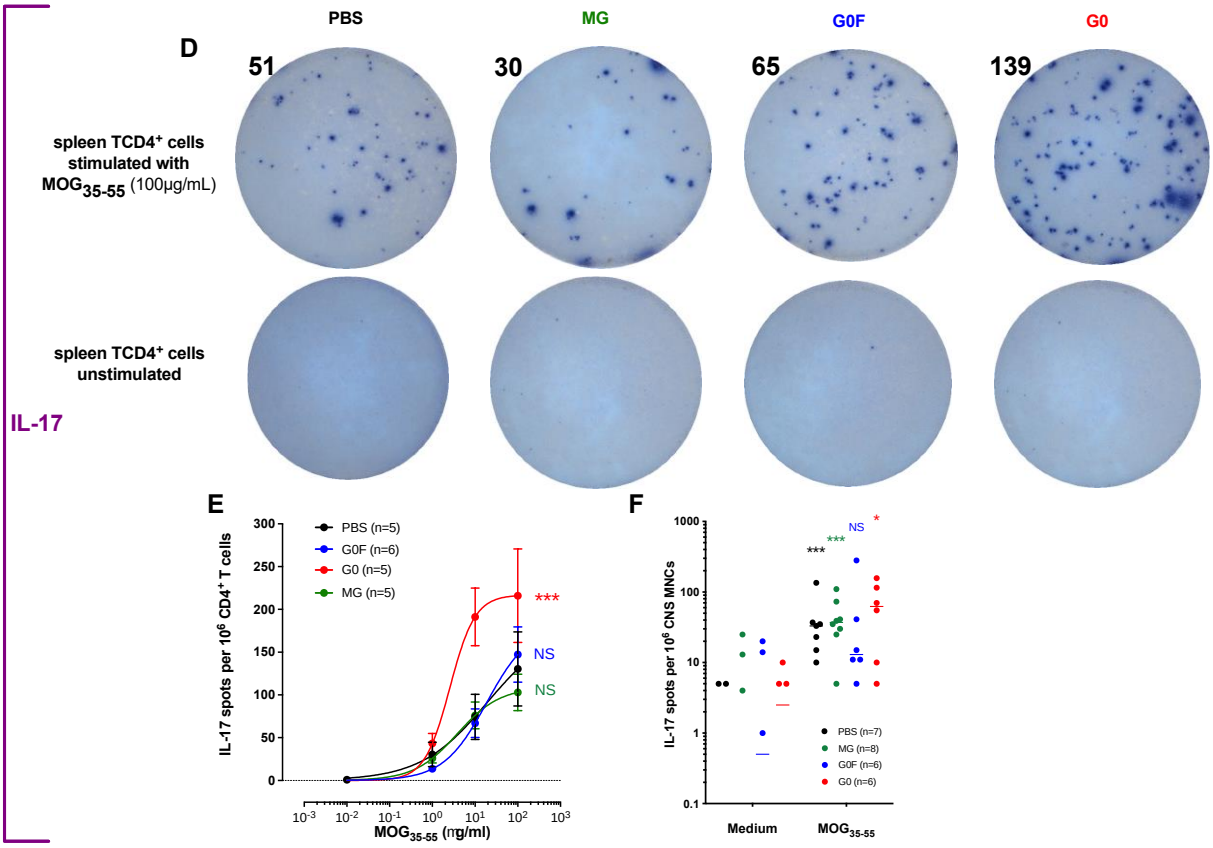

Figure 31: G0 and G0F 8-18C5 induced CD4 T cell response is MOG-specific.

(**A-F**) Elispot analysis of purified CD4⁺ T cells from the spleen (A,B,D,E) or percoll purified mononuclear cells from the brain (C,F) on day 16 after immunization. 8-18C5 variants (50 µg) were injected i.v. 9 days after immunisation with MOG_{35-55}. (**A**,**D**) Representative IFNγ (A) and IL-17 (D) Elispot on splenic CD4⁺ T cells co-incubated with irradiated splenocytes with or without MOG_{35-55}. (**B,E**) CD4⁺ T cells co-cultured with irradiated splenocytes in the presence of serial dilutions of MOG_{35-55}. IFNγ (B) and IL-17 (E) Elispot from individual mice treated with PBS (Black), MG (Green), G0F (Blue), G0 (Red).+/- SEM. (**C,F**) Total mononuclear cells stimulated with medium or MOG_{35-55}. IFNγ (C) and Il-17 (F) Elispot from 4 pooled mice treated with PBS (Black), MG (Green), G0F (Blue), G0 (red). Statistical comparison performed with two way ANOVA.

H. Hypofucosylated 8-18C5 antibodies augment the in situ expansion of autoreactive effector T cells.

To dissociate de novo priming of naïve CD4 T cells in secondary lymph nodes versus *in situ* expansion of effector T cells after 8-18C5 immune enhancement a fate mapping approach was used. Tracer MOG_{35-55}-specific TCR transgenic 2D2 T cells were transferred at two timepoints, 105 homozygous CD45.1$^{+/+}$ were transferred 24 hours before MOG_{35-55} immunisation and 105 heterozygous CD45.1$^{+/-}$ 2D2 T cells were transferred on day 9 in parallel with the injection of the 8-18C5 glycovariants. On the day of 8-18C5 injection (day 9), the 2D2 T cells transferred 24 hours before immunisation will have integrated the effector T cell response, while the concomitantly transferred 2D2 T cells will integrate the naïve T cell response. 7 days later, day 16 after immunisation, the magnitude and composition of the pathogenic CD4 T cell response will be analysed in the CNS (schema in Figure 33). The G0 8-18C5 treated mice again demonstrated a strikingly augmented endogenous CD45.2$^{+/+}$ CD4 T cell response and MOG_{35-55}-specific CD4^{+} 2D2 T cell response within the spinal cord and brain (**Error! Reference source not found.**A,B,C,D).

Within the spinal cord of PBS control mice the 2D2 T cell response comprised newly primed (CD45.1$^{+/-}$) and effector (CD45.1$^{+/+}$) 2D2 T cells at a 40/60 ratio (**Error! Reference source not found.**E,F,G). For the G0F 8-18C5 treated mice the spinal cord infiltrate comprised a similar 40/60 ratio of newly activated / effector 2D2 T cells. In the G0 8-18C5 treated mice the spinal cord infiltrate indicated a preferential in situ expansion of effector 2D2 T cells at a ratio of 30/70 for newly activated / effector 2D2 T cells. Taken together these data further demonstrate that T accumulation in the CNS is an antigen-driven response which in the case of the G0 8-18C5 variant is preferentially driven by the in situ expansion of MOG_{35-55} specific effector T cells that were originally primed by the MOG_{35-55}/CFA immunisation.

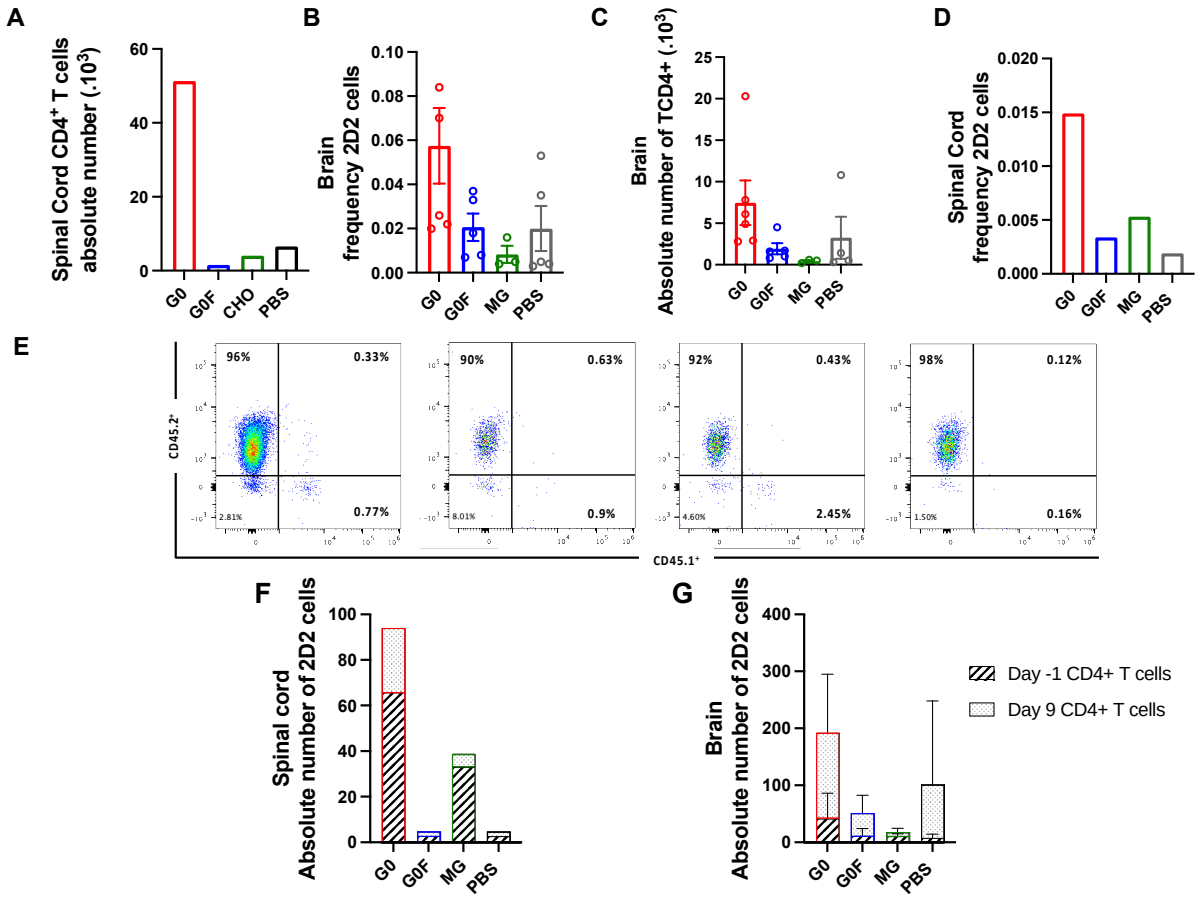

Figure 32: Hypofucosylated G0 8-18C5 drives the in situ expansion of MOG-specific effector CD4 T cells

(**A-G**) CD45.2$^{+/+}$ C57Bl/6 mice received CD45.1$^{+/+}$ 2D2 T cells transferred 24 hours before MOG_{35-55} immunisation and CD45.1$^{+/-}$ 2D2 T cells transferred on day 9 in parallel with the injection of treated with PBS (Black), or MG (Green), G0F (Blue), G0 (Red) 8-18C5 glycovariants. Analysis was performed on day 16. (**A,C**) Enumeration of the endogenous and transferred (2D2) CD4^{+} T cells in the spinal cord (A) and brain (C). (**B,D**) Identification of CD45.1$^{+/+}$ 2D2 T cells transferred 24 hours before immunisation and CD45.1$^{+/-}$ 2D2 T cells transferred on day 9. (**E**) The mononuclear infiltrate of 4 pooled spinal cords revealed that both the G0F, G0, MG 8-18C5 variants enhanced the accumulation of CD4 CD45.2$^{+/+}$ and also the infiltrate of CD4 CD45.1$^{+/+}$ cells. (**F,G**) Proportion of newly primed (stripes) and effector (point) MOG-specific 2D2 T cells in the spinal cord (**F**) and brain (**G**). Data represent 4 pooled mice (Spinal Cord) or 4-6 individual mice (brain).

I. Part A : A Evaluation of MOG-specific B cells dynamics at the initiation of spontaneous EAE in secondary lymphoid organs and the brain

Multiple sclerosis is a chronic neuroinflammatory disease of the central nervous system. This disease is complex because the clinical and pathological manifestations are variable and involve different pathogens. MS is undoubtedly an autoimmune disease that mobilizes both the innate and adaptive immune response. Current evidence suggests that the complexity of MS goes beyond self-reactivity, involving immune dysregulation caused by environmental factors and genetic predisposition, as well as immunosenescence due to progressive aging.

The humoral response is strongly involved in MS. Indeed, the diagnosis is based in part on the intrathecal production of antibodies detected by the presence of oligoclonal bands in the cerebrospinal fluid [190]. These antibodies are produced by B cells that have undergone clonal expansion and this process is directed by antigens [102,191]. Somatic hypermutation responsible for antibody production that occurs in brain draining cervical lymph nodes and possibly in ectopic meningeal lymphoid structures [192]. Finally it should be noted that the specificity of the adaptive immune response in MS is composite and evolves over time [68].

Spontaneous models of EAE allow the study of myelin-specific B cells during CNS autoimmune disease. In this study, the model used is TCR^{1640} transgenic SJL/j mice, which display a restricted I-As TCR specific for the MOG 92-106 peptide (MOG_{92-106}) on 70% of CD4 T cells [193]. The effector B cells are recruited from a non-transgenic B cell repertoire. Indeed, germinal centers are detected in the cervical lymph nodes of young non-diseased RR mice, implying that TCR^{1640} follicular helper T cells are responsible for the isotype change and maturation of the affinity of the MOG-specific B cell response [77]. It is therefore of interest to study the humoral response in this model.

In this work to investigate the involvement of B cells in disease initiation and progression, we used recombinant MOG tetramers to monitor the self-antigen-specific B cell response in TCR^{1640} mice, which developed late-onset acute EAE in our animal facility. Thus we reaffirm that spontaneous EAE in genetically predisposed animals is influenced by the environment in which they are housed. The microbiota may be informative for the encephalitogenic immune

response, as transplantation of the microbiota of homozygous twins discordant for MS into TCR^{1640} mice, induced demyelination only in the mice receiving the microbiota of the sick child [194].

Moreover, these results highlight the role of the lymph nodes draining the brain since this is where the humoral autoimmune demyelinating response matures. This lymph node maturation starts before the onset of the disease since we detected anti-MOG antibodies as early as 7 weeks of age. With serum transfers it was shown that only sera containing anti-MOG antibodies from diseased TCR^{1640} mice proved to be pathogenic. The expanded MOG-specific B cell response demonstrated clonal selection as consensus sequences for the junction region of MOG reactive kappa light chains could be identified. Finally, shared light chain rearrangements between B cell clones from TCR^{1640} mice were demonstrated, suggesting clonal expansion and this was achieved by sequencing the expanded iGB clones. However, this analysis should be performed on unexpanded ex-vivo B cells to study clonality and antigen-induced somatic hypermutations in TCR^{1640} mice.

II. Part B : Does Fc-glycosylation influence the pathogenicity of antibodies in MOGAD?

The strength by which immune complexes engage the immune system is controlled by the structural diversity of the Fc-domains. Isotypes and post-translational modifications decisively construct the inflammatory efficacy of the humoral response. In infectious diseases, the absence of a branching fucose may favour neutralising antibody responses. During Dengue virus infection mounting afucosylated antibodies ensures dengue clearance, while dengue viral persistence in the presence of fucosylated antibodies predisposes to dengue shock syndrome [167]. In critically ill COVID-19 patients a high proportion of afucosylated IgG antibodies specific for severe acute respiratory syndrome coronavirus 2 (SARS-CoV-2) was detected and contribute to the amplification of the cytokine storm that characterize progression to life-threatening pneumonia [195,196]. In tuberculosis patients, the Fc-glycosylation of latent and active TB patients differed [166]. Latency was associated with di-galactosylation with or without sialylated N-linked glycans on the Fc of IgGs that improved bacterial clearance. Conversely, Fc-fucosylation or agalactosylation failed to control TB infection, predisposing to overt infection.

Here we analysed the Fc-glycosylation profile of two paradigmatic inflammatory demyelinating diseases of the CNS. In MS, a chronic disease, we assessed the disease-related IgG response within the CSF compared to circulating IgG. Within the serum no significant modifications were observed relative to IgG of healthy individuals. By contrast, we observed the diversity of IgG1 Fc-domains evolve in favour of inflammatory Fc-domains. Concurrent with previous studies we observed an increase of bisecting GlcNAc and reduced galactosylation on CSF IgG [170,171]. This IgG1 Fc-glycosylation profile of bisecting GlcNAc and reduced galactosylation conserves the pro-inflammatory properties endowed by Fc-binding to activating FcγRs. This extends beyond MS, as other chronic inflammatory, including rheumatoid arthritis, lupus, diabetes, Sjogren's disease are associated with loss of Fc-galactosylation even at onset of disease activity [168,169].

Fucose and sialic acid have the strongest impact on the inflammatory activity of the Fc-domain [186]. In healthy individuals the majority of IgG are fucosylated owing to the expression of α-(1,6)-fucosyltransferase (FUT8) [173,174]. The singular absence of fucose increase the affinity of the IgG1 Fc domain 10- to 50-fold for FcγRIIIa (CD16a) [175,197]. This augmented affinity activates the IgG1 Fc for interaction with CD16a expressing NK cells and monocytes/macrophages [176,177,198]. Absence of the branching fucose residue is therefore critical in controlling antibody-dependent cell cytotoxicity and antibody-dependent immune enhancement [199]. In this study we demonstrate that this striking feature is observed among disease-related antibodies of patients with inflammatory demyelinating diseases. In MS, the proportion of afucosylated Fc-domains increased mildly among the disease-related IgG1 in the

CSF at the time of disease diagnosis. During a MOGAD attack hypofucosylation proved a hallmark of the IgG1 response. Lack of fucose was abundant among total IgG1 and dominant among the MOG-specific IgG1 response reaching over 95% in two of the patients. Other antibody mediated autoimmune diseases have demonstrate a similar polarisation. Fetal or neonatal alloimmune thrombocytopenia, caused by maternal IgG raised against fetal human platelet antigens demonstrate diminished levels of Fc-fucosylation [200]. Like in our study, the proportion of auto-antibodies integrating fucose in their Fc-domains fell to 10%. Combined, our observations may point to IgG1 hypofucosylation as a common feature of acute autoimmune diseases with a focused antibody response.

Molecularly, the increased affinity afforded by hypofucosylation is explained by the interaction between carbohydrates positioned on the glycan moieties present on N162 of the FcγRIIIa and those on the N297 of the IgG1 Fc domain [164]. Fucosylation disturbs this interaction by sterical hindrance causing a 10-50 fold reduction in affinity. In mice, the N162 is conserved within the FcγRIV, the homologue of human CD16A [157]. This endows fucosylation with the control of the inflammatory activity of mouse IgG2a. Absence of fucose improves affinity by 8-fold [201]. The mouse IgG1 response binds the activating FcγRIII which comes in three haplotypes, H, V and T [187]. We observed a small gain in affinity for our hypofucosylated mouse IgG1 antibodies for the CD16 T haplotype, warranting our choice for the C57BL/6 genetic background. Unlike the other haplotypes, the T haplotype includes a R74S substitution that introduces a consensus N-glycosylation sequence Asn-X-Ser for the N72 located in the FcγRIII sequence [202]. However, unlike the N162 in the human CD16A, this N-glycosylation site locates diagonally opposite to the Fc-domain binding site. An indirect effect may be implicated. The human CD16a receptor includes multiple N-glycosylation sites, with the homologues N74 being sensitive to highly processed complex-type N-glycans with N-acetyllactosamine repeats. These post-translational modifications influence receptor-ligand interactions, with the complex-type N-glycans lowering binding affinity [186,203]. The glycan complexity may further vary between cell types, with notable differences observed between CD16A isolated from human monocytes or NK cells. We speculate such modifications may underly the mildly augmented affinity detected for the G0 vs G0F variant of the 8-18C5 mAb.

The capacity of glycans to dictate the pathogenicity of MOG-specific antibodies was assessed using a punctual injection of 50 μg of the 8-18C5 glycovariants prior to active EAE onset. Observations from our animal model indicate a hierarchy in which the pathogenicity of G0 IgG1 supersedes that of G0F which supersedes the partially un-glycosylated MG variant. 3 days after MOG-Ab injection the G0 variant caused significant more tissue damage flaring the clinical severity and accelerating mortality as compared to their fucosylated counterparts. At this early timepoint lesions were characterized by the infiltration of macrophages, NK cells and T cells. The G0 variant most strongly promoted the accumulation of the NK and CD4 T cell response coherent with FcγRIII mediated antibody dependent cell-cytotoxicity (ADCC) and

antibody-dependent enhancement [199]. ADCC mediating killing of oligodendrocytes would augment tissue destruction, increase macrophage phagocytosis of tissue debris and promote the adaptive immune response by antigen-presentation. Antibody-dependent enhancement would promote these mechanisms by favouring FcγRIII phagocytosis of opsonised MOG-complexes. The striking MOG-Ab induced infiltration of the CD8 T cell response, nearly absent in the PBS control group, illustrates the efficacy of opsonised MOG-complexes in priming the adaptive immune response. Immune complexes promote priming *via* DC cell-maturation and opsonised antigen uptake via FcγR priming [204], as well as the neonatal FcRn receptor [205]. At sites of inflammation macrophages phagocytose opsonized immune-complexes permitting antigen presentation to local effector T cells to elicit their activation and phagolysosomal fusion [206]. The striking augmentation of the in situ $CD4^+$ T cell response induced by the G0 vs G0F 8-18C5 strongly points to antibody-dependent enhancement of the local inflammatory response. This augmentation was consistently shown among our different experimental paradigms, and show to be antigen-driven via MOG-recall experiments and fate-mapping of the monoclonal 2D2 T cell response. Reactivation of both Th1 and Th17 responses were implicated. With the 8-18C5 mAb recognizing a conformational epitope we expected a focused *in situ* enhancement by the MOG-specific antibodies. The observation that both the G0 and G0F 8-18C5 variants potentiated the MOG-specific $CD4^+$ T cell response in the spleen clearly indicate repercussions beyond the demyelinating lesions. This may implicate diffusion of opsonized MOG-complexes or migration of antigen-loaded myeloid cells back to the spleen in order to engage the adaptive immune response. The ability of G0F 8-18C5 to selectively promote the Th1 response indicates a qualitative difference with the G0 8-18C5 variant requiring further clarification. Fate mapping studies using traceable naïve 2D2 T cells confirmed the accumulation of the MOG-specific $CD4^+$ T cell response in the CNS. Transferring distinct 2D2 T cells 24hrs before immunization and concomitantly with the injection of the 8-18C5 glycovariants allowed the distinction between local *in situ* expansion of 2D2 effector cells primed upon MOG_{35-55} immunization (-24hrs) and the recruitment of recently activated effector cells (Day 9). The MOG_{35-55} induced immune response drives EAE onset integrating the 2D2 T cells transferred at -24hrs and principally targets MOG during onset with progressive implication of a heteroclitic neuronal antigen NF-M_{15-35} [207,208]. One week later, the MOG-specific T cell response in the spinal cord comprises both the disease inducing effector cells and newly primed effectors at equal proportion. The G0 8-18C5 variant enhanced the expansion of the MOG-specific T cell response 5 fold over this one week period. Strikingly, this predominantly implicated the *in situ* effector 2D2 T cells as 3 out of 4 were effector 2D2-24hrs T cells. This strongly indicates that local phagocytosis of immune-complexes opsonized with G0 IgG1 enhances lesional myeloid cells in expanding *in situ* effector T cells.

Demyelination and neurodegeneration characterize both MOGAD and MS lesions and similar mediators of inflammation can be detected including complement, antibodies and infiltrating

immune cells [132]. Poignant differences underscore that distinct immune mechanisms drive these paradigmatic neuroinflammatory diseases. Oligoclonal bands are absent in the cerebrospinal fluid of MOGAD patients. Unlike the focal MS lesions, MOGAD white matter demyelination is perivenous and confluent. The composition of the *in situ* immune response is dominated by macrophages and CD4 T cells, while CD8 T cells and B cells are present in more modest numbers [135]. Meningeal inflammation and B cell follicles as seen during disease progression in MS are absent in MOGAD. The lesional anatomy of MOGAD is recapitulated in our experimental model induced with a punctual injection of MOG-specific antibodies. The induced CD8 response remains perivascular, as opposed to the parenchymal CD8 infiltrates in MS [209]. The pathogenicity of the MOG-immune response was enhanced for the G0 Fc-glycovariants which strikingly enhanced the dominance of the MOG-specific CD4 T cell response *in situ*. Absence of fucose residues was a hallmark of the disease-related Ab response in MOGAD, while reduced galactosylation and increased bi-secting N297 glycans characterised disease-related Abs in MS. By translation these observations point to a decisive contribution of the hypofucocylated MOG-antibodies to the orchestration of the *in situ* inflammatory response in MOGAD. The increased affinity for CD16 potentiates NK-mediated ADCC and improves phagocytosis of opsonized MOG-complexes by local inflammatory myeloid cells endowing enhanced antigen activation of pathogenic T cells. Inflammatory Fc-domains are thus a hall mark of MOGAD pathology and dictate the inflammatory intensity orchestrated by the causal autoantibody response.

.

CONCLUSION

Currently, more than 80 autoimmune diseases have been described, affecting approximately 5-8% of the world's population and causing enormous suffering to patients, as well as representing a major global socioeconomic problem. Clinical issues remain a key challenge as treatments are not disease specific and are associated with many adverse effects [50]. Furthermore, although many detailed molecular, immunological, genetic, and clinical studies have led to a better understanding of the mechanisms underlying some autoimmune diseases, the drivers of human autoimmune diseases, including environmental triggers, and the subsequent pathogenesis remain incompletely understood and therefore important to study as a better comprehension of the disease may lead to better management of patients.

This work focuses on two paradigmatic inflammatory and demyelinating CNS diseases: MS and MOGAD. To date, there is no curative treatment for these two diseases and their complex pathophysiology remains a much studied field. More specifically, we have studied the impact of B lymphocytes and the humoral response in these two pathologies.

The study of the B cell repertoire in an experimental model of MS and more specifically in a spontaneous model of EAE in SJL/J TCR^{1640} mice allowed us to study the key role of these B cells in the pathophysiology of the disease. We have demonstrated that clonal selection and brain infiltration of specific MOG B cells are key factors in this spontaneous model of autoimmune demyelination.

The study of the impact of the glycosylation of the Fc fragment of autoantibodies in the context of MOGADs and MS by a translational approach allowed us to highlight the importance of this Fc glycosylation. Indeed, the study of the glycan profiles on the IgG1 response specific to MOG allowed us to identify a striking glycan signature in favor of hypofucosylation in MOGAD patients. The study of the impact of this hypofucosylation on the effector functions allowed us to highlight the pro-inflammatory aspect of this glycan profile due to its increased affinity for the Fc receptor CD16. This study allowed us to better understand the physiopathology of MOGAD. Fc-glycosylation seems to be a key factor in the disease and the study of the glycosylation profile of anti-MOG autoantibodies of patients could be an early diagnostic tool to improve the management of patients.

Furthermore, the study of Fc glycosylation can be extrapolated beyond the context of autoimmune diseases. Although Fc-glycosylation represents only 2 to 3% of the total mass of antibody. These glycans play a crucial role in the biological activity, pharmacokinetics, toxicity

or immunogenicity. It can be interesting to take into account this Fc-glycosylation in the production of monoclonal antibodies. Fc-engineering is critical for Next Generation Antibodies (NGA) and represent a key area in the improvement of monoclonal antibodies. With the example of obinutuzumab, produced with this technology and used in oncology in the treatment of previously untreated chronic lymphocytic leukemia This glycoengineered, humanized anti-CD20 monoclonal antibody present reduced core fucosylation and enhanced ADCC [210–212]. Moreover, the application of the Fc-engineering could be multiple in technical applications.

I. Molecular biology techniques

1. Production of recombinant vectors

All vectors were constructed by GeneArt from cDNA sequences defined trough UNIPROT data bases. (c.f **Annexe 2** and **Annexe 3**). Tetramer MOG come from the Max Planck institute.

a) Bacterial transformation

Recombinant vectors were produced by transformation of NEB®10-beta chemo-competent Escherichia coli bacteria (One shot max efficiency DH10B T1, Invitrogen) via heat shock. After 5 min of thawing on ice, the bacteria were put in contact with 2.5 µL of vector (i.e. between 1 and 10 ng of DNA) and, after a short incubation time (less than 30 min), they were placed in a water bath at 42°C for 30 to 45 sec and then again on ice for 1 min. The heat shock allows the incorporation of the vector into the bacteria by breaking the bacterial wall. Bacteria were then cultured for 45 min at 37°C under agitation (225 rpm) in 250 µL of SOC medium (BioLabs) then a fraction is plated on Petri dish containing LB medium (Luria Bertani) (SIGMA) supplemented with 50 µg/mL ampicillin (Gibco) for one night at 37°C. The addition of ampicillin ensures a selection pressure so that only bacteria that have integrated the vector carrying the ampicillin resistance gene multiply.

b) Amplification and purification

From 50 µL of glycerol stock, bacteria are grown in 500 mL of LB/ampicillin overnight before being centrifuged at 3500 rpm for 30 min. Then purification is done from the supernatant using the Nucleobond Xtra Maxi EF kit (Macherey-Nagel), its concentration is determined by measuring its absorbance at 280 nm with the Nanodrop and adjusted to 1000 ng/µL.

II. Cell culture ; antibody and protein production

A. Cell lines used

1. HEK293F cell line:

HEK293F (ATCC CRL-1573) cells for Human embryonic Kidney (HEK) are human embryonic kidney cells adapted to grow in suspension and under agitation with condition of culture: 37°C, 5% CO_2, 135rpm. For culture we use the Freestyle medium (Gibco). They are kept once a week with a cell density of : $3*10^5$ cells/mL.

2. YB2/0-E cell line:

YB2/0 cells (ATCC CRL-1662) are rat myeloma cells adapted to serum-free custom-made EMABPROI culture (Invitrogen) supplemented with 4mM L-glutamine (Gibco) and 0.3% cholesterol as LS1000 (Perbio). Upon thawing, the cells were cultured first under static and then under agitation with the following conditions: 37°C 5% CO_2, 135 rpm. Cell maintenance is carried out three times a week at a density of $3*10^5$ cells/mL (Monday and Wednesday) or $2*10^5$ cells/mL (Friday)

3. CHOs cell line:

CHO (Chinese Hamster Ovary) cells are chinese hamster ovary cells adapted for growth in suspension and under agitation: 37°C, 5% CO_2, 135rpm. Medium used is ProCHO4 (Lonza) supplemented with 4mM L-glutamine. Cell maintenance is carried out three times a week at a density of $3*10^5$ cells/mL (Monday and Wednesday) or $2*10^5$ cells/mL (Friday)

4. Jurkat cells transfected

Jurkat cells (ATCC® TIB-152™, Clone E6-1 are an immortalized human CD4 T cell line. For culture, the medium used is: RPMI 1640 (Invitrogen Corporation) supplemented with 10% FCS, 1% HEPES (Gibco), 1% Sodium Pyruvate (Gibco), 1% Penicilline/Streptomycine at 37°C under 7% CO2 in air. Cell maintenance is carried out once a week at a density of $3*10^5$ cells/mL.

B. Production of MOG protein and 8-18C5 antibodies

1. 8-18C5 in cell line production

a) Transient transfection and production in HEK293Fcells

The cells are amplified to a density of $1x10^6$ cells/ml in the desired volume on the day of transfection. A volume of 30 ml of cells to be transfected requires a total amount of 37.5 µg of DNA. The transfection is performed by lipofection, i.e. the DNA is complexed with a lipid transfection agent and enters the cell by endocytosis. Lipofection allows transient expression of the protein because the vector is not integrated into the cell genome. To transfect HEK293F cells, PEI (Polyethylenimine, Polysciences) is used as the transfectant and Opti-MEM (Opti-MEM Reduced serum medium, Gibco) as the transfection buffer. The DNA (37.5 µl concentrated to 1000 ng/µl) is first diluted in 1 ml of Opti-MEM before being mixed with the IAP (37.5 µl previously diluted in 1 ml of Opti-MEM). After incubating the complex for 20 min at room temperature, it is gently added to the cell suspension. Two "control" transfections are carried out in parallel, a growth control (without DNA) and a transfection control (transfection by the pMAX-GFP vector coding for GFP (Green Fluorescent Protein, Invitrogen)). The latter allows the transfection rate to be estimated (generally around 30% in HEK cells and 60% in CHO cells) by fluorescence microscopy 24 h after transfection. After 7 days of culture, the cells are harvested and centrifuged at 3500 rpm for 45 min. The supernatant was then filtered through a 0.22 µm filter (Millipak, Merck) and stored at +4°C before purification.

b) Stable transfection, cloning and production in CHOs cells

$1x10^6$ cells/ml is required on the day of transfection. The cells are centrifuged to RPMI medium (RPMI1640) (Gibco). A volume of 10 ml of cells to be transfected requires 60 µg of DNA. The linearised DNA (60 µl concentrated to 1000 ng/µl) is first diluted in 1 ml of RPMI and incubated for 15 min at room temperature. Similarly, 60 µl of Fecturin (Ozyme), the transfecting agent, is diluted in 1 ml of RPMI and incubated for 15 min at room temperature. The Fecturin solution is then rapidly added to the DNA solution for 30 min of complexation at room temperature. After addition of the complex to the cells, they are incubated under static conditions (37°C, 8% CO2) for 4h and then the medium is replaced by ProCHO4/L-glutamine culture medium. 2 days after transfection, the cells are placed in selective medium in the presence of 1 g/l of geneticin (G418) (Gibco) at a density of $5x10^5$ cells/ml. Geneticin is a toxin neutralised by the neomycin resistance gene product. Thus, only cells that have integrated the vector carrying the neomycin resistance gene are able to proliferate. This stable pool is then maintained conventionally and shaken when viability is above 50%, and a fraction is frozen when viability is above 80%.

If production is satisfactory, cloning is performed using a limit dilution method. The most productive clones are then amplified to a volume of 30 ml and a production test is performed for each clone. The best clones are frozen (3 cryotubes containing $10*10^6$ cells per clone).
To carry out a production run, the selected clone is thawed and then classically amplified under agitation (37°C, 7% CO2, 135 rpm) in ProCHO4/L-glutamine until the desired cell volume is reached. On the day of production start (d0), the cells are diluted to a density of $2x10^5$ cells/ml. The cells are harvested on day 10 and centrifuged at 4000 rpm for 30 min. The supernatant is then filtered through a 0.22 µm filter (Millipak, Merck) and stored at +4°C before purification.

c) Stable transfection, cloning and production in YB2/0-E cells

This transfection is carried out by electroporation, i.e. by means of a brief electrical pulse inducing a potential difference at the membrane and allowing the entry of DNA by opening the pores, using the Electrobuffer kit (Ozyme). On the day of transfection, the cells are centrifuged at 680 rpm for 8 min, the supernatant is retained. The cells are then washed in buffer A by centrifugation at 1200 rpm for 5 min and then rewashed in buffer A at a density of $1*10^7$ cells/ml and $5*10^6$ cells are then transferred into a conical microtube and centrifuged again. The amount of DNA required for transfection depends on the size of the vector, e.g. for a quantity of $5*10^6$ cells, 51.4 µg of a vector of 12950 bp (amount of DNA = 25*(vector size/reference vector size of 6292 bp)) is required. A mix is prepared by blending the 2X electroporation buffer (250 µl) composed of solutions B, C and D of the kit with the linearized DNA (51.4 µl concentrated to 1000 ng/µl) qsp 500 µl of ppi water. Once in this mix, the cells are immediately transferred to an electroporation dish (4 mm wide) and placed in the electroporator. Electroporation is enabled by the delivery of a 230 V / 950 µF exponential pulse, the pulse time should be between 18 and 25 msec. The cells are then resuspended in 15 ml of medium composed of 50% EMABPROI and 50% of the supernatant kept at a density of $3*10^5$ cells/ml. A "control" transfection was also performed (no DNA was added to the mix). Three days after transfection, the cells were placed in MCO10 optimised clonal medium (composed of 37.5% EMABPROI complemented, 22.5% DMEM (Gibco), 20% two-day supernatant and 20% BIT 9500 (Stemcell)) and under selection pressure (G418 1g/l) Ten days after transfection, the cells are placed in complemented EMABPROI medium while maintaining the selection pressure. This stable pool is then maintained under static conditions (37°C, 7% CO2) and a fraction is frozen when viability is above 80%.

If production is satisfactory, cloning is performed using a limit dilution method. For this, the cells of the stable pool are subcultured the day before at a density of $3*10^5$ cells/ml. On the day of plating, the cells were diluted in MCO10 without G418 and divided into 5 96-well plates (100 µl/well) containing 40 cells/plate. The culture medium is then renewed by adding

supplemented EMABPROI once a week until clones appear. When the wells have reached a sufficient cell density, the supernatants are screened by Fast-ELYSA assay. The most productive clones are then amplified to a volume of 30 ml and a production test is performed for each clone. The best clones are frozen (3 cryotubes containing $10*10^6$ cells per clone).
To carry out a production run, the selected clone is thawed and then classically amplified under agitation (37°C, 7% CO2, 135 rpm) in complemented EMABPROI (with the addition of 1 g/l G418 if it is the stable pool) until the desired cell volume is reached. On the day of production initiation (d0), cells were diluted in ProPow medium to a density of $3.5*10^5$ cells/ml and incubated under agitation (35°C, 7% CO2, 150 rpm). A nutrient supplement based on L-glutamine (4 mM) (Gibco) and D-glucose (2 g/l) (Sigma) is added to the cells at d3, d5 (and d7 depending on cell viability). Depending on cell viability, the cells are harvested at d6, d7 or d9 and centrifuged at 4000 rpm for 30 min. The supernatant was filtered through a 0.22 µm filter (Millipak, Merck) and stored at +4°C before purification.

2. 8-18C5 in hybridoma production

The production of the murine 8-18C5 antibody is performed by culturing the original hybridoma [143]. For this, cells were thawed and amplified under static conditions (37°C, 5% CO2) in amplification medium (IMDM (Iscove's Modified Dulbecco Medium, supplemented with 1% Penicillin/Streptomycin, 10% FBS (fetal bovine serum), and 0.1% mercaptoethanol; (Gibco)) until the desired cell volume was reached. On the day of production initiation (d0), cells are diluted to a density of $4*10^5$ cells/ml in production medium (IMDM (Iscove's Modified Dulbecco Medium, supplemented with 1% Penicillin/Streptomycin, 2% low IgG FBS (Fetal Bovine serum), and 0.1% mercaptoethanol; (Gibco)). The cells are harvested on day 7 and centrifuged at 4000 rpm for 30 min. The supernatant is then filtered through a 0.22 µm filter (Millipak, Merck) and stored at +4°C before concentration. Sequence is in Annexe 5.

3. Recombinant MOG monomere and MOG tetramer production

Polyethylenimine linear (PEI, CliniSciences) treated HEK cells were transfected with a pTT5 plasmid encoding for a histidine and Avi tagged $MOG_{1-125,}$ according to the protocol described in Perera NC and al**.** 2013 [213], Transfection efficiency of 21% was determined using a GFP plasmid. After 7 days of culture, supernatants were collected and rhMOG was purified by affinity chromatography using His TrapTM HP columns (Cytivia, Marlborough, MA). rMOG was eluted using an imidazole gradient (Sigma-Aldrich), followed by dialysis against PBS. A single biotin molecule was attached to the AviTag using the biotinylating kit (BirA500 kit, Avidity, Aurora, CO). The single-biotin rMOGm monomer was tetramerized at a ratio of 4mol of biotin rMOGm monomer to 1 mol of FITC or PE-conjugated streptavidin (Biolegend, San Diego, CA). The rMOGm tetramer that we refer to as MOG_{tet} was validated by flow cytometry using splenocytes from IgH^{MOG} mice. Validated MOG_{tet} labelled at least 70% of MOG-specific B cells present among IgH^{MOG} splenocytes.

4. Production of Avitag MOG_{1-132}

Avitag MOG_{1-132} is used for the purification of anti-MOG IgG1 from patients samples (c.f **VI.A**). (Vector and sequence in Annexe 6). HEK-EBNA cells were seeded at a density $1x10^6$ cells/mL in 100 mL medium (FreeStyle™293 expression medium, Gibco™) in T250 flask. 100 μg of extracellular domain hMOG DNA plasmid (inserted into pcDNA3.1(+) vector encoding with N-terminal avi-tag, $hMOG_{1-132}$, and C-terminal histidine tag) in 5 mL Opti-MEM™ medium (Gibco™) was prepared, and 200 μg of PEI (polyethylenimine, linear, MW 25K Da, Polysciences, Inc) was prepared in 5 mL Opti-MEM™ medium. PEI was added into DNA mixture, followed by incubation at room temperature, for 30 minutes. The DNA-PEI mixture was added dropwise into the cells while swirling. Cells were cultured at 135 rpm orbital shaker at 37 ℃, 5% CO_2 incubator for 7 days.

Supernatant was harvested by centrifugation at 1500 rpm, at 4 ℃ for 10 minutes. Before protein purification by HisTrap™ HP column (5mL, GE healthcare), supernatant was filtered through 0.22 μm filter membrane, followed by added imidazole to final concentration 20 mM. $rhMOG_{1-132}$ was loaded into HisTrap™ HP column and eluted by 500 mM Imidazole by using AKTA start protein purification system. The eluted fraction was dialyzed with dialysis membrane MWCO 6-8K Da against 50mM Tris-HCl pH8, at 4 ℃, overnight.

a) Biotinylation of avitag MOG_{1-132}

rhMOG protein was biotinylated by BirA biotin-protein ligase reaction kit (AVIDITY LLC) enzyme according to the instructions of the manufacturer. In brief, 10 nmole of rhMOG (at final concentration of 40 μM) was mixed with 1x Biomix-A (10x concentration, 0.5 M bicine buffer), 1x Biomix-B (100 mM ATP, 100 mM MgOAC, 500 μM d-biotin) and 2.5 μg of birA enzyme, at 30 ℃, overnight. Then, the biotinylated $rhMOG_{1-132}$ was dialyzed against PBS at 4 ℃, overnight to remove excess biotin.

b) Charging Ni-NTA beads and Streptavidin magnetic beads with $rhMOG_{1-132}$

Dynabeads™ MyOne™ Streptavidin C-1 beads (Invitrogen) and Dynabeads™ His-Tag beads (Invitrogen) were chosen to couple with biotinylated $rhMOG_{1-132}$ to test the coating capacity and the efficiency of pull-down anti-MOG antibodies. 1 mg of Dynabeads™ were taken and suspended in 1 mL of PBS followed by placed on DynaMag™-2 Aimant (Invitrogen) for 1 minute and the supernatant was discarded, for a total 3 washes. 100 μL of biotinylated $hMOG_{1-132}$ (around 1 mg/mL) was incubated with 1 mg of Dynabeads™ MyOne™ Streptavidin C-1 beads and the same amount of biotinylated $hMOG_{1-132}$ was incubated with 1 mg of Dynabeads™ His-Tag beads, respectively, rotate gently at room temperature, for 1 hour. The protein-coated beads were placed on magnet for 2 minutes to remove the supernatant. The amount of coated protein was known by measuring the remaining protein in the supernatant

by Nanodrop. The rhMOG$_{1-132}$-coated beads were washed by 500μL of PBS, vortex at room temperature, followed by placed on magnet to discard the supernatant, for a total 3 washes. Then, the rhMOG$_{1-132}$-coated beads were blocked by 200 μL of 0.1% BSA in PBS at room temperature, for 30 minutes. The rhMOG$_{1-132}$-coated beads were placed on magnet to remove the supernatant, and washed by PBS.

III. Concentration and purification techniques: Purification of antibodies and recombinant MOG protein

A. Antibody concentration

In order to reduce the volume of cell supernatant to be purified, it is concentrated on a cassette with a passage threshold of 50,000 Dalton (Pellicon P3B050A01 membrane, Millipore). To do this, the membrane is first washed with 15 L of ultrapure water and then the cell supernatant driven by a pump passes through the membrane at a speed of 200 rpm. The filtrate (containing components smaller than 50,000 Dalton) is removed while proteins larger than 50,000 Dalton such as IgG are concentrated in the retentate. To avoid leakage into the filtrate, the membrane should have a cut-off size 2-3 times smaller than the size of the protein to be concentrated. The membrane is then cleaned with 10% bleach in re-circulation for 30 min, washed with 15 L of ultrapure water and stored in 0.1M NaOH at +4°C. After concentration, the supernatant is filtered again on a 0.22 µm filter (Millipak, Merck) and stored at +4°C before purification.

B. Antibody purification

The antibodies produced are purified by affinity chromatography on a protein G column (5mL HiTrap Protein G HP column, GE Healthcare Bio-Sciences). Protein G is a surface protein of Streptococcus group G bacteria capable of binding IgG via its Fc fragment. This purification is performed on AKTA Purifier 10 (equipped with a P-960 pump and a Frac-950 fraction collector) using UNICORN software. All purification steps are performed at a flow rate of 5 ml/min except for elution at 2 ml/min. The column was first equilibrated with 20 mM Sodium Phosphate buffer pH7 (10 CV) and the supernatant was injected into the column. The column was then washed in equilibration buffer (10 CV) and the antibody was eluted at acidic pH with 0.1 M Glycine buffer pH2.7 and the eluate was collected in 1 ml fractions. After elution, the column was washed in 1 M NaCl buffer (2 CV) and re-equilibrated (10 CV) before being stored in 20% ethanol at +4°C. The absorbance at 280 nm of the elution fractions is checked with a UV-Visible Spectrophotometer (Ultrospec 3300 pro, Amersham Biosciences) and the fractions with absorbance above 0.05 are pooled. The pH of the eluate is adjusted to 5 by adding 1 M pH9 TRIS buffer. The eluate is then dialysed in a cassette (Slide-A-Lyzer Dialysis Kit, MWCO 3500 Dalton, Thermo) overnight in 10 mM Sodium acetate buffer pH4.75, concentrated (antibody concentration between 3000 and 5000 µg/ml) (Vivaspin 6, MWCO 5000 Dalton PES, Sartorius) and sterile filtered on a 0.22 µm filter (PES filter, Thermo).

C. MOG protein purification

Due to the affinity of the Histidine Tag for metal ions, the MOG protein (vector shown in Appendix 4) is purified by affinity chromatography on a Cobalt ion column (1mL HiTrap TALON crude column, GE Healthcare Bio-Sciences). This purification is performed on AKTA Purifier 10 with UNICORN software. All purification steps are performed at a flow rate of 1 ml/min except for elution at 0.5 ml/min. The column was first equilibrated in 50 mM Sodium Phosphate, 300 mM NaCl pH7.4 buffer (10 CV) and the supernatant was injected into the column. The column is then washed in equilibration buffer (10 CV) and the protein is eluted using a gradient of 0 to 300 mM imidazole (50 mM Sodium Phosphate, 300 mM NaCl, 300 mM Imidazole pH7.4) which competes with the Histidine Tag to bind to the metal ions on the column. The eluate is collected in 0.5 ml fractions. After elution, the column was re-equilibrated (10 CV) before being stored in 20% ethanol at +4°C. The absorbance at 280 nm of the elution fractions is checked and the fractions with an absorbance greater than 0.05 are pooled. The eluate is then dialysed in vivaspin (MWCO 5000 Dalton) in PBS 1X pH7.4 and sterile filtered on a 0.22 µm filter (PES filter, Thermo).

IV. *In vitro* studies and antibody functional characterization

A. Affinity ELISA test of recombinants FcRs, FcRn and MOG

1. FcRs ELISA

The binding of anti-MOG Ac produced in HEK (G0F), YB2 (G0) and CHO, 8-18C5 and deglycosylated 8-18C5 to murine recombinant FcγRIII is measured by ELISA. For this purpose, a coating of the receptors is performed on NiNTA plates (PierceTM Nickel Coated Plates, Thermo Scientific) with 100 ng/well. The plates are then incubated at 37°C for one to two hours. Prior to plating, Ab at a concentration of 1 µg/mL is complexed to the secondary HRP Anti-human $F(ab')^2$ Ab concentrated at 1.2 µg/mL for 2h at room temperature with gentle agitation on an orbital wheel at 12 rpm. These complexes are then plated onto the plates, with a 1:2 dilution over 8 spots, with deposits of 100 µL/well. The plates are then incubated for 1h at 30°C under agitation at 115 rpm. All washings and dilution were performed in PBS 1X Tween 0,05%.

Revelation is done by adding 100 µL/well of TMB (BioLegend™), then incubating for a maximum of 15 minutes in the dark. After neutralisation by adding 50 µL/well of sulphuric acid H_2SO_4, the absorbance at 450 nm is measured with the BMGLabTech FluoStarOmega spectrophotometer and recorded on the Omega software.

2. FcRn ELISA

The binding of anti-MOG Ac produced in HEK (G0F), YB2 (G0) and CHO, 8-18C5 and deglycosylated 8-18C5 to murine recombinant FcRn is measured by ELISA. For this purpose, a coating of the receptors is performed on NiNTA plates (PierceTM Nickel Coated Plates, Thermo Scientific) with 250 ng/well. The plates are then incubated at 37°C for one to two hours. In the same time, Abs at a concentration of 0.3 µg/mL are complexed to the secondary HRP Anti-human $F(ab')^2$ Ab concentrated at 3 µg/mL for 2h at room temperature with gentle agitation on an orbital wheel at 12 rpm. These complexes are then plated on the plates, with a 1:2 dilution over 8 spots, with deposits of 100 µL/well. The plates are then incubated for 1h at 30°C under agitation at 115 rpm. All washings and dilution were performed in P6 buffer ($Na_2HPO_412H_2O$ (1,08g) $NaH_2PO_42H_20$ (6,86g) NaCl (1,46g) qsp 500mL H_20 PPI at pH6) Tween 0,05% Skim milk 4%.

Revelation is done by adding 100 µL/well of TMB (BioLegend™), then incubating for a maximum of 15 minutes in the dark. After neutralisation by adding 50 µL/well of sulphuric acid H_2SO_4, the absorbance at 450 nm is measured with the BMGLabTech FluoStarOmega spectrophotometer and recorded on the Omega software.

Listing of mouse recombinants use for affinity ELISA of mouse FcRs and FcRn:

Recombinant Mouse FcγRIII/CD16 Protein, CF	1960-FC	Bio-Techne
Recombinant Mouse FcγRIIB/CD32b Protein, CF	1460-CD	Bio-Techne
Recombinant Mouse FcγRI/CD64 Protein, CF	2074-FC	Bio-Techne
Recombinant Mouse FcγR4/CD16-2 Protein, CF	1974-CD	Bio-Techne
Recombinant Mouse FcRn Protein, CF	6775-FC	Bio-Techne

Listing of others reagents :

Peroxidase-AffiniPure F(ab')2 Fragment Goat anti-mouse IgG, F(ab')2 Fragment Specific	115-035-006	Jackson ImmunoResearch
Tween-20	P1379	Sigma
Bovine serum albumin	A-7906	Sigma
TMB Substrate Set	421101	BioLegend
Stop Solution for TMB Substrate	423001	BioLegend
Pierce™ Nickel Coated Plates	15442	ThermoFisher Scientific
Na_2HPO_4 $12H_20$	71650	Sigma
$NaH_2P0_42H_20$	71505	Sigma
NaCl	27808.297	Sigma

3. MOG ELISA

MOG affinity of the different glycovariants is measured by ELISA. For this purpose a coating of recombinant MOG at a concentration of 1µg/mL is performed on Nunc Maxisorp plates with a deposit of 100µL. After Blocking solution, 8-18C5 glycovariants are plated with a 1:2 dilution over 16 points starting at a concentration of 0.4µg/mL. The plate is incubated 2h at room temperature. The secondary HRP Anti-human $F(ab')^2$ Ab is used for detection with a concentration of 1.2µg/mL and then incubated 1h30 at 37°C. Revelation is done by adding 100 µL/well of TMB (BioLegend™), then incubating for a maximum of 15 minutes in the dark. After neutralisation by adding 50 µL/well of sulphuric acid H_2SO_4, the absorbance at 450 nm is measured with the BMGLabTech FluoStarOmega spectrophotometer and recorded on the Omega software.

B. Detection of IL-2 production after JKT mCD16 activation

A coating of recombinant MOG at a concentration of 10µg/mL is performed on NiNTA plates (PierceTM Nickel Coated Plates, Thermo Scientific) with a deposit of 100µL. plate were incubate for one hour at 37°C, then wash with PBS Tween 0,05%. During incubation, mCD16 JKT cells and DC-SIGN JKT cells are counted to ensure that the final concentration is $0.5.10^6$ cells/mL (i.e. $0.5.10^5$ cells/well). Dilutions of cells are made in RPMI medium supplemented with phorbol myristate acetate (PMA) at 1 µg/mL.

Dilutions of different Abs are then prepared in Eppendorf tubes: 8 serial dilutions to 1:2, with an initial concentration of 2.5 µg/mL. JKT mCD16 cells are tested for activation in the presence of murine anti-MOG 8-18C5, G0, G0F, MG, and deglycosylated 8-18C5 at different concentrations. Each condition is tested in triplicates, depositing 100 µL/well of Ac. A reliability check is performed by coating one column of each plate with DC-SIGN JKT instead of mCD16 JKT. The plate is incubate for 16 h at 37°C, then centrifuge for 5 min at 1700 rpm. The supernatants are collected in two new 96-well plates (Greiner Bio-OneTM CELLSTAR), which are then placed in a freezer at -80°C. The aim is to detect the production of interleukin 2 (IL-2). This will be done by ELISA with the Human IL-2 DuoSet® ELISA kit (Bio-techne). Absorbance is measured at 450 nm with the BMGLabTech FluoStarOmega spectrophotometer and recorded on the Omega software.

C. Antibody cytotoxicity dependent on complement assay

The objective is to study CDC assay using JKT cells expressing MOG protein and our 8-18C5 anti-MOG antibody. This CDC assay is performed on the Incucyte Live-Cells Analysis System (Sartorius). In a 96-well conical plate (Greiner Bio-OneTM CELLSTAR), 100 µL/well of JKT MOG at a concentration of 40,000 cells/mL (i.e., 4,000 cells/well) is loaded. The different antibodies used for this experiment are: hybridoma produced 8-18C5 and its deglycosylated variant by PNGaseF treatment and lastly an anti-CD303 antibody used as control. 5 dilutions are performed in series, with an initial concentration at 100 µg/mL. 10 µL of each dilution is placed in the individual wells in duplicate, supplemented with 10 µL of fetal bovine serum (FBS). Two lines of wells are also filled with 10 µL of inactivated FBS. To decomplement or inactivate the SVF, it is heated to 56°C for 1 h. Finally, two wells are filled with 10 µL of Triton: these wells will serve as cell death controls.

Complement action is monitored for six hours, capturing images every fifteen minutes with the Incucyte Live-Cells Analysis System. The data is collected on the Incucyte Software

V. Mass spectrometry analysis

1. In-gel protease digestion

The antibody was loaded into 10% reducing SDS-PAGE. The position of gel around 50-55 kD corresponding to heavy chain of antibody was cut, and in-gel digestion was performed with an automated protein digestion system, a MassPrep Station (Waters, Manchester, U.K.). The gel plugs were washed twice with 50 µL of 25 mM ammonium bicarbonate and 50 µL of acetonitrile. Disulfide bonds were reduced by addition of 50 µL of 10 mM dithiothreitol at 57 °C followed by alkylated by addition of 50 µL of 55 mM iodoacetamide. After dehydration with acetonitrile, the proteins were cleaved in-gel with a 12.5 ng/µL solution of Trypsin/Lys-C protease mix, MS Grade (Pierce) in 25 mM ammonium bicarbonate, room temperature, overnight. Tryptic peptides were extracted twice: the first time with 60% acetonitrile in 5% formic acid for 1 h, and the second time with a 100% acetonitrile solution until the gel pieces were dehydrated. The collected extracts were pooled and dried by SpeedVac.

2. Nano-LC-ESI-MS/MS analyses

Nano-LC-MS/MS analysis was performed on an UltiMate 3000 RSLCnano System (Thermo Fisher Scientific) coupled to a Q-Exactive mass spectrometer (Thermo Fisher Scientific). Peptides were automatically fractionated onto a C18 reverse-phase column (75 µm × 150 mm, 2 µm particle, PepMap100 RSLC column, Thermo Fisher Scientific) at a temperature of 35°C. Trapping was performed during 4 min at 5 µl/min, with solvent A (98% H2O, 2% ACN and 0.1% FA). Elution was performed using two solvents A (0.1% FA in water) and B (0.1% FA in ACN) at a flow rate of 300 nl/min. Gradient separation was 24 min from 3% B to 20% B, 3 min from 20% B to 40% B, 2 min to 80% B, and maintained for 4 min. The column was equilibrated for 8 min with 3% solvent B prior to the next sample analysis. The electrospray voltage was 1.9 kV, and the capillary temperature was 275°C. Full MS scans were acquired over m/z 300–2,100 range with resolution 70,000 (m/z 200). The target value was 10^6. Ten most intense peaks with charge state between 2 and 5 were fragmented in the HCD collision cell with normalized collision energy of 22.5%, and tandem mass spectrum was acquired with resolution 70,000 at m/z 200. The target value was 5×10^6. The ion selection threshold was 1.3×10^5 counts, and the maximum allowed ion accumulation times were 250 ms for full MS scans and 200 ms for tandem mass spectrum. Dynamic exclusion was set to 30 s.

3. Quantitative glycopeptide analysis

NanoLC-MS/MS data was processed by using Byonic™ (Protein Metrics, San Carlos, CA), with a custom protein sequence database consisting of human IgG1, IgG2, IgG3, and IgG4 sequences to assign peptide and glycopeptide tandem mass spectra. For all data sets, cleavage rules were applied for each specific protease (trypsin/Lys-C: K, R,) and peptides with up to two missed cleavages were considered. The following peptide modifications were considered: methionine oxidation (variable), deamidation (variable), carbamidomethylation (fixed), and a Byonic N-glycan database consisting of 182 human N-glycans. Identification of glycopeptide mathes were accepted by confirmation manually.

The Full scan MS1 filtering in Skyline, an open source software (https://skyline.ms/wiki/home/software/Skyline/page.view?name=default) was chosen to extract quantitative information from data-dependent acquisition of LC-MS/MS experiment. Raw data was processed by Byonic™ search engine to generate spectral libraries before Skyline MS1 filtering. The peptide settings in Skyline are (1) Trypsin was chosen and the number of max missed cleavages was set as 2; (2) Structural modifications are common amino acid modifications happened during in-gel digestion and glycan modification which were observed in glycan analyses. Precursor isotopic import filter was set to a count of three, (M, M+1, and M+2) at a resolution of 60,000 for Orbitrap. After spectral library and raw data were imported, the graphical display of chromatogram was shown and report can be exported by the format of Excel file. The glycoform and intensity of IgG glycopeptides containing the conserved N297 residue were extracted to determine the relative ratios of each N297 glycoform represented.

4. Quantitative analysis of glycans

The isotopic cluster area of each permeated glycan is extracted from the Data Explorer software. The relative percentage of permeylated glycans is calculated by dividing the area of the glycan by the sum of the areas of all annotated glycans, multiplied by 100.

VI. *In vivo*, cellular and functional studies

A. Purification of IgG from human blood and CSF samples

Serum and CSF samples were obtained thanks to the biobank of the NOMADMUS and OFSEP protocols thanks to Pr Helene Zephir (Lille) and Romain Mariginier (Lyon).

5 mL of patient's serum was diluted with 45 mL of PBS, followed by filtered through 0.45 μm filter membrane. The filtered serum was loaded into a continuous connection of HiTrap™ Protein G HP column and HiTrap™ Protein A HP column (5 mL, GE healthcare), which were connected with AKTA start protein purification system. Total IgGs were eluted by 100 mM glycine, pH 2.5, and neutralized by Tris-base buffer. The purified IgGs were desalted and concentrated until 1 mL by 30 kDa Vivaspin® (Sartorius) at 4000 rpm at 4 ℃.

For glycosylation analysis, the antibodies were digested in trypsin gel. The resulting peptides were treated with PNGaseF to isolate the N-glycans. The glycopeptides were then analysed on a nanoRP C18-LC-ESI-MS/MS as described in *chapter III-C: Mass spectrometry analysis.*

1 mg rhMOG$_{1-132}$-coated C-1 beads were incubated with 2 mg total IgGs of patient in 1 mL of 0.025% Tween20 in PBS buffer (PBST 0.025%), rotate vigorously until beads suspension evenly in the solution, at 4 ℃, overnight. The beads were collected by placed on magnet and then, beads were added in 1 mL of PBST, 0.05%, vortex for 10 minutes, followed by removal of supernatant. The wash step was repeated 6 times. The anti-MOG antibodies were eluted from beads by adding 50 μL of 100 mM glycine with 0.1% SDS, pH 2.5, vortex vigorously for 15 minutes, and the supernatant was collected. The elution step was repeated in a total of 4 times, and all the supernatant was collected in the same tube followed by neutralization until pH 6. The neutralized antibodies were lyophilized.

B. Animal experimentation

- 2D2 mice have a C57BL/6 genetic background with homozygous CD45.1 congenic marker. They express a transgenic (Tg) TCR restricted CMH-II, I-A^b. These mice come from an endowment from Professor V. Kuchroo, Harvard University in Boston, USA. They carry a transgene encoding Vα3.2 and Vß11 allowing the expression of a MOG$_{35-55}$ specific TCR [53]. mouse strain is maintained in the heterozygous status by pairing 2D2 TCR Tg mice with WT mice. FACS phenotyping is performed as control of the strain
- RR mice with an SJL/J background were provided by Professor H. Wekerle of the Max Planck Institute in Martinsried, Germany. RR mice express a transgenic TCR restricted to MHC-II, I-A^s specific for MOG$_{92-16}$. The transgene encodes a Vα8.3 chain and a Vß4.
- C57Bl/6J mice were obtained from the Janvier laboratory (Le Genest Saint Isle, France). 8 week old females were used for the experiments.

- For the double fate mapping, an F1 was developed by crossing C57Bl/6J mice CD45.2$^+$ and a 2D2 CD45.1$^+$ to obtain 2D2 CD45.1$^+$CD45.2$^+$. FACS phenotyping is performed as control of the strain.

The breeding and housing of the mice is carried out in the High-Tech animal house with EOPS (Exempt from Specific Pathogenic Organisms) status at the research centre of the University of Lille, which is accredited by the Ministry of Agriculture (License # A59-3515). All experimental protocols are approved by the CEEA75 (Comité d'Éthique en Expérimentation Animale Nord - Pas de Calais region) and are in conformity with the directives of the European Union.

C. Peptides and recombinants proteins

MOG_{35-55} peptide (MEVGWYRSPFSRVVHLYRNGK) and NFM_{15-35} peptide (RRVTETRSSFSRVSGSPSSGF) come from GeneCust.

Recombinant human MOG protein (rhMOG) is produced by transient transfection in HEK. It is then purified from cell supernatant, clarified and concentrated on column (1mL HiTrap® TALON®) by affinity chromatography thanks to the affinity of the Histidine Tag for Cobalt ions. The rhMOG sequence is composed of 132 amino acids: « MGQFRVIGPRHPIRALVGDEVELPCRISPGKNATGMEVGWYRPPFSRVVHLYRNGKDQD GDQAPEYRGRTELLKDAIGEGKVTLRIRNVRFSDEGGFTCFFRDHSYQEEAAMELKVEDPF YWVSPGHHHHHH ».

D. EAE

1. Induction of Active EAE C57bl/6 mice

Female mice aged 7 to 15 weeks are anaesthetised with Xylasine (10mg/kg) and Ketamine (100mg/kg) intraperitoneally. Then they are immunised by an intradermic injection at the base of the tail of 100 µg of MOG_{35-55} peptide emulsified in CFA (Freund's complete adjuvant) completed with 500µg of *Mycobacterium Tuberculosis* inactivated strain H37RA.

On the day of immunization and on day 2, 200ng/mouse of pertussis toxin (PT) (List Biological Laboratories) is injected intravenously (i.v) into the retro orbital sinus. The day before the induction of EAE, at day 9, a single injection of 50µg of our 8-18C5 glycovariants antibodies (diluted in PBS to a concentration of 500µg/mL) is performed into I.V retro orbital sinus. The clinical follow-up of the mice is carried out according to the *Body Condition Score* (BCS). The BCS is monitored daily for 30 to 40 days. With the following score scale: 0: No signs; 1: Tail atony; 2: Delayed reversal; 3: Paraplegia of one o both hind limbs; 4: Paraplegia of both hind limbs; 5: Quadriparesis / Quadriplegia; 6: Death or moribund state.

2. Double fate mapping

To study the origin of CD4⁺ T cells activation in our experimental MOGAD model we performed a double fate mapping allowing us to dissociate *de novo* activation of naive CD4⁺ T cells in secondary lymph nodes from *in situ* expansion of effector T cells in 8-18C5-mediated exacerbation of autoimmune demyelination, we used a double fate mapping approach with two adoptive transfer of MOG specific CD4⁺ T with the use of the congenic markers CD45.1 and CD45.2 for their mapping. Thus, MOG-specific CD4⁺ CD45.1⁺ T cells from TCR-specific 2D2 transgenic mice were transferred 24 hours prior to immunization with the MOG_{35-55} peptide. On day 9, MOG-specific CD4⁺ T cells from 2D2 CD45.1⁺/CD45.2⁺ mice. This adoptive transfer is performed in parallel with the injection of 8-18C5 glycovariants .

MOG specific CD4⁺ T cells are purified from 2D2 mouse spleen. Red blood cells are lysed with ACK lysis buffer. CD4⁺ T cells are then purified via negative selection with magnetic sorting using the Miltenyi Biotec kit. Purified TCD4⁺ resuspended in PBS were injected intravenously (i.v) into the retro orbital sinus (**Figure 33**).

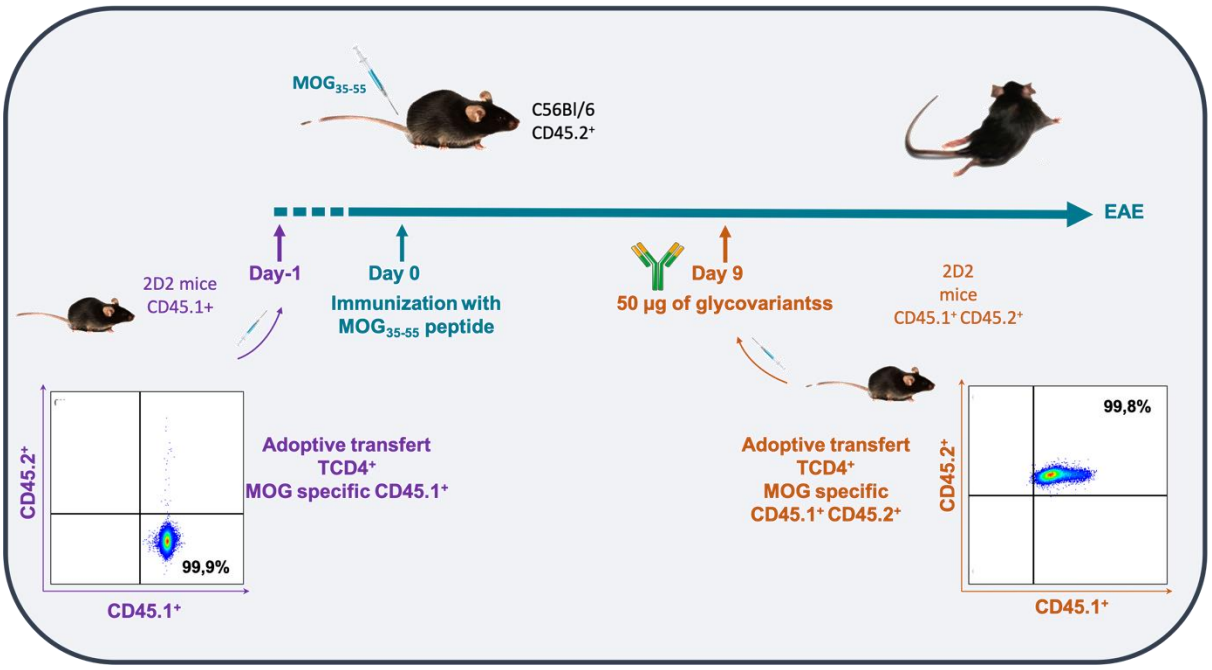

Figure 33: Illustrative picture of double fate mapping experiment

3. Spontaneous EAE SJL/J mice

EAE severity was scored as follows: 0: healthy/ No signs; 1: Tail atony; 2: hind limb weakness; 3: hind limb paralysis; 4: Quadriparesis / Quadriplegia; 5: Death or moribund state.

4. Transfer of Serum into 2D2 mice

Serum samples are taken after sacrifice. They are collected by intracardiac route. Serum was extracted after blood centrifugation at 1000G à 4°C stored at -20°C.

Sera were transferred with I.V injection by retro-orbital sinus in disease-prone 2D2 TCR transgenic recipients. Each recipient received the serum of a single, distinct, donor. On day 0, 2D2 mice received 200 ng of PT I.V by retro-orbital injection. Two days later a second i.v. injection of pertussis toxin was accompanied by either 50 µL of serum from disease-free TCR^{1640}, diseased TCR^{1640} or NTL mice or either 50 µL of PBS.

E. Cells isolation

For single-cell suspensions: cells were isolated from spleen and cervical lymph nodes by mechanical disruption via forcing through 40-µm cell strainers. B-cells were purified using a mouse B-cell isolation kit (EasySTep^{TM} Mouse B cell Isaolation Kit, Stemcell).

For isolation of murine CNS mononuclear cells : mice are given a lethal dose of sodium pentobarbital (50-60mg/kg) intraperitoneally and then perfused with PBS intracardially. The brains and spinal cords are removed. This tissues were dissociated using potters and then digested in digestion buffer (2mg/mL collagenase D (SIGMA), 0.01mg/mL TCLK (Na-Tosyl-L-Lysine Chloromethyl Ketone HY from SIGMA), 0.02mg/mL DNase (SIGMA)) under agitation at 37°C for 1h for brains and 30min for spinal cord. The mononuclear cells were then isolated via a triple gradient of Percoll (30%, 37% and 70%) after centrifugation for 20 min at 2000rpm.

F. Flow cytometry

Analyses were performed on the BD LSR Fortessa or SONY SP6800 at the Cytometry and Cell Sorting platform (Bio lmaging Center of Lille, Lille University). To avoid aspecific labelling due to Fc fragments, a CD16/CD32 Fc Block is performed before labelling. Viability was evaluated with fixable viability dye staining with APC-efluor780 or with 7AAD staining.

Intracellular labelling is performed following fixation/permeabilization using the kit: "Fixation/Permeabilization, Foxp3" (eBioscience^{TM}). An activation is carried out for cytokine labelling: PMA / Iono (PMA / Iono for Phorbol 12 mystrate 13-acetate / Inomycin (Ionomycin (1/500) + PMA (1/1000) + Brefeldin A (1/500))

To identify MOG-specific B cells analyse, they are detected with single-biotin recombinant mouse MOG_{tet} using streptavidin-FITC or -PE.

Cell-sorting was used for the iGB cultures $CD19^+CD20^+CD4^-$ singlets or MOG-tetramer$^+$ $CD19^+CD20^+CD4^-$ singlets were directly sorted into individual wells containing CD40LB feeder cells.

Cell-sorting was performed using a FACS Aria III (Becton Dickinson).

Analysis was performed using FlowJo (FlowJo, LLC, Ashland, OR) software V10.5.3.

The list of antibodies used is found in Annexe 1.

G. Histochemistry and Immunohistochemistry

Female mice immunized with MOG_{35-55} peptide and injected with 8-18C5 glycovariants were sacrificed on day 12 treated with intracardiac perfusion in PBS and then with 4% PFA. Mice were then sent to the brain institute after a post-fixation of minimum 24h in PFA 4%.

Histochemistry and immunohistochemistry was performed thanks to the Vienna Brain Institute and Dr. Jan Bauer. Brain and spinal cord sections (4 µm) of paraffin were stained with haematoxylin/eosin, Nissl stain for neurons and Luxol fast blue for myelin.

Immunohistochemical staining and confocal fluorescence double staining were performed according to published protocols [214] using the primary antibodies (CD3, CD8, CD161).

H. ELISPOT IFN-γ and IL-17A

- To analyze the immune infiltrate in the brain and marrow: mononuclear cells are isolated from the brain or bone marrow (as described above). 1 x 10^5 cells were stimulated or not with 10μg of MOG_{35-55} peptide. Supernatants were collected 48h later and ELSIPOT assay performed with CTL kit.
- To analyze the peripheral $TCD4^+$ immune response: The spleens are dissociated between two slides. Red blood cells are lysed with ACK lysis buffer. $CD4^+$ T cells are then purified via negative selection with magnetic sorting using the Miltenyi Biotec kit (CD4+ T Cell Isolation Kit, mouse 130-104-454). 2.5 x 10^5 purified CD4 T Cell were stimulated in the presence of MOG_{35-55} peptide (0.1μg ; 1μg ; 10μg or 100μg) along with 5 x 10^5 irradiated APCs (X ray (X-RAD 320)) from the spleen of C57Bl/6 mice. Supernatants were collected 48h later and ELSIPOT assay performed with CTL kit.

Elispots were perfomerd with with Cellular Technology Ltd(CTL) ELISPOT assay with Mu IFN-γ SCE Kit (MIFNG-2M/5) and Mu IL-17 SCE Kit (MIL17-2M/5). Plates have been sent for analyze to Dr. Romieu-Mourez from the Human immunomonitoring platform of INFINITy laboratory (Inserm UMR1291 – CNRS UMR5051 – Université Toulouse II) having the ELISPOT S6 Ultra-V analyzer de Cellular Technology Ltd.

I. Determination of serum titers of MOG-specific antibodies and of total IgG1 antibodies (ELISA)

Serially diluted serum collected from the indicated mice were transferred to 96-well ELISA plates Nunc MaxiSorp™ precoated with recombinant MOG. ELISA assay was performed like the ELISA MOG (from chapter IV.3.MOG ELISA). The absorbance at 450 nm is measured with the BMGLabTech FluoStarOmega spectrophotometer and recorded on the Omega software.

VII. Statistical test

The logiciel PRISM 9 (Graphpad software Inc.) was used for the statistical analysis and graphs.

- For the presentation of the results of EAE clinical follow-ups: the continuous quantitative variables were described by the mean and +/- SEM (Standard error of the mean) and compared with the two way ANOVA test.
- For statistical analyses of the mean cumulative score, an unpaired Student's T- test with a 5% risk was used. (p-values < 0.05)
- For the survival fraction, a Chi 2 tests were performed to analyze the difference between the two groups.
- For EAE incidence a Kaplan-Meier plots was used and statistical significance was calculated using the log rank test.
- Linear regression was used to evaluate correlations.

1. Allen NJ, Barres BA. Glia — more than just brain glue. Nature. 2009;457(7230):675-7.

2. Barres BA. The mystery and magic of glia: a perspective on their roles in health and disease. Neuron. 2008;60(3):430-40.

3. Prinz M, Jung S, Priller J. Microglia Biology: One Century of Evolving Concepts. Cell. 2019;179(2):292-311.

4. Masuda T, Sankowski R, Staszewski O, Prinz M. Microglia Heterogeneity in the Single-Cell Era. Cell Reports. 2020;30(5):1271-81.

5. Mrdjen D, Pavlovic A, Hartmann FJ, Schreiner B, Utz SG, Leung BP, et al. High-Dimensional Single-Cell Mapping of Central Nervous System Immune Cells Reveals Distinct Myeloid Subsets in Health, Aging, and Disease. Immunity. 2018;48(2):380-395.e6.

6. Mundt S, Greter M, Flügel A, Becher B. The CNS Immune Landscape from the Viewpoint of a T Cell. Trends Neurosci. 2019;42(10):667-79.

7. Medawar PB. Immunity to homologous grafted skin; the fate of skin homografts transplanted to the brain, to subcutaneous tissue, and to the anterior chamber of the eye. Br J Exp Pathol. 1948;29(1):58-69.

8. Owens GP. A Neuroprimer: Principles of CNS Immunity. Semin Pediatr Neurol. 2017;24(3):145-51.

9. Rustenhoven J, Drieu A, Mamuladze T, de Lima KA, Dykstra T, Wall M, et al. Functional characterization of the dural sinuses as a neuroimmune interface. Cell. 2021;184(4):1000-1016.e27.

10. Shechter R, London A, Schwartz M. Orchestrated leukocyte recruitment to immune-privileged sites: absolute barriers versus educational gates. Nat Rev Immunol. 2013;13(3):206-18.

11. Mildenberger W, Stifter SA, Greter M. Diversity and function of brain-associated macrophages. Current Opinion in Immunology. 2022;76:102181.

12. Cugurra A, Mamuladze T, Rustenhoven J, Dykstra T, Beroshvili G, Greenberg ZJ, et al. Skull and vertebral bone marrow are myeloid cell reservoirs for the meninges and CNS parenchyma. Science. 2021;373(6553):eabf7844.

13. Louveau A, Harris TH, Kipnis J. Revisiting the concept of CNS immune privilege. Trends Immunol. 2015;36(10):569-77.

14. Ransohoff RM, Engelhardt B. The anatomical and cellular basis of immune surveillance in the central nervous system. Nat Rev Immunol. 2012;12(9):623-35.

15. Ransohoff RM, Kivisäkk P, Kidd G. Three or more routes for leukocyte migration into the central nervous system. Nat Rev Immunol. juill 2003;3(7):569-81.

16. McGavern DB, Kang SS. Illuminating viral infections in the nervous system. Nature Reviews Immunology. 2011;11(5):318-29.

17. Dranoff G. Cytokines in cancer pathogenesis and cancer therapy. Nat Rev Cancer. 2004;4(1):11-22.

18. Mebius RE, Kraal G. Structure and function of the spleen. Nat Rev Immunol. 2005;5(8):606-16.

19. Martinon F, Burns K, Tschopp J. The inflammasome: a molecular platform triggering activation of inflammatory caspases and processing of proIL-beta. Mol Cell. 2002;10(2):417-26.

20. Tonegawa S. Somatic generation of antibody diversity. Nature. 1983;302(5909):575-81.

21. Grakoui A, Bromley SK, Sumen C, Davis MM, Shaw AS, Allen PM, et al. The Immunological Synapse: A Molecular Machine Controlling T Cell Activation. Science. 1999;285(5425):221-7.

22. Kersh GJ, Kersh EN, Fremont DH, Allen PM. High- and low-potency ligands with similar affinities for the TCR: the importance of kinetics in TCR signaling. Immunity. 1998;9(6):817-26.

23. Wucherpfennig KW, Allen PM, Celada F, Cohen IR, De Boer R, Garcia KC, et al. Polyspecificity of T cell and B cell Receptor Recognition. Semin Immunol. 2007;19(4):216-24.

24. Nemazee D. Receptor editing in lymphocyte development and central tolerance. Nat Rev Immunol. 2006;6(10):728-40.

25. Feederle R, Schepers A. Antibodies specific for nucleic acid modifications. RNA Biol. 2017;14(9):1089-98.

26. Backhaus O. Generation of Antibody Diversity [Internet]. Antibody Engineering. IntechOpen; 2018 [cité 27 juin 2022]. Disponible sur: https://www.intechopen.com/chapters/undefined/state.item.id

27. Swain SL, McKinstry KK, Strutt TM. Expanding roles for CD4+ T cells in immunity to viruses. Nat Rev Immunol. 2012;12(2):136-48.

28. Young C, Brink R. The unique biology of germinal center B cells. Immunity. 2021;54(8):1652-64.

29. Victora GD, Nussenzweig MC. Germinal centers. Annu Rev Immunol. 2012;30:429-57.

30. De Silva NS, Klein U. Dynamics of B cells in germinal centres. Nat Rev Immunol. 2015;15(3):137-48.

31. Basso K, Dalla-Favera R. Germinal centres and B cell lymphomagenesis. Nat Rev Immunol. 2015;15(3):172-84.

32. Xu Z, Zan H, Pone EJ, Mai T, Casali P. Immunoglobulin class-switch DNA recombination: induction, targeting and beyond. Nat Rev Immunol. 2012;12(7):517-31.

33. Tendeiro Rego R, Morris EC, Lowdell MW. T-cell receptor gene-modified cells: past promises, present methodologies and future challenges. Cytotherapy. 2019;21(3):341-57.

34. Kuhns MS, Davis MM. TCR Signaling Emerges from the Sum of Many Parts. Front Immunol. 2012;3:159.

35. Francis Elliott J, Rock EP, Patten PA, Davis MM, Chien Y hsiu. The adult T-cell receptor 5-chain is diverse and distinct from that of fetal thymocytes. Nature. 1988;331(6157):627-31.

36. Nikolich-Žugich J, Slifka MK, Messaoudi I. The many important facets of T-cell repertoire diversity. Nat Rev Immunol. 2004;4(2):123-32.

37. Koch U, Radtke F. Mechanisms of T cell development and transformation. Annu Rev Cell Dev Biol. 2011;27:539-62.

38. Singer A, Bosselut R. CD4/CD8 coreceptors in thymocyte development, selection, and lineage commitment: analysis of the CD4/CD8 lineage decision. Advances in Immunology. 2004;83:91-131.

39. Laufer TM, Glimcher LH, Lo D. Using thymus anatomy to dissect T cell repertoire selection. Semin Immunol. 1999;11(1):65-70.

40. Peterson P, Org T, Rebane A. Transcriptional regulation by AIRE: molecular mechanisms of central tolerance. Nature Reviews Immunology. 2008;8(12):948-57.

41. Kyewski B, Peterson P. Aire, Master of Many Trades. Cell. 2010;140(1):24-6.

42. Pohar J, Simon Q, Fillatreau S. Antigen-Specificity in the Thymic Development and Peripheral Activity of CD4+FOXP3+ T Regulatory Cells. Front Immunol. 2018;9:1701.

43. Bennett CL, Christie J, Ramsdell F, Brunkow ME, Ferguson PJ, Whitesell L, et al. The immune dysregulation, polyendocrinopathy, enteropathy, X-linked syndrome (IPEX) is caused by mutations of FOXP3. Nature Genetics. 2001;27(1):20-1.

44. Vignali DAA, Collison LW, Workman CJ. How regulatory T cells work. Nat Rev Immunol. 2008;8(7):523-32.

45. Feuerer M, Hill JA, Mathis D, Benoist C. Foxp3+ regulatory T cells: differentiation, specification, subphenotypes. Nat Immunol. 2009;10(7):689-95.

46. Vyas JM, Van der Veen AG, Ploegh HL. The known unknowns of antigen processing and presentation. Nat Rev Immunol. 2008;8(8):607-18.

47. Mahon BP, Katrak K, Nomoto A, Macadam AJ, Minor PD, Mills KH. Poliovirus-specific CD4+ Th1 clones with both cytotoxic and helper activity mediate protective humoral immunity against a lethal poliovirus infection in transgenic mice expressing the human poliovirus receptor. J Exp Med. 1995;181(4):1285-92.

48. Abbas AK, Murphy KM, Sher A. Functional diversity of helper T lymphocytes. Nature. 1996;383(6603):787-93.

49. Nurieva R, Yang XO, Martinez G, Zhang Y, Panopoulos AD, Ma L, et al. Essential autocrine regulation by IL-21 in the generation of inflammatory T cells. Nature. 2007;448(7152):480-3.

50. Fugger L, Jensen LT, Rossjohn J. Challenges, Progress, and Prospects of Developing Therapies to Treat Autoimmune Diseases. Cell. 2020;181(1):63-80.

51. Miller SD, Vanderlugt CL, Begolka WS, Pao W, Yauch RL, Neville KL, et al. Persistent infection with Theiler's virus leads to CNS autoimmunity via epitope spreading. Nat Med. 1997;3(10):1133-6.

52. Katz-Levy Y, Neville KL, Padilla J, Rahbe S, Begolka WS, Girvin AM, et al. Temporal development of autoreactive Th1 responses and endogenous presentation of self myelin epitopes by central nervous system-resident APCs in Theiler's virus-infected mice. J Immunol. 2000;165(9):5304-14.

53. Scheikl T, Pignolet B, Mars LT, Liblau RS. Transgenic mouse models of multiple sclerosis. Cell Mol Life Sci. 2010;67(23):4011-34.

54. Scammell TE. Narcolepsy. The New England Journal of Medicine. 2015;373(27):2654-62.

55. Latorre D, Kallweit U, Armentani E, Foglierini M, Mele F, Cassotta A, et al. T cells in patients with narcolepsy target self-antigens of hypocretin neurons. Nature. 2018;562(7725):63-8.

56. Bjornevik K, Cortese M, Healy BC, Kuhle J, Mina MJ, Leng Y, et al. Longitudinal analysis reveals high prevalence of Epstein-Barr virus associated with multiple sclerosis. Science. 2022;375(6578):296-301.

57. Bar-Or A, Pender MP, Khanna R, Steinman L, Hartung HP, Maniar T, et al. Epstein–Barr Virus in Multiple Sclerosis: Theory and Emerging Immunotherapies. Trends in Molecular Medicine. 2020;26(3):296-310.

58. Tengvall K, Huang J, Hellström C, Kammer P, Biström M, Ayoglu B, et al. Molecular mimicry between Anoctamin 2 and Epstein-Barr virus nuclear antigen 1 associates with multiple sclerosis risk. Proceedings of the National Academy of Sciences. 2019;116(34):16955-60.

59. Lünemann JD, Jelcić I, Roberts S, Lutterotti A, Tackenberg B, Martin R, et al. EBNA1-specific T cells from patients with multiple sclerosis cross react with myelin antigens and co-produce IFN-gamma and IL-2. J Exp Med. 2008;205(8):1763-73.

60. Jog NR, McClain MT, Heinlen LD, Gross T, Towner R, Guthridge JM, et al. Epstein Barr virus nuclear antigen 1 (EBNA-1) peptides recognized by adult multiple sclerosis patient sera induce neurologic symptoms in a murine model. J Autoimmun. 2020;106:102332.

61. Lanz TV, Brewer RC, Ho PP, Moon JS, Jude KM, Fernandez D, et al. Clonally expanded B cells in multiple sclerosis bind EBV EBNA1 and GlialCAM. Nature. 2022;603(7900):321-7.

62. Robinson WH, Steinman L. Epstein-Barr virus and multiple sclerosis. Science. 2022;375(6578):264-5.

63. Kang MS, Kieff E. Epstein–Barr virus latent genes. Exp Mol Med. 2015;47(1):e131-e131.

64. Polman CH, Reingold SC, Banwell B, Clanet M, Cohen JA, Filippi M, et al. Diagnostic criteria for multiple sclerosis: 2010 revisions to the McDonald criteria. Ann Neurol. 2011;69(2):292-302.

65. Filippi M, Bar-Or A, Piehl F, Preziosa P, Solari A, Vukusic S, et al. Multiple sclerosis. Nat Rev Dis Primers. 2018;4(1):43.

66. Compston A, Coles A. Multiple sclerosis. Lancet. 2008;372(9648):1502-17.

67. Dendrou CA, Fugger L, Friese MA. Immunopathology of multiple sclerosis. Nat Rev Immunol. 2015;15(9):545-58.

68. Goebels N, Hofstetter H, Schmidt S, Brunner C, Wekerle H, Hohlfeld R. Repertoire dynamics of autoreactive T cells in multiple sclerosis patients and healthy subjects: epitope spreading versus clonal persistence. Brain. 2000;123 Pt 3:508-18.

69. Atlas of MS [Internet]. MS International Federation. Disponible sur: http://www.msif.org/wp-content/uploads/2014/09/Atlas-of-MS.pdf

70. Attfield KE, Jensen LT, Kaufmann M, Friese MA, Fugger L. The immunology of multiple sclerosis. Nat Rev Immunol. 2022;1-17.

71. Wallin MT, Culpepper WJ, Nichols E, Bhutta ZA, Gebrehiwot TT, Hay SI, et al. Global,

regional, and national burden of multiple sclerosis 1990–2016: a systematic analysis for the Global Burden of Disease Study 2016. The Lancet Neurology. 2019;18(3):269-85.

72. Koch-Henriksen N, Sørensen PS. The changing demographic pattern of multiple sclerosis epidemiology. The Lancet Neurology. 2010;9(5):520-32.

73. International Multiple Sclerosis Genetics C. Multiple sclerosis genomic map implicates peripheral immune cells and microglia in susceptibility. Science. 2019;365(6460).

74. Barcellos LF, Oksenberg JR, Begovich AB, Martin ER, Schmidt S, Vittinghoff E, et al. HLA-DR2 Dose Effect on Susceptibility to Multiple Sclerosis and Influence on Disease Course. Am J Hum Genet. 2003;72(3):710-6.

75. Olsson T, Barcellos LF, Alfredsson L. Interactions between genetic, lifestyle and environmental risk factors for multiple sclerosis. Nat Rev Neurol. 2017;13(1):25-36.

76. Hedström AK, Sundqvist E, Bäärnhielm M, Nordin N, Hillert J, Kockum I, et al. Smoking and two human leukocyte antigen genes interact to increase the risk for multiple sclerosis. Brain. 2011;134(Pt 3):653-64.

77. Berer K, Mues M, Koutrolos M, Rasbi ZA, Boziki M, Johner C, et al. Commensal microbiota and myelin autoantigen cooperate to trigger autoimmune demyelination. Nature. 2011;479(7374):538-41.

78. Brahic M. Multiple sclerosis and viruses. Ann Neurol. 2010;68(1):6-8.

79. Sundqvist E, Sundström P, Lindén M, Hedström AK, Aloisi F, Hillert J, et al. Epstein-Barr virus and multiple sclerosis: interaction with HLA. Genes Immun. 2012;13(1):14-20.

80. Pakpoor J, Disanto G, Gerber JE, Dobson R, Meier UC, Giovannoni G, et al. The risk of developing multiple sclerosis in individuals seronegative for Epstein-Barr virus: a meta-analysis. Mult Scler. 2012;

81. Palacios N, Alonso A, Brønnum-Hansen H, Ascherio A. Smoking and increased risk of multiple sclerosis: parallel trends in the sex ratio reinforce the evidence. Ann Epidemiol. 2011;21(7):536-42.

82. Pierrot-Deseilligny C, Souberbielle JC. Vitamin D and multiple sclerosis: An update. Multiple Sclerosis and Related Disorders. 2017;14:35-45.

83. Salzer J, Hallmans G, Nyström M, Stenlund H, Wadell G, Sundström P. Vitamin D as a protective factor in multiple sclerosis. Neurology. 2012;79(21):2140-5.

84. Vidal SA, Caulin Charles, Roguet Isabelle. Vidal Recos: recommandations en pratique 2016 185 stratégies thérapeutiques / [édité par l'équipe rédactionnelle du Vidal ; sous la direction du professeur Charles Caulin et Isabelle Roguet]. [6e édition]. Issy-les-Moulineaux: Vidal; 2015. 2799 p.

85. Maillart E. Treatment of progressive multiple sclerosis: Challenges and promising perspectives. Rev Neurol (Paris). 2018;174(6):441-8.

86. Goverman J. Autoimmune T cell responses in the central nervous system. Nat Rev Immunol. 2009;9(6):393-407.

87. Lucchinetti C, Brück W, Parisi J, Scheithauer B, Rodriguez M, Lassmann H. Heterogeneity of multiple sclerosis lesions: implications for the pathogenesis of demyelination. Ann Neurol.

2000;47(6):707-17.

88. Babbe H, Roers A, Waisman A, Lassmann H, Goebels N, Hohlfeld R, et al. Clonal expansions of CD8(+) T cells dominate the T cell infiltrate in active multiple sclerosis lesions as shown by micromanipulation and single cell polymerase chain reaction. J Exp Med. 2000;192(3):393-404.

89. Jacobsen M, Cepok S, Quak E, Happel M, Gaber R, Ziegler A, et al. Oligoclonal expansion of memory CD8+ T cells in cerebrospinal fluid from multiple sclerosis patients. Brain. 2002;125(Pt 3):538-50.

90. Lovato L, Willis SN, Rodig SJ, Caron T, Almendinger SE, Howell OW, et al. Related B cell clones populate the meninges and parenchyma of patients with multiple sclerosis. Brain. 2011;134(Pt 2):534-41.

91. Trapp BD, Stys PK. Virtual hypoxia and chronic necrosis of demyelinated axons in multiple sclerosis. Lancet Neurol. 2009;8(3):280-91.

92. Mahad DH, Trapp BD, H. Lassmann. Pathological mechanisms in progressive multiple sclerosis. Lancet Neurol. 2015;14(2):183-93.

93. Lassmann H, van Horssen J, Mahad D. Progressive multiple sclerosis: pathology and pathogenesis. Nature Reviews Neurology. 2012;8(11):647-56.

94. Magliozzi R, Howell O, Vora A, Serafini B, Nicholas R, Puopolo M, et al. Meningeal B-cell follicles in secondary progressive multiple sclerosis associate with early onset of disease and severe cortical pathology. Brain. 2007;130(Pt 4):1089-104.

95. Serafini B, Rosicarelli B, Magliozzi R, Stigliano E, Aloisi F. Detection of ectopic B-cell follicles with germinal centers in the meninges of patients with secondary progressive multiple sclerosis. Brain Pathol. 2004;14(2):164-74.

96. Vaughn CB, Jakimovski D, Kavak KS, Ramanathan M, Benedict RHB, Zivadinov R, et al. Epidemiology and treatment of multiple sclerosis in elderly populations. Nat Rev Neurol. 2019;15(6):329-42.

97. Peterson JW, Trapp BD. Neuropathobiology of multiple sclerosis. Neurol Clin. 2005;23(1):107-29, vi-vii.

98. Grebenciucova E, Berger JR. Immunosenescence: the Role of Aging in the Predisposition to Neuro-Infectious Complications Arising from the Treatment of Multiple Sclerosis. Curr Neurol Neurosci Rep. 2017;17(8):61.

99. Weber MS, Hemmer B, Cepok S. The role of antibodies in multiple sclerosis. Biochim Biophys Acta. 2011;1812(2):239-45.

100. Lassmann H, Bruck W, Lucchinetti C. Heterogeneity of multiple sclerosis pathogenesis: implications for diagnosis and therapy. Trends Mol Med. 2001;7(3):115-21.

101. Storch MK, Piddlesden S, Haltia M, Iivanainen M, Morgan P, Lassmann H. Multiple sclerosis: in situ evidence for antibody- and complement-mediated demyelination. Ann Neurol. 1998;43(4):465-71.

102. Obermeier B, Mentele R, Malotka J, Kellermann J, Kümpfel T, Wekerle H, et al. Matching of

oligoclonal immunoglobulin transcriptomes and proteomes of cerebrospinal fluid in multiple sclerosis. Nat Med. 2008;14(6):688-93.

103. von Budingen HC, Harrer MD, Kuenzle S, Meier M, Goebels N. Clonally expanded plasma cells in the cerebrospinal fluid of MS patients produce myelin-specific antibodies. Eur J Immunol. 2008;38(7):2014-23.

104. Farrell MA, Kaufmann JC, Gilbert JJ, Noseworthy JH, Armstrong HA, Ebers GC. Oligoclonal bands in multiple sclerosis: clinical-pathologic correlation. Neurology. 1985;35(2):212-8.

105. Keegan M, Konig F, McClelland R, Bruck W, Morales Y, Bitsch A, et al. Relation between humoral pathological changes in multiple sclerosis and response to therapeutic plasma exchange. Lancet. 2005;366(9485):579-82.

106. Zettl UK, Hartung HP, Pahnke A, Brueck W, Benecke R, Pahnke J. Lesion pathology predicts response to plasma exchange in secondary progressive MS. Neurology. 2006;67(8):1515-6.

107. Molnarfi N, Schulze-Topphoff U, Weber MS, Patarroyo JC, Prod'homme T, Varrin-Doyer M, et al. MHC class II-dependent B cell APC function is required for induction of CNS autoimmunity independent of myelin-specific antibodies. J Exp Med. 2013;210(13):2921-37.

108. Baxter AG. The origin and application of experimental autoimmune encephalomyelitis. Nat Rev Immunol. 2007;7(11):904-12.

109. Jelcic I, Al Nimer F, Wang J, Lentsch V, Planas R, Jelcic I, et al. Memory B Cells Activate Brain-Homing, Autoreactive CD4(+) T Cells in Multiple Sclerosis. Cell. 2018;175(1):85-100 e23.

110. Cree BAC, Bennett JL, Kim HJ, Weinshenker BG, Pittock SJ, Wingerchuk DM, et al. Inebilizumab for the treatment of neuromyelitis optica spectrum disorder (N-MOmentum): a double-blind, randomised placebo-controlled phase 2/3 trial. Lancet. 2019;394(10206):1352-63.

111. Zephir H, Bernard-Valnet R, Lebrun C, Outteryck O, Audoin B, Bourre B, et al. Rituximab as first-line therapy in neuromyelitis optica: efficiency and tolerability. J Neurol. 2015;262(10):2329-35.

112. Jarius S, Wildemann B. The history of neuromyelitis optica. J Neuroinflammation. 2013;10:8.

113. Lennon VA, Wingerchuk DM, Kryzer TJ, Pittock SJ, Lucchinetti CF, Fujihara K, et al. A serum autoantibody marker of neuromyelitis optica: distinction from multiple sclerosis. Lancet. 2004;364:2106-12.

114. Lennon VA, Kryzer TJ, Pittock SJ, Verkman AS, Hinson SR. IgG marker of optic-spinal multiple sclerosis binds to the aquaporin-4 water channel. The Journal of Experimental Medicine. 2005;202:473-7.

115. Wingerchuk DM, Banwell B, Bennett JL, Cabre P, Carroll W, Chitnis T, et al. International consensus diagnostic criteria for neuromyelitis optica spectrum disorders. Neurology. 2015;85(2):177-89.

116. Redenbaugh V, Montalvo M, Sechi E, Buciuc M, Fryer JP, McKeon A, et al. Diagnostic value of aquaporin-4-IgG live cell based assay in neuromyelitis optica spectrum disorders. Mult Scler J Exp Transl Clin. 2021;7(4):20552173211052656.

117. Sechi E, Cacciaguerra L, Chen JJ, Mariotto S, Fadda G, Dinoto A, et al. Myelin Oligodendrocyte

Glycoprotein Antibody-Associated Disease (MOGAD): A Review of Clinical and MRI Features, Diagnosis, and Management. Frontiers in Neurology [Internet]. 2022 [cité 22 juill 2022];13. Disponible sur: https://www.frontiersin.org/articles/10.3389/fneur.2022.885218

118. Sato DK, Callegaro D, Lana-Peixoto MA, Waters PJ, Jorge FM de H, Takahashi T, et al. Distinction between MOG antibody-positive and AQP4 antibody-positive NMO spectrum disorders. Neurology. 2014;82(6):474-81.

119. Cobo-Calvo A, Ruiz A, Maillart E, Audoin B, Zephir H, Bourre B, et al. Clinical spectrum and prognostic value of CNS MOG autoimmunity in adults: The MOGADOR study. Neurology. 2018;90(21):e1858-69.

120. Mader S, Gredler V, Schanda K, Rostasy K, Dujmovic I, Pfaller K, et al. Complement activating antibodies to myelin oligodendrocyte glycoprotein in neuromyelitis optica and related disorders. J Neuroinflammation. 2011;8:184.

121. Mori M, Kuwabara S, Paul F. Worldwide prevalence of neuromyelitis optica spectrum disorders. J Neurol Neurosurg Psychiatry. 2018;89(6):555-6.

122. Quek AML, McKeon A, Lennon VA, Mandrekar JN, Iorio R, Jiao Y, et al. Effects of age and sex on aquaporin-4 autoimmunity. Arch Neurol. 2012;69(8):1039-43.

123. Borisow N, Kleiter I, Gahlen A, Fischer K, Wernecke KD, Pache F, et al. Influence of female sex and fertile age on neuromyelitis optica spectrum disorders. Mult Scler. juill 2017;23(8):1092-103.

124. Sepúlveda M, Armangue T, Martinez-Hernandez E, Arrambide G, Sola-Valls N, Sabater L, et al. Clinical spectrum associated with MOG autoimmunity in adults: significance of sharing rodent MOG epitopes. J Neurol. 2016;263(7):1349-60.

125. Jarius S, Paul F, Weinshenker BG, Levy M, Kim HJ, Wildemann B. Neuromyelitis optica. Nature Reviews Disease Primers. 2020;6(1):1-32.

126. Bruijstens AL, Wong YYM, Pelt DE van, Linden PJE van der, Haasnoot GW, Hintzen RQ, et al. HLA association in MOG-IgG– and AQP4-IgG–related disorders of the CNS in the Dutch population. Neurology - Neuroimmunology Neuroinflammation [Internet]. 2020 [cité 24 juill 2022];7(3). Disponible sur: https://nn.neurology.org/content/7/3/e702

127. Graves J, Grandhe S, Weinfurtner K, Krupp L, Belman A, Chitnis T, et al. Protective environmental factors for neuromyelitis optica. Neurology. 2014;83(21):1923-9.

128. Matiello M, Lennon VA, Jacob A, Pittock SJ, Lucchinetti CF, Wingerchuk DM, et al. NMO-IgG predicts the outcome of recurrent optic neuritis. Neurology. 2008;70(23):2197-200.

129. Kim SM, Go MJ, Sung JJ, Park KS, Lee KW. Painful tonic spasm in neuromyelitis optica: incidence, diagnostic utility, and clinical characteristics. Arch Neurol. 2012;69(8):1026-31.

130. Chen JJ, Flanagan EP, Jitprapaikulsan J, Lopez-Chiriboga ASS, Fryer JP, Leavitt JA, et al. Myelin Oligodendrocyte Glycoprotein Antibody-Positive Optic Neuritis: Clinical Characteristics, Radiologic Clues, and Outcome. Am J Ophthalmol. 2018;195:8-15.

131. Dubey D, Pittock SJ, Krecke KN, Morris PP, Sechi E, Zalewski NL, et al. Clinical, Radiologic, and Prognostic Features of Myelitis Associated With Myelin Oligodendrocyte Glycoprotein

Autoantibody. JAMA Neurol. 2019;76(3):301-9.

132. Hennes EM, Baumann M, Schanda K, Anlar B, Bajer-Kornek B, Blaschek A, et al. Prognostic relevance of MOG antibodies in children with an acquired demyelinating syndrome. Neurology. 2017;89(9):900-8.

133. Jurynczyk M, Messina S, Woodhall MR, Raza N, Everett R, Roca-Fernandez A, et al. Clinical presentation and prognosis in MOG-antibody disease: a UK study. Brain. 2017;140(12):3128-38.

134. Reindl M, Di Pauli F, Rostasy K, Berger T. The spectrum of MOG autoantibody-associated demyelinating diseases. Nat Rev Neurol. 2013;9(8):455-61.

135. Hoftberger R, Guo Y, Flanagan EP, Lopez-Chiriboga AS, Endmayr V, Hochmeister S, et al. The pathology of central nervous system inflammatory demyelinating disease accompanying myelin oligodendrocyte glycoprotein autoantibody. Acta Neuropathol. 2020;

136. Kleiter I, Gahlen A, Borisow N, Fischer K, Wernecke KD, Wegner B, et al. Neuromyelitis optica: Evaluation of 871 attacks and 1,153 treatment courses. Ann Neurol. 2016;79(2):206-16.

137. Bonnan M, Valentino R, Debeugny S, Merle H, Fergé JL, Mehdaoui H, et al. Short delay to initiate plasma exchange is the strongest predictor of outcome in severe attacks of NMO spectrum disorders. J Neurol Neurosurg Psychiatry. 2018;89(4):346-51.

138. Ciron J, Audoin B, Bourre B, Brassat D, Durand-Dubief F, Laplaud D, et al. Recommendations for the use of Rituximab in neuromyelitis optica spectrum disorders. Rev Neurol (Paris). 2018;174(4):255-64.

139. Kieseier BC, Stüve O, Dehmel T, Goebels N, Leussink VI, Mausberg AK, et al. Disease amelioration with tocilizumab in a treatment-resistant patient with neuromyelitis optica: implication for cellular immune responses. JAMA Neurol. 2013;70(3):390-3.

140. Traboulsee A, Greenberg BM, Bennett JL, Szczechowski L, Fox E, Shkrobot S, et al. Safety and efficacy of satralizumab monotherapy in neuromyelitis optica spectrum disorder: a randomised, double-blind, multicentre, placebo-controlled phase 3 trial. Lancet Neurol. 2020;19(5):402-12.

141. Rivers TM, Sprunt DH, Berry GP. OBSERVATIONS ON ATTEMPTS TO PRODUCE ACUTE DISSEMINATED ENCEPHALOMYELITIS IN MONKEYS. J Exp Med. 1933;58(1):39-53.

142. Krogsgaard M, Wucherpfennig KW, Canella B, Hansen BE, Svejgaard A, Pyrdol J, et al. Visualization of Myelin Basic Protein (Mbp) T Cell Epitopes in Multiple Sclerosis Lesions Using a Monoclonal Antibody Specific for the Human Histocompatibility Leukocyte Antigen (Hla)-Dr2–Mbp 85–99 Complex. Journal of Experimental Medicine. 2000;191(8):1395-412.

143. Linnington C, Webb M, Woodhams PL. A novel myelin-associated glycoprotein defined by a mouse monoclonal antibody. J Neuroimmunol. 1984;6(6):387-96.

144. Shetty A, Gupta SG, Varrin-Doyer M, Weber MS, Prod'homme T, Molnarfi N, et al. Immunodominant T-cell epitopes of MOG reside in its transmembrane and cytoplasmic domains in EAE. Neurol Neuroimmunol Neuroinflamm. 2004;1(2):e22.

145. Lucca LE, Axisa PP, Aloulou M, Perals C, Ramadan A, Rufas P, et al. Myelin oligodendrocyte glycoprotein induces incomplete tolerance of CD4(+) T cells specific for both a myelin and a neuronal

self-antigen in mice. Eur J Immunol. 2016;46(9):2247-59.

146. Delarasse C, Daubas P, Mars LT, Vizler C, Litzenburger T, Iglesias A, et al. Myelin/oligodendrocyte glycoprotein-deficient (MOG-deficient) mice reveal lack of immune tolerance to MOG in wild-type mice. J Clin Invest. 2003;112(4):544-53.

147. Nimmerjahn F, Ravetch JV. Fcγ receptors as regulators of immune responses. Nat Rev Immunol. 2008;8(1):34-47.

148. Schwab I, Nimmerjahn F. Intravenous immunoglobulin therapy: how does IgG modulate the immune system? Nat Rev Immunol. 2013;13(3):176-89.

149. Zhu X, Meng G, Dickinson BL, Li X, Mizoguchi E, Miao L, et al. MHC class I-related neonatal Fc receptor for IgG is functionally expressed in monocytes, intestinal macrophages, and dendritic cells. J Immunol. 2001;166(5):3266-76.

150. Ward ES, Ober RJ. Multitasking by Exploitation of Intracellular Transport Functions: The Many Faces of FcRn. Adv Immunol. 2009;103:77-115.

151. Roopenian DC, Akilesh S. FcRn: the neonatal Fc receptor comes of age. Nat Rev Immunol. 2007;7(9):715-25.

152. Heyman B. Regulation of antibody responses via antibodies, complement, and Fc receptors. Annu Rev Immunol. 2000;18:709-37.

153. Ravetch JV, Kinet JP. Fc receptors. Annu Rev Immunol. 1991;9:457-92.

154. Hulett MD, Hogarth PM. Molecular basis of Fc receptor function. Adv Immunol. 1994;57:1-127.

155. Mechetina LV, Najakshin AM, Volkova OY, Guselnikov SV, Faizulin RZ, Alabyev BY, et al. FCRL, a novel member of the leukocyte Fc receptor family possesses unique structural features. European Journal of Immunology. 2002;32(1):87-96.

156. Nimmerjahn F, Bruhns P, Horiuchi K, Ravetch JV. FcgammaRIV: a novel FcR with distinct IgG subclass specificity. Immunity. 2005;23(1):41-51.

157. P B, F J. Mouse and human FcR effector functions. Immunological reviews [Internet]. 2015 [cité 15 juin 2022];268(1). Disponible sur: http://pubmed.ncbi.nlm.nih.gov/26497511/?holding=ifrunillib_fft&myncbishare=ifrunillib&otool=ifrunillibdds

158. Nimmerjahn F. Activating and inhibitory FcγRs in autoimmune disorders. Springer Semin Immun. 2006;28(4):305-19.

159. Meyer D, Schiller C, Westermann J, Izui S, Hazenbos WL, Verbeek JS, et al. FcgammaRIII (CD16)-deficient mice show IgG isotype-dependent protection to experimental autoimmune hemolytic anemia. Blood. 1998;92(11):3997-4002.

160. Pincetic A, Bournazos S, DiLillo DJ, Maamary J, Wang TT, Dahan R, et al. Type I and type II Fc receptors regulate innate and adaptive immunity. Nature Immunology. 2014;15:707-16.

161. Wang TT, Ravetch JV. Functional diversification of IgGs through Fc glycosylation. J Clin

Invest. 2019;129(9):3492-8.

162. Zauner G, Selman MHJ, Bondt A, Rombouts Y, Blank D, Deelder AM, et al. Glycoproteomic analysis of antibodies. Mol Cell Proteomics. 2013;12(4):856-65.

163. Sondermann P, Huber R, Oosthuizen V, Jacob U. The 3.2-A crystal structure of the human IgG1 Fc fragment-Fc gammaRIII complex. Nature. 2000;406(6793):267-73.

164. Ferrara C, Grau S, Jäger C, Sondermann P, Brünker P, Waldhauer I, et al. Unique carbohydrate–carbohydrate interactions are required for high affinity binding between FcγRIII and antibodies lacking core fucose. 2011;6.

165. Quast I, Keller CW, Maurer MA, Giddens JP, Tackenberg B, Wang LX, et al. Sialylation of IgG Fc domain impairs complement-dependent cytotoxicity. J Clin Invest. 2015;125(11):4160-70.

166. Lu LL, Chung AW, Rosebrock TR, Ghebremichael M, Yu WH, Grace PS, et al. A Functional Role for Antibodies in Tuberculosis. Cell. 2016;167(2):433-443 e14.

167. Wang TT, Sewatanon J, Memoli MJ, Wrammert J, Bournazos S, Bhaumik SK, et al. IgG antibodies to dengue enhanced for FcgammaRIIIA binding determine disease severity. Science. 2017;355(6323):395-8.

168. Alter G, Ottenhoff THM, Joosten SA. Antibody glycosylation in inflammation, disease and vaccination. Semin Immunol. 2018/06/16 éd. 2018;39:102-10.

169. Seeling M, Bruckner C, Nimmerjahn F. Differential antibody glycosylation in autoimmunity: sweet biomarker or modulator of disease activity? Nat Rev Rheumatol. 2017;13(10):621-30.

170. Decker Y, Schomburg R, Nemeth E, Vitkin A, Fousse M, Liu Y, et al. Abnormal galactosylation of immunoglobulin G in cerebrospinal fluid of multiple sclerosis patients. Mult Scler. 2016;22(14):1794-803.

171. Wuhrer M, Selman MHJ, McDonnell LA, Kümpfel T, Derfuss T, Khademi M, et al. Pro-inflammatory pattern of IgG1 Fc glycosylation in multiple sclerosis cerebrospinal fluid. J Neuroinflammation. 2015;12(1):235.

172. Jefferis R, Lund J, Pound JD. IgG-Fc-mediated effector functions: molecular definition of interaction sites for effector ligands and the role of glycosylation. Immunological Reviews. 1998;163:59-76.

173. Arnold JN, Wormald MR, Sim RB, Rudd PM, Dwek RA. The impact of glycosylation on the biological function and structure of human immunoglobulins. Annu Rev Immunol. 2007;25:21-50.

174. Kobata A. The N-linked sugar chains of human immunoglobulin G: their unique pattern, and their functional roles. Biochim Biophys Acta. 2008;1780(3):472-8.

175. Shields RL, Lai J, Keck R, O'Connell LY, Hong K, Meng YG, et al. Lack of fucose on human IgG1 N-linked oligosaccharide improves binding to human Fcgamma RIII and antibody-dependent cellular toxicity. The Journal of Biological Chemistry. 2002;277:26733-40.

176. Shinkawa T, Nakamura K, Yamane N, Shoji-Hosaka E, Kanda Y, Sakurada M, et al. The absence of fucose but not the presence of galactose or bisecting N-acetylglucosamine of human IgG1 complex-type oligosaccharides shows the critical role of enhancing antibody-dependent cellular

cytotoxicity. J Biol Chem. 2003;278(5):3466-73.

177. Zou G, Ochiai H, Huang W, Yang Q, Li C, Wang LX. Chemoenzymatic synthesis and Fcγ receptor binding of homogeneous glycoforms of antibody Fc domain. Presence of a bisecting sugar moiety enhances the affinity of Fc to FcγIIIa receptor. Journal of the American Chemical Society. 2011;133:18975-91.

178. Anthony RM, Wermeling F, Karlsson MC, Ravetch JV. Identification of a receptor required for the anti-inflammatory activity of IVIG. Proc Natl Acad Sci U S A. 2008;105(50):19571-8.

179. Temming AR, Dekkers G, van de Bovenkamp FS, Plomp HR, Bentlage AEH, Szittner Z, et al. Human DC-SIGN and CD23 do not interact with human IgG. Sci Rep. 2019;9(1):9995.

180. Anthony RM, Kobayashi T, Wermeling F, Ravetch JV. Intravenous gammaglobulin suppresses inflammation through a novel T(H)2 pathway. Nature. 2011;475(7354):110-3.

181. Wang TT, Maamary J, Tan GS, Bournazos S, Davis CW, Krammer F, et al. Anti-HA Glycoforms Drive B Cell Affinity Selection and Determine Influenza Vaccine Efficacy. Cell. 2015;162(1):160-9.

182. Salvador F, Deramoudt L, Leprêtre F, Figeac M, Guerrier T, Boucher J, et al. A Spontaneous Model of Experimental Autoimmune Encephalomyelitis Provides Evidence of MOG-Specific B Cell Recruitment and Clonal Expansion. Front Immunol. 2022;13:755900.

183. Pfeifle R, Rothe T, Ipseiz N, Scherer HU, Culemann S, Harre U, et al. Regulation of autoantibody activity by the IL-23-TH17 axis determines the onset of autoimmune disease. Nat Immunol. 2017;18(1):104-13.

184. O'Connor KC, McLaughlin KA, De Jager PL, Chitnis T, Bettelli E, Xu C, et al. Self-antigen tetramers discriminate between myelin autoantibodies to native or denatured protein. Nat Med. 2007;13(2):211-7.

185. Breithaupt C, Schubart A, Zander H, Skerra A, Huber R, Linington C, et al. Structural insights into the antigenicity of myelin oligodendrocyte glycoprotein. Proc Natl Acad Sci U S A. 2003;100(16):9446-51.

186. Roberts JT, Patel KR, Barb AW. Site-specific N-glycan Analysis of Antibody-binding Fc γ Receptors from Primary Human Monocytes. Mol Cell Proteomics. 2020;19(2):362-74.

187. Andrén M, Johanneson B, Alarcón-Riquelme ME, Kleinau S. IgG Fc receptor polymorphisms and association with autoimmune disease. Eur J Immunol. 2005;35(10):3020-9.

188. Urich E, Gutcher I, Prinz M, Becher B. Autoantibody-mediated demyelination depends on complement activation but not activatory Fc-receptors. Proc Natl Acad Sci U S A. 2006;103(49):18697-702.

189. Flach AC, Litke T, Strauss J, Haberl M, Gómez CC, Reindl M, et al. Autoantibody-boosted T-cell reactivation in the target organ triggers manifestation of autoimmune CNS disease. Proc Natl Acad Sci USA. 2016;113(12):3323-8.

190. Meinl E, Krumbholz M, Hohlfeld R. B lineage cells in the inflammatory central nervous system environment: migration, maintenance, local antibody production, and therapeutic modulation. Ann

Neurol. 2006;59(6):880-92.

191. Beltrán E, Obermeier B, Moser M, Coret F, Simó-Castelló M, Boscá I, et al. Intrathecal somatic hypermutation of IgM in multiple sclerosis and neuroinflammation. Brain. 2014;137(Pt 10):2703-14.

192. Stern JNH, Yaari G, Vander Heiden JA, Church G, Donahue WF, Hintzen RQ, et al. B cells populating the multiple sclerosis brain mature in the draining cervical lymph nodes. Sci Transl Med. 2014;6(248):248ra107.

193. Pollinger B, Krishnamoorthy G, Berer K, Lassmann H, Bosl MR, Dunn R, et al. Spontaneous relapsing-remitting EAE in the SJL/J mouse: MOG-reactive transgenic T cells recruit endogenous MOG-specific B cells. J Exp Med. 2009;206(6):1303-16.

194. Berer K, Gerdes LA, Cekanaviciute E, Jia X, Xiao L, Xia Z, et al. Gut microbiota from multiple sclerosis patients enables spontaneous autoimmune encephalomyelitis in mice. Proceedings of the National Academy of Sciences of the United States of America. 2017;114(40):10719-24.

195. Chakraborty S, Gonzalez J, Edwards K, Mallajosyula V, Buzzanco AS, Sherwood R, et al. Proinflammatory IgG Fc structures in patients with severe COVID-19. Nat Immunol. janv 2021;22(1):67-73.

196. Larsen MD, de Graaf EL, Sonneveld ME, Plomp HR, Nouta J, Hoepel W, et al. Afucosylated IgG characterizes enveloped viral responses and correlates with COVID-19 severity. Science. 2021;371(6532):eabc8378.

197. Nimmerjahn F, Ravetch JV. Divergent immunoglobulin g subclass activity through selective Fc receptor binding. Science. 2005;310(5753):1510-2.

198. Umana P, Jean-Mairet J, Moudry R, Amstutz H, Bailey JE. Engineered glycoforms of an antineuroblastoma IgG1 with optimized antibody-dependent cellular cytotoxic activity. Nat Biotechnol. 1999;17(2):176-80.

199. Bournazos S, Gupta A, Ravetch JV. The role of IgG Fc receptors in antibody-dependent enhancement. Nat Rev Immunol. 2020;20(10):633-43.

200. Kapur R, Kustiawan I, Vestrheim A, Koeleman CA, Visser R, Einarsdottir HK, et al. A prominent lack of IgG1-Fc fucosylation of platelet alloantibodies in pregnancy. Blood. 2014;123(4):471-80.

201. Dekkers G, Bentlage AEH, Plomp R, Visser R, Koeleman CAM, Beentjes A, et al. Conserved FcγR- glycan discriminates between fucosylated and afucosylated IgG in humans and mice. Mol Immunol. 2018;94:54-60.

202. Mellquist JL, Kasturi L, Spitalnik SL, Shakin-Eshleman SH. The amino acid following an asn-X-Ser/Thr sequon is an important determinant of N-linked core glycosylation efficiency. Biochemistry. 1998;37(19):6833-7.

203. Patel KR, Roberts JT, Subedi GP, Barb AW. Restricted processing of CD16a/Fc γ receptor IIIa N-glycans from primary human NK cells impacts structure and function. J Biol Chem. 2018;293(10):3477-89.

204. Regnault A, Lankar D, Lacabanne V, Rodriguez A, Théry C, Rescigno M, et al. Fcgamma

receptor-mediated induction of dendritic cell maturation and major histocompatibility complex class I-restricted antigen presentation after immune complex internalization. J Exp Med. 1999;189(2):371-80.

205. Baker K, Rath T, Flak MB, Arthur JC, Chen Z, Glickman JN, et al. Neonatal Fc receptor expression in dendritic cells mediates protective immunity against colorectal cancer. Immunity. 2013;39(6):1095-107.

206. Guilliams M, Bruhns P, Saeys Y, Hammad H, Lambrecht BN. The function of Fcγ receptors in dendritic cells and macrophages. Nat Rev Immunol. 2014;14(2):94-108.

207. Mars LT, Araujo L, Kerschen P, Diem S, Bourgeois E, Van LP, et al. Invariant NKT cells inhibit development of the Th17 lineage. Proc Natl Acad Sci U S A. 2009;106(15):6238-43.

208. Ramadan A, Lucca LE, Carrié N, Desbois S, Axisa PP, Hayder M, et al. In situ expansion of T cells that recognize distinct self-antigens sustains autoimmunity in the CNS. Brain. 2016;139(Pt 5):1433-46.

209. Mars LT, Saikali P, Liblau RS, Arbour N. Contribution of CD8 T lymphocytes to the immuno-pathogenesis of multiple sclerosis and its animal models. Biochim Biophys Acta. 2011;1812(2):151-61.

210. Sachdeva M, Dhingra S. Obinutuzumab: A FDA approved monoclonal antibody in the treatment of untreated chronic lymphocytic leukemia. International Journal of Applied and Basic Medical Research. 2015;5(1):54-7.

211. Evans JG, Chavez-Rueda KA, Eddaoudi A, Meyer-Bahlburg A, Rawlings DJ, Ehrenstein MR, et al. Novel suppressive function of transitional 2 B cells in experimental arthritis. J Immunol. 2007;178(12):7868-78.

212. Makita S, Yoshimura K, Tobinai K. Clinical development of anti-CD19 chimeric antigen receptor T-cell therapy for B-cell non-Hodgkin lymphoma. Cancer Sci. 2017;108(6):1109-18.

213. Perera NC, Wiesmüller KH, Larsen MT, Schacher B, Eickholz P, Borregaard N, et al. NSP4 Is Stored in Azurophil Granules and Released by Activated Neutrophils as Active Endoprotease with Restricted Specificity. JI. 2013;191(5):2700-7.

214. Bauer J, Elger CE, Hans VH, Schramm J, Urbach H, Lassmann H, et al. Astrocytes are a specific immunological target in Rasmussen's encephalitis. Ann Neurol. 2007;62(1):67-80.

APPENDIX

Annexe 1 : List of antibodies coupled to a fluorochrome used in flow cytometry

4-1BBL	PE	CD137L	BioLegend
B220	PerCP-Cy5	RA3-6B2	BD Biosciences
CCR6	PE dazzle 294	29-2L17	BioLegend
CD138	PE	281-2	BD Biosciences
CD16	PE	3G8	BioLegend
CD16	PE	S17014E	BioLegend
CD16/32	FC Block	93	BioLegend
CD19	APC	6D5	BioLegend
CD19	PE-Cy5	6D5	BD Biosciences
CD19	Pacific Blue	6D5	BD Biosciences
CD19	Bv605	1D3	BD Biosciences
CD2	Pacific Blue	RPA-2.10	BioLegend
CD209	FITC	9E9A8	BioLegend
CD32	FITC	S17012B	BioLegend
CD335	FITC	NKp46	BioLegend
CD38	Pacific Blue	90	BD Biosciences
CD3e	PE/Dazzle594	KT3.1.1	BioLegend
CD4	Bv570	GK1.5	BioLegend
CD4	PE	RMA-5	BioLegend
CD4	APC-Cy7	RMA-5	BioLegend
CD4	BV786	RMA-5	BioLegend
CD44	PerCP Cy5.5	IM7	BioLegend
CD44	Bv605	IM7	BioLegend
CD44	AF700	IM7	BioLegend
CD45	PE-TR	30-F11	BioLegend
CD45	PerCP Cy5.5	30-F11	BioLegend
CD45.1	FITC	A20	BioLegend
CD45.1	APC	A20	BD Biosciences
CD45.2	Bv605	104	BioLegend
CD45.2	PE	104	BD Biosciences

CD56	Bv650	5.1H11	BioLegend
CD62L	PE Cy5	MEL-14	BioLegend
CD62L	Bv650	MEL-14	BioLegend
CD64	PE	10.1	BioLegend
CD64	PE	X54-5/7.1	BioLegend
CD8b	PE Cy7	YTS156.7.7	BioLegend
CD90.2	Pacific Blue	53-2.1	BioLegend
CMHII I-Ab	Efluor450	AF6-120.1	eBioscience
CXCR3	BV 650	CXCR3-173	BioLegend
CXCR3	PerCP/Cy5.5	CXCR3-173	BioLegend
FAS	PE-Cy7	Jo2	BD Biosciences
Fixable Viability Dye	APC efluor 780		Life Technologies
GL7 antigen	Alexa Fluor 647	GL7	BD Biosciences
GM-CSF	FITC	MP1-22E9	BioLegend
IgG1	FITC	A85-1	BD Biosciences
IgM^a	PE	DS-1	BD Biosciences
IgM^b	FITC	AF6-78	BD Biosciences
IL-17A	BV 650	TC11-18H10.1	BioLegend
INFγ	FITC	AN-18	BioLegend
INF**γ**	AF 700	AN-18	BioLegend
Mouse IgG2a κ	/	MOPC-173	BioLegend
NK1.1	FITC	PK136	eBioscience
PE rat IgG2a κ CTL	/	G013CL2	BioLegend
RORγT	PE	AFKJ5-9	BioLegend
T-bet	BV711	4B10	BioLegend
TCR Vα3.2	PE	RR3-16	BioLegend
TCR Vα8.3	PE	B21.14	BD Biosciences
TCR Vβ4	FITC	KT4	BD Biosciences
TNFα	PE Cy7	MP6-XT22	BioLegend
Viability	7AAD		BioLegend

❖ **UNIPROT N° P08508 - FCGR3_MOUSE**

- *sp|P08508|FCGR3_MOUSE Low affinity immunoglobulin gamma Fc region receptor III*

MFQNAHSGSQWLLPPLTILLLFAFADRQSAALPKAVVKLDPPWIQVLKEDMVTLMCEGTHN
PGNSSTQWFHNGRSIRSQVQASYTFKATVNDSGEYRCQMEQTRLSDPVDLGVISDWLLLQ
TPQRVFLEGETITLRCHSWRNKLLNRISFFHNEKSVRYHHYKSNFSIPKANHSHSGDYYCKG
SLGSTQHQSKPVTITVQDPATTSSISLVWYHTAFSLVMCLLFAVDTGLYFYVRRNLQTPREY
WRKSLSIRKHQAPQDK

- *m CD16-pcDNA3.1(-)hygro vector map*

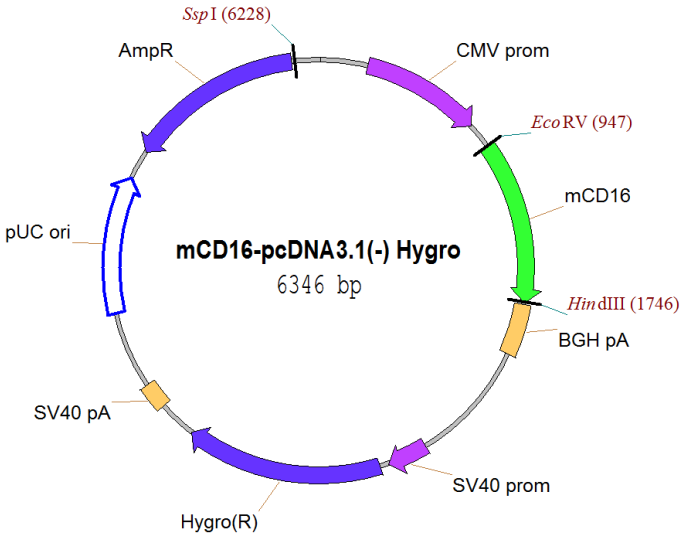

Annexe 2: Murin CD16 protein sequence and vector map

❖ **Human DC-SIGN (CD209 antigen)**

DC-SIGN for Dendritic cell-specific intercellular adhesion molecule-3-grabbing nonintegrin

- *sp|Q9NNX6|1-404 Accession number : Q9NNX6*

MSDSKEPRLQQLGLLEEEQLRGLGFRQTRGYKSLAGCLGHGPLVLQLLSFTLLAGLLVQVS
KVPSSISQEQSRQDAIYQNLTQLKAAVGELSEKSKLQEIYQELTQLKAAVGELPEKSKLQEIY
QELTRLKAAVGELPEKSKLQEIYQELTWLKAAVGELPEKSKMQEIYQELTRLKAAVGELPEK
SKQQEIYQELTRLKAAVGELPEKSKQQEIYQELTRLKAAVGELPEKSKQQEIYQELTQLKAA
VERLCHPCPWEWTFFQGNCYFMSNSQRNWHDSITACKEVGAQLVVIKSAEEQNFLQLQSS
RSNRFTWMGLSDLNQEGTWQWVDGSPLLPSFKQYWNRGEPNNVGEEDCAEFSGNGWN
DDKCNLAKFWICKKSAASCSRDEEQFLSPAPATPNPPPA

- *DC-SICN-pcDNA3 vector map*

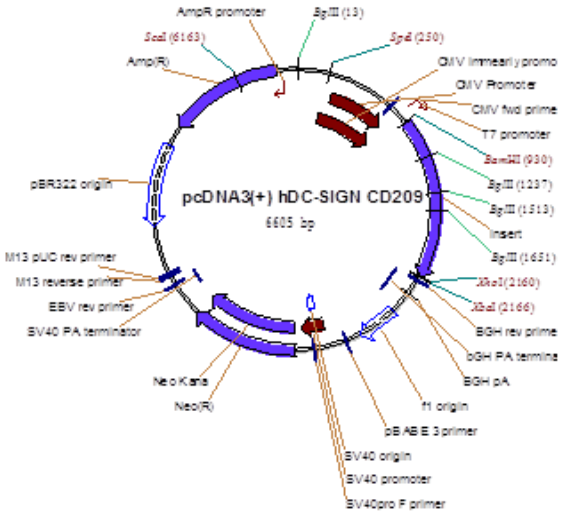

Annexe 3: DC-SIGN protein sequence and vector map

❖ **Myelin Oligodendrocyte Glycoprotein (MOG), used for the JKT expressing MOG**

- *>sp|Q61885|1-246 Accession number : Q61885*

MACLWSFSWPSCFLSLLLLLLQLSCSYAGQFRVIGPGYPIRALVGDEAELPCRISPGKNATG
MEVGWYRSPFSRVVHLYRNGKDQDAEQAPEYRGRTELLKETISEGKVTLRIQNVRFSDEG
GYTCFFRDHSYQEEAAMELKVEDPFYWVNPGVLTLIALVPTILLQVPVGLVFLFLQHRLRGK
LRAEVENLHRTFDPHFLRVPCWKITLFVIVPVLGPLVALIICYNWLHRRLAGQFLEELRNPF

- *MOG - vector : pcDNA3*

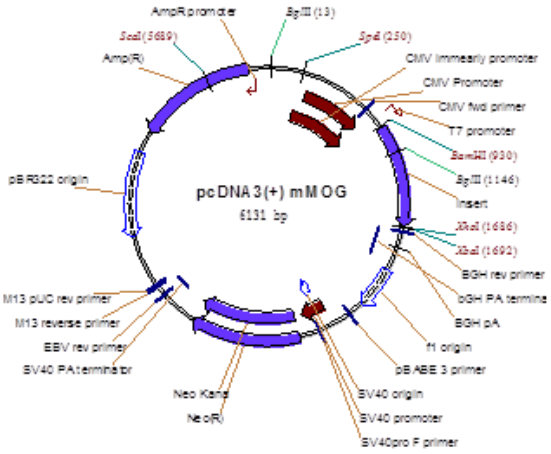

Annexe 4: MOG protein sequence and vector map

❖ 8-18C5

- Heavy chain (HC):

EVKLHESGAGLVKPGASVEISCKATGYTFSSFWIEWVKQRPGHGLEWIGEILPGRGRTNYN
EKFKGKATFTAETSSNTAYMQLSSLTSEDSAVYYCATGNTMVNMPYWGQGTTVTVSSAKT
TPPSVYPLAPGSAAQTNSMVTLGCLVKGYFPEPVTVTWNSGSLSSGVHTFPAVLESDLYTL
SSSVTVPSSPRPSETVTCNVAHPASSTKVDKKIVPRDCGCKPCICTVPEVSSVFIFPPKPKD
VLTITLTPKVTCVVVDISKDDPEVQFSWFVDDVEVHTAQTQPREE$_{171}$QFN174STFRSVSELP
IMHQDWLNGKEFKCRVNSAAFPAPIEKTISKTKGRPKAPQVYTIPPPKEQMAKDKVSLTCMI
TDFFPEDITVEWQWNGQPAENYKNTQPIMNTN$_{278}$GSYFVYSKLNVQKSNWEAGNTFTCSV
LHEGLHNHHTEKSLSHSPGK

- Light chain (LC):

DIELTQSPSSLAVSAGEKVTMSCKSSQSLLNSGNQKNYLAWYQQKPGLPPKLLIYGASTRE
SGVPDRFTGSGSGTDFTLTISSVQAEDLAVYYCQNDHSYPLTFGAGTKLEIKRADAAPTVSI
FPPSSEQLTSGGASVVCFLNNFYPKDINVKWKIDGSERQNGVLNSWTDQDSKDSTYSMSS
TLTLTKDEYERHNSYTCEATHKTSTSPIVKSFNRNEC

- *8-18C5 bicistronique vector- pCEP4-H8-18C5-GK*

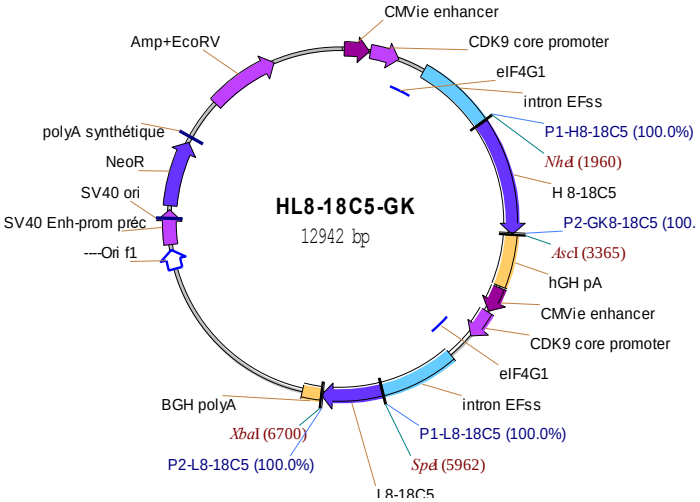

Annexe 5: 8-18C5 protein sequence and vector map

❖ 8-18C5 produced with hybridoma

- Heavy chain (HC):

QVQLQQSGAELMKPGASVEISCKATGYTFSSFWIEWVKQRPGHGLEWIGEILPGRGRTNY
NEKFKGKATFTAETSSNTAYMQLSSLTSEDSAVYYCATGNTMVNMPYWGQGTTLTVSSAK
TTPPSVYPLAPGSAAQTNSMVTLGCLVKGYFPEPVTVTWNSGSLSSGVHTFPAVLQSDLYT
LSSSVTVPSSTWPSETVTCNVAHPASSTKVDKKIVPRDCGCKPCICTVPEVSSVFIFPPKPK
DVLTITLTPKVTCVVVDISKDDPEVQFSWFVDDVEVHTAQTQPREEQFNSTFRSVSELPIMH
QDWLNGKEFKCRVNSAAFPAPIEKTISKTKGRPKAPQVYTIPPPKEQMAKDKVSLTCMITDF
FPEDITVEWQWNGQPAENYKNTQPIMDTDGSYFVYSKLNVQKSNWEAGNTFTCSVLHEG
LHNHHTEKSLSHSPGK

- Light chain (LC):

DIVMTQSPSSLSVSAGEKVTMSCKSSQSLLNSGNQKNYLAWYQQKPGLPPKLLIYGASTRE
SGVPDRFTGSGSGTDFTLTISSVQAEDLAVYYCQNDHSYPLTFGAGTKLELKRADAAPTVSI
FPPSSEQLTSGGASVVCFLNNFYPKDINVKWKIDG

❖ **Myelin Oligodendrocyte Glycoprotein 1-125 (MOG^{1-125})**

Used for the production of MOG tetramer and for Ni-NTA beads and Streptavidin magnetic beads with MOG_{1-132}
Avitag is a short sequence implicate in the biotinylation of MOG protein. MOG_{1-125} is the coding sequence of the extracellular part of MOG. 6His is a tag histidin used for purify the MOG_{1-125} protein.

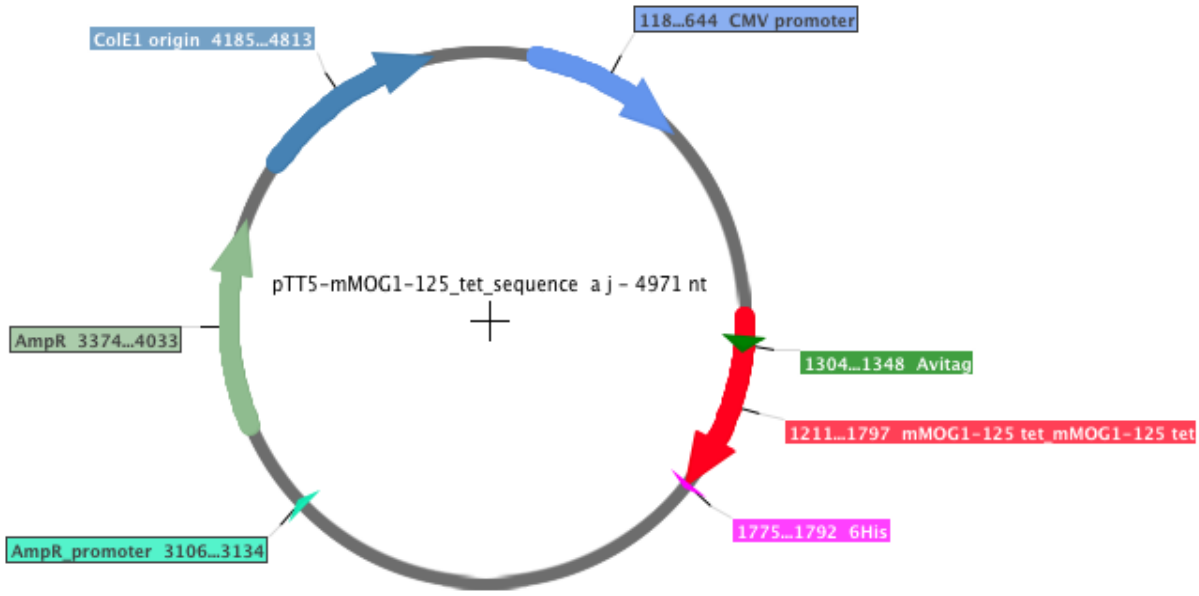

Annexe 6: Myelin Oligodendrocyte Glycoprotein 1-125

Lille University
Academic year 2021/2022

First Name: Laure
Name: Deramoudt
Title:

"B cells and humoral immunity in demyelinating disease of the central nervous system"

Key words: Humoral response, autoantibodies, neuro inflammation, demyelinating disease, Fc-glycosylation

Abstract:

This work investigates the involvement of the humoral response in inflammatory demyelinating diseases of the central nervous system. The study focuses on two autoimmune diseases: multiple sclerosis (MS) and diseases associated with anti-MOG (myelin oligodendrocyte glycoprotein) autoantibodies, called MOGAD. In both diseases, the pathogenic target is myelin, a protective sheath that protects axons and facilitates nerve impulses. Demyelination resulting from tissue and cell damage is responsible for the clinical presentation. MOG antibodies (Abs), which recognize a protein component of myelin, are key determinants in MOGAD, whereas in MS Abs are not a relevant biomarker due to the variable and evolving nature of antigen specificity. This work highlights the importance of Fc fragment glycosylation, which greatly expands the functional potential of Abs in the context of MOGAD. The B cell repertoire is also studied in parallel by analyzing the dynamics of MOG-specific B cells during the initiation of a spontaneous mouse model of MS.

Jury members:

President:

Monsieur le Professeur Patrick Vermersch
MD, PhD, PU-PH – Neurologist – Lille University

Reviewers:

Monsieur le Professeur Alexander Flügel
Professor and director of the Institute for Neuroimmunology and Multiple Sclerosis Research, University of Göttingen

Monsieur le Docteur Guillaume Dorothée
Research Director – inserm UMR-S 938 – Team leader « *Système Immunitaire et Neuroinflammation* » – Saint Antoine research centre, Paris

Examinateur:

Madame le Docteur Anneli Peters
Research Group Leader – *T:B cell interactions* – institute of Clinical – Neuroimmunology, Munich

Thesis Director :

Monsieur le Docteur Lennart MARS
Researcher – inserm UMR-S 1172 – Team leader NEMESIS « *Neuroinfammation & Multiple Sclerosis* » – Lille University